CHAPTER 1

INTRODUCTION

1.1 General introduction

This thesis embraces six chapters. An overview for the subject and objectives of the work is presented in Chapter 1. The literature review, background and current status of mcl-PHA, PVC and plasticized PVC are presented in Chapter 2 of the thesis. Chapter 3 deals with the experimental methods and analytical techniques undertaken in order to structurally, thermally and physically characterize the biopolyester, degradation products (oligoesters), PVC and plasticized PVC compounds. The results and discussions for the thermal degradation of mcl-PHA are presented in Chapter 4. Chapter 5 discusses the results from the assessment of PHA and its oligoesters as environmentally friendly and renewable plasticizers for PVC. Chapter 6 gives the overall summaries of the research done and suggestions for future works.

1.2 Biodegradable polymer

Petroleum based plastics are considered one of the biggest environmental pollutants, and this had led to intense research activities to develop alternative materials which are more environmentally friendly. The alternative materials should be biodegradable into harmless intermediates and end products. Poly(3-hydroxyalkanoates) (PHA) are natural polyesters which are good alternative materials to petrochemical-based polymers as PHA are non-toxic, biodegradable, biocompatible and possess thermoplastic properties similar to conventional plastics. They are synthesized by several groups of microorganisms, usually in response to unfavorable growth conditions *e.g.* when an essential nutrient such as nitrogen, phosphorus, oxygen or sulfur becomes limiting (Dawes & Senior, 1973; Du & Yu, 2002; Annuar et al., 2008). PHA are accumulated as water-insoluble granules in the cells, and they are believed to be the

carbon and energy storage compounds (Dawes & Senior, 1973; Wang & Bakken, 1998; Madison & Huisman, 1999). In these microbial polyesters, the carboxyl group of one monomer forms an ester bond with the hydroxyl group of the neighboring monomer. Each monomer contains the chiral carbon and has the (*R*) stereochemical configuration, thus PHA are optically active and isotactic (Lee et al., 1999; Ballistreri et al., 2001).

Medium-chain-length poly(3-hydroxyalkanoates) (mcl-PHA) are microbial polyesters comprised of six to fourteen carbon-chain-length 3-hydroxyalkanoic acids as monomers. This class of PHA is primarily produced by the fluorescent pseudomonades belonging to rRNA homology group I (Huisman et al., 1989; Timm & Steinbuchel, 1990; Kiska & Gilligan, 1999) and the monomeric composition of mcl-PHA is closely related to the structure of the carbon substrate that was fed to the bacteria (Brandl et al., 1988; Lageveen et al., 1988; Huisman et al., 1989; Eggink et al., 1992). Mcl-PHA have low crystallinity and glass transition temperature and are elastic, less stiff and brittle (Huisman et al., 1989; Preusting et al., 1990; Timm & Steinbuchel, 1990; Madison & Huisman, 1999). Different combinations of monomers yield polymers with a wide variety of chemical and physical properties, and thus broaden the potential applications of mcl-PHA.

1.3 Thermodegradation of mcl-PHA

Low molecular weight oligoesters can be produced from medium-chain-length polyhydroxyalkanoates by thermal degradation process. These oligomeric hydroxyalkanoic acids possess favorable end groups, and such fragments could be served as precursors or intermediates for the synthesis of biodegradable polymeric materials and optically active compounds. For example, they could be used as biodegradable carriers for medicines, drugs and hormones, biodegradable additives, coatings and plasticizers, or being used as blending materials in a co-polymerization process (Reeve et al., 1993; Hiki

et al., 2000; Nguyen et al., 2002). As the thermal degradation process takes place in the absence of organic solvents and other chemicals, this justified the method of producing low molecular weight oligoesters as green chemistry.

In this study, mcl-PHA were produced by *Pseudomonas putida* PGA1 *via* fermentation using oleic acid (OA) and saponified palm kernel oil (SPKO) as carbon substrate. Subsequently, they were thermally degraded at moderately high temperatures. The changes in thermal, physical and structural properties of the control and thermally-degraded oligoesters were analyzed and the chain scission mechanism of the biopolymer during thermal degradation process was proposed.

1.4 Mcl-PHA and its oligoesters as natural based plasticizer for PVC

Poly(vinyl chloride) (PVC) constitutes one of the largest global consumption of commodity plastics, approximately 16 million tonnes per annum (PVC Information Council, 1995). PVC compounds in the plasticized form are widely used in the industry for various flexible applications such as packaging, toys, medical and household products. Conventional petrochemical-based plasticizers for PVC, particularly phthalates, e.g. diethylhexyl phthalates (DEHP) and diisonyl phthalates (DINP) are the most commonly used PVC plasticizers (Marcilla et al., 2004). Nevertheless, these phthalate-based plasticizers are found to be detrimental to the environment and human health (Third National Report on Human Exposure to Environmental Chemicals, 2005), as they might migrate out from the PVC compound during end-use applications, into the human body or the environment. In 1995, European Community had banned for the usage of phthalates in the applications intended for children usage under the age of 3 years ("Official Journal of the European Communities", 1999). Recently in the 2011 Taiwan Food Scandal, DEHP and DINP were reported as the carcinogenic plasticizer agents, implicated in human infertility problem and developmental problems in children as these

plasticizers mimic human hormones and could served as the endocrine disruptors (National Toxicology Program, 1982).

Recent research activities have been carried out to seek for alternative greener materials which impart low toxicity, total or partial biodegradability and are economical and technical viable to substitute those conventional petrochemical-based plasticizers. Mcl-PHA which have the biodegradable, biocompatible and non-toxic properties fulfill all the desired traits of an alternative eco-friendly plasticizer material and have the great potential to function as compatible plasticizer for PVC.

In this work, the OA and SPKO-derived mcl-PHA and their low molecular weight oligoesters were mixed with PVC at the compositions of 2.5 and 5 parts per hundred parts (phr) of PVC through solution blending. The lightly plasticized PVC films were solvent casted and characterized to study the PVC-PHA interactions, microstructures, polymer film morphology, miscibility between the two polymers, viscoelastic properties, thermal behavior, thermal stability and thermo-kinetic parameters of the PVC/PHA polymer blends.

1.5 Objectives of study:

1.5.1 In the study of thermodegradation of mcl-PHA

1. To produce mcl-PHA *via* bacterial fermentation using oleic acid and saponified palm kernel oil as renewable carbon feedstock;
2. To produce oligomeric materials with useful end groups and desirable structures *via* thermal degradation of mcl-PHA;
3. To characterize the degradation products and study the possible chain scission mechanism during the thermal degradation of the mcl-PHA.

1.5.2 In the study of assessment of biopolyesters and oligoesters as natural based plasticizer for PVC

1. To investigate the ability of mcl-PHA and their low molecular weight oligoesters to act as a compatible, biodegradable plasticizer for poly(vinyl chloride) (PVC);
2. To structurally, thermally and mechanically characterize the lightly plasticized PVC films;
3. To investigate the thermal stability and thermo-kinetics parameters of the polymer blends.

CHAPTER 2

LITERATURE REVIEW

2.1. Poly(3-hroydroxyalkanoates) as biodegradable polymer

Since the non-degradable plastics were introduced in our daily lives, the postconsumer plastic waste disposal has created a pressing global environmental issue. Nevertheless, researchers from all over the world are aware of the intricate link between xenobiotics, petrochemicals and sustainable environment, and intense research activities have been carried out to develop alternative biopolymers from renewable resources such as plant oils, fatty acids and organic wastes.

Poly(3-hydroxyalkanoates) (PHA) are a new generation of polymers which are completely biodegradable, biocompatible, non-toxic and can be synthesized from natural renewable resources (Tan et al., 1997; Braunegg et al., 1998; Reddy et al., 2003; Annuar et al., 2007). PHA have the potential to replace the conventional plastic due to their structural diversity and the close similarites to petrochemical thermoplastics, and the ability to degrade in the environment. These biopolymers can be broken down into carbon dioxide, water and biomass in aerobic conditions or to methanol in anaerobic conditions such as soil, sea, stagnant water or sewage water (Lee, 1996). Besides being biodegradable, PHA are recyclable just like the conventional petrochemical plastics.

PHA are biological polyesters of various hydroxyl acids which are synthesized by a wide range of microorganisms. PHA are accumulated in response to nutrient limiting environment e.g. when an essential nutrient such as nitrogen, phosphorous, oxygen or sulfur is in deficiency (Dawes & Senior, 1973; Doi, 1995; Du & Yu, 2002; Verlinden et al., 2007; Annuar et al., 2008), but in the presence of excess carbon source. These polyesters serve as carbon and energy reserve materials which are osmotically inert and occurred as hydrophobic intracellular granules in the cell (Dawes & Senior, 1973; Tan et

al., 1997; Wang & Bakken, 1998; Madison & Huisman, 1999). Fig. 2.1 shows the electron microscopy of a bacterium harbouring PHA granules.

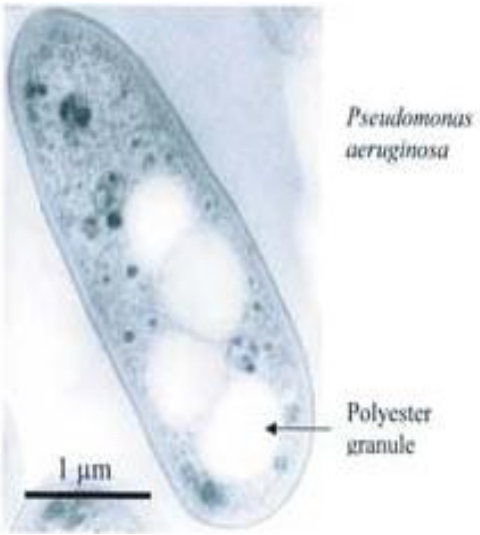

Fig. 2.1 Electron microscopy of *Pseudomonas aeruginosa* harbouring PHA granules (Rehm, 2003)

By polymerizing water-soluble intermediates into hydrophobic compounds, the cell does not undergo osmotic shock and at the same time leakage of these valuable compounds out of the cell is prevented (Madison & Huisman, 1999). Under starved conditions, these natural products can be catabolized by the cell itself and subsequently consumed by enzymatic depolymerization reactions (Dawes & Senior, 1973; Sudesh et al., 2000).

Since PHA are produced by naturally occurring microorganisms, this makes these polyesters a natural material and thus they can be degraded upon subsequent exposure to soil, compost, sewage, river or marine sediment (Lee, 1996; Ho et al., 2002; Lim et al., 2005). The biodegradation of PHA is dependent upon a number of factors such as the microbial activity of the environment and the exposed surface area. In addition,

temperature, pH, molecular weight are also important factors (Boopathy, 2000; Reddy et al., 2003) for the degradation process. Biodegradation starts when microorganisms begin growing on the surface of the polymers and secrete enzymes like PHA hydrolases and PHA depolymerases that break down the polymer into its monomer building blocks, called hydroxyacids. The hydroxyacids are then taken up by the microorganisms and used as carbon sources for growth. Their biodegradability property distinguishes PHA from petroleum-based polymers. Despite their biodegradability the PHA have good resistance to water and moisture vapor, and thus they are stable during use and under normal storage conditions (Reddy et al., 2003; Ojumu et al., 2004).

2.1.1 Chemical structure of PHA

Poly(3-hydroxyalkanoates) are natural polyesters which composed of repeating units of 3-hydroxyalkanoic acids, each of which carries an aliphatic alkyl side chain (R) as shown in Fig. 2.2.

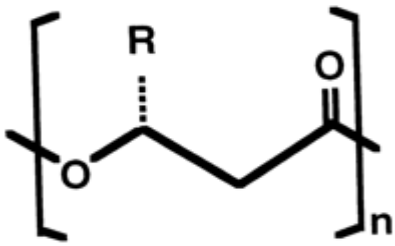

Fig. 2.2 Chemical structure of PHA (Madison & Huisman, 1999)

Carbon, oxygen and hydrogen are the main components in the structure formation of PHA. In these polymers, the carboxyl group of one monomer forms an ester bond with the hydroxyl group of the adjacent monomer (Madison & Huisman, 1999). Each monomer contains the chiral carbon atom and has the (R) stereochemical configuration on the hydroxyl-substituted carbon, thus PHA are optically active and isotactic (Lee et al.,

1999; Ballistreri et al., 2001; Nguyen et al., 2002). To date, many different PHA that have been identified are primarily linear, head-to-tail polyesters composed of 2- to 6-hydroxy fatty acid monomers. They can have various monomer compositions and functional groups in the side chains, depending on the carbon substrate that is fed to the bacteria (Brandl et al., 1988; Lageveen et al., 1988; Huisman et al., 1989; Eggink et al., 1992) as well as the metabolic pathways involved in the utilization of the carbon source (Steinbüchel & Valentin, 1995). Variation in the length and composition of the side chains is the basis for the diversity of the PHA polymer family (Madison & Huisman, 1999). The alkyl side chain is not necessarily saturated (Abe et al., 1990); unsaturated (Tan et al., 1997), halogenated (Kim et al., 1992), aromatic (Fritzsche et al., 1990b), and branched alkyl (Fritzsche et al., 1990a) groups have been reported in PHA as side chain as well. These polymer structures can be manipulated to have wide range of chemical and mechanical properties through the modifications of their monomers and the side chains. For instance, reactive substituents in the polymer side chains can be modified chemically by cross-linking of unsaturated bonds (de Koning et al., 1994).

2.1.2 Medium-chain-length poly(3-hydroxyalkanoates)

PHA are classified into two broad groups based on their monomer chain length, that is, short-chain-length poly(3-hydroxyalkanoates) (scl-PHA) and medium-chain-length poly(3-hydroxyalkanoates) (mcl-PHA). Scl-PHA contain monomers with the carbon atom length ranging from 3 to 5. Typical examples of the scl-PHA are poly(3-hydroxybutyrate) (PHB) and poly(3-hydroxybutyrate-co-valerate) (PHBV). A well known producer of scl-PHA is *Alcaligenus eutrophus*. For mcl-PHA, they are comprised of monomers having 6 to 14 carbon atoms. Medium-chain-length PHA are always heteropolymers, having monomers like 3-hydroxyhexanoate (3HHx), 3-hydroxyoctanoate (3HO), 3-hydroxydecanoate (3HD), 3-hydroxydodecanoate (3HDD),

3-hydroxytetradecanoate (3HTD). Fig. 2.3 shows the structure of the mcl-PHA with various types of monomers.

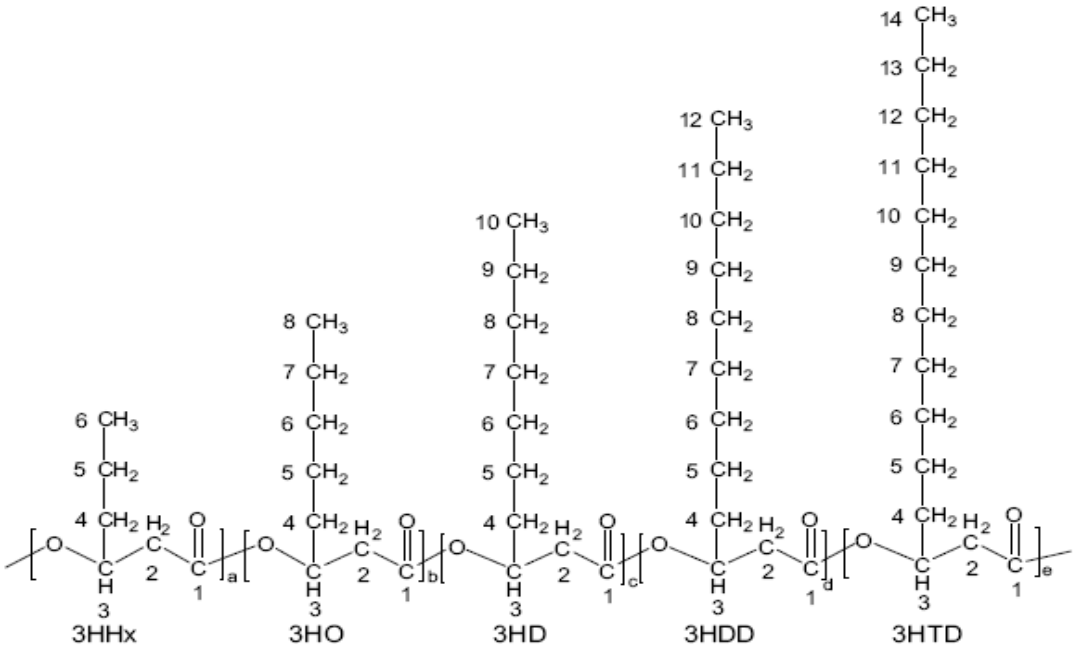

Fig. 2.3 Medium-chain-length PHA with different types of monomers

(Chen et al., 2009)

This class of PHA is primarily synthesized by the fluorescent pseudomonads belonging to rRNA homology group I (Huisman et al., 1989; Timm & Steinbuchel, 1990; Kiska & Gilligan, 1999). For example, *Pseudomonas putida, Pseudomonas oleovorans* and *Pseudomonas aeruginosa* are well-known mcl-PHA producers which have the ability to use variety of carbon substrates such as alkanes, alkanols, medium- and long-chain fatty acids for growing and accumulating PHA (Brandl et al., 1988; Lageveen et al., 1988; Khanna & Srivastava, 2005; Chen et al., 2009).

2.1.3 Physical properties of mcl-PHA

The family of PHA exhibits a wide variety of physical and mechanical properties, ranging from hard crystalline to elastic, depending on the monomer compositions of the polymer. Compared to scl-PHA, mcl-PHA have lower level of crystallinity and lower

glass transition temperature. They are more elastic, less stiff and less brittle (Huisman et al., 1989; Preusting et al., 1990; Timm & Steinbuchel, 1990; Madison & Huisman, 1999). Hence mcl-PHA are easier to process and have potentially wider applications. For instance, mcl-PHA being the amorphous elastomers, have low melting temperature, low tensile strength and high elongation to break and they can be used as biodegradable rubber after cross-linking (Khanna & Srivastava, 2005).

Medium-chain-length poly(3-hydroxyalkanoates) are partially crystalline polymers in which within the bacterial cell they exist as amorphous and water-soluble inclusions (Barnard & Sanders, 1989; Sudesh et al., 2000). Upon disruption of cells where the polymers are extracted, rapid crystallization occurs. These bacterially produced polymers have sufficiently high molecular weight in the range of 50,000 to 300,000 Dalton, making them to possess polymer characteristics that are similar to conventional plastics (Marchessault, 1996).

2.1.4 Thermal degradation and stability of mcl-PHA

Most high molecular weight organic polymers tend to decompose when heated to moderate high temperature. The thermal instability of these polymers can be due to the fact that degradation of a polymer to a low-molecular-weight compound is favored at high temperature by entropy effects. In practice, depolymerization is often favored at high temperature and this is the main reason for the thermal instability of most polymers at high temperature. When processing biopolymers, it is important to know the point of thermal degradation for the polymer.

The thermal stability of mcl-PHA is one of the important factors to determine the processing and application of the biopolymer. Owing to their thermal instability and high susceptibility to a rapid thermal degradation at processing temperature, broad application

of mcl-PHA as a thermoplastic is sterically hindered currently. Therefore the thermal properties and thermal stability of mcl-PHA have to be well studied in order to develop desired modifications for the application of the biopolymer as a thermoplastic. There are many thermoanalytical techniques to study the thermo-kinetics of mcl-PHA thermal degradation and one of them could be dynamic thermogravimetric analysis (TGA), which is a fast and simple method to evaluate the kinetic parameters of thermal degradation.

PHA can be thermally depolymerized at moderate high temperature into chiral oligomers with favorable end groups. These oligomeric hydroxyl acids could serve as precursors for the synthesis of optically active compounds, which are useful as biodegradable carriers for medicines, drugs and hormones (Williams, 1996), biodegradable coatings, additives and plasticizers (van der Walle et al., 2001), or being used as blending materials in a polymerization process (Hiki et al., 2000; Chen & Wu, 2005). However, decomposition of these biopolymers at moderate high temperature is a complex phenomenon as the observed decomposition products could be formed as a result of primary, secondary or a mixture of both decomposition processes (Liggat et al., 1999). For PHA which consists of a long chain of carbon, hydrogen and oxygen atoms, the ester skeletal bonds could be served as the weak points for the hydrolytic chain cleavage during the thermal polyester breakdown process. Consequently, a complex spectrum of (R)-hydroxyacid fragments would be generated and these fragments are not easy to characterize in detail. Moreover abnormal structure such as terminal unsaturated fragments could be formed during subsequent decomposition which could affect the product functionalities, especially for the usage particularly in relation to the hydroxyl and carboxyl end groups. Therefore the degradation products of mcl-PHA generated at certain temperature range need to be studied before drastic decomposition of the biopolymer occurs.

2.1.5 Industrial and medical applications of mcl-PHA

Medium-chain-length polyhydroxyalkanoates (mcl-PHA) have wide range of applications owing to the unique properties of biodegradability, biocompatibility, isotacticity, stereochemistry, light weight, water and air proof. They are natural thermoplastic polyesters, and hence the majority of their applications are as replacements for petrochemical based polymers in the use of packaging applications. The mcl-PHA which possess low melting temperature and high elasticity could be used in the paint formulations and biodegradable coatings (Gagnon et al., 1992; van der Walle et al., 2001).

Polyhydroxyalkanoates can serve as chiral precursors for the chemical synthesis of optically active compounds (Oeding and Schlegel, 1973), which are particularly useful as biodegradable carriers for long-term dosage of drugs, medicines, hormones, insecticides and herbicides. Besides that, PHA promise to be new source of small molecules as they can be depolymerized into chiral monomers and oligomers. The monomers can be converted to commercially attractive molecules such as -hydroxy acids, -alkenoic acids, -hydroxyalkanols, -acyllactones, -amino acids, and -hydroxyacid esters (Williams, 1996). Hydroxyacid esters are currently receiving attention because of the potential applications as biodegradable solvents. These monomeric, dimeric, trimeric and oligomeric hydroxyacids can be prepared through various methods. For example, by degradation of high molecular weight PHA *via* thermal degradation (Morikawa & Marchessault, 1981; Grassie et al., 1984; Kunioka & Doi, 1990; Lehrle & Williams, 1994; Williams, 1996) or acid-catalyzed methanolysis (Reeve et al., 1993) or acid/base hydrolysis (Lauzier et al., 1994).

Thermal degradation of PHA is a promising method to produce low molecular weight hydroxyacids as no chemical and organic solvents are used in the process and hence this method of producing hydroxyacids can be considered as green chemistry.

These hydroxyl acids possess functional end groups *e.g*. hydroxyl and carboxyl group, and such fragments could be used as desirable building blocks or intermediates for synthesis of useful biomaterials. For example, they could be polymerized together with other monomers in the synthesis of biodegradable coatings, additives and plasticizers, as well as the blending materials in a co-polymerization process (Morikawa & Marchessault, 1981; Reeve et al., 1993; Hiki et al., 2000; Nguyen et al., 2002).

2.1.6 Carbon feedstock for PHA production

Carbon substrate is one of the determining factors in optimizing the production, structural and material properties of PHA (Huijberts & Eggink, 1996; Salehizadeh & Van Loosdrecht, 2004). Besides that, using economical substrates such as plant oil and fatty acids to produce PHA can effectively reduce the cost of production of these biopolymers. Palm oil and palm kernel oil are inexpensive and renewable carbon resources which are readily available in Malaysia. These oils are good growth substrates for PHA producing bacteria and the high energy content of vegetable oil results in high biomass yields.

2.1.6.1 Oleic acid as a sole carbon source

Oleic acid is a monounsaturated omega-9 fatty acid (cis-Δ^9-octadecenoic acid, $C_{18:1}$) which is derived from vegetable oil, e.g. palm oil. In local palm oil industry, fatty acid substrates could be produced at lower cost than a single purified fatty acid as the oil palm (*Elaeis guineensis Jacq.*) produce more oil per hectare than any other oil-bearing plant (Tan et al., 1997). In addition, using this long chain fatty acid which contains the unsaturated functional group as carbon source can result in synthesis of PHA with unsaturated monomers. This makes the PHA amenable to modifications as the unsaturated double bonds in the PHA side chain provide sites for chemical modifications (Madison & Huisman, 1999).

2.1.6.2 Palm kernel oil as a sole carbon source

Palm kernel oil is the extract from the nut kernel of the palm oil fruit. It is a highly saturated vegetable oil with almost 82% of major fatty acids are saturated, thus it exist as semi-solid at room temperature. The oil consists of a mixture of C_6 to $C_{18:2}$ fatty acids with lauric acid (C_{12}) as the main composition. Table 2.1 shows the fatty acid compositions in palm kernel oil (Elson, 1992). Furthermore, palm kernel oil which is the side product from palm oil industry is an economical carbon source for PHA production. As it is non-edible oil, production of PHA using palm kernel oil will also reduce the competition of oil in food industry.

Table 2.1 Fatty acid compositions in palm kernel oil (Adapted from Elson, 1992).

Fatty acids	Percentage (%)
$C_{6:0}$ (Caproic acid)	0.2
$C_{8:0}$ (Caprylic acid)	3.0
$C_{10:0}$ (Capric acid)	4.0
$C_{12:0}$ (Lauric acid)	48.0
$C_{14:0}$ (Myristic acid)	16.0
$C_{16:0}$ (Palmitic acid)	8.0
$C_{18:0}$ (Stearic acid)	3.0
$C_{18:1}$ (Oleic acid)	15.4
$C_{18:2}$ (Linoleic acid)	2.4
$C_{20:0}$ (Arachinoic acid)	0.1

2.2 Poly(vinyl chloride)

Poly(vinyl chloride) (PVC) is an amorphous thermoplastic. Due to the presence of chlorine atoms, it has a significant polarity within the polymer molecule structure.

PVC usually comes in the form of white powder with countless micro voids present within the particles, each with the average particle size of 100 to 150 μm and apparent density of 0.4 to 0.7 g cm^{-1} (PVC Fact Book, 2008).

Generally, additives such as plasticizers, thermal stabilizers, lubricants, pigments and fillers are added to the PVC resin during processing to improve the overall performance of the product. Plasticizers in particular are added to change the moldability of PVC and provide desired flexibility to the end products. By adding in different levels of plasticizers, the PVC products could be formulated with physical properties ranging from rigid to flexible. PVC without any plasticizers are called rigid PVC, while PVC that include plasticizers are called flexible PVC (PVC Fact Book, 2008).

2.2.1 Chemical structure

PVC has a unique chemical structure with the chlorine atoms bound to the carbon atoms. Fig. 2.4 illustrates the general structure of a PVC monomer unit. The letter 'n' showing the repeating unit of vinyl chloride monomer and α-hydrogen is the hydrogen that attached to the electropositive carbon atom.

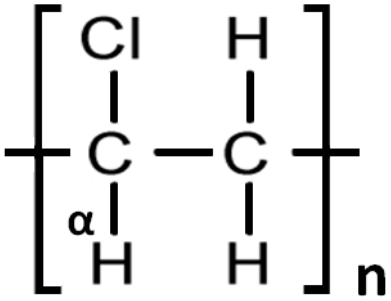

Fig. 2.4 General structure of PVC monomer

Generally, PVC can exhibit three basic structures. Firstly, isotactic in which all the chlorine (Cl) atoms are on the same side of a polymer chain. Secondly, atactic in

which Cl atoms are randomly distributed within the chain. The last one is syndiotactic where the Cl atoms are regularly distributed on both sides of the chain in an alternate arrangement.

Chlorine is one of the most active halogen in the world. Owing to the electronegative property of chlorine atom, formation of hydrogen bonds within and between PVC polymer chains is theoretically possible. This is shown in Fig. 2.5:

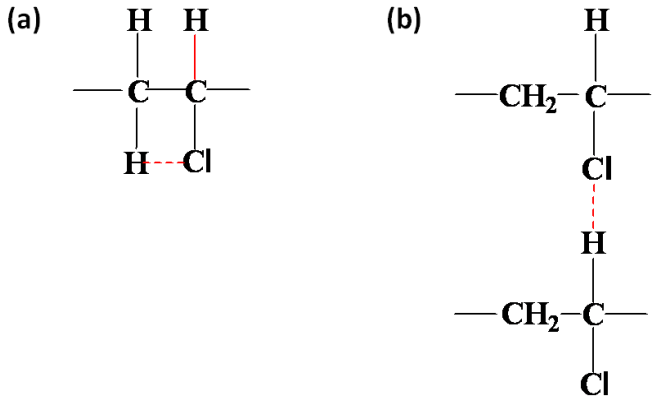

Fig. 2.5 (a) Formation of intramolecular hydrogen bonding within polymer and (b) Formation of intermolecular hydrogen bonding between polymers (Wypych, 2008)

The C-Cl bond has a pronounced electron-withdrawing effect upon other bonds joined with the same carbon atom. Thus the hydrogen atom bonded to the carbon atom may become sufficiently acidic to act as an electron-acceptor atom in a hydrogen bond. Nevertheless when the proton-donor and proton acceptor atoms are collinear, as illustrated in structure (a), the most stable forms of hydrogen bond would occur. Structure (b) suggests the formation of an intermolecular hydrogen bond between two PVC chains (Wypych, 2008).

2.2.2 PVC Morphology

PVC, being a polymer with low degree of crystallinity, cannot be studied effectively by the conventional methods applied to crystalline materials. It is difficult to interpret the morphology of PVC due to the fact that the morphology is a not a parameter, but a desciptive feature which is influenced by variables like chain length or molecular weight of polymer, configuration and conformation, chain folds and chain thickness, entanglements, crystalline structure and grain morphology (Wypych, 2008).

The morphology of PVC is generally determined by the size of the molecule, structure or chain segments, chain spatial distribution and interaction, as well as structure of particles. The particle size distribution of suspension PVC is difficult to determine due to the very complex morphology. For PVC grains obtained from suspension polymerization, it exhibits a hierarchical morphology (Diego et. al., 2004) which is illustrated in the schematic diagram in Fig. 2.6.

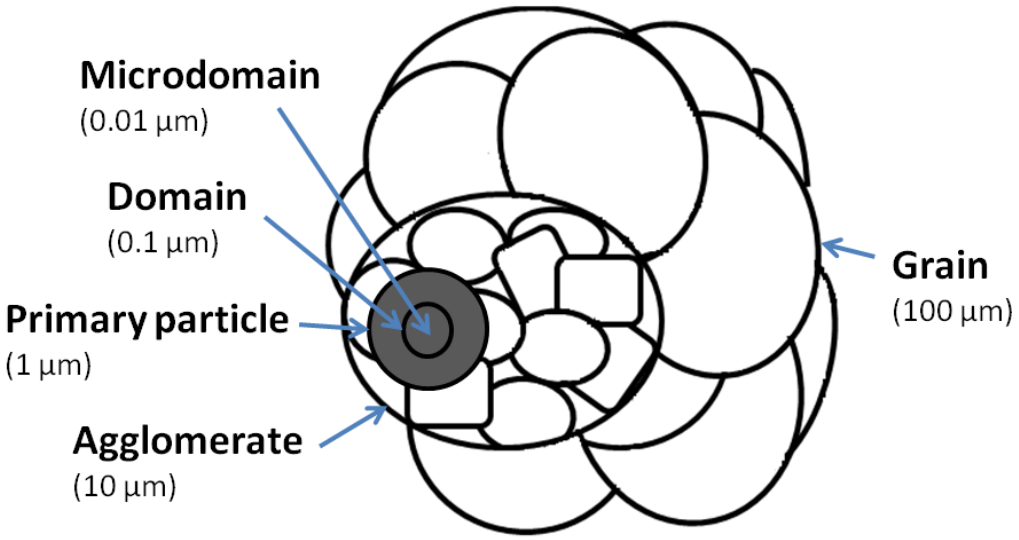

Fig. 2.6 Model of PVC grain (Adapted from Saeki, 2000)

As depicted in the figure, the PVC grains are composed of agglomerates trapped inside a skin made of hydrosoluble polymers. The agglomerates are made up of primary particles. Inside the primary particles, domains are visible (Diego et al., 2004). The details of the morphology of PVC are discussed in Table 2.2.

Table 2.2 Nomenclature for the morphology of suspension PVC grain (Adapted from (Allsopp, 1981; Geil, 1977; Saeki, 2000)

Structural element	Size range, µm	Description
Skin	-	Formed on the surface of the PVC grain. Inside of the skin layer are the subparticles and interconnected pores
Grain	50-250	Visible constituent of free flowing powder
Agglomerate	1-10	Formed by coalescence of primary particles
Primary particle	0.5-1	Grown droplet of monomer
Domain	0.1-0.2	Formed inside of primary particle
Microdomain	0.01-0.02	Smallest visible particle made out of approximately 50 chains

2.2.3 Molecular weight

A measure of the molecular weight of PVC is classified by K-value and it is based upon a viscosity measurement of a PVC solution. According to (Lorenz, 1971), the term "K-value" refers to the empirical molecular weight value of the polymer. For PVC, the K-value can range from 55 to 80.

Low K-value implies low molecular weight and high K-value implies high molecular weight (Dynisco Corporate, 2011). Medium molecular weight PVC ranging from K-value of 60 to 67 is more widely used compared to low molecular weight and high molecular weight PVC. Low molecular weight PVC grades are easy to process but

have inferior properties. They are usually used for rigid products. High molecular weight PVC grades are difficult to process but they have outstanding properties. Normally they are used to obtain special properties like matt surface finish or better toughness (Plastermart, October 2010). Table 2.3 illustrates the relationship between viscosity index, K-value and general applications for different types of PVC.

Table 2.3 Relationship between the viscosity index, K-value and general uses for different types of PVC

(Adapted from "PVC SPEC", quality standard: GB/T 5761-93)

	Type of PVC							
Viscosity index	136-144	143-136	135-127	126-119	118-107	106-96	95-87	86-73
K-value	77-75	77-73	72-71	70-69	68-66	65-63	62-60	59-55
Applications	High grade insulator	Insulator, film, soft plastic	Insulator, agricultural film and tube, normal tube, leatheroid, plastic shoes, normal soft plastic	Industrial and agricultural film, tube, leatheroid, high strength pipe	Film, pipe, building material	Disc, transparent hard film, PVC board, welding rod	Bottle, transparent hard film, PVC pipe connector	Bottle, transparent hard film, PVC pipe connector

2.2.4 Thermal degradation of PVC

Thermal degradation of poly(vinyl chloride) is a complex phenomenon. Two different types of degradation products are usually generated as a result of two stage degradation processes (Radhakrishnan Nair et al., 2007). They are volatile small molecules which are readily separated as well as the larger molecules that represent the remaining fragments of the chain. These fragments are particularly formed upon the internal rearrangements of the polymer backbone, i.e. the intramolecular cyclisation of the conjugated sequences (Wypych, 1985).

A two-stage degradation pattern as shown in Fig. 2.7 is commonly seen in the PVC decomposition, where the first stage of degradation is due to the dehydrochlorination process, whereby elimination of HCl occurred leaving behind the unsaturated hydrocarbons. Second degradation is attributed to the cracking of –C=C– hydrocarbon backbone, yielding volatile saturated and unsaturated, aliphatic and aromatic hydrocarbons, where benzene and toluene will be the major products in high yield (Wypych, 1985; Marcilla & Beltran, 1996a).

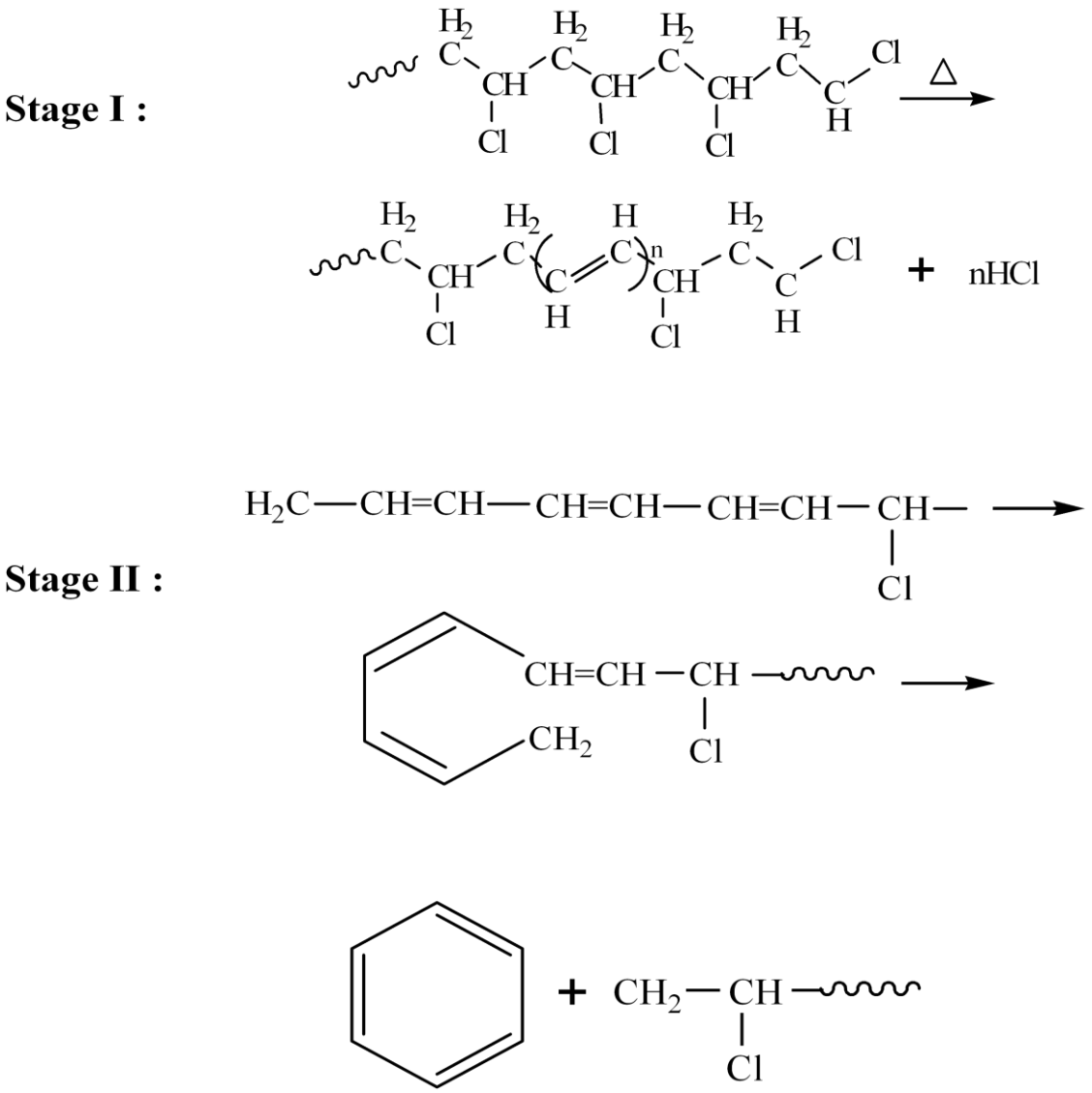

Fig. 2.7 Two-stage degradation occurred during thermal decomposition of PVC. Stage 1: Hydrogen chloride elimination of PVC and Stage 2: Decomposition of unsaturated hydrocarbon structures followed by intramolecular cyclization of conjugated sequences and benzene formation (Adapted from Wypych, 1985)

2.2.5 Chemical and physical properties of PVC

PVC has the molecular structure with polar chlorine atoms bound to the carbon atoms. Since the polymer is comprised of single bonds of carbon atoms with little change in molecular structure, PVC is chemically stable and has excellent chemical resistance. It is resistant to acid, alkali and almost all inorganic chemicals. Besides that, PVC is a polar

polymer and so its mechanical properties are excellent owing to the strong interaction among the molecular chains (PVC Fact Book, 2008).

PVC has inherently superior fire retarding properties due to its chlorine content. When PVC products are burned, hydrogen chloride gas resulting from thermal cracking stops the continuous combustion reaction and prevents further burning by warding off the PVC product surface from oxygen (PVC Fact Book, 2008).

Having the values of solubility parameter lie in the range of 9.48 to 9.7 (Mark, 1971), a wide range of organic solvents could be used to dissolve PVC. As such, tetrahydrofuran, cyclohexane, ethyl methyl ketone were found to be best solvents for PVC (Koleske, 1969), while halogenated hydrocarbons, ketones and aromatic compounds could also be used as solvents for PVC.

In overall, PVC shows excellent chemical and physical properties such as chemical stability, fire retarding properties, toughness, durability and resistance to oxidative reaction.

2.2.6 General applications

PVC constitutes one of the largest globally consumed commodity plastics, approximately 16 million tonnes per annum (PVC Information Council, March 1995). About 70% of world consumption of PVC is for the usage like pipes, fittings, siding, windows, fencing etc. It could be seen that the current global demand for PVC majority originates from building construction, civil engineering applications and automotive production, as to replace for the traditional construction materials like wood and metals (Ebner, November 2008). Since the electrical insulating properties of PVC are excellent, PVC is also widely used as telecommunications and electrical cables, vehicles and

household electrical appliances, cable coverings and protecting tubes for power, insulating tapes and switch boxes (PVC Fact Book, 2008).

According to the technical articles and reports on plastic industry reported by Plastermart in year 2010, PVC demand is high for the usage of piping and fittings in telecommunications and natural gas in industrialized countries. Meanwhile, the demand of PVC pipe is high in developing world, especially for infrastructure for drinking water, sewage and drainage. Fig. 2.8 shows the projected growth for regional PVC consumption from year 1990 to 2025.

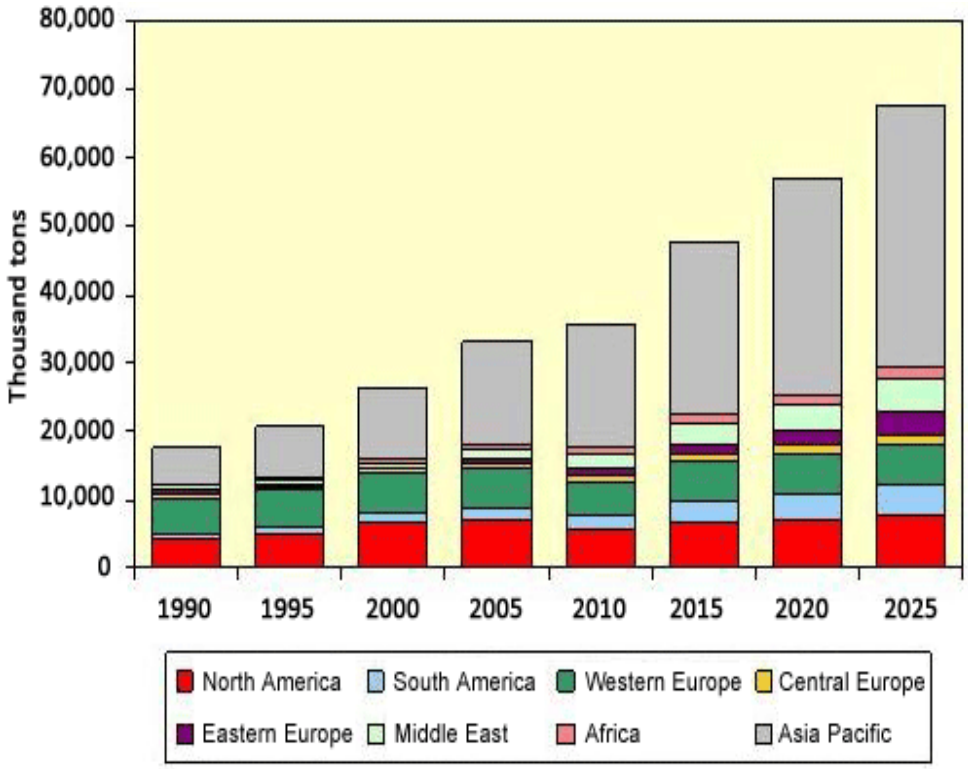

Fig. 2.8 Regional growth of PVC consumption from year 1990 and projected up to year 2025

PVC possesses rigidity property in nature and has the applications as profiles, house siding, hollow parts, etc in the rigid form. A lot of researches have been done on improving the properties of PVC for various applications as the high T_g of rigid PVC will

still restrict the wide application as a result of heat deformation temperatures. Some additives were added to the PVC, resulting in new compositions that are commonly known as PVC compounds. Plasticized PVC compounds are the most well-known PVC compounds which present high flexibility and are commonly used in films and packaging, toys and household products, medical products such as intravenous drip lines and transfusion bags, food wear and clothing, flooring and wall-covering, etc.

2.2.7 Miscibility of PVC

PVC is well known for its efficiency to form miscible systems with various structurally different polymers (Varughese et al., 1988). This is due to the presence of α-hydrogen in PVC which is capable of forming hydrogen bonding (Lieberman, 1962). Many of the polymers exhibiting miscibility with PVC have as a common entity, the carbonyl unit. The interaction allowed a large variation in the composition of the polymer with retention of miscibility with PVC.

Hydrogen bonding-type interactions have been proposed as the key to achieving miscibility in many of the blends cited in this treatise. PVC which is a hydrogen bond donor exhibits miscibility with many polymers containing H^+ acceptor units. The chlorine atoms of the PVC appear to render the polymer capable of interaction with polyesters, possibly by enabling hydrogen bonding to occur with the carbonyl groups of the polyester.

2.3 Polymer miscibility

Polymer miscibility delineates the polymer-polymer blends with behavior expected to be similar to a single-phase system. It not necessary connotes the ideal molecular mixing**,** but at least the level of molecular mixing is adequate to yield macroscopic properties, for example, showing a single-phase behavior (Olabisi et al.,

1979). Usually a polymer blend with a single glass transition will be classified as miscible. For the investigator interested in macroscopic properties useful in industrial application, the miscibility connotes the homogeneity of the polymer mixture in which the dimension is similar to the segmental size responsible for the major glass transition. Mechanical compatibility with a property compromise between the components is also assured for a miscible polymer mixture. Under microscopic inspection, a miscible polymer blend consists of a single phase; on a molecular level, two different polymer molecules may intermingle with each other (Olabisi et al., 1979).

Usually polar polymers are compatible only with some polar plasticizers. Interaction of polar polymers and plasticizers depends on the presence and arrangement of groups capable of donor-acceptor interactions. Polar plasticizers with a proton-acceptor character (esters, ethers, and nitriles) are most useful for polymers having average polarity (e.g., PVC, PC and butadiene-acrylonitrile copolymers).

Similar polarity, hydrogen-bonding and other strong intermolecular attraction are the optimum requirements for two polymers to be completely miscible. Types of molecular forces of attraction normally found in miscible polymer system are random dipole-induced dipole, dipole-induced dipole and hydrogen bonding. It should be noted that intermolecular forces contributed by hydrogen bonding are stronger than the dipole-dipole forces.

For random dipole-induced dipole, this type of interaction is possible between any two molecules regardless of the structure, because the only requirement is the ground-state oscillation of charge in the molecule (Scott, 1949; Hinshelwood, 1951; Olabisi et al., 1979). The result of such oscillation is a temporary dipole moment, which immediately induces dipoles in all other neighboring molecules. These dipoles can then interact. Polarizability, the susceptibility of a molecule to charge separation, is the key

parameter in this type of interaction. Halogen substitution and unsaturation tend to increase polarizability. If one component of the polymer system has a permanent dipole moment, it will induce a dipole in neighboring symmetrical molecules, leading to an interaction which is called dipole-induced dipole.

The prerequisites for a hydrogen bond of significant strength are as following: firstly, a hydrogen atom must be covalently bound to an electron-withdrawing atom; secondly, a structure with donatable electrons as the acceptor must locate at about 180 ° with respect to the first bond. This geometric consideration is quite important as the energy falling off rapidly with angle. In fact, hydrogen bonding is perhaps responsible for more miscible system than any other types of interactions. For example, the large number of miscible system in which PVC is a component can probably be ascribed to the donating character of the Cl-C-H groups in an interacting situation with polyester as shown in Fig. 2.9.

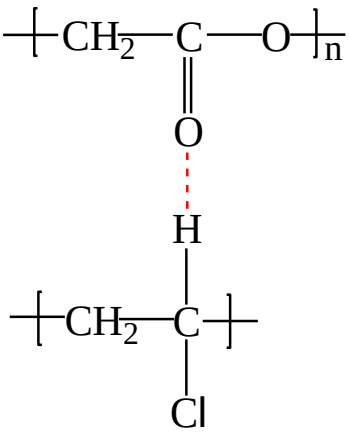

Fig. 2.9 Hydrogen bonding between the hydrogen acceptor of carbonyl group and hydrogen donator of C-Cl-H group

The hydrogen bond involves the establishment of electron-containing molecular orbitals but the proton is not transfer. If the proton is transferred, an organic salt is formed and the interaction is classified as acid-base.

Burrell (1955) and Lieberman (1962) have qualitatively classified the hydrogen bonding capability of polar units. Hydrogen bonding interactions between polymer chains provide necessary driving force for miscibility. This classification is illustrated in Table 2.4. Many miscible polymer blends can be hypothetically rationalized to exhibit miscibility based on the specific interactions chosen from this list.

Table 2.4 Classification of hydrogen bonding for various functional groups[1]

H-bond strength[2]	**Electron donors (H^+ acceptors)**	**Electron acceptors (H^+ donors)**	**Electron/H^+ donors-acceptors**
Strong	Pyridine	-	Water, alcohols, carboxylic acids
Moderate	Ketones, ethers, esters	-	-
Weak	Nitriles, nitros, olefins, aromatic hydrocarbons	Halogenated hydrocarbons	-
Unclassified	Aldehydes, tertiary amines, sulfones, sulfoxides	-	Primary and secondary amines

[1]Adapted from Burrell, 1955; Lieberman, 1962 and Olabisi et al., 1979; [2]Mixtures of strong acceptors and donors may result in proton transfer, giving an acid-base (electrostatic) interaction, rather than a resonance interaction.

2.3.1 Analytical techniques for determining polymer-polymer miscibility

2.3.1.1 Glass transition temperature

Glass transition temperature (T_g) is the most important property for a polymer where the position of the T_g determines the physical state of the polymer, affecting the properties like mechanical stiffness and toughness (Tobolsky, 1960). The T_g represents the temperature at which the polymeric chains have a combination of energies from the vibrational, translational and rotational forces, and these energies equal to the forces of attractions in the polymer (Olabisi et al., 1979).

Below T_g, the polymer chains are locked into a network with motion of the small units restricted to vibrational, rotational and translational movement. As temperature approaches T_g, the configurational structures become more and more compact. At T_g, the polymer segments are so densely packed that the internal mobility is negligible (Marcilla & Beltran, 2004). Above T_g, the molecules have enough energy to move or rotate and the translational movement of the entire polymer chain is possible. Besides that, dramatic changes in modulus also occur at T_g.

The level of miscibility is qualitatively assessed by the features of the T_g behavior. Existence of a single and distinctive, single and broad, shifted, or separate individual transition for a polymer blend actually reveals the macroscopic property characteristics of the blend. Broadening of transition will occur in the case of borderline miscibility. With cases of limited miscibility, two separate transitions between those of the components may result. In cases where strong specific interactions occur, the T_g may go through a maximum as a function of the composition (Olabisi et al., 1979). Experimental evidence of miscibility is often found when a single T_g is observed (Thomas & George, 1992) in between the T_gs of the individual components.

Nevertheless, T_g versus composition of a miscible polymer blend may not be a predictable relationship, indeed it has many variations over the entire composition range,

i.e., the linear relationship, minimum and maximum deviations from linearity (Olabisi et al., 1979). These three generalized curves pattern are depicted in Fig. 2.10. It should be noted that if the T_g of the polymer blends is higher than the expected, the T_g of the system could be probably elevated as a result of intermolecular interaction between the electron donating and accepting functional groups on separate component of the blend (Slark, 1997).

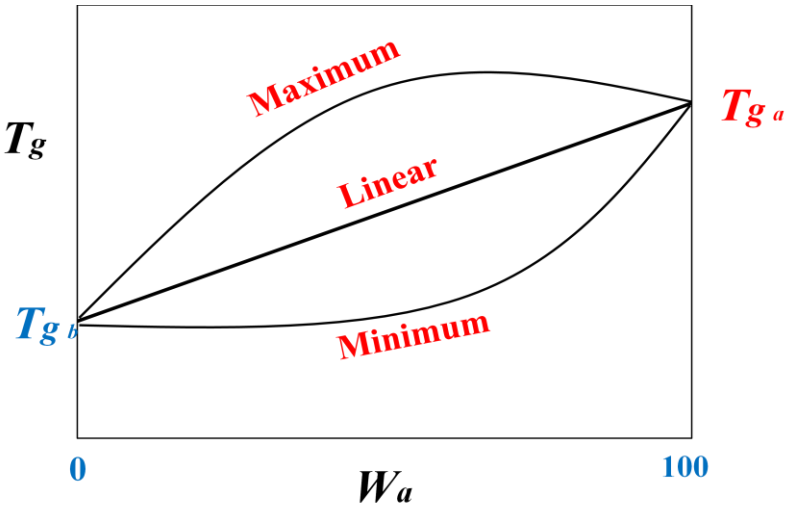

Fig. 2.10 Generalized behavior of T_g relationships for miscible polymer blends

Deviations from linearity in T_g-composition are quite common in miscible polymer blends. In these cases, data may fit relationships, the Fox equation (Fox, 1956) as shown in Equation (2.1) and the Gordon-Taylor equation (Gordon & Taylor, 1952) as shown in Equation (2.2) are commonly adopted to describe the T_g relationship for polymer-diluent blends, particularly plasticized PVC.

$$1/T_g = (W\text{a}/\, T_g\text{a}\,) + (W\text{b}\,/\, T_g\text{b}\,) \quad (2.1)$$

$$T_g = (W\text{a}\; T_g\,\text{a} + k\;(1\text{-}W\text{a})\; T_g\,\text{b}) \,/\, [W\text{a} + k\;(1\text{-}W\text{a})] \quad (2.2)$$

where T_ga and T_gb represent the glass transitions of the individual polymer components; Wa and Wb are the weight fractions of the blend; and k is the ratio of the thermal expansion coefficients between the rubber and glass states of the component polymers.

Successful applications of the Fox expression to miscible blends include poly(vinyl chloride)-butadiene/acrylonitrile copolymers (Zakrzewski, 1973) and poly(vinyl chloride)-poly(ethylene/vinyl acetate/sulfur dioxide) (Hickman & Ikeda, 1973). Examples of miscible polymer blends in which the T_g-composition data are satisfied by the Gordon-Taylor equation include freeze-dried poly(methyl methacrylate)-poly(vinyl acetate) and styrene/butadiene copolymer with polybutadiene (Zlatkevich, 1973).

2.3.1.1.1 Calorimetric methods

Differential scanning calorimetry (DSC) is the most common technique used in calorimetric method for determination of T_g. DSC measures the change in heat capacity as a function of temperature. Under normal condition, the heat capacity will change gradually with temperature. However it exhibits a drastic change when passing through the glass transition (Olabisi et al., 1979), as the sample may undergo a change in physical state. At this point, the polymer blend experiences enthalpies of relaxation which appear as a positive deviation from the baseline (Sin, 1998).

Generally the T_g is defined as the onset or midpoint of the steep change in energy, depending on certain circumstances. Fig. 2.11 shows the T_g of a sample which could be exhibited as either the onset or midpoint of the steep change in energy. Usually

immiscible blends will exhibit distinctly two different T_g's as opposed to a miscible blend which has a single T_g.

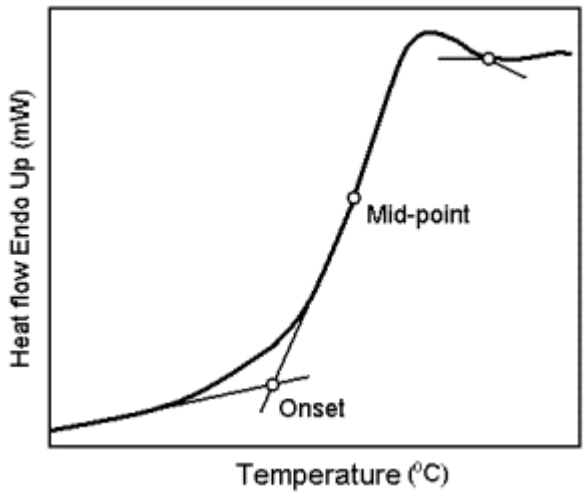

Fig. 2.11 T_g , as exhibited as the onset or midpoint of the steep change in energy in the DSC endothermic curve (Adapted from Mazurin, 2007)

2.3.1.1.2 Mechanical methods

Dynamic mechanical analysis (DMA) is another method commonly employed to provide a direct quantitative measurement of modulus, phase transition, as a function of temperatures occurring on the molecular scale (Olabisi et al., 1979; Sin, 1998). Data obtained over a broad temperature range can be used to study the molecular response of a polymer with other polymer.

The difference between homogeneous and heterogeneous blends is easily detected in the mechanical loss and modulus-temperature data. The generalized data are usually shear modulus (G'), loss modulus (G") and mechanical loss (tan δ, defined as G"/G'). For example, the shear modulus and mechanical loss for polymer-polymer blends versus temperature are illustrated in Fig. 2.12, for behavior expected of two-phase blend. This figure illustrates the highly phase-separated polymer blend, where the

transitional behavior of the individual constituents will be unchanged. On the other hand, a miscible polymer with a single and unique transition is shown in Fig. 2.13.

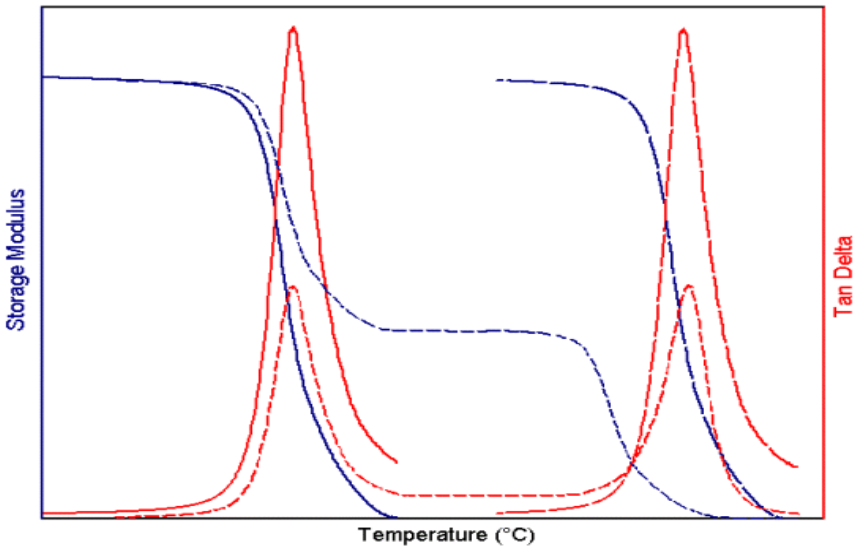

Fig. 2.12 Generalized behavior of the dynamic mechanical properties of a two-phase blend. Solid line: pure component A; Hyphenated line: mixture; Dashed line: pure component B (Adapted from Perkin Elmer)

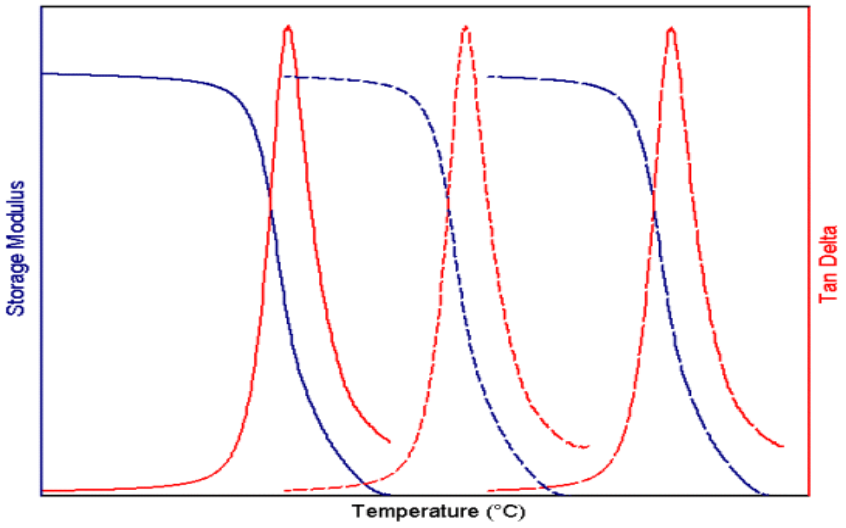

Fig. 2.13 Generalized behavior of the dynamic mechanical properties of a miscible blend. Solid line: pure component A; Hyphenated line: mixture; Dashed line: pure component B (Adapted from Perkin Elmer)

2.3.1.2 Microscopy

Direct visual validation of the presence of inhomogeneous phase has been used as a preliminary indication of the degree of miscibility in a polymer-polymer system. Many researchers have turned to microscopy to aid in determining not only the presence but the connectivities of the phases (Olabisi et al., 1979). For instance, Fig. 2.14 and Fig. 2.15 show the scanning electron micrographs of the PVC and PVC-plasticizer. It could be seen from the images in Fig. 2.14 for the presence of voids in PVC and Fig. 2.15 for the swollen voids in which the PVC had interacted with the miscible plasticizer.

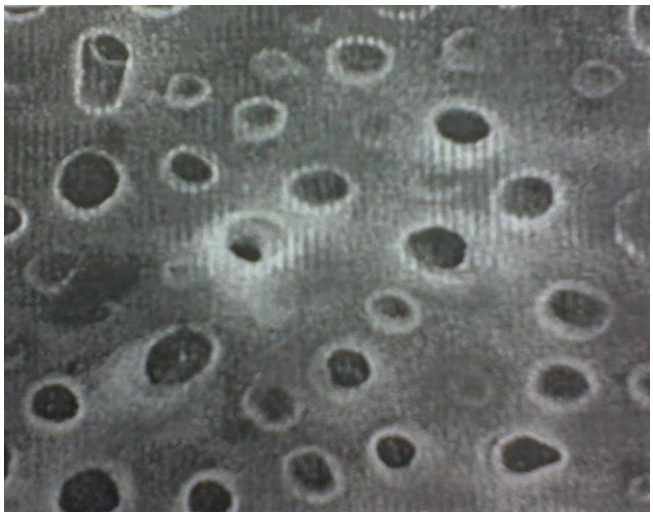

Fig. 2.14 SEM photograph of a PVC film (Adapted from Stephan et al., 2000)

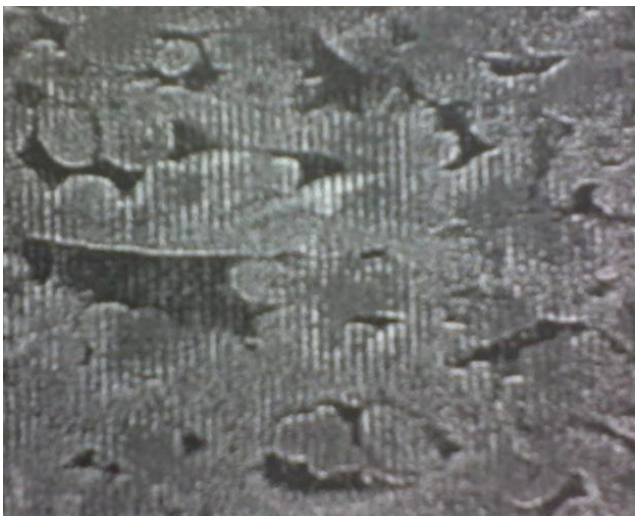

Fig. 2.15 SEM photograph of a plasticized PVC film (Adapted from Stephan et al., 2000)

However, this technique is not suitable to be used to identify certain components of the polymer blends (Fang, 2000).

2.3.1.3 Spectroscopic techniques

Spectroscopy can also be used to investigate the interaction of the polymer molecule with its environment (Dyer, 1965). Polymer systems of high miscibility will generate spectra showing strong deviations from an average of the spectra of the two components in the blend. The degree of deviation as a function of miscibility cannot be satisfactorily predicted but it can only verify the findings from other analysis for demonstrating miscibility. Nevertheless this technique does provide valuable insight into the nature of the specific interactions between the macromolecules (Olabisi et al., 1979).

2.4 Plasticizer for PVC

PVC is unique in its acceptance of plasticizers. The polarity and balance of amorphous and crystalline regions in its molecular geometry provide compatibility for a variety of plasticizer structures over relatively wide concentration and temperature ranges (Graham, 1973). The most commonly used plasticizers for PVC are phthalates (Tai, 1999), phosphate (Ferm & Shen, 1997), adipate (Audic et al., 2001) and polyester (Eapen, 1994) based which give the PVC various desired flexibility.

Plasticizers were added to the PVC resin to allow movement between the PVC molecules. They are interfused with polymers to increase flexibility, extensibility and workability, making the polymer changed from a hard, glasslike solid to a flexible, tough elastomer. They have a strong affinity for PVC polymers, but they do not undergo a chemical reaction with PVC that causes bonding or crafting to the polymer (Krauskopf & Godwin, 2005).

2.4.1 Types of plasticizers

Plasticizers could be classified as either monomeric or polymeric plasticizers. It is preferred to categorize plasticizers on the basis of their chemical structure and associated performance when employed in PVC. Three subgroups which are related to the performance characteristics in PVC are classified as General Purpose Plasticizers (GP), Performance Plasticizers (PP) and Specialty Plasticizers (SP).

2.4.1.1 General Purpose Plasticizers

These types of plasticizers provide desired flexibility to PVC at the lowest cost, with an overall balance of optimum properties. They are dialkyl phthalates ranging from diisoheptyl (DIHP) to diisodecyl (DIDP) (Krauskopf & Godwin, 2005).

2.4.1.2 Performance Plasticizers

These types of plasticizers contribute secondary performance properties desired in flexible PVC beyond the GP type, but they impose higher costs than GP type. These include specific phthalates and other types of plasticizers. For example, high molecular weight plasticizers e.g. trimellitates and polymeric polyesters which were used in low volatility performance (Krauskopf & Godwin, 2005).

2.4.1.3 Specialty Plasticizers

These types of plasticizers provide specialty characteristics and properties beyond those designed for general purpose. Only a few phthalates meet these special requirements. Examples of specialty plasticizers are polyester plasticizers which provide low volatility and low diffusivity under fire conditions; epoxy plasticizers provide adjuvant thermal stability to PVC; phosphates and halogenated plasticizers provide fire

retardant properties. These types of plasticizers impose even higher costs than PP grade plasticizers (Krauskopf & Godwin, 2005).

2.4.2 Phthalate-based plasticizer

Phthalic acid esters, generally known as phthalate plasticizers are the predominant type of PVC plasticizer produced in the world and accounted for almost 86% of world consumption of plasticizers in year 2008 (Bizzari, 2009). Phthalate plasticizers are colourless, odourless liquids which are produced by a simple chemical reaction between alcohol and phthalic anhydride. The most commonly used phthalates are di-2-ethyl hexyl phthalate (DEHP, also called dioctyl phthalate (DOP)), diisodecyl phthalate (DIDP), diisononyl phthalate (DINP), benzyl butyl phthalate (BBP) and dibutyl phthalate (DBP) (Plastermart, April 2008).

However, several issues regarding the use of phthalates were raised recently, concerning about the effects of phthalates on the environment, human hormones and reproductive system as well as their exposures to children *via* breast milk, toys and baby care products. Based on a study in Norway, the bronchial obstruction in children was directly related to the amount of plasticizer-releasing materials present in the indoor environment (Plastermart, April 2008). According to Bornehag et al. (2005), plasticizers that present in the dust are the main elements causing allergy, asthma and inducing puberty among the children since they spent most of the time in indoor. There was a study conducted in the same year showing that phthalates actually mimicked female hormones and could serve as the endocrine disruptors in human body, resulting in feminization of boys (Third National Report on Human Exposure to Environmental Chemicals, July 2005).

Research showed that phthalates were shown to be responsible of cancer proliferation in mice and rats (National Toxicology Program, 1982). These phthalate-based plasticizers are found to be harmful to human beings when direct contact with skin and tissues. They have the risk of leaching out from PVC compounds during end-used applications, to the environment or human body. As a result of these concerns, the European Commission in year 1999 temporarily banned the usage of six phthalates (DEHP, DINP, DNOP, DIDP, DBP and BBP) in toys which were used in oral applications designed for children under the age of three years and the permanent ban was adapted in year 2005. Current regulation is more restrictive regarding their use in application related to food contact, medical devices and toys (Shea, 2003). In July 2005, the European Union permanently banned the use of DEHP, DBP and BBP in all children's items and additionally banned the use of DINP, DIDP, and DNOP in children's items which can be put in the mouth. This ban became effective on January 16, 2007. Taiwan took a similar approach and banned the use of six phthalate plasticizers (DEHP, DINP, DNOP, DIDP, DBP and BBP) after the ban in Europe. Furthermore, large cosmetic companies in the USA such as L'Oreal and Revlon, have taken the action of banning the use of DBP in their cosmetic products (Plastermart, April 2008).

2.4.3 Polymeric plasticizer

Polymeric plasticizers are regularly polyester-type, with molecular weights ranging from 1,000 to 8,000 M_n. The greater is the plasticizer molecular weight, the greater is its permanence property. Examples of polymeric plasticizers are polyethylene copolymers and terpolymers which can range up to >500,000 M_n (Krauskopf & Godwin, 2005). Nevertheless aliphatic polyesters with molecular weight less than 4000 M_n have also been used to improve the permanence of plasticized PVC for applications requiring intermediate performance (Olabisi et al., 1979).

Polymeric plasticizers comprised of branched structures are more resistant to migration loss than those linear structures. The polarity also influences the extraction resistance of the polymeric plasticizers. For example, lower polarity plasticizers exhibit better extraction resistance towards polar extraction fluids such as soapy water (Krauskopf & Godwin, 2005).

Recent concern in the potential toxicity as a result of leaching of phthalate based plasticizers into food and medical products has catalyzed interest in permanent high molecular weight polymeric plasticizers for PVC.

2.4.4 Functions of plasticizers

The main functions performed by plasticizers are to make products more flexible, affect packing density and free volume (Borek & Osoba, 1996), affect chain mobility (Elicegui et al., 1997), lower glass transition and processing temperature (Vilics et al., 1997; Biju, 2007), affect thermal degradation of PVC (Minsker, 1996; Marcilla & Beltran, 1996b) and make products of varying rigidity.

Plasticizers work by embedding themselves between the polymer chains, spacing them further apart to increase the free volume in the system, thus significantly lowering the glass transition temperature for the polymer and making it softer. In order to have a good compatibility, plasticizers should have a minimal degree of branching. This is because branching in the plasticizer structure always worsens compatibility with polymers due to the steric restrictions effect (Senichev, 2004).

Part of PVC can be more easily solvated by plasticizer due to its characteristics of lower molecular weight (Nakajima & Ward, 1983) and lower crystalline content (Wypych, 1985), while other parts of the resin reveal higher resistance to the plasticizer

action. Nevertheless, only a certain fraction of the plasticizer is involved in the interaction and remaining plasticizer behaves just like the pure component.

2.4.5 Performance of plasticizers

The key performance properties of a PVC compounds are influenced by the chemical type of plasticizer as well as the plasticizer level (part per hundred of PVC). Various types of plasticizers give various plasticization effects due to the differences in the strengths of plasticizer-plasticizer and plasticizer-polymer interactions. At low plasticizer levels, the plasticizer-PVC interactions are the dominant interactions, while at high plasticizer concentrations, plasticizer-plasticizer interactions become more significant (Krauskopf & Godwin, 2005). In formulations at higher level of plasticizers, some leaching out of excess plasticizers to the polymer surface would be occurred. This is because plasticizing effect will ultimately reach constant once the critical point of plasticizer concentration is passed, where further addition of the plasticizer may lead to an inhomogeneous mixture of the PVC compound.

In the selection of a suitable plasticizer for a given application, the first consideration would be compatibility. Other criteria relating to processing, performance and permanence properties would be obtained, depending on the specific application. For each application, the desirable balance of properties should be achieved within a prescribed cost framework. It should be noted that no single plasticizer exhibits the perfect balance of properties for every application. Each end use will demand certain essential properties and thus some properties of lower importance need to be sacrificed to some extent (Graham, 1973).

2.5 Plasticization Steps

Sears and Darby (1982) identified six steps of plasticization of PVC. During the first step, plasticizer molecules penetrate the porous structure of PVC in an irreversible way. Adsorption of plasticizer takes place. Subsequently, there is an induction period where the plasticizer slowly solvates the resin surface. During the third step, the absorption of plasticizer takes place. During this step the PVC particles swell while the total volume of the material decreases. A diffusion process takes place with low activation energy. In the fourth step, drastic changes take place that transcur with high activation energy. The plasticizer forms clusters among the polymer segments and penetrates into the molecular segments of polymer, solvating hydrogen bonding and polar groups available. During this step the PVC particles lose their identity, and the mixture can be seen as a melted homogeneous material. If heating progresses the material behaves like a fluid melt. The clusters of polymer or plasticizer molecules disappear and a homogeneous material is formed. The last step takes place during cooling. The polymer hardens due to crystallization and creation of weak van der Waals forces and hydrogen bonding between the plasticizer molecules and the polymer segments.

2.5.1 Mechanism of plasticizers action

For a plasticizer to be effective, it must be thoroughly mixed and incorporated into the PVC polymer matrix. This is typically obtained by heating and mixing until either the resin dissolves in the plasticizer or the plasticizer dissolves in the resin.

Several theories have been developed to account for the observed characteristics of the plasticization process. A significant review of the theoretical treatment of plasticization is described by Sears and Darby (1982). In this treatment, plasticization is

described by three primary theories: Lubricity Theory, Gel Theory and Free Volume. Lubricity and Gel Theory describe the action of plasticizer in the polymer. Free volume is a measure of the internal space available within a polymer and the theory describes the effect of increasing free volume to the molecule or polymer chain movement.

2.5.1.1 Lubricity theory

In Lubricity theory, the function of plasticizer is to reduce the intermolecular frictions between polymer molecules and prevent the formation of a rigid network. The plasticizer acts by lubricating the movement of the polymer molecules and reducing their internal resistance to sliding where the polymer molecules can slip over each other. According to Clark (1941) (as cited in Marcilla & Beltran, 2004), plasticizing involves the filling of the large voids in the molecular space lattice, thus leading to the formation of planes of easy glide. This supports the Lubricity theory that the plasticizer acts as a lubricant to fill the voids between the gliding planes to reduce polymer-polymer interactive forces. As a consequence, T_g of PVC is lowered and the polymer chains are allowed to move rapidly, resulting in increased softness and flexibility.

2.5.1.2 Gel theory

The Gel theory describes the polymer structure is sustained by an internal tridimensional honeycomb or gel structure, maintained by loose attachment of the macromolecules along their chains. The rigidity of an unplasticized resin is due to the resistance of this tridimensional network (Marcilla & Beltran, 2004). The principal resistance to distortion in a polymer is viewed as the elastic resistance of interlocked segments of the resin to slip. Plasticization reduces the relative number of polymer-polymer unions, letting the polymer to be deformed without breaking. Thereby reducing

the aggregation of polymer molecules which eventually reducing the rigidity of polymers (Doolittle, 1954; Doolittle, 1965).

In plasticized polymers, there exists a dynamic equilibrium involving solvation-desolvation of the polymer by the plasticizer and aggregation-disaggregation of the polymer chains themselves. In these systems, the plasticizer and resin molecules engage in continuous solvation-desolvation equilibrium while the resin macromolecules are joining and separating from each other in a continuous aggregation-disaggregation.

Aiken et al. (1947) tried some correlations between plasticizer effectiveness and softening, compatibility and molecular structure. They concluded that polar groups in plasticizer and polymer could be arranged in a manner as to form solvating dipoles on the PVC chains. The non-polar tails, being incompatible with PVC would tend to cluster together, leaving a large amount of unshielded polar polymer chains. According to Aiken, plasticizer facilitates micro-Brownian motion of polymer chain segments, thus permitting elasticity to develop. They proposed that in the dynamic equilibrium of the solvation-desolvation process, the plasticizer diffuses through the polymer structure, opening up polymer-polymer contacts temporarily and wandering about, allowing the structure to close behind it in a different position. The solvation-desolvation process described by Aiken to explain plasticization effect matches the basic ideas of the gel theory.

2.5.1.3 Free Volume theory

Free volume is considered as the remaining space between atoms and molecules when no movement is allowed in a polymer. Free volume is low in the glassy state with the molecules packed tightly and cannot move past each other very easily, resulting the polymer appear to be rigid and hard. When the polymer is heated above its glass

transition temperature (T_g), additional free volume was created as a result of the molecular vibrations, allowing the polymer molecules to move past each other rapidly (Krauskopf & Godwin, 2005). This has the effect of making the polymer system to be more flexible and rubbery.

Incorporation of plasticizer into PVC mass is expected to lead to a change in free volume. Free volume can be decreased by: increase the molecular weight of polymer or plasticizers; decrease in chain hydrodynamic volume in the system (e.g. presence of numerous long side chains); decrease in chain mobility (e.g. less end groups present) and higher interaction between chains (e.g. high polarity, increased hydrogen bonding). As plasticizers are added to the polymer system, the T_g of the polymer is lowered by increasing the free volume and molecules are separated further in the system, making the PVC soft and rubbery. With that the PVC molecules can then be able to move past each other rapidly (Krauskopf & Godwin, 2005).

Generally the amorphous areas in polymer are associated with more free volume and tend to be more flexible since conformational changes are permitted in these areas (Marcilla & Beltran, 2004). Plasticizers preferentially position themselves in the amorphous areas. As the free volume theory predicts, the introduction of plasticizers into the polymer involves addition of more free volume and thus, imparting more flexibility and ease of movement to the polymer molecules.

2.5.2 Prerequisites for plasticization

According to Krauskopf and Godwin (2005), the plasticizer molecules are not permanently bound to the PVC resin molecules but are free to self-associate and associate with the resins at certain sites like amorphous sites. As these interactions are weak, there is a dynamic exchange process whereby plasticizer molecule is readily

dislodged and replaced by one another. Therefore, the plasticizer must be selective in entering the amorphous PVC part but not enter and destroy the crystalline part of PVC.

Moorshead (1962) analyzed requirements for a polymer to be plasticized. Firstly, the polymer chains must be sufficiently long to have some strength although the plasticizer forces them apart. Secondly, in highly crystalline polymers the chains are held together by primary bonds and crystalline forces where both forces are too strong to permit plasticizer to penetrate into the polymer. Hence crystallinity of the polymers should not be too high.

On the other hand, the structure of the plasticizer also has a significant effect on plasticization. Both polar and non-polar groups are required in a plasticizer if good compatibility and flexibility is to be achieved. Polar and polarizable groups in a plasticizer improve tensile strength of a polymer, but flexibility is only moderately improved since there are many points of high cohesion along the chain. If the plasticizer also contains non-polar and non-polarizable groups, these groups separate the polymer dipoles without introducing intermediate links, thereby providing high flexibility in plasticized compounds (Marcilla & Beltran, 2004).

The polarities of polymer and plasticizer were useful in assisting the choices of plasticizers. Polar groups in a plasticizer are essential for good compatibility as it is the case of like dissolving like. When plasticizer molecules are introduced into the polymer mass, polymer chains are separated by the plasticizer molecules, which are able to line up their dipoles with the polymer dipoles. Polymer chains separated in this way are more easily moved relative to the one that are bonded very closely. Besides that it should be pointed out that branching of aliphatic chain and high molecular weight of a plasticizer reduces its ability to shield polymer dipoles, this subsequently reducing the mobility

among the polymer chain, and accordingly reducing its softening properties (Marcilla & Beltran, 2004).

2.6 Market of PVC plasticizer

In general, the demand for plasticizer markets is greatly influenced by general economic conditions and thus it largely follows the patterns of the leading world economies. Fig. 2.16 shows the pie chart of world consumption of plasticizers in year 2008.

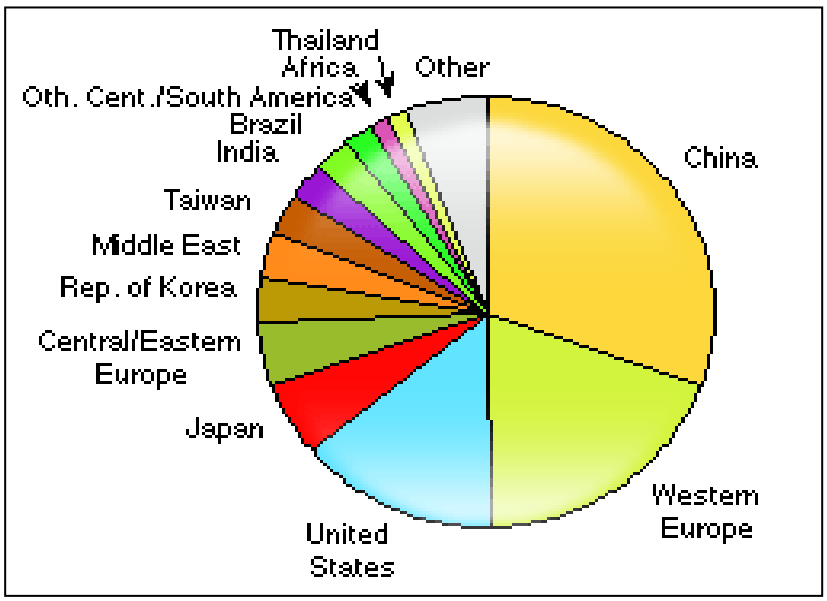

Fig. 2.16 World consumption of plasticizers in year 2008

(Adapted from Bizzari et al., 2009)

In recent years, the price of plasticizers (per Ib) has hiked up the price of PVC resin than before. This cost relationship between PVC resin and plasticizer has urged PVC formulator to find solutions to lower the overall cost of plasticizers used. Therefore the formulator needs to be knowledgeable about the exact type and amount of plasticizer needed to meet product specifications and to produce a satisfactory product with overall lower cost (Rugen et al., 1981).

CHAPTER THREE

MATERIALS AND METHODS

The study in the thesis comprised of two parts; the first part studies the thermal degradation of medium-chain-length poly(3-hydroxyalkanoates) (mcl-PHA) synthesized *via* bacterial fermentation process; and the second part investigates the ability of the mcl-PHA and its low molecular weight oligoesters to serve as a compatible plasticizer for poly(vinyl chloride) (PVC).

3.1 Thermodegradation of medium-chain-length poly(3-hydroxyalkanotes)

3.1.1 Materials

3.1.1.1 Renewable fermentation carbon substrates

Oleic acid and palm kernel oil were kind gifts from Southern Acids (M) Ltd., Klang, Malaysia. Oleic acid ($C_{18}H_{34}O_2$, M_w 282.46 g mol^{-1}, ρ = 0.90 g ml^{-1}) was the refined mono unsaturated fatty acid from palm oil. Palm kernel oil (M_w 217 g mol^{-1}) is the extract from the nut kernel of oil palm (*Elaeis guineensis Jacq.*) fruit. It is highly saturated oil, consists of a mixture of C_6 to $C_{18:2}$ fatty acids with almost 82% saturated fatty acids and 18% unsaturated fractions (Elson, 1992). The major fatty acid compositions are: lauric acid (C_{12}, 48%), myristic acid (C_{14}, 16%), oleic acid ($C_{18:1}$, 15.4%), palmitic acid (C_{16}, 8%), capric acid (C_{10}, 4%), caprylic acid (C_8, 3%), stearic acid (C_{18}, 3%), linoleic acid ($C_{18:2}$, 2.4%), caproic acid (C_6, 0.2%) and arachinoic acid (C_{20}, 0.1%). Same batch of oleic acid and palm kernel oil were utilized throughout the study without further purification in order to minimize the compositional variations.

3.1.1.2 Bacterial strain

Pseudomonas putida PGA1 was used throughout the study. It was the culture collection of Prof. Dr. Irene Tan Kit Ping in Biotechnology Laboratory, University of

Malaya, which was a kind gift from Prof. Dr. Gerrit Eggink, from the Agrotechnological Research Institute, Wageningen, The Netherlands. The bacterial strain was maintained at 4˚C on nutrient agar plate and agar slant, and periodically subcultured.

3.1.1.3 Media

3.1.1.3.1 Stock culture medium

Pseudomonas putida PGA1 was maintained on a sterile nutrient agar plate as shown in Fig. 3.1 and agar slant which was prepared from 20.0 g L^{-1} nutrient agar (Merck), contained the following ingredients (g L^{-1}): 5.0 meat peptone, 3.0 meat extract and 12.0 agar.

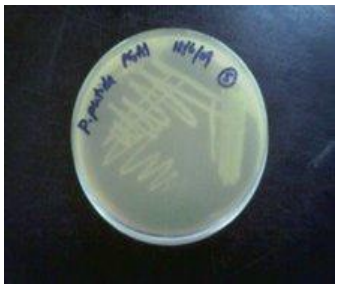

Fig. 3.1 *Pseudomonas putida* PGA1 grown on a nutrient agar plate

3.1.1.3.2 Rich medium

Rich medium is a complex medium which contains some major ingredients of natural origin. It provides carbon source and a full range of growth factors that enhance the growth of the bacterium. Since rich medium supports good growth for bacterium, it does not promote the biosynthesis and accumulation of PHA in the bacterial cell.

In shake flasks fermentations, the nutritionally rich medium contained 8 g L^{-1} nutrient broth (Merck), in which per liter solution comprised of the following ingredients (g L^{-1}): 10.0 meat extract, 2.0 yeast extract and 10.0 peptone. For fed-batch fermentation, the rich medium contained the following components (g L^{-1}): 2.0 yeast extract (Yeast

extract granulated, Merck), 10.0 meat extract (Extract of meat dry, Merck), 10.0 bacteriological peptone (Merck).

3.1.1.3.3 PHA production medium used in shake flasks fermentation

The minimal salt medium used in the oleic acid derived mcl-PHA production was modified M9 medium (Maniatis et al., 1982). It is a nitrogen-limiting medium which was used to induce PHA accumulation in bacteria. It contained the following ingredients (g L^{-1}): 12.8 di-sodium hydrogen phosphate heptahydrate ($Na_2HPO_4.7H_2O$, M_w 268.06 g mol^{-1}, ChemAR), 3.0 potassium di-hydrogen phosphate anhydrous (KH_2PO_4, M_w 136.09 g mol^{-1}, ChemAR), 0.5 ammonium chloride (NH_4Cl, M_w 53.49 g mol^{-1}, ChemAR) and 0.5 sodium chloride (NaCl, M_w 58.44 g mol^{-1}, J.T. Baker); trace elements which consisted of 2.0 ml of 1.0 M magnesium sulfate heptahydrate ($MgSO_4 \cdot 7\ H_2O$, M_w 246.47 g mol^{-1}, Merck) stock solution and 1ml of 0.1 M calcium chloride ($CaCl_2$, M_w 74.10 g mol^{-1}, ChemAR) stock solution. The medium is designed in a way that the essential nutrient, in this case nitrogen, is limiting. Ammonium chloride was the sole nitrogen source for the bacterium in the PHA production medium and limited concentration of it promoted the accumulation of PHA. Generally, nitrogen, phosphorus, oxygen and sulfur are the essential nutrients for bacterial cell growth, and if one of them is in limiting concentration, the cells will be in stress condition and start to reserve the carbon and energy source in the form of PHA.

Nitrogen limitation could be exploited in the PHA production medium since it is relatively easier to make the bacterial culture ammonium-limited than other mineral ions. In addition, the growth of microorganism is more dependent on nitrogen (Suzuki et al., 1986). On the other hand, phosphorous amount is not easy to limit as it was an important component in the medium's buffering system. The amount of dissolved oxygen also could not be easily manipulated in this study as *P. putida* PGA1 is an aerobic

microorganism. Sulfur is just part of the trace element ingredients present in the M9 medium so the sulfur concentration could not be exploited.

3.1.1.3.4 PHA production medium used in fed-batch fermentation

E2 medium (Marsudi et al., 2007) is a defined formulation of major and minor elements and minerals. Modified E2 formulation was used as the palm kernel oil derived PHA production medium in the fed-batch fermentation. It composed of (g L^{-1}): 1.2 potassium di-hydrogen phosphate anhydrous (KH_2PO_4, M_w 136.09 g mol^{-1}, ChemAR), 11.0 di-sodium hydrogen phosphate heptahydrate ($Na_2HPO_4.7H_2O$, M_w 268.06 g mol^{-1}, ChemAR), 16.0 ammonium chloride (NH_4Cl, M_w 53.49 g mol^{-1}, ChemAR), 170.0 ml 100.0 mM magnesium sulfate heptahydrate ($MgSO_4 \cdot 7\ H_2O$, M_w 246.47 g mol^{-1}, Merck) and 1.0 ml trace element solution having the following components (g L^{-1}) in 0.1 M HCl: 0.22 cobalt (II) chloride hexahydrate ($CoCl_2.6H_2O$, M_w 237.93 g mol^{-1}, Merck), 9.70 iron (III) chloride hexahydrate ($FeCl_3.6H_2O$, M_w 270.33 g mol^{-1}, Merck), 7.80 calcium chloride ($CaCl_2$, M_w 74.10 g mol^{-1}, ChemAR), 0.12 nickel chloride hexahydrate ($NiCl_3.6H_2O$, M_w 237.70 g mol^{-1}, Sigma), 0.11 chromium (III) chloride hexahydrate ($CrCl_3.6H_2O$, M_w 266.40 g mol^{-1}, Sigma) and 0.16 cupric sulfate pentahydrate ($CuSO_4.5\ H_2O$, M_w 249.68 g mol^{-1}, BDH).

3.1.1.4 Chemicals and test reagents

3.1.1.4.1 Preparation of 100.0 mM and 1.0 M magnesium sulfate heptahydrate stock solution

A stock solution of 100.0 mM magnesium sulfate heptahydrate ($MgSO_4 \cdot 7\ H_2O$, M_w 246.47 g mol^{-1}, Merck) was prepared by adding 24.65 g $MgSO_4 \cdot 7\ H_2O$ into 1.0 L volumetric flask and the volume was made up to 1.0 L with distilled water. For the stock

solution of 1.0 M magnesium sulphate heptahydrate, 246.47 g $MgSO_4 \cdot 7\ H_2O$ was prepared in 1.0 L distilled water.

3.1.1.4.2 Preparation of 0.1 M calcium chloride stock solution

A stock solution of 0.1 M calcium chloride ($CaCl_2$, M_w 74.10 g mol^{-1}, ChemAR) was prepared by adding 7.41 g $CaCl_2$ into 1.0 L volumetric flask and made up to 1.0 L with distilled water.

3.1.1.4.3 Preparation of 0.85% saline solution

A stock solution of 0.85% saline was prepared by dissolving 8.50 g sodium chloride (NaCl, M_w 58.44 g mol^{-1}, J.T. Baker) in 1.0 L distilled water.

3.1.1.4.4 Preparation of 10% antifoam stock solution

A stock solution of 10% Antifoam A (30% aqueous emulsion of silicon polymer, Fluka Chemical) was prepared by adding 10.0 ml of Antifoam A in 990.0 ml distilled water.

3.1.1.4.5 Preparation of 1.0 M hydrochloric acid solution

1.0 M hydrochloric acid (37% HCl, M_w 36.36 g mol^{-1}, ρ 1.19 g ml^{-1}, Fisher Scientific) was prepared by adding 82.81 ml of 37% HCl into 1.0 L volumetric flaks and made up to 1.0 L with distilled water.

3.1.1.4.6 Preparation of 3.0 M potassium hydroxide solution

3.0 M potassium hydroxide solution (KOH, M_w 56.11 g mol^{-1}, Merck) was prepared by adding 168.33 g KOH into 1.0 L volumetric flask and made up to 1.0 L with distilled water.

3.1.1.4.7 Preparation of phenolphthalein indicator solution

1% phenolphthalein indicator solution was prepared by dissolving 1.0 g phenolphthalein ($C_{20}H_{14}O_4$, M_w 318.33 g mol^{-1}, Merck) in 100 ml of 95% denatured ethanol (C_2H_5OH, M_w 46.07 g mol^{-1}, HmbG Chemicals).

3.1.1.4.8 Preparation of standardized potassium hydroxide solution

Potassium hydroxide (KOH, M_w 56.11 g mol^{-1}, Merck) solution was standardized with potassium hydrogen phthalate (KHP) first prior to the determination of acid number in end group analysis. About 0.02 M concentration of KOH solution was prepared by dissolving 1.18 g of KOH in 1.0 L of 95% denatured ethanol (C_2H_5OH, M_w 46.07 g mol^{-1}, HmbG Chemicals). A small amount of potassium hydrogen phthalate ($C_8H_5KO_4$, M_w 204.23 g mol^{-1}, R&M Chemicals) was dried in oven at 110 ℃ for at least 2 hours and allowed to cool in a desiccator before use to remove moisture. About 0.1 g of KHP was weighed and dissolved in 50.0 mL of distilled water and added with 2 drops of 1% phenolphthalein indicator. The mixture was swirled gently until the salt had completely dissolved and titrated with 0.02 M ethanolic KOH solution to the first appearance of a permanent pink colour. The molarity (M) of standardized potassium hydroxide (KOH) solution was calculated using Equation (3.1):

$$M_{KOH} = W_{KHP}\ x\ (V_{KOH}\ x\ 0.2042)^{-1} \qquad (3.1)$$

where W_{KHP} is weight of potassium hydrogen phthalate (KHP) in g; V_{KOH} is volume of KOH solution used for sample titration in ml.

3.1.1.4.9 Methyl ester standards for gas chromatography analysis

3-hydroxyalkanoaic acid methyl ester standards were used as reference for identification of the monomers present in the mcl-PHA. The standards used were mainly saturated even carbon methyl esters, i.e. methyl 3-hydroxybutanoate ($C_5H_{10}O_3$, M_w

118.13 g mol^{-1}, Sigma Chemical), methyl 3-hydroxyhexanoate ($C_7H_{14}O_3$, M_w 146.19 g mol^{-1}, SAFC), methyl 3-hydroxyoctanoate ($C_9H_{18}O_3$, M_w 174.24 g mol^{-1}, Larodan), methyl 3-hydroxydecanoate ($C_{11}H_{22}O_3$, M_w 202.29 g mol^{-1}, Larodan), methyl 3-hydroxydodecanoate ($C_{13}H_{26}O_3$, M_w 230.34 g mol^{-1}, Larodan), methyl 3-hydroxytetradecanoate ($C_{15}H_{30}O_3$, M_w 258.40 g mol^{-1}, Larodan), methyl 3-hydroxyhexadecanoate ($C_{17}H_{34}O_3$, M_w 286.45 g mol^{-1}, Larodan). By comparing with the retention times of the standards in the chromatogram, the C-even monomers present in the polymer could be identified.

3.1.1.5 Shaker incubator set-up

Shake flask fermentation was carried out in the orbital shaker incubator (HOTECH, Model 718, Taiwan) as shown in Fig. 3.2. The incubation temperature and agitation speed for the incubator was set at 30 ℃ and 200 rpm throughout the experiments.

Fig 3.2 Orbital shaker incubator used in the shake flasks fermentation

3.1.1.6 Bioreactor set-up

The fed-batch fermentation was performed in a 5.0 L fermenter (Biostat®B, B. Braun International, Germany), a culture vessel made of borosilicate glass equipped with an outer thermostat jacket. The pH, temperature and partial pressure of oxygen (pO_2) of the culture media were measured and regulated by a digital system.

All the sampling bottles which contained the carbon substrate, magnesium sulfate, antifoam, acid and base solutions were connected to the bioreactor with autoclavable peroxide-cured silicone tubings. Before autoclaving, all the tubes and filters were clamped except the exhaust pump filter. The filters were wrapped with non-absorbant wool and aluminium foil to prevent water vapor from entering into the filters. The temperature sensor, pH probe (Mettler-Toledo) and pO_2 probe (Mettler-Toledo) were checked and calibrated prior to the experiments. The pH probe and temperature sensors were connected to the bioreactor and calibration of pH probe was carried out using pH 4 and pH 7 buffer solutions at 25℃ before autoclaving. After the whole system was autoclaved at 121℃ for 15 min using the large capacity autoclave machine (P. SELECTA, Spain), the pO_2 electrode was connected to the digital system to polarize the pO_2 probe for at least 6 hours. Upon polarization, the pO_2 probe was calibrated using industrial grade nitrogen gas followed by industrial grade oxygen gas. The peristaltic pumps on the machine were also calibrated. After the temperature of the whole system had cooled down to room temperature, the cooling jacket machine was switched on. Cool circulating water was allowed to fill in the thermostat to remove trapped air inside the machine and bioreactor. The motor was then fitted to the reactor and the pH regulation and temperature of the medium was set at pH 7 and 30℃, respectively. The impeller speed was set at 600 rpm throughout the fermentation. The setup of the bioreactor during fed batch fermentation is shown in Fig. 3.3.

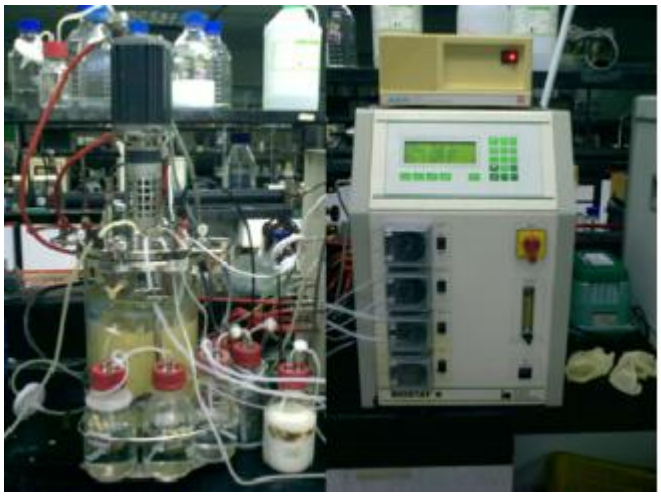

Fig. 3.3 Setup of 5-L bioreactor for fed batch fermentation system

3.1.2 Methods

3.1.2.1 Saponification of palm kernel oil

According to Tan et al. (1997), *Pseudomonas putida* PGA1 cannot utilize palm kernel oil (PKO) directly due to the absence of lipase gene. Therefore it is necessary to saponify the PKO with sodium hydroxide to produce sodium salts of free fatty acids to be used as the feedstock for bacterial growth and PHA production. PKO at room temperature is in semi-solid form therefore it was first warmed in the oven at 40^{o}C until it melted completely. An ethanolic sodium hydroxide solution was prepared by dissolving 28.0 g of sodium hydroxide (NaOH, M_w 40.00 g mol^{-1}, Merck) in 1.0 L of absolute 99.5% ethanol (C_2H_5OH, M_w 46.07 g mol^{-1}, ChemAR); 80.0 g of PKO was then weighed and added to the round bottom flask containing the ethanol/NaOH solution. The mixture was refluxed gently at 70˚C for 1 hour. Upon completion, the reaction mixture was poured into a glass petri dish and dried in an oven to evaporate off the excess ethanol, leaving behind the sodium salt of the fatty acids.

3.1.2.2 Sterilization

All medium and solutions used in the shake flasks fermentation were sterilized at 121˚C, 1 atm for 15 min using autoclave machine (TOMY Model SS-325, Japan). The carbon substrate was sterilized separately from the nutrient-limiting medium to avoid possible reactions with other medium's components where possibly toxic and inaccessible compounds for growth may be formed. To avoid precipitation during autoclaving, the trace element solutions of modified M9 medium were heat sterilized separately before adding to the rest of the formulation.

The 5 L bioreactor containing the nutrient-limiting medium and the sampling bottles which contained the carbon substrate, magnesium sulfate, antifoam, acid and base solutions were sterilized at 121˚C, 1 atm for 15 minutes using large capacity autoclave machine (P. SELECTA, Spain). The trace element solution of the modified E2 medium was filter sterilized separately before adding to the rest of the medium.

3.1.2.3 Production of oleic acid derived mcl-PHA through shake flasks fermentation

In shake flasks fermentation, 0.5% (v/v) oleic acid was utilized by *Pseudomonas putida* as the sole carbon and energy source. The bacterium was cultured at 30℃ and agitated at 200 rpm in the HOTECH orbital shaker incubator under aerobic condition.

PHA production was performed in a two-stage culture system which consists of cell-growth phase and PHA-accumulation phase. In the first phase, the bacteria were grown in nutrient broth (8.0 g L^{-1}), a nutritionally rich medium, to produce high concentration cell cultures. After 20 hours of incubation, the cells were harvested by centrifugation, washed with 0.85% saline, and transferred to the modified nitrogen-limiting M9 medium to induce PHA biosynthesis by the cells. The bacteria were further cultivated in PHA production medium for 72 hours at 200 rpm and 30^{o}C.

3.1.2.4 Production of palm kernel oil derived mcl-PHA through fed-batch fermentation

For fed-batch fermentation, bacterial cells were pre-cultured overnight in the orbital shaker orbital at 30˚C and agitated at 200 rpm for 15 hours in a rich medium. The resulting culture was used to inoculate the inoculum medium containing the same composition as the rich medium but supplemented with additional 5.0 g L^{-1} SPKO. This was used as the inoculum for the PHA production medium in the 5 L bioreactor. SPKO was added to the inoculum medium so that the bacterial cells will be more easily adapted to the new environment in the PHA production medium with similar carbon source, and therefore reduced the period of lag phase for cell growth.

Fed-batch cultures were cultivated at 30˚C in the 5 L bioreactor (Biostat®B, B. Braun International, Germany) with 5.0 g L^{-1} SPKO as the sole carbon substrate in the initial feed and 3 g L^{-1} in the subsequent fed-batch feeding. 10% inoculum (v/v) was used to inoculate 3.0 L PHA production medium in the bioreactor. The carbon substrate was added at intermittent intervals at a constant flow rate *via* bottom feeding. The SPKO solution was kept warm in the hot water bath (Memmert, Germany) throughout the experiments so that homogeneous feeding to the culture medium will be achieved. 100.0 mM $MgSO_4.7H_2O$ solution was also intermittently fed into the bioreactor in order to minimize precipitation in the culture medium. Stirrer speed was kept constant at 600 rpm in all experiments. The partial pressure of dissolved oxygen was maintained around 80% of oxygen saturation during the cell growth phase and 50% of oxygen saturation during PHA accumulation phase by feeding oxygen-enriched gas. The pH of the culture was maintained at 7.0 by addition of acid (1.0 M HCl) and base (25% NH_3 at initial growth and 3.0 M KOH after 48 hours of cultivation). The NH_3 feed simultaneously served as the nitrogen source for bacterial growth during exponential phase and as a basic solution for pH control. Under the specific cultivation conditions, PHA

accumulation phase began after 48 hours of fed-batch cultivation. To maintain nitrogen-limiting condition after 48 hours of cultivation, the pH was regulated by the addition of 3.0 M KOH instead of 25% NH_3. Foaming was likely to occur when the SPKO solution was pumped into the culture medium. To control the foaming problem, 10% antifoam was added to the medium to suppress the foam formation. Foaming could also be controlled by the installation of two mechanical foam breakers on the central shaft and above the surface of the liquid, adjustment of the impeller speed and aeration. Automatically regulated gas-mix mode was chosen to supply oxygen to the culture alternative to constant airflow method.

After 60 hours of fermentation, the culture medium was pumped out from the bioreactor by increasing the air pressure in the bioreactor. The bacterial culture was subsequently harvested by centrifugation.

3.1.2.5 Cell harvesting

The bacterial cells were aseptically harvested by centrifugation (CONTINENT R large capacity refrigerated centrifuge, Korea) at 8000 rpm for 30 minutes at 4℃ after bacterial cultivation. The cells were washed twice with sterile 0.85% saline and dried at 70˚C in a hot air oven (Memmert, Germany) to constant weight.

3.1.2.6 Removal of oily remnants from the cells by biomass pretreatment

The dried cells were washed with polar solvent to remove remnants from the carbon substrates and metabolic wastes from the biomass by suspending them in 95% analytical grade ethanol (C_2H_5OH, M_w 46.07, HmbG Chemicals) and shaking for 30 minutes at 22$\pm$1 ℃ and 160 rpm in the orbital shaker incubator (HOTECH Model 718). Oily residues and other polar lipids attached to the cells would dissolve in the alcohol

which was decanted off. The washed cells were then dried in oven at 70 ℃ to constant weight.

3.1.2.7 PHA extraction and purification

Intracellular PHA were extracted by suspending the dried cells in analytical grade chloroform ($CHCl_3$, M_w 119.38 g mol^{-1}, Merck) and refluxed for 6 hours at 70˚C. The PHA-chloroform solution was filtered through Whatman number 1 filter paper to remove the cellular debris, and the filtrate was concentrated by rotary evaporation (EYELA N-1000 rotary evaporator). The polymers were purified by dropwise addition of the extract into rapidly stirred analytical grade methanol (CH_3OH, M_w 32.04 g mol^{-1}, Merck) chilled with ice bath. Further purification was carried out by re-dissolving the PHA in a small amount of chloroform and re-precipitating it in excess methanol. It was then dried in a vacuum oven (JEIOTECH Model OV-11/12, Korea) at 37˚C, 0.6 atm for 48 hours. The purified mcl-PHA derived from oleic acid and SPKO were obtained, with the oleic acid derived PHA appeared as viscous gel and SPKO derived PHA appeared as elastic film, as shown in Fig. 3.4.

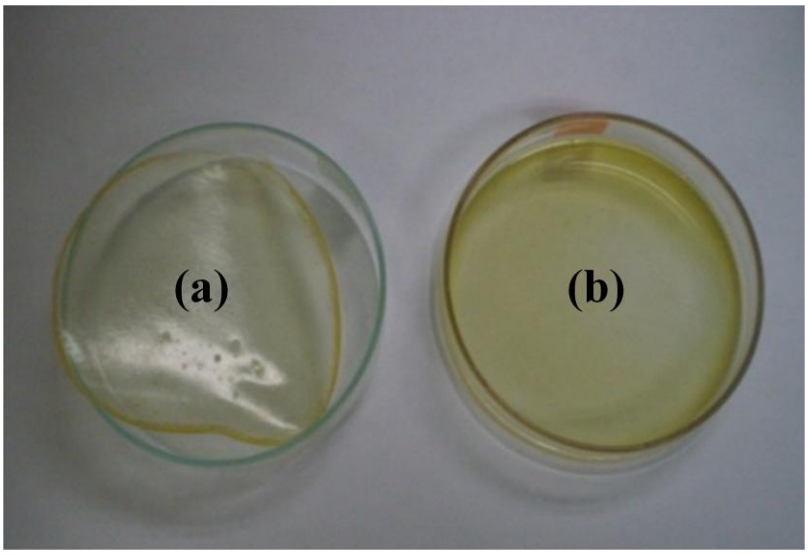

Fig. 3.4 Morphology of mcl-PHA derived from two different substrates: (a) mcl-PHA derived from SPKO and (b) mcl-PHA derived from oleic acid

3.1.2.8 Thermal degradation of mcl-PHA

Thermal degradation was carried out at three temperatures: 160±2 ℃, 170±2 ℃ and 180±2 ℃ for mcl-PHA derived from oleic acid; and at four temperatures: 160±2 ℃, 170±2 ℃, 180±2 ℃ and 190±2 ℃ for mcl-PHA derived from palm kernel oil. The thermal degradation of oleic acid derived PHA was conducted in the temperature range of 160-180 ℃ as the initial degradation temperature for this polymer was around 183 ℃. Meanwhile the initial degradation temperature of SPKO derived PHA was around 195 ℃, hence, the thermal degradation was conducted in the temperature range of 160-190 ℃. The PHA samples were pre-dried for 48 hours in vacuo to remove moisture. Approximately 5.0 g of sample was placed in a 250 ml conical flask with socket, which was connected to a Leibig condenser, as shown in Fig. 3.5. The reaction flask was placed in thermostated silicon oil (Polydimethylsiloxane, for melting point and boiling point apparatus, ACROS organics) bath and heated from ambient temperature to the desired degradation temperatures. The level of the oil bath was kept at approximately 2 cm above the sample in the reaction flask and the oil bath apparatus was covered with

aluminium foil to allow uniform heat transfer during thermal degradation. The sample was then kept isothermal for 30 minutes. The reactor was removed from the oil bath after the reaction was completed and allowed to cool down to room temperature. A small volume of chloroform was added to dissolve the degradation products. The solution was poured into a glass petri dish followed by complete evaporation in fume hood at room temperature and subsequently dried in vacuum oven to remove moisture.

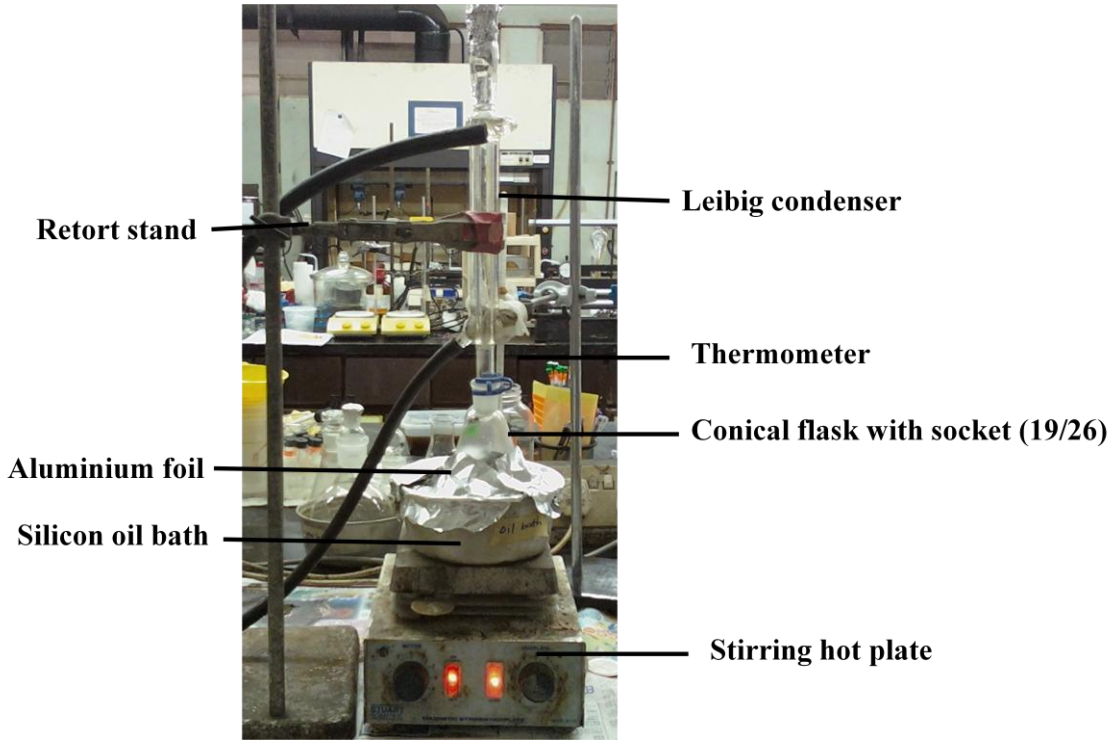

Fig. 3.5 The set-up of thermodegradation process

3.1.3 Characterizations of un-degraded and heat-treated mcl-PHA

3.1.3.1 End-group analysis

End group analysis was performed in accordance with ASTM D 1980-87 Standard Test Method and PORIM Test Method (PORIM p2.5 Acidity) to measure the amount of free acids present in the sample. Acid number titration was carried out to determine the concentration of carboxylic acid end groups in the PHA polymer. The PHA samples (non-degraded control and heat-treated ones) were dissolved in a 2:1

mixture of toluene and ethanol. The acid values were determined by titrating the polymer solutions with standardized ethanolic potassium hydroxide solution. Each titration was added with two drops of 1% phenolphthalein indicator as titration end-point visual indicator. All experiments were performed in duplicate. As acid number is the number of mg of KOH used to neutralize the free fatty acids in 1.0 g of PHA, the number average molecular weight and concentration of terminal carboxyl groups of the polymer could therefore be determined.

3.1.3.2 Determination of acid number for PHA sample

3.1.3.2.1 Blank and sample titration

A stock solution of a solvent mixture consisted of analytical grade toluene ($C_6H_5CH_3$, M_w 92.14, Fisher Scientific) and analytical grade 95% denatured ethanol (C_2H_5OH, M_w 46.07, HmbG Chemicals) in a ratio of 2:1 was prepared. The blank solution was prepared by adding 50.0 mL of the solvent mixture and 2 drops of phenolphthalein indicator into a conical flask. The solution was then titrated with standardized KOH solution until the first appearance of a permanent pink color and the volume of KOH used in the blank titration was recorded.

About 1 g of PHA sample was weighed into a conical flask followed by addition of 50.0 mL of the solvent mixture (toluene/ethanol) and 2 drops of phenolphthalein indicator. The mixture was swirled gently until the polymer was completely dissolved. The sample solution was then titrated with the standardized KOH solution until the first appearance of a permanent pink color and the volume of KOH used in the sample titration was recorded. Both the blank and sample titrations were performed in duplicates.

3.1.3.2.2 Theoretical calculation of acid number

The acid number (*AN*) of the PHA sample was calculated using the following formula:

$$AN = [56.1\ x\ M_{KOH}\ x\ (V - V_{blank})] / W_{PHA} \quad (3.2)$$

where M_{KOH} is molarity of the potassium hydroxide solution in M; W_{PHA} is weight of PHA sample in g; V is volume of the potassium hydroxide solution used for the sample titration in ml; V_{blank} is volume of the potassium hydroxide solution used for the blank titration in ml.

Duplicate results of acid values were obtained and the acid number was reported by averaging the results. The acid values obtained from the two determinations should not differ by more than 5% of the mean acid number.

3.1.3.3 Determination of thermal properties of control and heat-treating mcl-PHA

Thermal behavior of reference control (non-degraded) and heat-treated mcl-PHA were characterized using Thermogravimetric Analysis (TGA) (Perkin-Elmer TGA6) and Differential Scanning Calorimetry (DSC822e, Mettler Toledo).

3.1.3.3.1 Thermogravimetric Analysis

Thermogravimetric analysis (TGA) has been widely employed to characterize the thermal behavior of a polymer and to estimate the thermo-kinetic parameters e.g. activation energy, frequency factor, reaction order and rate of decomposition (Carrasco et al., 2006).

Measurements from TGA are usually displayed as a thermogram in which the weight/ weight percentage is plotted against temperature. The rate of weight changes is derived from the TGA curve with respect to the temperature and is known as the

derivative thermogravimetric (DTG) curve. The tip of the DTG curve usually corresponds to the maximum rate of decomposition.

For TGA, about 10.0 mg of PHA sample was loaded in the ceramic pan and scanned at heating rate of 10˚C min^{-1} in the temperature range between 50˚C and 900˚C under an atmospheric nitrogen flow of 20 mL min^{-1}. Thermal data were recorded on Perkin-Elmer Pyris 1 TGA software.

3.1.3.3.2 Differential Scanning Calorimetry

Differential scanning calorimetry (DSC) is designed to determine the change of enthalpy for a material as heat is absorbed or released when it undergoes a physical transformation (Sin, 1998). The thermal transitions for the polymer are determined by directly measuring the difference of the amount of heat supplied to the sample and the reference.

DSC analysis was carried out in the temperature range of -100 to 180 ℃ at a heating rate of 20 ℃ min^{-1} under a nitrogen gas flow. Cryospeed nitrogen was used to achieve the sub-ambient temperature. Approximately 5.0 mg of samples were used and encapsulated in aluminium pans. The sampling pan was placed aside with a blank aluminium pan as a reference in the sample chamber. T_g of the sample was determined as the onset of steep change in energy; T_m and enthalpy of fusion (ΔH_m) were determined from the DSC endothermic peak. All temperatures were recorded in degrees Celsius.

3.1.3.3.3 Determination of kinetic parameters for thermal degradation of mcl-PHA

Thermodegradation kinetics of mcl-PHA was studied using Kissinger's method through Thermogravimetric Analysis (Doyle, 1961). PHA samples were analyzed by TGA non-isothermal procedures at multiple heating rates of 10, 15, 20, 25 and 30 K min^{-1}. The nitrogen flow rate was fixed at 20 ml min^{-1}. The degradation activation energy and

pre-exponential factor of the process were estimated using Kissinger expression as shown in Equation (3.3):

$$-ln\,(q/{T_p}^2) \;=\; E_d/RT_p \;-\; ln\,(AR/T_p) \qquad (3.3)$$

where q is heating rate (K min^{-1}); T_p is maximum degradation temperature (K); R is universal gas constant (8.3143 J K^{-1} mol^{-1}); E_d is degradation activation energy (kJ mol^{-1}); A is pre-exponential factor (s^{-1}).

Kissinger's method for calculating degradation activation energy uses the temperature at maximum degradation rate. From the linear plot of –ln (q/T_p^2) versus $1/T_p$, activation energy and pre-exponential factor could be calculated from the slope and the intersection at *y*-axis respectively (Lee et al., 1997).

The entropy of activation (ΔS) for PHA thermal degradation was also calculated using the relationship as shown in Equation (3.4) (Radhakrishnan Nair et al., 2007):

$$A \;=\; (kT_p/\,h)\; e^{\Delta S/R} \qquad (3.4)$$

where A is Arrhenius parameter (s^{-1}); k is Boltzman constant (1.3807x10^{-23} J K^{-1}); T_p is peak temperature (K); h is Planck constant (6.626x10^{-34} J s); ΔS is entropy of activation (J K^{-1} mol^{-1}); R is general gas constant (8.3143 J K^{-1} mol^{-1}).

3.1.3.4 Gel Permeation Chromatography

The relative molecular weight and molecular weight distribution of mcl-PHA polymers were determined by using gel permeation chromatography (GPC). GPC could not be used to determine the exact molecular weight of a polymer as it separates the components on the basis of size only. The most common eluent used in the GPC analysis is tetrahydrofuran (THF), which is a good solvent for the polymer at room temperature.

In this study, GPC was performed using a Waters™ 600-GPC (USA) instrument equipped with Waters Styragel HR columns (7.8 mm internal diameter x 300 mm)

connected in series (HR1, HR2, HR5E and HR5E) and a Waters 2414 refractive index detector. Approximately 100.0 μl of 2.0 mg ml^{-1} polymer sample was eluted by THF at a flow rate of 1 mL min^{-1} at 40 ℃. The instrument was calibrated using monodisperse polystyrene standards.

3.1.3.5 Determination of acidity of degradation products

According to Material Safety Data Sheet (MSDS), solubility of hydroxyalkanoic acids in water at 20˚C is about 59.2% and at 100˚C is 84%, indicating hydroxyalkanoic acid is a weak acid in nature.

The aqueous acidity of oligomeric hydroxyalkanoic acids obtained from the thermal degradation process can be determined by measuring the pH of the non-degraded and the heat treated polymers in their respective boiled aqueous solutions, with boiled distilled water (95 ℃) as the control, using pH meter (HANNA instrument pH 211 microprocessor). All experiments were performed in duplicate. Subsequently, acid dissociation constant (K_a), pK_a value and the degree of dissociation (α) of the decomposition products could be determined. The spontaneity of the dissociation of hydroxyalkanoic acids into thermodynamically stable conjugate base and hydrogen ions in aqueous solution was determined from the changes in Gibbs free energy of the process. The change in standard Gibbs free energy of the process can be calculated from the following relationship:

$$\Delta G^\circ = RT\ 2.303\ pK_a \qquad (3.5)$$

where ΔG° is change in standard Gibbs free energy at 1 atm (kJ mol^{-1}); R is universal gas constant (8.3143 J K^{-1} mol^{-1}); T is temperature of the aqueous solution (368K).

3.1.3.6 Gas Chromatography

Gas chromatography (GC) is a technique used to separate various components of a polymer, to detect the individual monomers and to identify and quantify the monomers using reference standards. The separation is carried out inside a column in an oven programmed at certain temperature with the inert carrier gas flowing through the stationary phase. The individual components are separated based on differential migration rate of monomers in the polymer.

Analysis of PHA monomeric compositions before and after thermal treatment was performed using a GC 2014 Shimadzu (Japan) equipped with a SGE forte GC capillary column BP20 (30 m x 0.25 mm internal diameter x 0.25 μm) (Australia) and a flame ionization detector (FID). Approximately 8.0 mg of purified PHA was subjected to methanolysis by heating at 100˚C for 140 min in the mixture of 1.0 ml analytical grade chloroform ($CHCl_3$, M_w 119.38 g mol^{-1}, Merck), 0.85 ml analytical grade methanol (CH_3OH, M_w 32.04 g mol^{-1}, Merck), and 0.15 ml concentrated sulfuric acid (98% HCl, M_w 98.08 g mol^{-1}, ρ = 1.94 g ml^{-1}, Merck) in a screw-cap tube sealed with PTFE tape. The mixture was shaken occasionally throughout the heating process and subsequently cooled to room temperature. 1.0 mL of distilled water was added to the reaction mixture. The mixture was then vortexed for 1 min and allowed to stand for 10 min to induce phase separation. The organic phase at the bottom layer was recovered by glass Pasteur pipette and analyzed by gas chromatography.

In the GC analysis, 1.0 μl of sample was injected by split injection with a split ratio of 10:1 using a SGE 10.0 μl syringe. Nitrogen was used as the carrier gas at a flow rate of 3 ml min^{-1}. The column oven temperature was programmed from 120˚C for 2 min at the start, ramped up at a rate of 20˚C min^{-1} to 230˚C, and held at this temperature for 10 min. The temperatures of injector and detector were set at 225˚C and 230˚C respectively. 3-hydroxyalkanoic acid methyl ester standards: 3-hydroxybutyric acid

(3HB; C_4), 3-hydroxyhexanoic acid ($3HH_x$; C_6), 3-hydroxyoctanoic acid (3HO; C_8), 3-hydroxydecanoic acid (3HD; C_{10}), 3-hydroxydodecanoic acid (3HDD; C_{12}), 3-hydroxytetradecanoic acid (3HTD; C_{14}) and 3-hydroxyhexadecanoic acid ($3HH_xD$; C_{16}) methyl esters (Larodan) were used to determine the respective retention times for monomer identification.

3.1.3.7 Fourier Transform Infrared Spectroscopy

Infrared spectrometer is widely used in the qualitative and quantitative determination of polymeric composition by identifying the structural and functional groups, steric and geometric isomerism in the polymer (Teoh, 1998). The polymers can be handled in many forms, e.g. solutions, powder and cast film. Fourier transform infrared spectroscopy (FTIR) is a modern infrared spectrometer which is capable of collecting spectral data in a wide spectral range (Griffiths & de Haseth, 2007), with greater speed and sensitivity than a dispersive spectrometer.

In this study, FTIR analysis was conducted with a Perkin-Elmer FTIR RX Spectrometer (USA). PHA sample was first dissolved in small amount of chloroform to form a viscous solution, which was then spread onto a NaCl FTIR cell. The solvent was removed by blowing with hot air so that a thin polymer film was deposited on the surface of the NaCl cell. The spectrum was recorded after 16 scans and at a resolution of 4 cm^{-1} between 4000 and 650 cm^{-1}.

3.1.3.8 Proton Nuclear Magnetic Resonance Spectroscopy

Proton nuclear magnetic resonance (^{1}H-NMR) spectroscopy is a valuable technique used to elucidate the molecular structure of a polymer as the signals of the protons are very sensitive to the changes in molecular structure, producing narrow chemical shift with sharp signals. Deuterated chloroform is the most common used

solvent in NMR analysis, and it could be served as the internal reference in the spectrum, giving the signal of 7.27 ppm.

^{1}H-NMR analysis of the control and heat-treated PHA samples was carried out on a JEOL JNM-LA 400 FT-NMR spectrometer (Japan) operating at 400 MHz at ambient temperature. About 20.0 mg of PHA sample was dissolved in 1 mL of deuterated chloroform ($CDCl_3$, 99.9 atom % D, 0.03% (v/v) TMS, M_w 120.38 g mol^{-1}, Sigma Aldrich) and the 2% (w/v) PHA-$CDCl_3$ solution was recorded on the ^{1}H-NMR spectrum. Chemical shifts in ppm were relative to the signals of $CDCl_3$ as internal reference. The integration value of terminal methyl protons in the side chain of PHA was chosen as the reference and was assigned the value of 1.00.

3.2 Investigation of the ability of mcl-PHA and its oligoesters as compatible plasticizer for poly(vinyl chloride)

3.2.1 Materials

3.2.1.1 Poly(vinyl chloride)

Poly(vinyl chloride) (PVC) with viscosity number 87, and low molecular weight approximately 100,000 g mol^{-1} (BDH laboratory reagent) was used throughout the experiments.

3.2.1.2 Medium-chain-length poly(3-hydroxyalkanoates)

Medium-chain-length poly(3-hydroxyalkanoates) (mcl-PHA) were synthesized by *Pseudomonas putida* PGA1 from two different carbon substrates: oleic acid (OA) and saponified palm kernel oil (SPKO) at the concentration of 0.5% (v/v and w/v) using shake flasks fermentation. Similar culture media as shown in Section 3.1.1.3.2 and 3.1.1.3.3 were used for the bacterial cell growth and PHA production in the fermentation.

3.2.2 Methods

3.2.2.1 Heat treating of mcl-PHA at desired degradation temperature

The purified mcl-PHA samples were thermally degraded at temperatures of 170℃ for OA derived mcl-PHA and 170℃ for SPKO derived mcl-PHA. These temperatures were chosen as the degradation temperatures as the heat-treated PHA obtained were mainly composed of a mixture of oligomeric hydroxyacid fragments without terminal unsaturated fragments. The thermal degradation process was performed using similar procedure as detailed in section 3.1.2.8.

3.2.2.2 Characterizations of mcl-PHA and degradation products prior to solution blending

3.2.2.2.1 Differential Scanning Calorimetry

Differential Scanning Calorimetry **(**DSC) analysis of the non-degraded and heat-treated mcl-PHA used in the blending was performed using similar procedure as detailed in Section 3.1.3.3.2.

3.2.2.2.2 Gel Permeation Chromatography

The number average molecular weight (M_n), weight average molecular weight (M_w) and polydispersity index (*PDI*) of the control and heat-treated mcl-PHA used in the blending were determined by gel permeation chromatography (GPC) analysis using similar procedure as detailed in Section 3.1.3.4.

3.2.2.2.3 Gas Chromatography

The monomeric compositions of the non-degraded and heat-treated mcl-PHA used in the blending were characterized by gas chromatography (GC) using similar procedure as detailed in Section 3.1.3.6.

3.2.2.3 Solution blending of PVC and mcl-PHA

3.2.2.3.1 Preparation of PVC/mcl-PHA binary blends

A series of polymer blends comprised of poly(vinyl chloride) (PVC) and different types of medium-chain-length poly(3-hydroxyalkanaotes) (mcl-PHA) (polymeric PHA derived from OA; 170 ℃ heat-treated PHA derived from OA; polymeric PHA derived from SPKO; 170 ℃ heat-treated PHA derived from SPKO) were prepared from the common solvent. Chloroform ($CHCl_3$, M_w 119.38 g mol^{-1}, Merck) of analytical grade was used as the solvent for both polymers in the blending.

A 0.625% w/v of PHA solution (20.0 mL chloroform containing 0.125 g mcl-PHA) and 1.25% w/v of PHA solution (20.0 mL chloroform containing 0.25 g mcl-PHA) were prepared. These solutions were then added to the 5% w/v PVC solution (100.0 mL chloroform containing 5.0 g of PVC) at two ratios, yielding 2.5 phr (parts per hundred PVC resin) and 5 phr (parts per hundred PVC resin) of PVC/PHA binary blends, respectively. The binary blends were designated as, for example PVC/$PHA_{OA\text{-}2.5}$, the abbreviation meaning a blend of 97.5 parts of PVC and 2.5 parts of PHA derived from OA; PVC/$PHA_{SPKO\text{-}2.5}$, a blend of 97.5 parts of PVC and 2.5 parts PHA derived SPKO; PVC/deg$PHA_{OA\text{-}2.5}$, a blend of 97.5 parts of PVC and 2.5 parts 170 ℃ heat-treated PHA derived from OA; PVC/deg$PHA_{SPKO\text{-}2.5}$, a blend of 97.5 parts of PVC and 2.5 parts 170 ℃ heat-treated PHA derived from SPKO; PVC/$PHA_{OA\text{-}5}$, a blend of 95 parts of PVC and 5 parts of PHA derived from OA; PVC/$PHA_{SPKO\text{-}5}$, a blend of 95 parts of PVC and 5 parts PHA derived from SPKO; PVC/deg$PHA_{OA\text{-}5}$, a blend of 95 parts of PVC and 5 parts 170 ℃ heat-treated PHA derived from OA; PVC/deg$PHA_{SPKO\text{-}5}$, a blend of 95 parts of PVC and 5 parts 170 ℃ heat-treated PHA derived from SPKO.

The designation and compositions of the binary blends prepared are summarized in Table 3.1.

Table 3.1 Designations and compositions of PVC/PHA binary blends

Sample code	**Blend Composition**	
	PVC (phr)	**PHA (phr)**
PVC/$PHA_{OA-2.5}$	97.5	2.5
PVC/deg$PHA_{OA-2.5}$	97.5	2.5
PVC/PHA_{OA-5}	95	5
PVC/degPHA_{OA-5}	95	5
PVC/$PHA_{SPKO-2.5}$	97.5	2.5
PVC/deg$PHA_{SPKO-2.5}$	97.5	2.5
PVC/PHA_{SPKO-5}	95	5
PVC/degPHA_{SPKO-5}	95	5

The commercial code, method of preparation and molecular weight properties of the PVC and different types of mcl-PHA used in the blending was summarized in the Table 3.2.

Table 3.2 Average molecular weight and molecular weight distribution for the components in PVC/PHA samples. M_n, number-average molecular weight; M_w, weight-average molecular weight; *PDI*, polydispersity index, defined by M_w/M_n

Polymer	**Commercial code/Preparation**	***M_n**	***M_w**	***PDI**
PVC	Viscosity no. 87 (BDH laboratory reagent)	36700	96000	2.6
OA derived mcl-PHA	Batch-fermentation	22800	50700	2.2
170 ℃ heat-treated OA derived mcl-PHA	Thermal degradation	18400	75700	4.1
SPKO derived mcl-PHA	Batch-fermentation	32700	60000	1.8
170 ℃ heat-treated SPKO derived mcl-PHA	Thermal degradation	18200	42000	2.3

(*****The values of M_n, M_w and *PDI* were determined from the GPC chromatograms of the samples as shown in Appendix H)

3.2.2.3.2 Reaction set-up

The PVC/chloroform solution was first mixed at 500 rpm, and refluxed at 55 ℃ in a flat round bottom flask connected to Leibig condenser with a reduction adaptor (socket 24/29 and cone 34/35) for 30 minutes. After the specified reaction time, the PHA/ chloroform solution was added to the PVC solution and the mixture was allowed to mix at 500 rpm and 55 ℃ for one hour. The solution was mixed thoroughly using an 8 x 40 mm PTFE magnetic stirrer bar with pivot ring. The reactor was placed in a thermostated water bath and the level of the water was kept at least 2 cm above the level of the

solution in the reaction flask for homogeneous temperature equilibrium. Upon completion of blending, the PVC/PHA was solvent-casted in a glass petri dish and was stirred using an 8 x 30 mm PTFE magnetic stirrer bar, to slowly evaporate off the solvent in the fume hood at room temperature. When the mixture started to form a viscous solution, the magnetic stirrer bar was removed and sample was continued with drying until a homogenous film was obtained. The casted films were further dried under vacuum at 60 to 70 ℃ for two days followed by drying in hot air oven at 70 to 72 ℃ for one week to allow for complete removal of the traces of residual solvent. The solution blending and solvent casting set-up is as shown in Fig. 3.6:

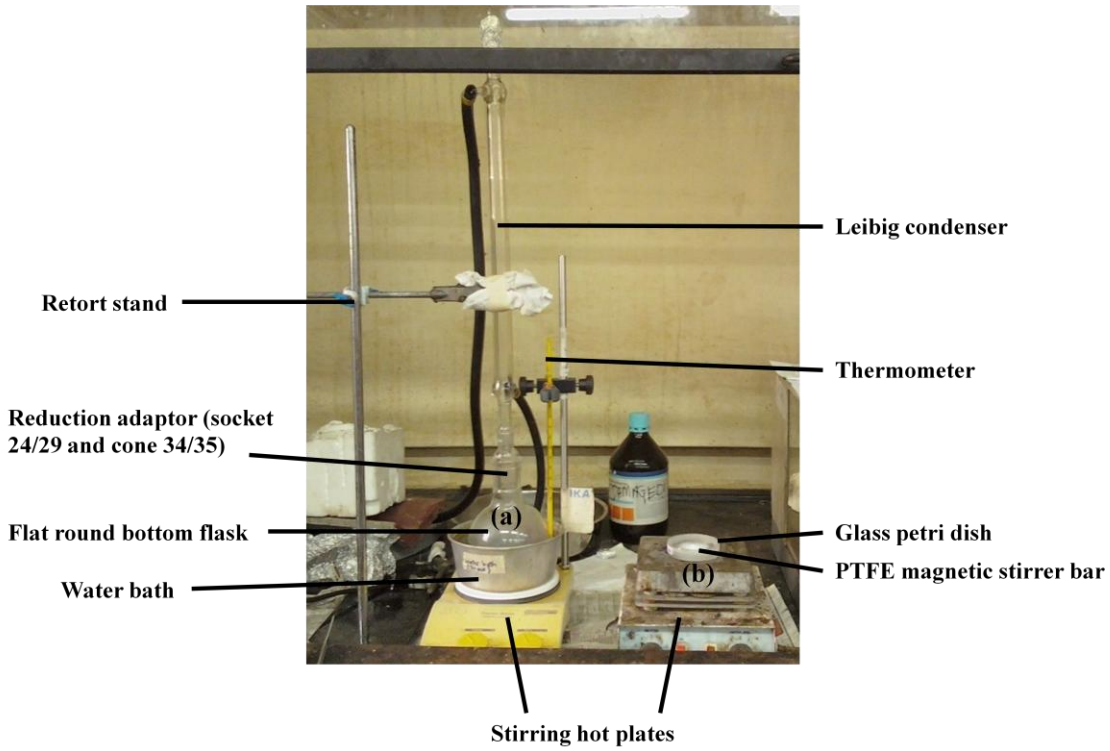

Fig. 3.6 Experiment set-up of (a) solution blending and (b) solvent casting

3.2.2.4 Characterizations of PVC-PHA binary blends

The casted PVC/PHA films were studied by various analytical techniques such as FTIR, ^{1}H-NMR, scanning electron microscopy (SEM), TGA, DSC and dynamic mechanical analysis (DMA).

3.2.2.4.1 Fourier Transform Infrared Spectroscopy

The structural and functional groups present in the PVC, PHA and PVC/PHA samples were analyzed by Perkin-Elmer FTIR-ATR spectrometer. The IR spectra of the thin films prepared were scanned at a wavelength of 4000 to 450 cm^{-1}, with a resolution of 4 cm^{-1} and recorded after 4 scans.

3.2.2.4.2 Proton Nuclear Magnetic Resonance Spectroscopy

The chemical structures of PVC, PHA and the binary blends on molecular level were characterized by proton nuclear magnetic resonance (^{1}H-NMR) spectroscopy using similar procedure as detailed in Section 3.1.3.8.

3.2.2.4.3 Scanning Electron Microscopy

The PVC/PHA sample films were examined by scanning electron microscopy (SEM) to study the microstructure and surface morphology of the thin films. SEM microscopy was performed using a SEM Zeiss Auriga (Germany) at operating voltage of 1 kV, under magnifications of 200 x and 500 x.

The use of SEM allows observation of morphological changes in PVC particles during plasticization process. The evolution of the initial structure, the solvation of PVC and plasticizer particles may offer valuable qualitative information. Thus SEM is a reliable technique to monitor the plasticizing effect of mcl-PHA to PVC.

Uncoated samples were used in this SEM study, using low operating voltage around 1 kV and LaB_6, Field Emission as electron source. Samples were mounted onto the specimen holder using conducting carbon-impregnated tape. At normal operating voltages (10 to 30 kV), the contrast differences between phases with different compositions are inherently lower in resolution in the backscattered (BS) image than the secondary image (Hobbs & Watkins, 2000). By working at low operating voltages,

subtle variations in the chemical compositions of blend components are sufficient to produce contrast in the secondary images and therefore high-quality images are possible to be obtained.

3.2.2.4.4 Thermal analysis of PVC/mcl-PHA binary blends

3.2.2.4.4.1 Thermal profile and thermal stability of the blends studied by TGA

Before subjected to further analysis, the dried PVC/mcl-PHA films were subjected to thermogravimetric analysis (TGA 6, Perkin Elmer, USA). The samples were heated at a heating rate of 30 K min^{-1} with the scanning temperature ranging from 50 to 900 ℃, under an atmospheric nitrogen flow at the flow rate of 20 ml min^{-1}, to check for the presence of trapped solvent contained in the sample.

The thermal profile of the binary blends was then characterized using TGA by scanning the samples in the similar temperature range at 10 K min^{-1}, under the similar flow rate of nitrogen gas.

3.2.2.4.4.2 Thermo-kinetic analysis of PVC/mcl-PHA

Thermo-kinetics of PVC and the PVC/PHA binary blends were studied by using the data from TGA measurements following similar procedure as detailed in Section 3.1.3.3.3.

3.2.2.4.4.3 Thermal behavior of PVC/mcl-PHA studied by DSC

T_g measurements for PVC and the binary blends were carried out using a Perkin Elmer Pyris DSC 6 thermal analyzer (USA) at a programmed heating rate of 20 ℃ min^{-1}. The experiments were carried out in the temperature range of 35 to 130 ℃ under dry nitrogen atmosphere at a flow rate of 20 ml min^{-1}. For PVC, approximately 5.0 mg of sample in the compact powder form was loaded in the aluminium pan while for the

PVC/mcl-PHA blends, 5.0 mg of sample films were cut into small pieces and were used in the testing. The sample was scanned twice with the first scan heating from 35 to 120 ℃ to remove the thermal history of the sample, subsequently cooled to 35 ℃ and scanned for the second time up to the temperature of 130 ℃. The T_g of the sample was determined as the onset of steep change in enthalpy for the second scan. All temperatures were recorded in degrees Celsius.

3.2.2.4.4.3.1 Theoretical calculation of T_g using Gordon-Taylor equation

Calculation of k-values for Gordon-Taylor equation using Polymath software:

The theoretical value of T_g for the binary blends can be calculated from the Gordon-Taylor Equation whereby the *k*-fitting parameter was determined by solving simultaneous equations using the Polymath ® software as well as experimental T_g substitution approach. The Gordon-Taylor Equation is shown as:

$$T_g = (W_{PHA}\ T_{g_{PHA}} + k\ W_{PVC} T_{g_{PVC}}) / (W_{PHA} + k\ W_{PVC}) \quad (3.6)$$

where T_g is the glass transition temperature of the polymer blend; $T_{g\,\mathrm{PHA}}$ and $T_{g\,\mathrm{PVC}}$ is the glass transition temperature of the respective polymer; *W* is the weight fraction of the individual component; *k* is the model specific parameter

3.2.2.4.4.3.2 Theoretical calculation of T_g using Fox equation

The T_g of the binary blends can also be predicted from the Fox equation as shown in the following equation:

$$1/T_g = (W_1/\ T_{g_1}) + (W_2\ /\ T_{g_2}) \quad (3.7)$$

where W_1 and W_2 represents the weight fractions of mcl-PHA and PVC; T_g, T_{g1} and T_{g2} are the glass transition temperatures of the binary blend, mcl-PHA and PVC.

The difference of the experimental T_g and that T_g from the Fox equation can be used to correlate the polymer-plasticizer affinity as the intermolecular forces present in the polymer system were not taken into consideration in the Fox equation.

3.2.2.4.5 Dynamic Mechanical Analysis

Miscibility between two polymers is usually characterized using dynamic mechanical analysis (DMA). DMA is also an alternative method to study the viscoelastic properties of a polymer blend e.g. storage modulus (*E'*), loss modulus (*E''*) and loss angle tangent (tan δ) (Walsh et al., 1982). Generally for an immiscible blend, the loss modulus curves show the presence of two damping peaks corresponding to the T_gs of individual components (George et al., 1997). For a highly miscible blend, the curve shows only a single peak, whereas broadening of the transition occurs in the case of partially miscible systems (Varughese et al., 1988).

In this study, viscoelastic properties of PVC/PHA polymer blends were characterized by TA DMA Q800 dynamic mechanical analyzer using a tension film clamp. Before subjected to the mechanical testing, sample films were prepared using a hot press (Carver Instrument, Model C, S/N 40000-715). Specimens were heated pressed to a specific temperature at 4.5 psi applied load and held for 2 min, followed by cooling to ambient temperature.

Strips of thin films with 30.0 mm fixed length were then mounted to the TA DMA Instrument and the measurements were made under the temperature scan mode ranging from -40 to 120 ℃, under a heating rate of 5 ℃ min^{-1} and at a frequency of 1 Hz. Liquid nitrogen was used in the Cryospeed, the cooling accessory, to achieve sub-ambient temperature in this testing.

Mechanical properties of polymer show profound changes in the region of the glass transitions. For example, the elastic modulus may decrease by a factor of over 1000

times as the temperature is raised through the glass transition region. For this reason, T_g can be considered the most important material characteristic of a polymer as far as mechanical properties are concerned. Besides that, T_g has important theoretical implications for the understanding of the macromolecular mobility in the polymer. T_g can be determined from the onset of the storage modulus (*E'*) drop, the onset or peak of loss modulus (*E''*), and the onset or peak of the tan δ curve (Menard, 1999). In our analysis, the T_g values were determined from the maximum peak of loss modulus curves. All temperatures were recorded in degrees Celsius.

3.2.2.4.5.1 Study of elastic modulus of PVC/mcl-PHA blends

Elastic modulus is the mathematical description of a polymer's tendency to be deformed elastically when a force is applied to it. It is a measure of the stiffness of a component. A stiff component, with a high elastic modulus, will show much smaller changes in dimensions. In general, engineering applications view stiffness as a function of both the elastic modulus and the geometry of a component.

The elastic modulus equation was adapted from the model equation in the TA DMA Q800 Equation Guideline, with the relationship of the stiffness, elastic modulus and sample's geometry for the sample analyzed on a film tension clamp as shown below:

$$K = (A \, x \, E) \, / \, L \qquad (3.8)$$

where *K* is stiffness (N m^{-1}); *E* is elastic modulus (G N m^{-2}); *A* is sample cross-sectional area (cm^2) and *L* is sample length (cm). As the sample has a very small area as compared to its length, no end effects correction is needed, therefore the modulus equation is derived as followed:

$$E = K_s \, x \, L/A \quad (3.9)$$

where E is elastic modulus (G N m^{-2}); A is sample cross-sectional area (cm^2); L is sample length (cm); K_s is measured stiffness (N m^{-1})

3.2.2.4.5.2 Comparison of storage modulus for PVC and PVC/mcl-PHA blends

The storage modulus (*E'*) describes the ability of a polymer to absorb or store energy. This parameter provides an indication of rigidity of the polymer and its ability to resist deformation under an applied dynamic stress. High storage modulus indicates rigid material (Sin, 1998). The decrease in *E'* indicates a correlation between film stiffness and the temperature at which the films become rubbery.

The compositions possess a high storage modulus below the onset of the T_g, indicative of a rigid polymer. During the transition from glass to rubber, the modulus falls precipitously. At the end of the glass transition region, the curves display a short plateau which is followed by a drop in modulus due to viscous flow. This plateau defines the temperature regime where the composition is soft, flexible and rubber-like (Nielsen & Landel, 1994). A typical storage modulus versus temperature curve is shown in Fig. 3.7.

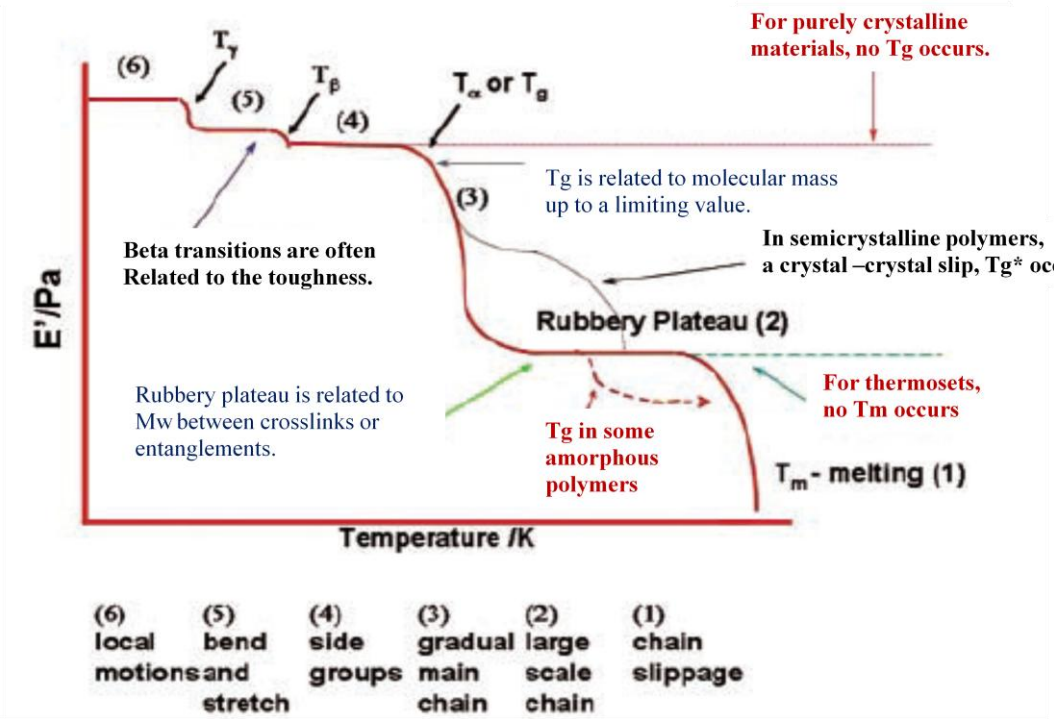

Fig. 3.7 Storage modulus values change with the temperature and transitions in polymers can be seen as changes in the E' curve (Perkin Elmer)

In this study, the storage moduli of the binary blends were compared with the control PVC to investigate the effect of mcl-PHA on the rigidity of the polymer blends.

CHAPTER 4

THERMAL DEGRADATION OF MEDIUM-CHAIN-LENGTH POLY(3-HYDROXYALKANOATES) (MCL-PHA)

4.1. Thermal properties of mcl-PHA before and after thermal treatment

4.1.1 Characterization by thermogravimetric analysis (TGA)

Thermogravimetric analysis (TGA) was employed to compare the thermal stability of oleic acid and SPKO-derived mcl-PHA. Fig. 4.1 showed the TGA thermogram of oleic acid-derived mcl-PHA, which appeared to proceed by one-step decomposition between 183 to 528 ℃, represented by a single peak in the corresponding derivative thermogravimetric (DTG) curve. During the degradation step, drastic weight loss of about 99.1% was observed with only traces of carbonaceous residues (carbon black) remained.

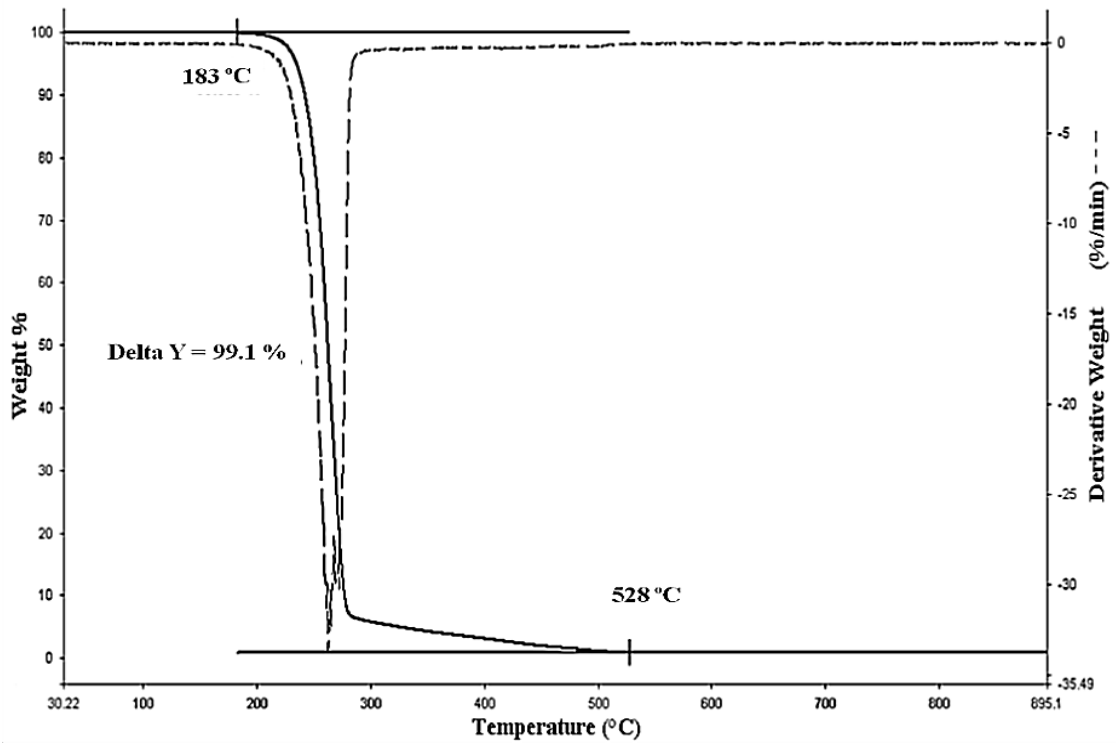

Fig. 4.1 TGA thermogram of mcl-PHA derived from oleic acid

For SPKO-derived mcl-PHA, the thermal degradation proceeded in one-step process between 196 to 555˚C as shown in Fig. 4.2, which was represented by a single peak in the DTG curve. During the degradation step, weight loss of about 97.7% was observed with only traces of residues remained.

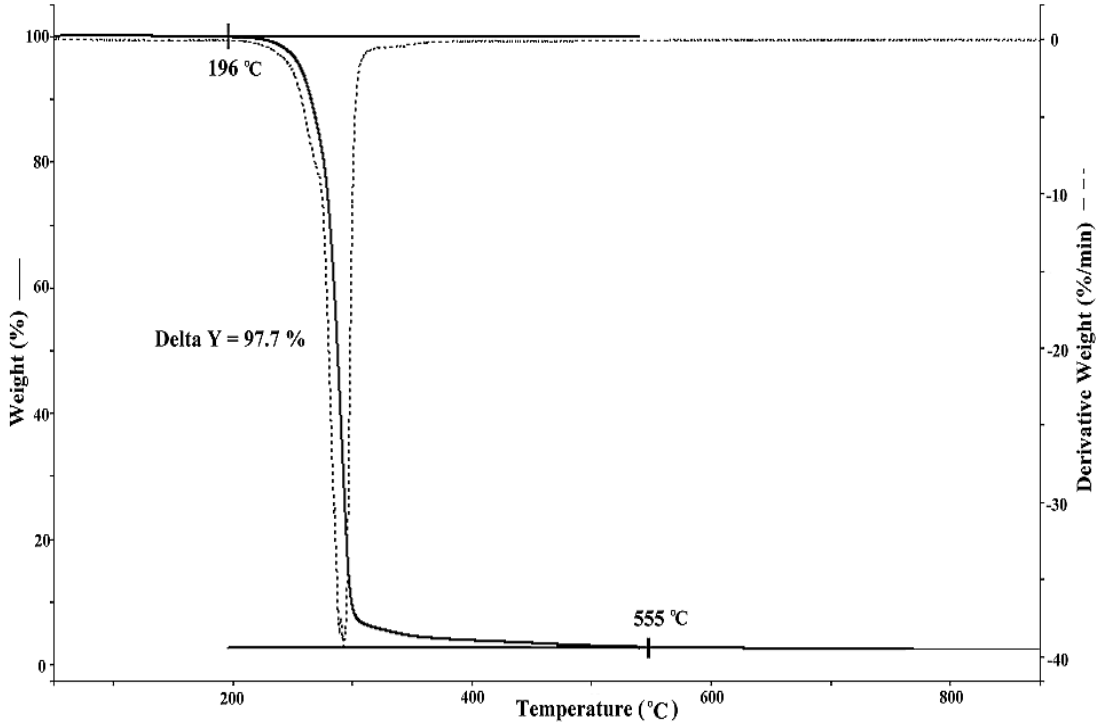

Fig. 4.2 TGA thermogram of mcl-PHA derived from SPKO

TGA was also employed to compare the thermal stability of control and heat-treated PHA. Fig. 4.3 showed the thermograms for mcl-PHA derived from oleic acid and those that had been subjected to thermal treatments. All the curves had the similar shape with one-stage of degradation. The control, 160˚C and 170˚C-treated PHA started to decompose at around 200 to 250˚C, with the control PHA registering a lower initial degradation temperature. The lowest initial degradation temperature was however registered by the 180˚C-treated PHA which started to decompose at around 100 ℃. A possible explanation could be that the 160˚C and 170˚C-treated PHA were slightly partially degraded, leaving behind polymer chains which were more heat stable, thus

showing higher thermal stability. The 180˚C-treated PHA sample contained lower-molecular weight species which could be more easily disintegrated by heating.

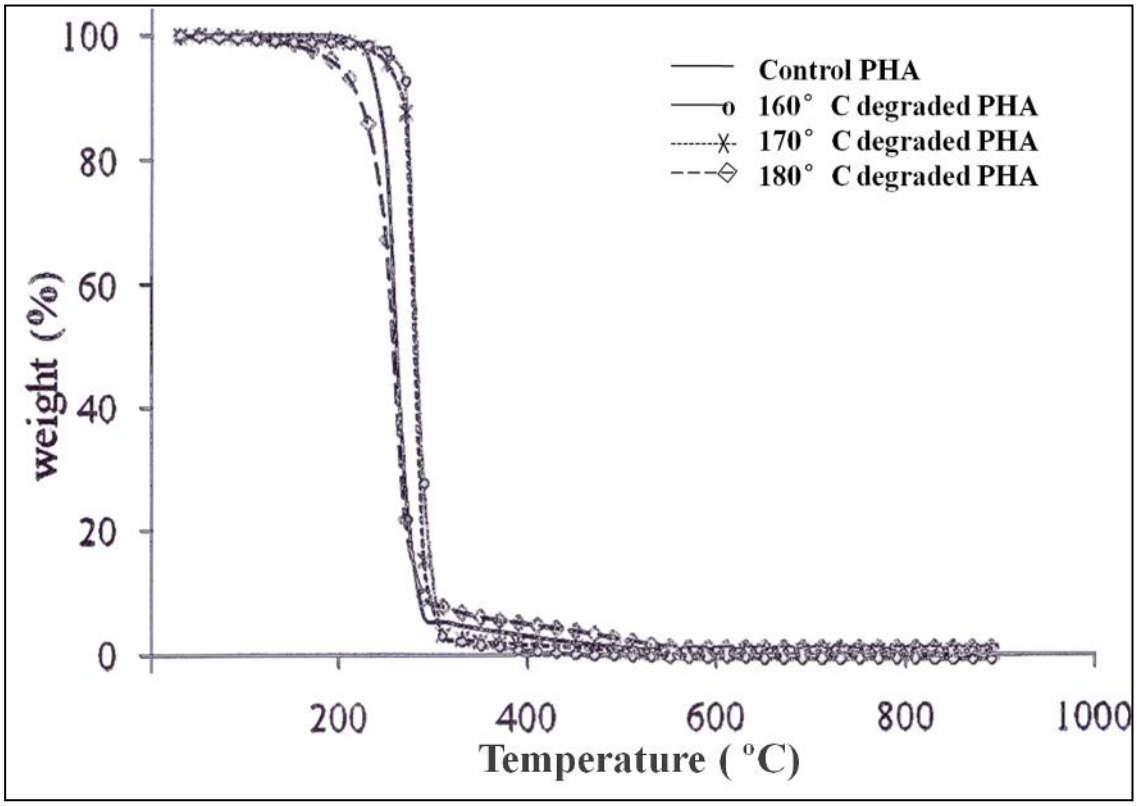

Fig. **4.3** Relative thermal stability of control and heat-treated mcl-PHA derived from oleic acid, as indicated by different TG curves at 10˚C min^{-1}

For mcl-PHA derived from SPKO, the weight loss curves (TG) for all heat treated and control PHA were shown in Fig. 4.4. As can be seen in the figure, PHA heat treated at 160°C and 170°C showed precipitous weight loss in the temperature range of 220 to 340°C, with the onset temperatures shifted to a higher temperature than the control PHA. However, the decomposition temperature for 180°C-treated PHA was shifted to lower temperature range of about 180 to 330°C. TGA indicated that 190˚C-treated PHA sample showed the lowest thermal stability. Heating mcl-PHA at 160°C, 170°C and 180℃ resulted in partially intact PHA with comparatively stable

decomposition products, whereas mcl-PHA was almost completely decomposed at 190°C, thus accounting for the relative thermal stability of the former.

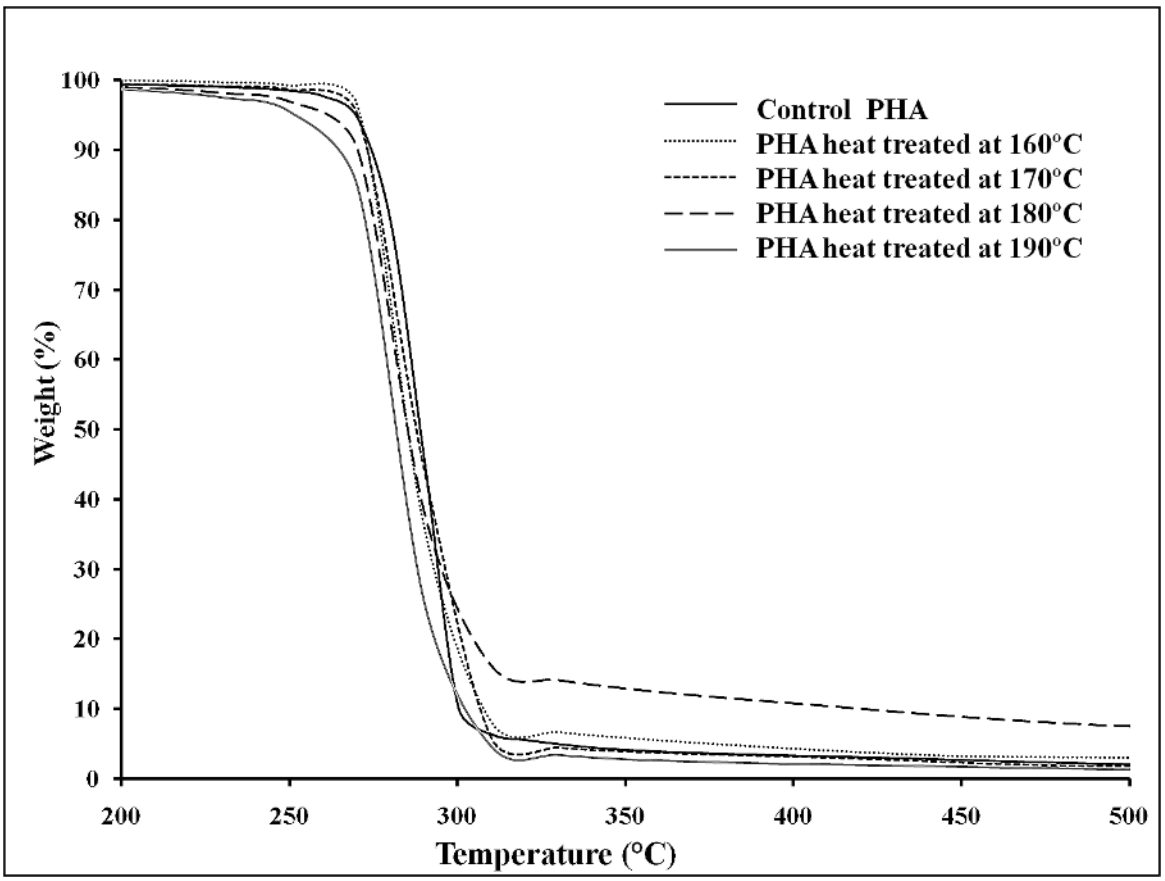

Fig. 4.4 Relative thermal stability of control and heat-treated PHA derived from SPKO as indicated by different TG curves at 10˚C min^{-1}

4.1.2 Kinetics of thermodegradation of mcl-PHA

Kinetics of mcl-PHA during thermal degradation was studied using Kissinger's method through TGA (Doyle, 1961; Erceg et al., 2005). PHA samples were analyzed by TGA non-isothermal procedures at different heating rates of 10, 15, 20, 25 and 30 K min^{-1}. Fig. 4.5 (a) and (b) showed TGA and DTG thermograms for oleic acid-derived mcl-PHA at multiple heating rates. All thermograms in Fig. 4.5 (A) showed only one-step degradation process between 200 to 400˚C. Increasing heating rate shifted the onset

temperature higher. From Fig. 4.5 (B), temperature at the lowest point of the DTG curve peak corresponded to the temperature where the rate of degradation was at maximum.

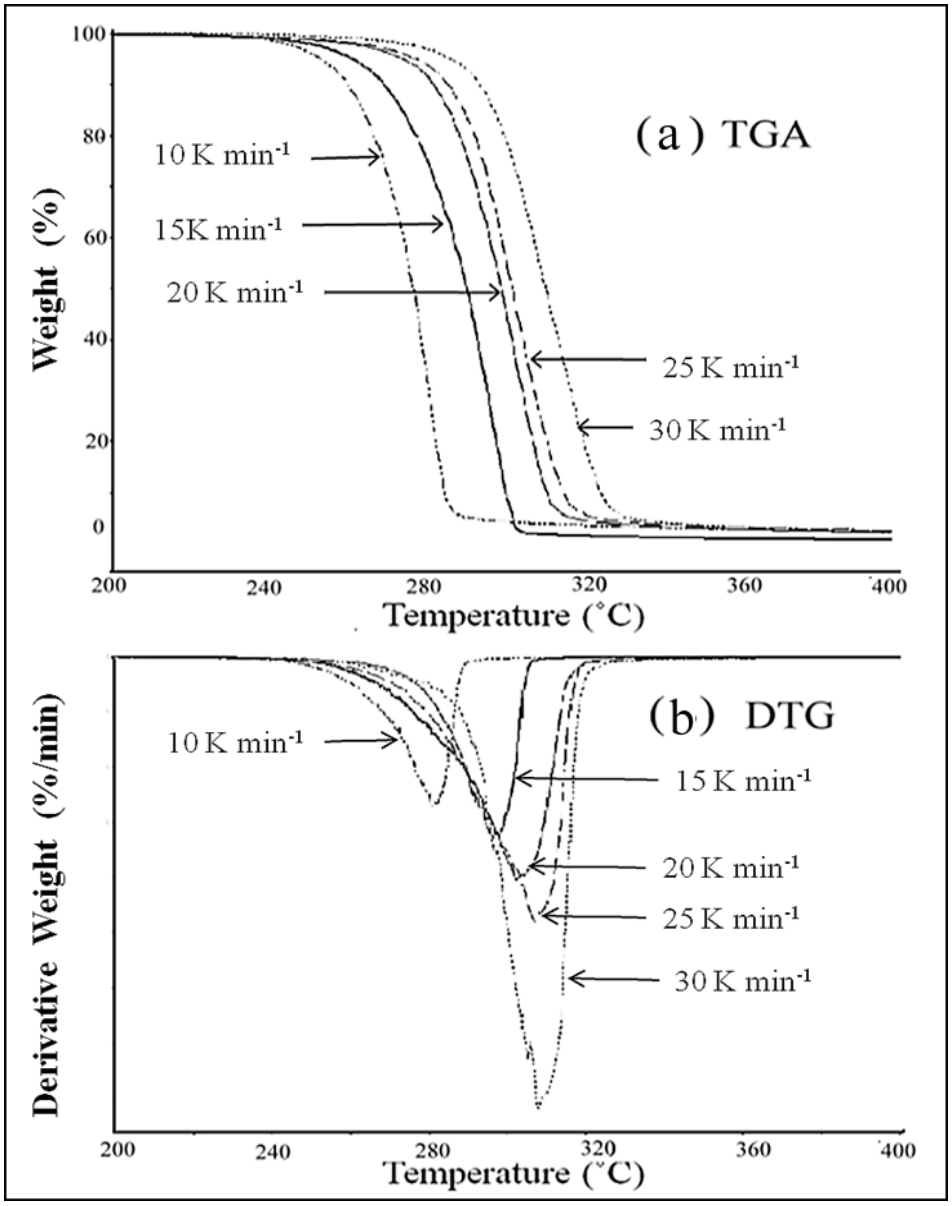

Fig. 4.5 (a) TGA and (b) DTG curves of oleic acid-derived mcl-PHA at multiple heating rates

To obtain thermo-kinetic parameters for oleic acid-derived mcl-PHA through Kissinger equation, the relationship between heating rates and temperature at maximum degradation was shown in Table 4.1, and the plot of $-\ln (q/T_p^2)$ vs. $1/T_p$ was displayed in Fig. 4.6. The gradient of the plot was E_d/R, thus degradation activation energy, E_d could

be calculated. The intercept at *y*-axis was equal to –ln (AR/E_d), which then enabled the pre-exponential factor, *A*, to be calculated. The calculations of E_d, *A* and ΔS for the PHA_{OA} samples were described in Appendix A.

Table 4.1 Data of thermo-kinetic parameters for thermal degradation of oleic acid-derived mcl-PHA

Heating rate, q / K min^{-1}	**Temperature at maximum degradation, T_p / K**	**$1/T_p$ (x10^3 K)**	**-ln (q/T_p^2)**
10	552	1.81	10.33
15	571	1.75	9.99
20	576	1.74	9.72
25	578	1.73	9.50
30	582	1.72	9.33

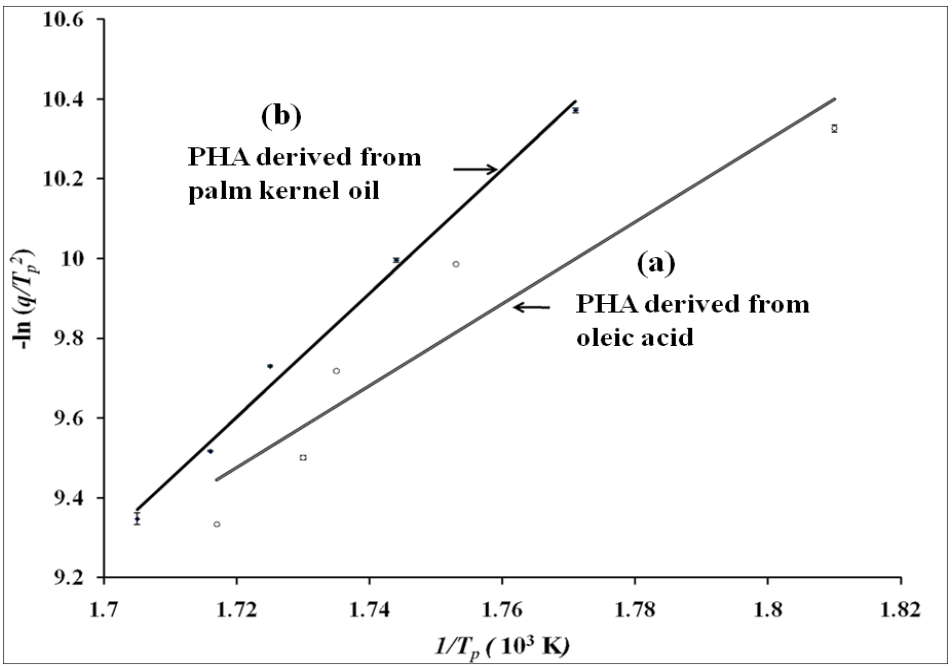

Fig. 4.6 Kissinger plot for determining the activation energy of thermal degradation, E_d, of the PHA produced from (a) oleic acid and (b) palm kernel oil

The degradation activation energy, E_d and pre-exponential factor, A for mcl-PHA derived from oleic acid were 85.3 kJ mol^{-1} and $6.07x10^5$ s^{-1} respectively. The change of activation entropy (ΔS) for the PHA degradation was -139.4 kJ K^{-1} mol^{-1}, and the relatively high E_d indicated that thermal degradation can only occur at high temperatures.

For SPKO-derived mcl-PHA, the TGA and DTG thermograms at five different heating rates were shown in Fig. 4.7 and Fig. 4.8, respectively. All the TGA thermograms showed a smooth one-step weight loss curve between 200 to 500˚C. Increasing heating rate shifted the TGA and DTG curves to higher temperature zone.

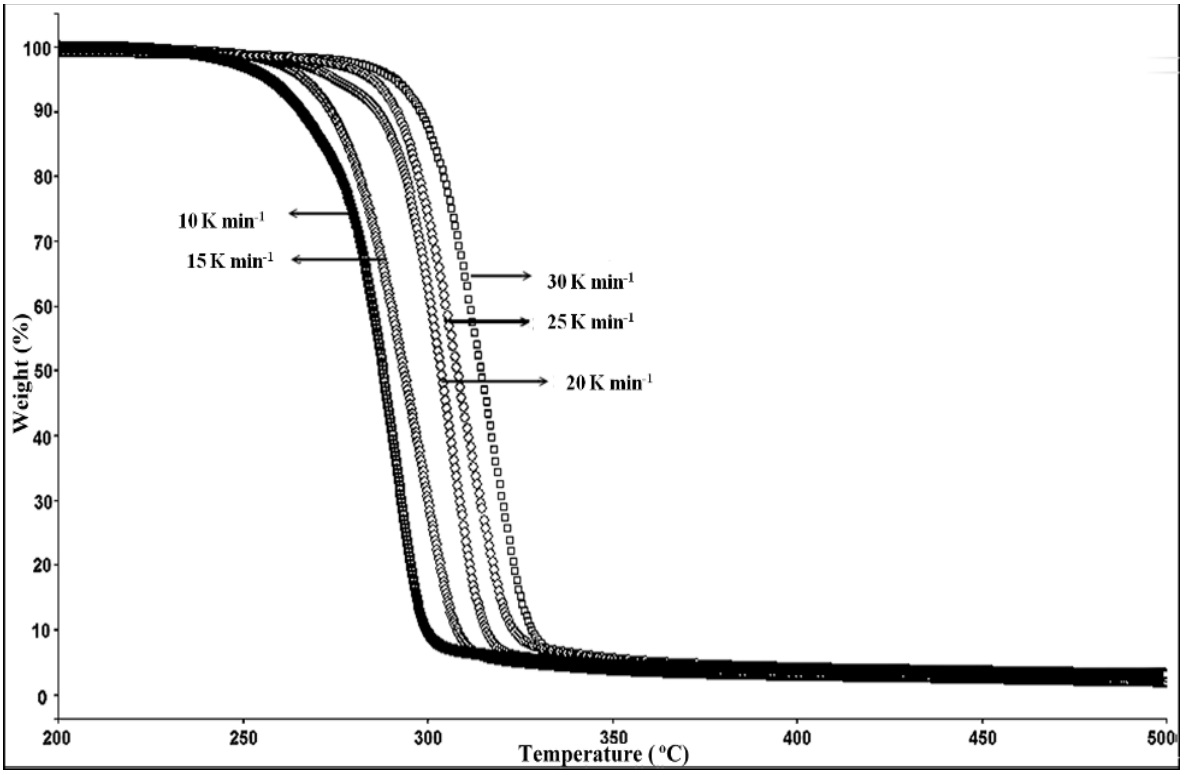

Fig. 4.7 TGA curves of SPKO-derived mcl-PHA measured at different heating rate

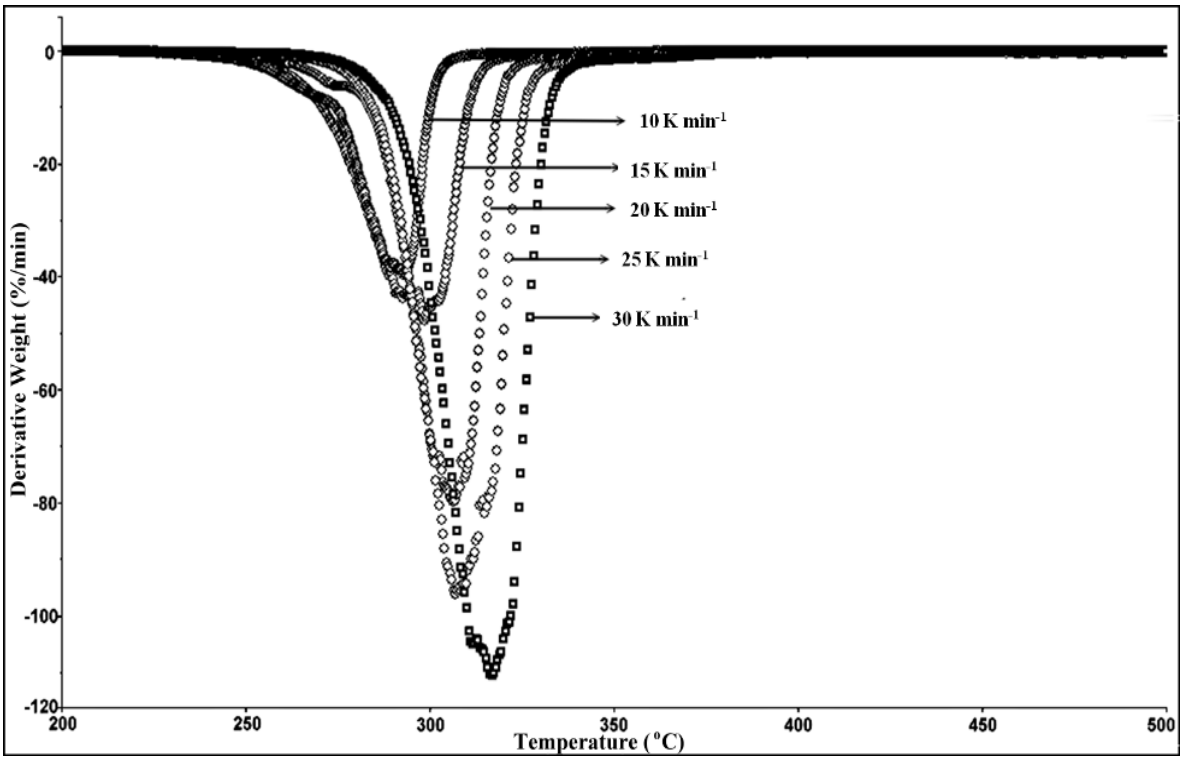

Fig. 4.8 DTG curves of SPKO-derived mcl-PHA measured at different heating rate

The relationship between heating rate and temperature of maximum degradation for SPKO-derived PHA was shown in Table 4.2. Calculations of E_d, A and ΔS for PHA_{SPKO} samples were described in Appendix A.

Table 4.2 Data of thermo-kinetic parameters for thermal degradation of SPKO-derived mcl-PHA

Heating rate, q / K min^{-1}	**Temperature at maximum degradation, T_p / K**	**$1/T_p$ (x10^3 K)**	**-ln (q/T_p^2)**
10	565	1.77	10.37
15	574	1.74	10.00
20	580	1.73	9.73
25	583	1.72	9.52
30	587	1.71	9.33

E_d and A for the SPKO-derived mcl-PHA were calculated to be 128.9 kJ mol^{-1} and $1.15x10^{10}$ s^{-1}, respectively. The change of activation entropy (ΔS) estimated from equation (3.4) had a value of -57.6 J K^{-1} mol^{-1}. The relatively small ΔS indicated that the mcl-PHA may be thermally unstable at high temperatures.

The E_d for mcl-PHA made from oleic acid was much lower than mcl-PHA made from SPKO. This indicated that mcl-PHA derived from SPKO was more thermal stable than that derived from oleic acid. The difference in the thermal stability was due to the fact that the mcl-PHA produced from SPKO consisted of a mixture of monomer units, derived from the carbon substrate of a mixture of medium- and long-chain fatty acids, whereas the oleic acid-derived mcl-PHA was produced from a single type of fatty acid.

4.1.3 Characterization by differential scanning calorimetry (DSC)

The thermal properties for both oleic acid and SPKO-derived mcl-PHA before and after thermal treatments, studied by DSC analysis were shown in Table 4.3. The DSC thermograms of PHA samples which indicated T_g, T_m and ΔH_m were shown in Appendix B.

Table 4.3 Thermal properties of mcl-PHA derived from oleic acid and SPKO before and after thermal treatments

Thermal properties	**Oleic acid derived PHA**			**SPKO derived PHA**		
	T_g (˚C)	T_m (˚C)	ΔH_m (J g^{-1})	T_g (˚C)	T_m (˚C)	ΔH_m (J g^{-1})
Control	-44.1	n.d	n.d	-44	45	9.7
PHA heat treated at 160˚C	-44.6	n.d	n.d	-44.2	40	8.6
PHA heat treated at 170˚C	-45	n.d	n.d	-45	38	8.3
PHA heat treated at 180˚C	-48.1	n.d	n.d	-48.2	n.d.	n.d.
PHA heat treated at 190˚C	-	-	-	-53	n.d.	n.d.

T_g: glass transition temperature; T_m: melting temperature; ΔH_m: enthalpy of fusion; n.d: not detected

For mcl-PHA derived from oleic acid, a low T_g around -44.1˚C was observed and there was a decrease in T_g from -44.6˚C to -48.1˚C when PHA were heat treated at 160˚C to 180˚C. The decrease was primarily due to the disruption in the tight arrangement of polymer chains where the weak intermolecular forces were no longer effective in holding the polymer chains together at high temperatures. However no melting temperature (T_m) and enthalpy changes were observed in both control and heat-treated mcl-PHA derived from oleic acid, indicating that this polyester was an amorphous elastomer.

For mcl-PHA derived from palm kernel oil, low T_g around -44˚C was observed and there was a shift of T_g from -44.2˚C to -53˚C when the PHA was heat treated at

160˚C to 190˚C. The decrease in T_g was attributed to the defects in arrangement of polymer chains in an ordered manner as the intermolecular attractions weakened at high temperatures. The melting temperature (T_m) and enthalpy of fusion (ΔH_m) of the polymer can be detected in control, 160 ℃ and 170 ℃-treated PHA only and the crystallinity of the polymer decreased as reflected in the decrease in ΔH_m. A loss in crystallinity in 180 ℃ and 190 ℃-treated PHA was mainly due to the increased mobility effect of the polymer chains where they overlapped at high temperature of decomposition. The crystalline portions of the polymer were destructed when thermal decomposition temperature exceeds a certain threshold (Chen et al., 2009).

4.2 Morphological properties of mcl-PHA degradation products

The morphology of the oleic acid-derived mcl-PHA was observed to change following the thermal treatment. During the heat-treatment at 160 ℃, 170 ℃ and 180 ℃, the color of the mcl-PHA changed from an initial yellow to brown and dark brown with black precipitates, while viscosity of the sample decreased. PHA that had been heat-treated at 160˚C and 170˚C produced compounds which did not vaporize. However, when heated at 180 ℃, evolution of gaseous products with pleasant odors accompanied by bubbles formation in the sample was observed. According to Gonzalez et al. (2005) when PHA was thermolyzed, monomeric and oligomeric (dimeric, trimeric or tetrameric) volatile products might be generated. However, oligomers larger than tetramers were not volatile enough and would remain within the sample. The vapors changed the color of moist blue litmus paper to red almost immediately indicating an acidic property. It is believed that the vapors were composed of low molecular weight esters and hydroxyl acids.

For SPKO-derived mcl-PHA, PHA film started to melt when the temperature reached 40˚C and formed a yellowish gel beyond 50ºC. As mcl-PHA derived from

SPKO had a melting point around 45℃, heating the polymer above the melting temperature will change the physical state from solid to gel through the weakening of intermolecular forces that hold the polymer chains together. However, in 160˚C and 170˚C-treated PHA, the elastic film formed back when cooled to room temperature while 180˚C and 190˚C thermal treatments produced the PHA in the permanent viscous liquid form. It is suggested that partial crystallinity remained in 160 ℃ and 170 ℃-treated PHA, which allowed them to form back the morphology resembling the original polymer. The color of mcl-PHA was changed from yellow to brown/ dark brown followed by dark brown with black carbon precipitates as the decomposition temperature increased from 160˚C to 190˚C. PHA heat treated at 160˚C and 170˚C produced species that did not vaporize during thermal processing. However evolution of vapors with a pleasant odor was detected when the PHA was heated at 180˚C and 190˚C. Vapors from the 190˚C degrading sample turned moist blue litmus paper to red almost immediately while vapors from the 180˚C degrading sample took a few minutes to change the color of moist litmus paper. It is suggested that the vapors were composed of low molecular weight oligoesters and acids.

4.3 Analysis of the changes in molecular weight and acidity of degradation products

4.3.1 End group analysis

A PHA polymer chain contains equimolar of hydroxyl end group and carboxyl end group. Thus, the acid number of PHA can be determined by titrating the carboxylic end groups with standardized potassium hydroxide solution. Number average molecular weight (M_n) and concentration of carboxylic acid terminals in the PHA are related to acid number and thus can be determined from the acid value of the polymer. The calculations of acid number, M_n and concentrations of -COOH terminals for mcl-PHA before and thermal treatments were shown in Appendix C.

The oleic acid-derived PHA had an acid number of 4.0 $\pm$ 0.04 mg KOH g^{-1}. This value increased following temperature treatment: 5.3 $\pm$ 0.01 mg KOH g^{-1} (160 ℃), 14.6 $\pm$ 0.02 mg KOH g^{-1} (170 ℃) and 33.1 $\pm$ 0.3 mg KOH g^{-1} (180 ℃). A PHA polymer chain contains one unit of hydroxyl and one unit of carboxylic end group. Thus the number of the carboxylic terminals is equal to the number of the polymer chain. The concentration of carboxylic acid terminals and the number average molecular weight (M_n) were then determined. The control mcl-PHA derived from oleic acid had the highest M_n of 13900 g mol^{-1}, while the M_n of the heat-treated PHA decreased with increasing degradation temperatures. The M_n of the 160 ℃, 170 ℃ and 180 ℃-treated PHA was 77%, 28%, and 12% of the M_n of the control PHA, respectively. The observed progressive decrease in M_n was proposed to proceed *via* the chain scission of the polymer during thermal degradation. Concentration of carboxyl end groups also increased with higher temperature, presumably due to faster rate of decomposition. The acid number, concentration of terminal carboxylic acid and the number average molecular weight of both control and heat-treated PHA were shown in Table 4.4. The data supported the view that mcl-PHA were thermally decomposed at 160 ℃, 170 ℃ and 180 ℃. However the M_n results obtained were absolute values and were independent of the distribution of molecular weights in the polymer.

Table 4.4 End group analysis of oleic acid-derived mcl-PHA before and after thermal treatments

PHA samples	**Control**	**Heat treated at 160 ℃**	**Heat treated at 170 ℃**	**Heat treated at 180 ℃**
Average acid number (*AN*) / mg KOH g^{-1}	4.0 ± 0.04	5.3 ± 0.01	14.6 ± 0.02	33. 1 ± 0.3
Number average molecular weight (M_n) /g mol^{-1}	13900 ± 145	10600 ± 28	3900 ± 6	1700 ± 14
-COOH terminal concentration /mol g^{-1}	7.2 x 10^{-5}	9.4 x 10^{-5}	2.6 x 10^{-4}	5.9 x 10^{-4}

Table 4.5 summarized the acid number, number average molecular weight and –COOH terminal concentration of the SPKO-derived PHA as well as the 160˚C, 170˚C, 180˚C and 190˚C-treated PHA. Mcl-PHA derived from SPKO contained an initial acid number of 5.2 ± 0.01 mg KOH g^{-1}. The acid number of PHA increased when they were heat treated at temperatures of 160˚C, 170˚C, 180˚C and 190˚C. The heat-treated PHA also showed higher concentration of carboxylic terminals than the control PHA. Control mcl-PHA showed initial M_n of 10900 ± 15 g mol^{-1}. Heating PHA polymer at 160˚C, 170˚C and 180˚C for 30 minutes resulted in the progressive reduction of M_n value, producing a mixture of low molecular weight hydroxyl alkanoic acids with 77.3%, 64.8% and 41.4% of initial M_n value, respectively. When PHA sample was heated at 190˚C under the same condition, the M_n value of the degradation products was drastically

reduced to 14.6% of initial M_n value. The observed progressive decrease in M_n was proposed to proceed *via* the chain scission of PHA at moderately high temperature decomposition. The M_n results obtained from end group analysis were absolute values and were independent of the distribution of molecular weights in the polymer.

Table 4.5 End group analysis of SPKO-derived mcl-PHA before and after thermal treatments

PHA samples	**Control**	**Heat treated at 160 ℃**	**Heat treated at 170 ℃**	**Heat treated at 180 ℃**	**Heat treated at 190 ℃**
Average acid number (*AN*) / mg KOH g^{-1}	5.2 $\pm$ 0.01	6.7 $\pm$ 0.2	7.9 $\pm$ 0.04	12.4 $\pm$ 0.2	35.3 $\pm$ 0.6
Number average molecular weight (M_n) / g mol^{-1}	10900 $\pm$ 15	8400 $\pm$ 197	7100 $\pm$ 32	4500 $\pm$ 64	1600 $\pm$ 26
-COOH terminal concentration /mol g^{-1}	9.2 x 10^{-5}	1.2 x 10^{-4}	1.4 x 10^{-4}	2.2 x 10^{-4}	6.3 x 10^{-4}

4.3.2 Gel permeation chromatography (GPC) analysis

The average molecular weight and molecular weight distribution of both oleic acid and SPKO-derived control and heat-treated polymers were determined by GPC analysis. The GPC column was calibrated using polystyrene (PS) standards, and hence the number-average molecular weight (M_n) and weight-average molecular weight (M_w) values were relative to PS. The GPC chromatograms of PHA samples were shown in Appendix D and the results were summarized in Table 4.6. Results showed that M_n of oleic acid-derived PHA decreased with increase in polydispersity index (*PDI*) when the polymers were heat treated from 160˚C to 180˚C. The decrease in M_n values followed the similar trend as in the observed results of the end group analysis. Increased *PDI* in heat-treated PHA indicated the polymers had broader molecular weight distribution with more lower-molecular-weight species generated by the random scission of the ester linkages, as a result of thermal decomposition at high temperature.

Table 4.6 Average molecular weight and molecular weight distributions of control and heat-treated mcl-PHA derived from oleic acid and SPKO

GPC analysis	**Oleic acid-derived mcl-PHA**			**SPKO-derived mcl-PHA**		
	[1]M_n (Da)	**[2]M_w (Da)**	**[3]*PDI***	**M_n (Da)**	**M_w (Da)**	***PDI***
Control PHA	30600	60900	2.0	44000	92200	2.1
PHA heat treated at 160˚C	29300	71400	2.4	41300	78700	1.9
PHA heat treated at 170˚C	3500	16200	4.7	39100	74400	1.9
PHA heat treated at 180˚C	2200	9000	4.0	13700	28500	2.1
PHA heat treated at 190˚C	-	-	-	3100	13300	4.3

[1]M_n: number-average molecular weight; [2]M_w: weight-average molecular weight; [3]*PDI*: polydispersity index, defined by M_w/M_n

Table 4.7 also showed that M_n of SPKO-derive PHA decreased from 41300 g mol^{-1} to 3100 g mol^{-1} when the polymers were heat treated from 160˚C to 190˚C. These results corroborated well with the decrease in M_n values in end group analysis as well. Increase in polydispersity index (*PDI*) in 180 ℃ and 190 ℃-treated PHA was observed, and this indicated that these polymers had broader molecular weight distribution, as various lower-molecular-weight species were generated at high temperature of degradation.

4.3.3 Acidity of degradation products: oligomeric hydroxyalkanoic acids

Low molecular weight hydroxyalkanoic acids are weak acids in nature and dissociate partially in aqueous environment as shown in the equilibrium expression below:

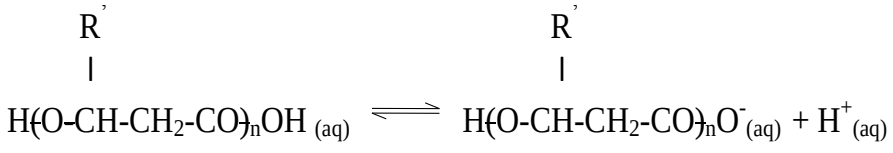

(4.1)

The acid dissociation constant, K_a of hydroxyl acid is given by the following equation:

$$K_a = [R\text{-}COO^-][H^+]/[R\text{-}COOH] \quad (4.2)$$

where 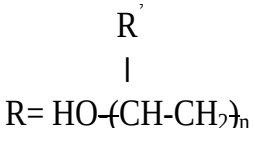

Ionization of these weak acids in water is an endothermic process. An increase in temperature would favor the formation of hydrogen ions and the conjugate base. Therefore dissolving the decomposition products in distilled water at 95 ℃ would results in higher dissociation of the weak acids in the aqueous solution.

Hydroxyalkanoic acid is acidic in nature because the dissociation of the weak acid gives a hydroxy-carboxylate ion and hydrogen ion in aqueous. Both the carboxyl group and the carboxylate anion are stabilized by resonance. This stabilization of conjugate base leads to an increased acidity of the carboxylic acid (R-COOH). This also shifts the tendency of the equilibrium to the right hand side. The resonance effect described here is the delocalization of the p-orbital π electron as shown in Fig. 4.9.

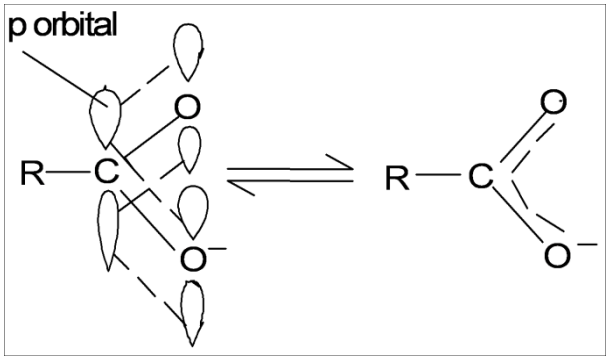

Fig. 4.9 Resonance structure of carboxyl group

Electronegative substituents increase the acidity of carboxylic acid by withdrawing electrons from the carboxyl group and lower the negative charge on carboxylate ion and therefore stabilize the ion. This is illustrated in Fig. 4.10.

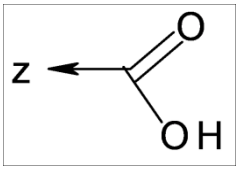

Fig. 4.10 Electron withdrawal by Z, an electronegative substituent

In the case of hydroxyalkanoic acids, hydroxyl group is the electronegative substituent which withdraw π electron from carboxyl group. The closer the substituent to the carboxyl group, the greater is its effect and thus the stronger is the acid. However, hydrogen and alkyl substituent on the α-carbon assist in inductive electron shift on the carboxyl group, where electrons are being donated to the carbonyl group and thus decreasing the acidity of carboxylic acid. This is illustrated in Fig. 4.11.

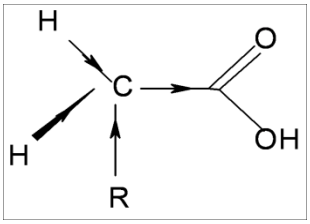

Fig. 4.11 Inductive effect of R, alkyl group

The influence of carbon chain length and structural features is significant for the acidity of oligomeric hydroxyalkanoic acids. The larger the number of carbon atoms in the acid, the stronger the electron donating effect of alky group and therefore the weaker is the acid. Bulky alkyl substituent will also insulate the electronegativity of hydroxyl group to the carboxyl group and thus reduce the acidity. This is the reason for the insolubility of high molecular weight hydroxyl alkanoic acids in water.

For oleic acid-derived mcl-PHA, the acidity of 160˚C degradation products could not be determined as they were partially degraded polymer with high M_n value of 10600 g mol^{-1}. These high molecular weight polyesters appeared to be insoluble in water and thus unable to ionize in aqueous environment. Both 170˚C and 180˚C degradation products were dissolved in distilled water at 95 ℃ and gave pH values of 5.7 $\pm$ 0.2 and 5.8 $\pm$ 0.01, respectively. However, experimental pH values obtained were not the actual pH values for the hydroxyl acids as hydrogen ions in the weak acid solution may contributed by the dissociation of weak carbonic acid as well as water molecule itself. Thus the actual pH values for both 170˚C and 180˚C degradation products were determined through the calculation of acid dissociation constant (K_a) and pK_a of dissociable hydroxyl acids. The smaller the pK_a value, the stronger is the acid.

The degree of dissociation (α) of the hydroxyl acids and the standard Gibbs free energy change (ΔG°) from the dissociation of PHA degradation product at 170˚C and 180˚C were also calculated using the K_a and pK_a values. Determinations of pH, K_a, pK_a, α and ΔG° of PHA degradation products were described in Appendix E. The calculated pH, K_a, pK_a, α and ΔG° values were shown in Table 4.7. At 95 ℃, $\Delta G^\circ > 0$ for both 170 ℃ and 180 ℃- treated PHA, showing that dissociation of the weak hydroxyalkanoic acids into hydroxyl-carboxylate ion and hydrogen ion was not spontaneous, requiring energy input into the system to occur. ΔG° was lower for 180 ℃-treated PHA compared

to 170 ℃-treated PHA, showing that dissociation of 180 ℃ decomposition products in aqueous solution occurred more readily in aqueous solution at 95 ℃ compared to 170 ℃ decomposition products.

Table 4.7 Effective concentration of carboxyl end groups, acid dissociation constant (K_a), pK_a, pH, degree of dissociation (α) and standard Gibbs free energy change (ΔG°) for 160 ℃, 170 ℃ and 180 ℃ degradation products derived from oleic acid

Oleic acid derived PHA	**Thermal degradation temperatures**		
	160ºC	**170ºC**	**180°C**
-COOH terminal concentration, mol g^{-1}	n.d.	2.6×10^{-4}	5.9×10^{-4}
Acid dissociation constant (K_a), mol dm^{-3}	n.d.	4.2×10^{-12}	1.3×10^{-10}
pK_a	n.d.	11.5 ± 0.3	9.9 ± 0.01
Acidity (pH)	n.d.	6.0 ± 0.2	5.1 ± 0.007
Degree of dissociation, α	n.d.	3.9×10^{-6}	1.5×10^{-5}
Standard Gibbs free energy change (ΔG°), kJ mol^{-1}	n.d	80.7 ± 2.4	69.7 ± 0.1

n.d.: not detected

For mcl-PHA derived from SPKO, the acidity of 160˚C and 170˚C decomposition products could not be determined as they were partially decomposed polymer with high M_n values. These high molecular weight polyesters were relatively insoluble in water with almost negligible ionization in aqueous solution. Both 180˚C and

190˚C decomposition products dissolved in distilled water at 95°C and gave pH values of 5.7 ± 0.09 and 4.7 ± 0.01, respectively. However, experimental pH values obtained were not the actual pH values for the hydroxyl acids as hydrogen ions in the weak acid solution were contributed by the dissociation of weak carbonic acid as well as water molecule itself. Thus the actual pH values for both 180˚C and 190˚C decomposition products were determined through the calculation of K_a and pK_a of dissociable hydroxyl acids.

The degree of dissociation (α) of the hydroxyl acids and the standard Gibbs free energy change (ΔG°) from PHA decomposition at 180˚C and 190˚C were calculated using the K_a and pK_a, and the calculations were shown in Appendix E. The standard Gibbs free energy change for both 180 ℃ and 190 ℃ heat treated PHA were positive, showing that formation of hydroxyl-carboxylate and hydrogen ions from the dissociation of weak hydroxyalkanoic acids in aqueous solution was not spontaneous. ΔG° was lower for 190 ℃-treated PHA compared to 180 ℃-treated PHA. This showed that dissociation of 190 ℃ decomposition products in aqueous solution occurred more readily than the 180 ℃ decomposition products at 95 ℃ in aqueous solution.

The calculated acid dissociation constant (K_a), pK_a, pH, degree of dissociation (α) and standard Gibbs free energy change (ΔG°) values were shown in Table 4.8.

Table 4.8 Effective concentration of carboxyl end groups, acid dissociation constant (K_a), pK_a, pH, degree of dissociation (α) and standard Gibbs free energy change (ΔG) for 160ºC, 170ºC, 180ºC and 190˚C-treated SPKO derived mcl-PHA degradation products

PHA sample	**Thermal degradation temperatures**			
	160 ℃	**170 ℃**	**180 ℃**	**190 ℃**
-COOH terminal concentration, mol g^{-1}	n.d.	n.d.	2.2×10^{-4}	6.3×10^{-4}
Acid dissociation constant (K_a), mol dm^{-3}	n.d.	n.d.	1.7×10^{-12}	4.7×10^{-10}
pK_a	n.d.	n.d.	11.8 ± 0.3	9.3 ± 0.03
Acidity (pH)	n.d.	n.d.	6.3 ± 0.2	4.8 ± 0.01
Degree of dissociation (α)	n.d.	n.d.	2.6×10^{-6}	2.7×10^{-5}
Standard Gibbs free energy change ($\Delta G°$), kJ mol^{-1}	n.d	n.d	83.4 ± 2.2	65.8 ± 0.1

n.d: not detected

4.4 Structural analysis of control and heat-treated mcl-PHA

4.4.1 Monomer composition analysis by gas chromatography (GC)

From the GC analysis, oleic acid-derived mcl-PHA contained four saturated monomers: 3-hydroxyhexanoate (C_6), 3-hydroxyoctanoate (C_8), 3-hydroxydecanoate (C_{10}) and 3-hydroxydodecanoate (C_{12}) and three unsaturated monomers: 3-hydroxydodecenoate ($C_{12:1}$), 3-hydroxytetradecenoate ($C_{14:1}$) and 3-hydroxytetradecenoate ($C_{14:2}$). The polyester mainly consisted of the saturated units, C_8 (42.3 wt %) and C_{10} (30 wt %), which seemed to be a common feature for homology

Group I Pseudomonads (Huisman et al., 1989; Madison & Huisman, 1999). The unsaturated monomer content in control PHA was 13.6% of the total units. The changes in monomeric composition of PHA before and after thermal treatments were shown in Fig. 4.12 and the GC chromatograms of PHA samples were shown in Appendix F. The trend of variation in monomeric compositions was almost similar in 160˚C and 170˚C-treated PHA. The unsaturated monomer content of the polymer decreased when PHA was heat treated at 160 ℃ (9.1 wt %) and 170 ℃ (8.9 wt %). A decrease in the number of unsaturated monomers supported the idea that oxidative cleavage at unsaturated linkages in the side chain could have occurred at high temperature. Indeed, the number of shorter saturated monomers (C_6, C_8, C_{10} and C_{12}) had increased in heat-treated PHA. However, the unsaturated monomer content in 180˚C-treated PHA (12.7 wt %) was higher than both 160˚C- and 170˚C- treated PHA. Besides that, small amounts of $C_{4:1}$ (1 wt %) and $C_{6:1}$ (1 wt %) monomers were detected in 180˚C-treated PHA. It is postulated that at 180˚C, in the presence of excess terminal carboxylic acids, a small proportion of low-molecular-weight fragments generated from the oxidative cleavage of unsaturated bond in the side chain would be dehydrated, generating non-hydroxylated $C_{4:1}$ and $C_{6:1}$ fragments.

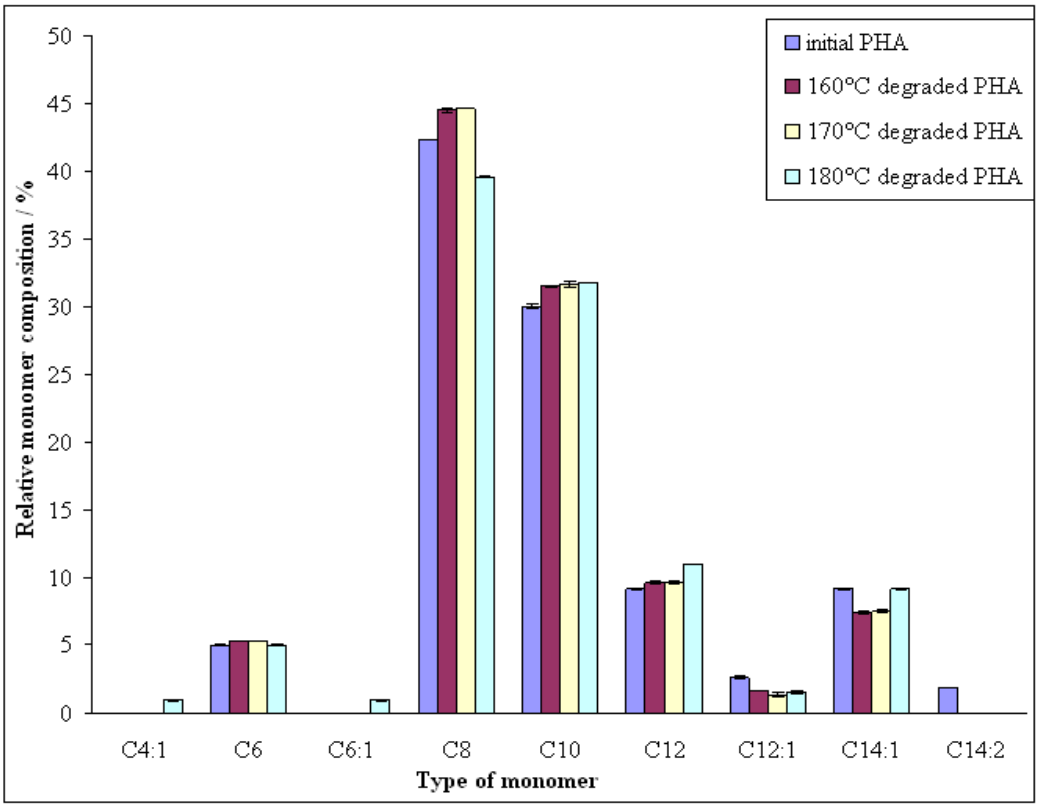

Fig. 4.12 Relative monomer compositions of control and partially degraded PHA derived from oleic acid

GC analysis showed that the methanolyzed mcl-PHA produced from SPKO composed of five saturated monomers: 3-hydroxyhexanoate (C_6), 3-hydroxyoctanoate (C_8), 3-hydroxydecanoate (C_{10}), 3-hydroxydodecanoate (C_{12}), 3-hydroxytetradecanoate (C_{14}) and one unsaturated monomer, 3-hydroxy-5-tetradecenoate ($C_{14:1\Delta}{}^5$) with C_8 as the predominant monomer. Since palm kernel oil contains only 18% of unsaturated fatty acids, the amount of unsaturated monomers present in the SPKO derived mcl-PHA will be lower compared to the PHA derived from unsaturated fatty acids i.e. oleic acid. The GC chromatograms of 160°C to 180˚C-treated PHA were almost identical to the chromatogram obtained from the control PHA (see Appendix F). On the other hand, the 190 ℃-treated PHA showed 3 additional peaks with the retention time of 4.1, 5.5 and 6.8 min which presumably corresponded to $C_{4:1}$, $C_{6:1}$ and $C_{8:1}$ monomers.

Fig. 4.13 showed the variation of monomer compositions for the control PHA derived from SPKO and the thermally decomposed products. The relative monomer compositions of the 160 ℃ to 180 ℃ decomposed products were almost similar to that of the control PHA i.e. they were mainly comprised (in wt %) of 5.8 C_6, 46.1 C_8, 31.0 C_{10}, 13.9 C_{12}, 1.3 C_{14} monomers and 1.9 of unsaturated units. The unsaturated monomer content increased to 8.1 wt % while the weight percentage of C_8 (43.2 wt %), C_{10} (29.0 wt %) and C_{12} (12.8 wt %) monomers had decreased when the PHA was decomposed at 190 ℃, with three new unsaturated monomers being detected: $C_{4:1}$ (3 wt %), $C_{6:1}$ (2.2 wt %) and $C_{8:1}$ (1.3 wt %). These were most likely to be formed from the dehydration of the terminal -OH and were consistent with the observations from FTIR and NMR measurements discussed later.

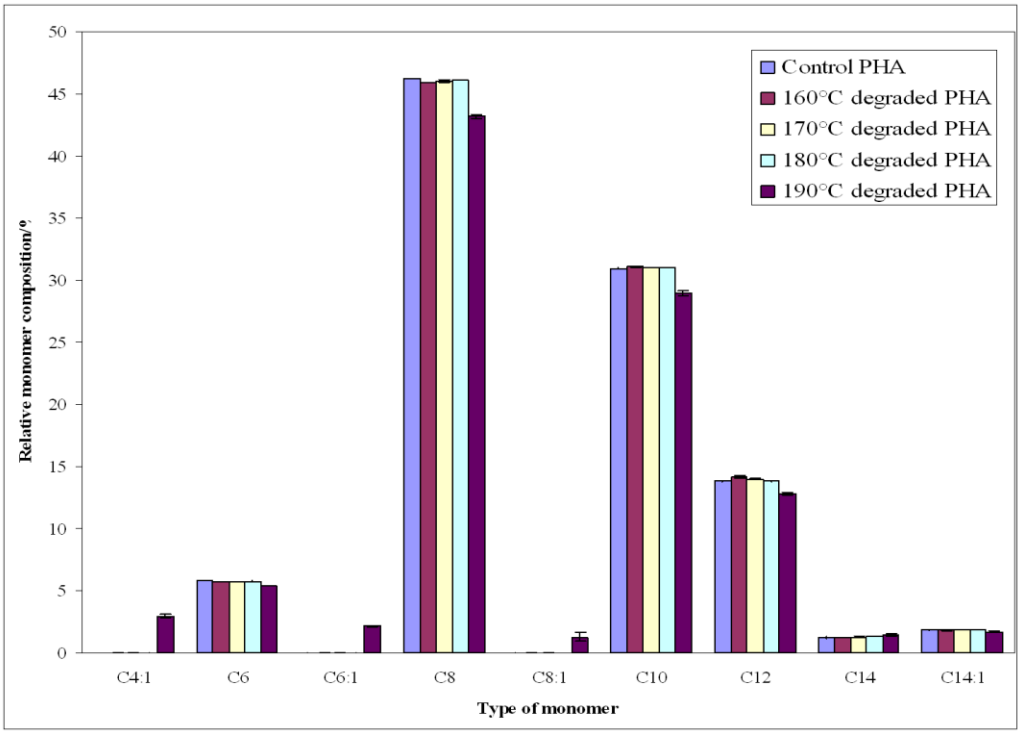

Fig. 4.13 Relative monomer compositions of control and partially degraded PHA derived from SPKO

When heat treated at 160 ℃ to 180 ℃, the palm kernel oil derived mcl-PHA generated a mixture of hydroxyl acids from the hydrolysis of the ester linkages. At 190 ℃, a proportion of the hydroxyl acids could have undergone dehydration to produce RCH=CH– terminals. These results supported the proposition that at high temperature such as 190˚C, some side chain fragments in the PHA would undergo thermal cracking, producing small proportions of volatile alkenes and thus shortened the side chain by elimination of two to four-carbon chain length molecules. The terminal alcohol of these shorter polymer chains would be dehydrated producing non-hydrated alkenoic acid with shorter polymer side chains.

4.4.2 Fourier transform infrared spectroscopic (FTIR) analysis

The FTIR spectrum of oleic acid-derived mcl-PHA was shown in Fig. 4.14. The presence of an ester structure was clearly indicated by the absorbance bands at frequency of 1742, 1259 and 1168 cm^{-1}: the first corresponded to the stretching of ester C=O and the latter two to the stretching of C-O in saturated aliphatic esters. The aliphatic nature was also clearly shown by the bands from 2800 to 3000 cm^{-1} (CH_3- and CH_2-stretching), bands at 1379 and 1459 cm^{-1} (C-CH_3 and C-CH_2 bending) and band at 724 cm^{-1} ($(CH_2)_n$ rocking). The C-O stretching of secondary alcohol structures contributed to the band at 1120 cm^{-1}. The weak absorption peak at 966 cm^{-1} indicated the presence of *trans*-configuration double bond (=C-H bending) in the side chain of some monomers in mcl-PHA.

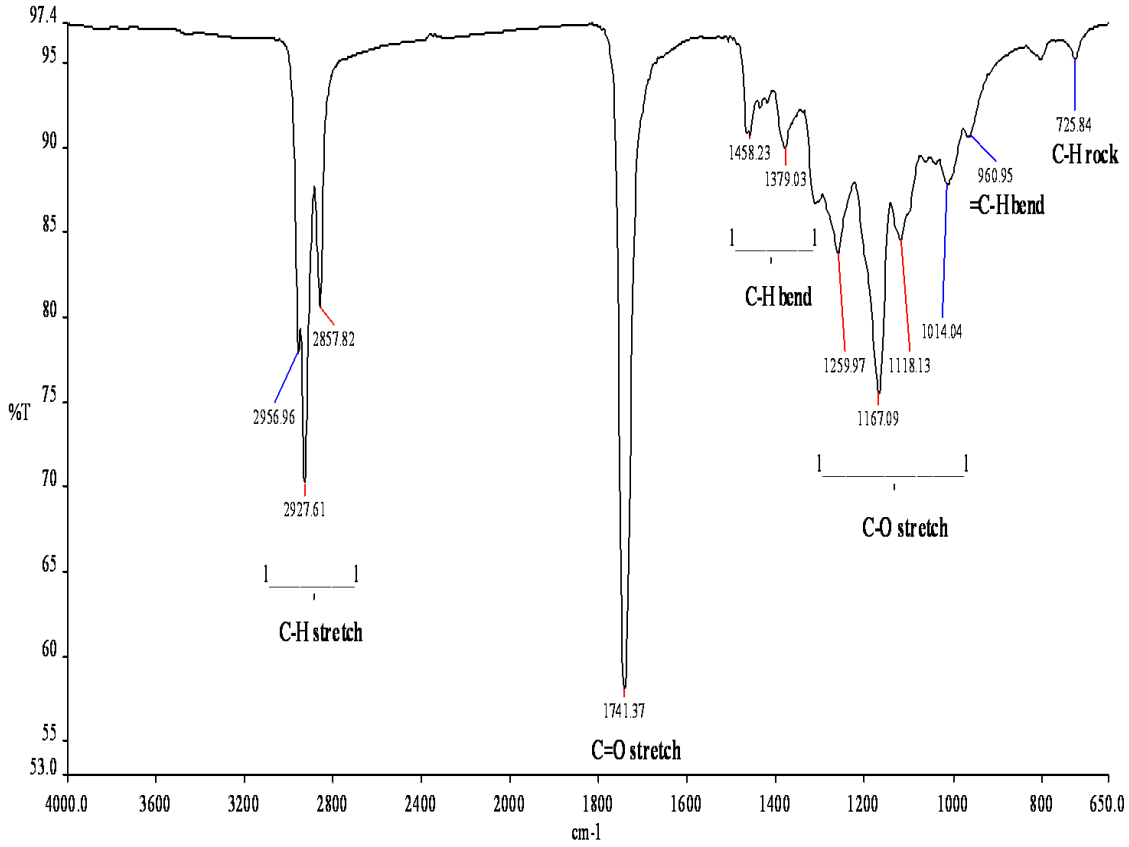

Fig. 4.14 Infrared spectrum of mcl-PHA derived from oleic acid

The band positions for all the major structural bonding types in control and heat- treated mcl-PHA were summarized in Table 4.9. This table showed that after 30 minutes heating at 180˚C, the carbonyl peak had shifted to 1716cm^{-1}, which was exclusive to the unsaturated C=O stretch, corresponded to the formation of α, β unsaturated ester. This revealed that unsaturated ester groups were present in 180˚C-treated polymer. Spectra of control, 160˚C and 170˚C-treated mcl-PHA derived from oleic acid were almost identical with the similar broadening of carbonyl stretching band (C=O) around 1736 cm^{-1}, which was attributed to the saturated aliphatic ester group in mcl-PHA.

Table 4.9 FTIR correlations of various functional groups in control and heat-treated mcl-PHA derived from oleic acid

Functional group	**Alkane**			**Ester**		**Alkene**	
Type of vibration /Bond Wave number/ cm^{-1}	C-H stretch (a) CH_3 - (b) $-CH_2$ - (c) $-CH_2$ -	C-H bend (a) $-CH_2-$ (b) CH_3-CH_2	C-H rock $-(CH_2)_n$ -	C=O stretch (a) saturated aliphatic (b) α, β unsaturated	C-O stretch	=C-H bend (out of plane)	(a) -C=C- Stretch =C-H bend (a) In plane (b) Out of plane
Control PHA	(a) 2956 (b) 2928 (c) 2858	(a) 1459 (b) 1379	724	(a) 1742	1000-1320	966	-
PHA heat treated at 160˚C	(a) 2956 (b) 2926 (c) 2857	(a) 1460 (b) 1379	724	(a) 1736	1000-1320	966	-
PHA heat treated at 170˚C	(a) 2951 (b) 2925 (c) 2857	(a) 1459 (b) 1379	723	(a) 1736	1000-1320	964 756	-
PHA heat treated at 180˚C	(a) - (b) 2920 (c) 2852	(a) 1461 (b) 1374	724	(b) 1716	1000-1320	-	(a) 1653 (b) 1414 (c) 983

Fig. 4.15 showed the FTIR spectra of the oleic acid-derived mcl-PHA and the degradation products at 160˚C, 170˚C and 180˚C. The FTIR spectra of the control, 160˚C and 170˚C-treated PHA (Fig. 4.15(a), (b) and (c)) were similar, with the carbonyl stretching band (C=O) at around 1736 cm^{-1}, which was attributed to the saturated aliphatic ester group in mcl-PHA. However the spectrum for the 180˚C-treated PHA (Fig. 4.15(d)) showed two additional absorption peaks, indicated by arrows at 1653 cm^{-1} and

1414 cm^{-1}. The band centered at 1653 cm^{-1} was assignable to non-conjugated C=C stretching vibration, and the one at 1414 cm^{-1} was due to =CH- bending. These signals indicated the presence of terminal vinyl groups.

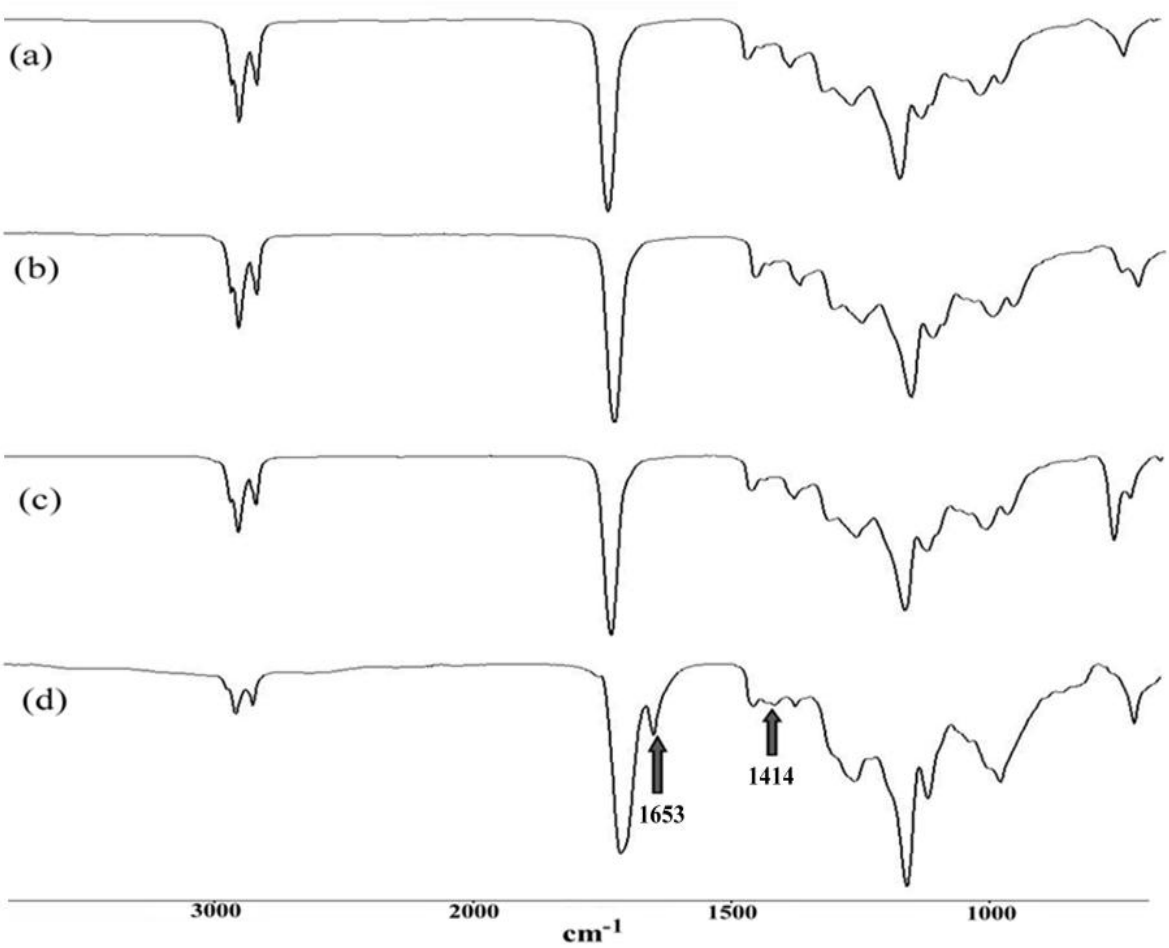

Fig. 4.15 FTIR spectra of oleic acid-derived mcl-PHA: (a) Control PHA, (b) PHA heat treated at 160˚C, (c) PHA heat treated at 170˚C and (d) PHA heat treated at 180˚C. Two distinct –C=C– peaks were observed in the 180˚C-treated PHA, corresponding to the unsaturated terminal group

The infrared spectrum of SPKO-derived mcl-PHA in Fig. 4.16 showed the following bands: 2800 to 3000 cm^{-1} corresponded to -CH_3 and -CH_2- stretching, respectively; 1379 and 1458 cm^{-1} for -C-CH_3 and -C-CH_2- bending, and 725 cm^{-1}

corresponded to -CH_2- rocking. The presence of an ester structure was clearly indicated by the bands at 1741, 1259 and 1167 cm^{-1}: the first corresponded to the stretching of ester C=O and the rest were assigned to the stretching of C-O in saturated aliphatic esters. The C-O stretching of secondary alcohol structures contributed to the band at 1118 cm^{-1}. The weak absorption peak at 965 cm^{-1} indicated the presence of double bond (=C-H bending) in the side chain of some monomers in the mcl-PHA.

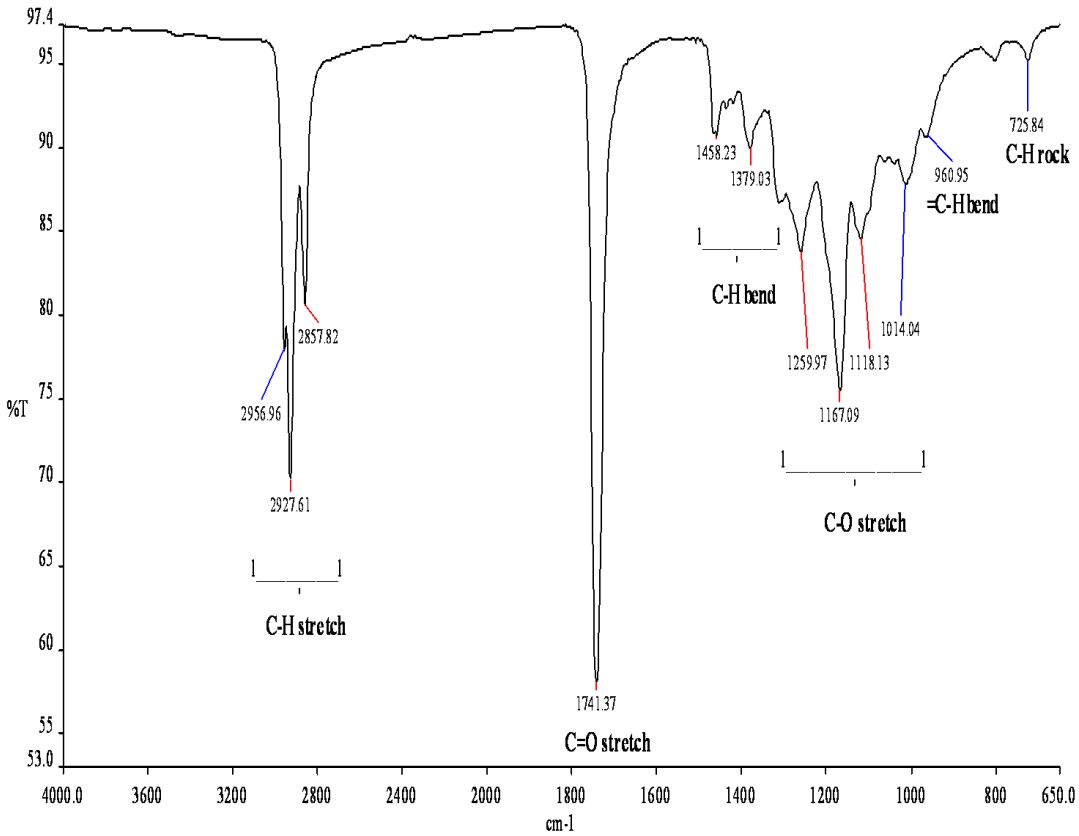

Fig. 4.16 Infrared spectrum of mcl-PHA derived from SPKO

The band positions for all the major structural bonding types in the control and heat-treated mcl-PHA derived from SPKO were summarized in Table 4.10.

Table 4.10 FTIR correlations of various functional groups in control and heat-treated mcl-PHA derived from SPKO

Functional group	**Alkane**			**Ester**		**Alkene**	
Type of vibration / Bond / Wave number/ cm^{-1}	C-H stretch (a) CH_3 - (b) $-CH_2$ - (c) $-CH_2$ -	C-H bend (a) $-CH_2-$ (b) CH_3-CH_2	C-H rock $-(CH_2)_n$ -	C=O stretch (saturated aliphatic)	C-O stretch	=C-H bend (out of plane)	-C=C- stretch
Control PHA	(a) 2957 (b) 2928 (c) 2858	(a) 1458 (b) 1379	726	1741	1000-1320	961	-
PHA heat treated at 160˚C	(a) 2952 (b) 2928 (c) 2858	(a) 1464 (b) 1386	721	1742	1000-1320	966	-
PHA heat treated at 170˚C	(a) 2957 (b) 2928 (c) 2858	(a) 1466 (b) 1379	725	1743	1000-1320	965	-
PHA heat treated at 180˚C	(a) 2952 (b) 2928 (c) 2858	(a) 1465 (b) 1379	725	1740	1000-1320	966	-
PHA heat treated at 190˚C	(a) 2957 (b) 2929 (C) 2859	(a) 1459 (b) 1379	725	1740	1000-1320	-	1654

Fig. 4.17 showed the overlay FTIR spectra of SPKO-derived mcl-PHA and those which were heat-treated at 160 ℃, 170 ℃, 180 ℃ and 190 ℃. For the infrared spectrum of 190˚C-treated PHA, an additional absorption peak was seen at 1654 cm^{-1}, which indicated the presence of non-conjugated RCH=CH– terminal vinyl group.

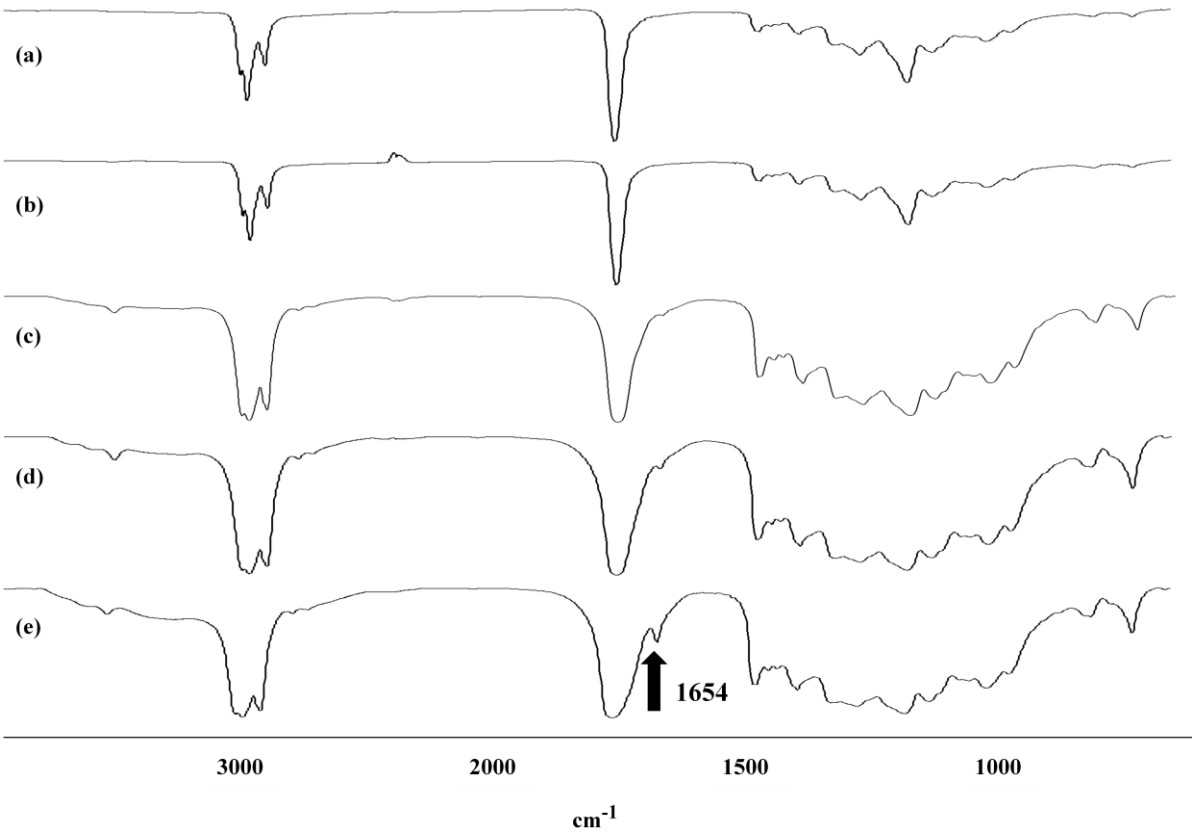

Fig. 4.17 FTIR spectra of SPKO-derived mcl-PHA. (a) Control PHA, (b) PHA heat treated at 160˚C, (c) PHA heat treated at 170˚C, (d) PHA heat treated at 180˚C and (e) PHA heat treated at 190˚C. The arrow indicated a distinct –C=C– peak, corresponding to the unsaturated terminal group in 190 ℃-treated PHA

4.4.3 Proton nuclear magnetic resonance (^{1}H-NMR) spectroscopic analysis

Fig. 4.18 showed the ^{1}H-NMR spectrum for the oleic acid-derived mcl-PHA. The peak *e* at 0.8 ppm and peak *d* at 1.2 ppm were assigned to the methyl and methylene group in the side chain respectively. The two peaks *b* and *a* around 2.5 ppm and 5.1 ppm represented the methylene group at the α-position and methine group at the β-position of the ester respectively. The α-hydrogens in esters were deshielded by the adjacent carbonyl group whereas β-hydrogens on the carbon attached to the single-bonded oxygen were deshielded directly by the electronegative oxygen. While the peak shown at 3.7 ppm was assigned to the proton of the hydroxyl groups and peak shown at 2.1 ppm was

assigned to the proton attached to the carbon next to carboxyl groups. The signals for the olefinic protons in the side chain appeared in the expected region between 5.2 and 5.3 ppm. Another characteristic signal was the one appeared at 1.9 and 2.4 ppm which belonged to protons adjacent to the double bonds. Remaining signal at 7.27 ppm was due to the $CHCl_3$ in $CDCl_3$.

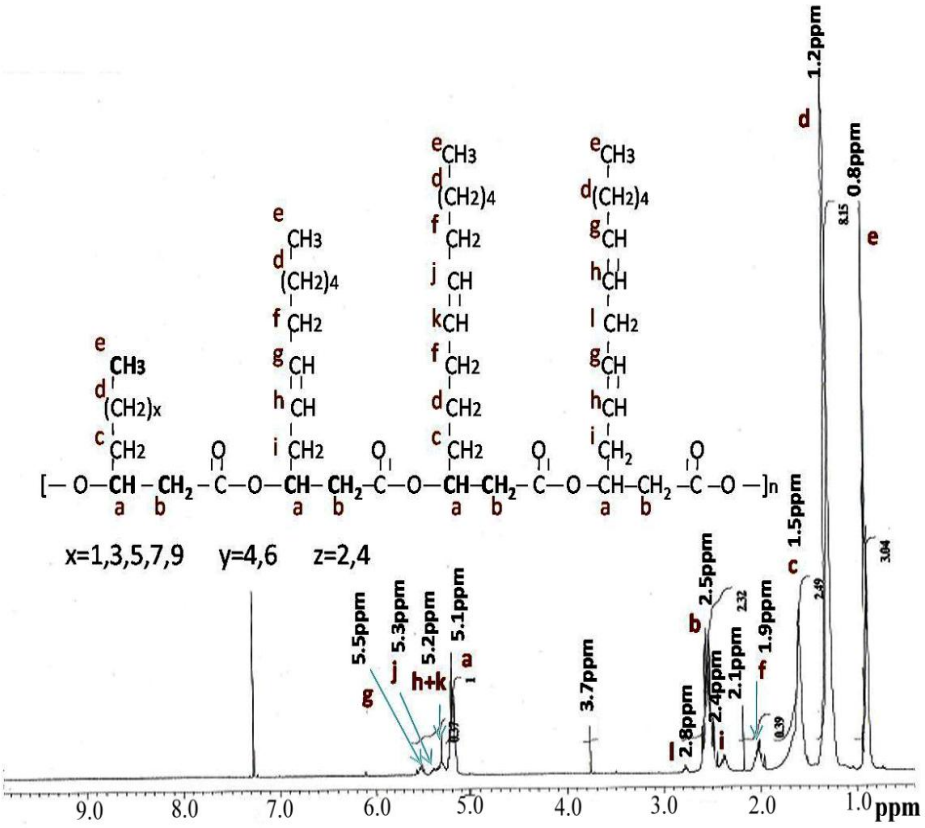

Fig. 4.18 400–MHz ^{1}H-NMR spectrum of oleic acid-derived mcl-PHA. The protons in the mcl-PHA structure were denoted by the corresponding letters in the spectrum

The ^{1}H-NMR spectrum of oleic acid-derived mcl-PHA produced by *Pseudomonas putida* showed peaks at almost identical chemical shift in the spectrum studied by Huijbert et al. (1992) and Tan et al. (1997). According to Huijbert et al., the chemical shifts of peak *j, k, g* and *h* indicated the presence of unsaturated groups in some of the monomers' side chains. The peak *f* and *l* with chemical shift 1.9 ppm and 2.8 ppm

were assigned to allylic methylene group and diallylic methylene group. Chemical shift of peak *i* was assigned to the methylene group between the double bond in the side chain and the hydroxyl group of ester.

Fig. 4.19 compared the ^{1}H-NMR spectra of oleic acid-derived mcl-PHA and those which had been heat treated at 160˚C, 170˚C and 180˚C. The intensity ratio of signal *a* (proton originated from *β*-methine group adjacent to esterified alcohol group) to signal *e* (proton originated from side chain methyl group) decreased in proportion to increasing temperature. This showed that hydrolysis of ester bond had occurred, generating free alcohol end groups as the *β*-hydrogen was no longer deshielded by the electronegative oxygen in the ester group. This corresponded to an increase of intensity of the alcohol end groups, as shown by the proton resonance at 3.7 ppm.

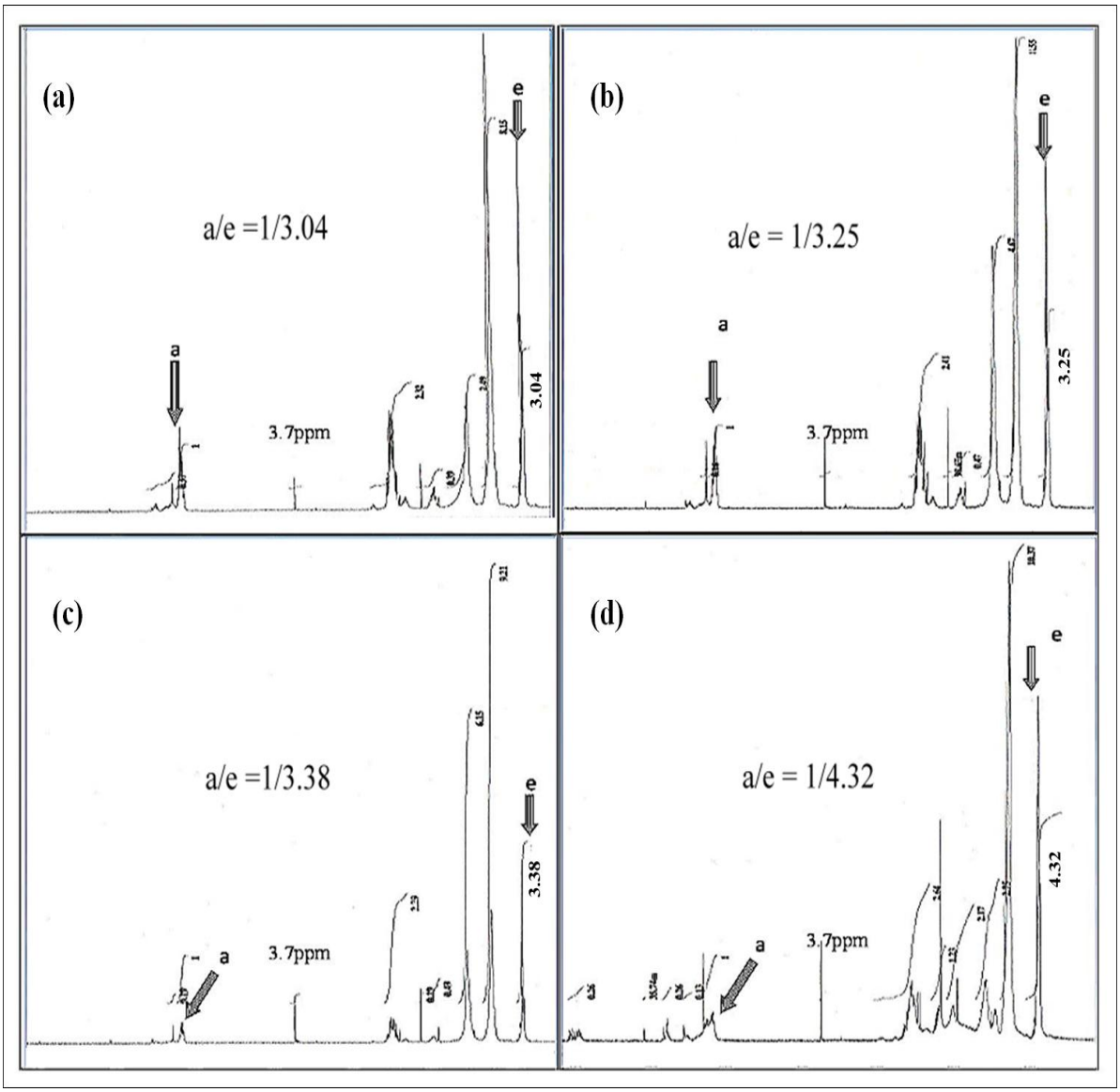

Fig. 4.19 ^{1}H–NMR spectra of oleic acid-derived mcl-PHA: (a) control, (b) heat-treated at 160˚C, (c) heat-treated at 170˚C and (d) heat-treated at 180˚C. The ratio of proton *a* (methine group) to proton *e* (methyl group) had decreased, as hydrolysis of ester linkages would producing more hydroxyl acids with the –OH end group at 3.7 ppm

The ^{1}H-NMR spectra of 160˚C and 170˚C-treated PHA were almost identical to the spectrum of control PHA. Nevertheless, two extra multiplet peaks (*m* and *n*) were observed at position between 5.0 to 7.0 ppm in the 180˚C-treated PHA as shown in Fig. 4.20. These could be attributed to the olefinic protons in the unsaturated end structure in the degradation product. This observation agreed with the presence of monounsaturated

terminal structure of CH_3-CH=CH-C(O)O-R in the thermally degraded short-chain-length poly(3-hydroxyalkanoates) (scl-PHA) as reported by Kunioka and Doi (1989).

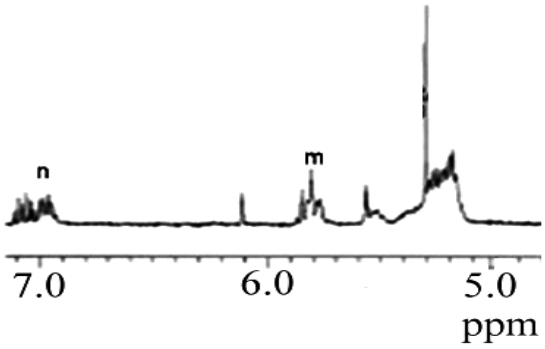

Fig. 4.20 Expanded ^{1}H-NMR spectrum of oleic acid-derived PHA heat treated at 180˚C, where the olefinic protons *m* and *n* were appeared at 5.8 and 6.9 ppm

The elucidation of intensity ratio of hydroxyl terminals to carboxyl terminals in 160˚C, 170˚C and 180˚C-treated PHA were shown in Fig. 4.21. From the ^{1}H-NMR spectra of the heat-treated PHA samples, amount of OH terminal groups and COOH terminal groups were almost similar in the 160˚C and 170˚C-treated PHA. These observations suggested that hydrolysis at ester linkages had occurred, leading to the production of a mixture of oligomeric hydroxyl acids methyl ester. However the presence of more carboxylic terminals than hydroxyl terminals was observed in spectrum of 180˚C-treated PHA. One plausible reason for this phenomenon was that the hydroxyl acids tend to dehydrate at high temperature.

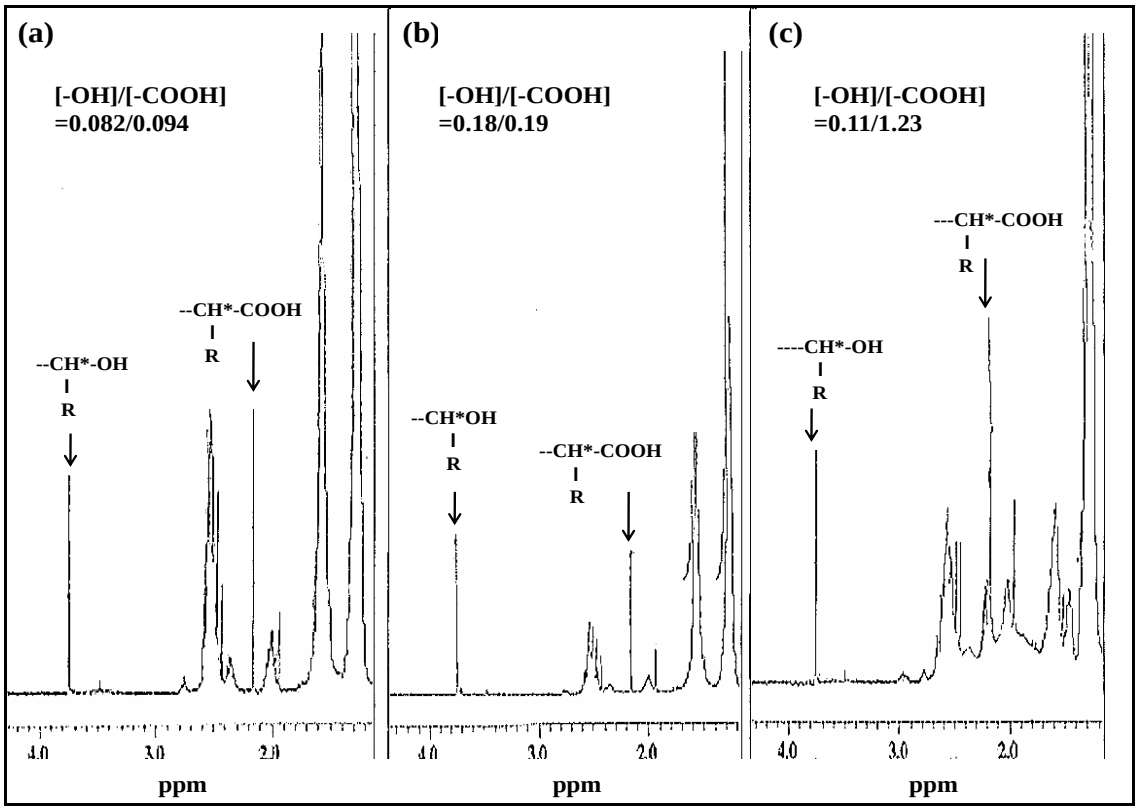

Fig. 4.21 ^{1}H-NMR spectra of the thermolyzed mcl-PHA samples derived from oleic acid: (a) heat treated at 160˚C, (b) heat treated at 170˚C and (c) heat treated at 180˚C. A lower level of -CH*-OH group than –CH*-COOH group was observed in the 180˚C-treated PHA

The ^{1}H-NMR spectrum for mcl-PHA derived from SPKO was shown in Fig. 4.22. In the spectrum, peak *e* at 0.8 ppm and peak *d* at 1.2 ppm were assigned to $–CH_3$ and $–CH_2–$ in the alkyl pendant groups respectively. The two peaks *a* and *b* around 5.1 ppm and 2.5 ppm represented the methine group at the β-position (~~COO-CHR~~) and methylene group at the *α*-position of the ester (~~CH_2-COO~~) respectively. Finally, the peaks for the olefinic protons in the side chain appeared in between 5.3 and 5.5 ppm. The peaks at 2.1 ppm and 3.7 ppm were assigned to the proton attached to carbon bonded to carboxyl group (HOOC-CH_2~~) and hydroxyl group (HO-CHR~~).

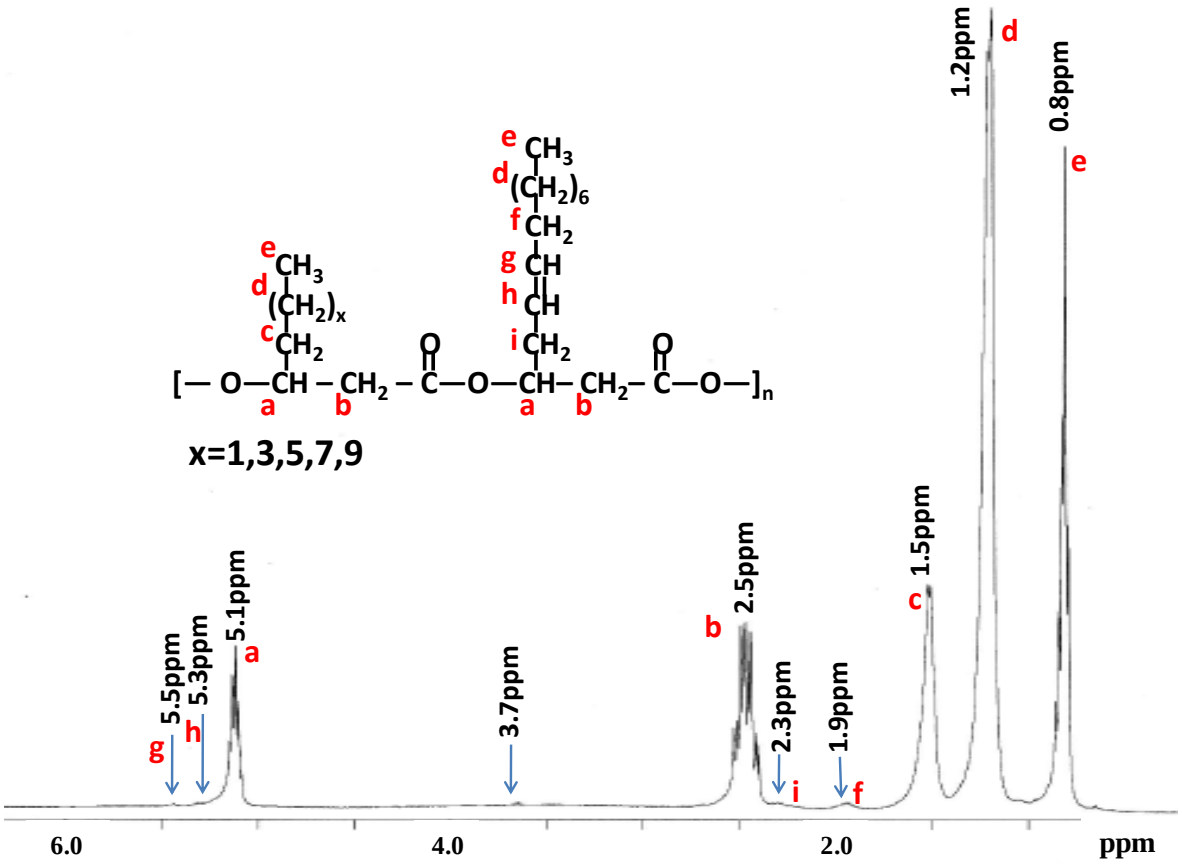

Fig. 4.22 The 400–MHz ^{1}H-NMR spectrum of mcl-PHA derived from SPKO. The protons in the mcl-PHA structure were denoted by the corresponding letters in the spectrum

Fig. 4.23(a) to (e) showed the ^{1}H-NMR spectra of the control and the PHA heat treated at 160 ℃, 170 ℃, 180 ℃ and 190 ℃ respectively. The initial ratio of peaks *a*/*e* was 0.32, and had decreased to 0.29 when the degradation temperature increased to 190 ℃. This could be interpreted as the occurrence of hydrolysis of some of the ester linkages generating -OH terminal group, when ~~COO-CHR~~ being hydrolyzed to HO-CHR~~. The actual peak due to –OH was not clearly observable, presumably because of the very low concentration and broadening due to hydrogen bonding.

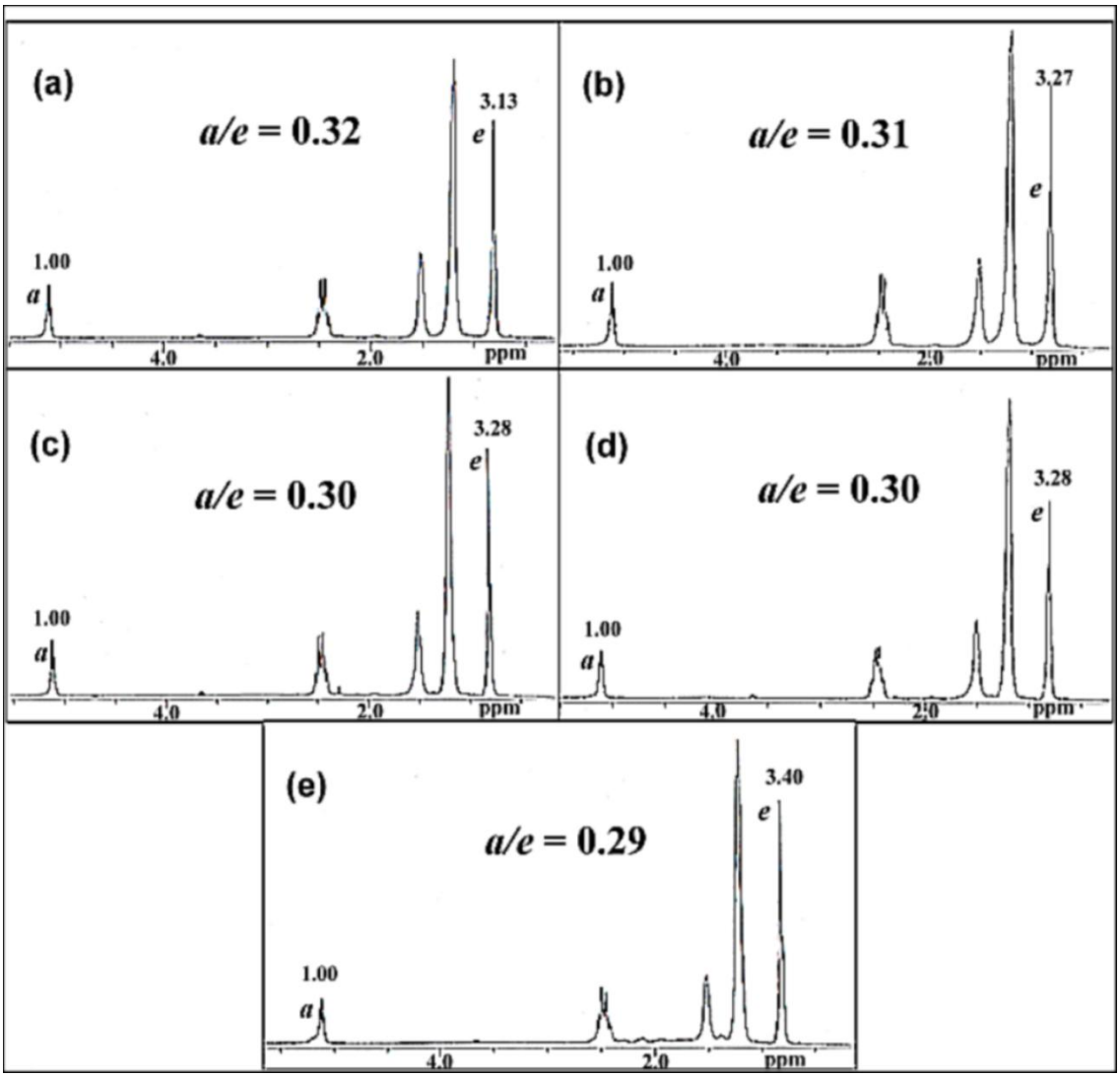

Fig. 4.23 ^{1}H–NMR spectra of mcl-PHA derived from SPKO: (a) Control PHA, (b) PHA heat treated at 160˚C, (c) PHA heat treated at 170˚C, (d) PHA heat treated at 180˚C and (e) PHA heat treated at 190˚C

While the spectra of 160°C to 180˚C treated mcl-PHA were very similar to the spectrum of the control PHA (Fig. 4.23 (a)-(d)), the spectrum of 190 ℃-treated PHA showed increased intensity of alcohol and carboxylic end groups, as shown by the peaks at 3.7 and 2.1 ppm in Fig. 4.24(a) with relatively higher amount of –COOH groups. This observation could be due to the dehydration of the HO-CHR-CH_2~~ to RCH=CH~~ at temperature around 190 ℃. Two extra multiplet peaks (*m* and *n*) between 5.0 to 7.0 ppm were also observed (expanded spectrum in Fig. 4.24(b)). These could be attributed to the

vinyl protons in the unsaturated terminal of the product as a result of the dehydration process.

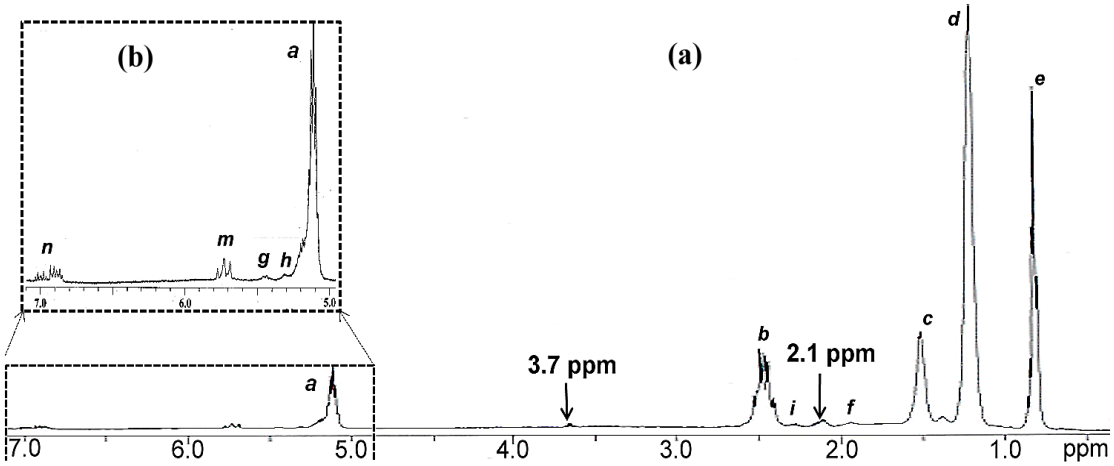

Fig. 4.24 400-MHz ^{1}H-NMR spectrum of mcl-PHA derived from SPKO: (a) the decomposed product obtained at 190 ℃ and (b) expanded region between 5.0 to 7.0 ppm

Both results from the degradation products of oleic acid and SPKO-derived mcl-PHA suggested that the thermal degradation of mcl-PHA at moderate high temperature involved a random chain scission which initiated at the ester linkages, producing hydroxyacids with free –OH and –COOH end groups. The hydroxyl acids tend to dehydrate in acidic and high temperature environment as the high amount of carboxylic terminals in the degradation products acted as the catalyst for dehydration to occur. These phenomena disagreed with the 6 membered-ring β-chain scission mechanism expoused for short-chain-length poly(3-hydroxyalkanoates) (scl-PHA) such as poly(3-hydroxybutyrate) (PHB) and poly(3-hydroxybutyrate-co-hydroxyvalerate) (PHBV), as such mechanism would induce the formation of carboxylic terminal and a crotonate structure instead of hydroxyl terminal. According to Morikawa and Marchessault (1981), no signal was observed at the position of 3.7 ppm in the NMR spectra of PHB pyrolysate, indicating that terminal OH group was absent from the oligomers. However, presence of hydroxyl end groups was observed in the spectra of partially degraded mcl-PHA. This

indicated that the chain scission mechanism pathway in mcl-PHA during thermal degradation could be different from scl-PHA.

4.5 Thermal degradation mechanism of mcl-PHA

The results obtained from GC, FTIR and ^{1}H-NMR analyses were simultaneously used as complementary techniques to determine the molecular structure of the partially degraded mcl-PHA, and with that to elucidate the mechanism of thermal degradation of the mcl-PHA.

The thermal degradation process appeared to involve α-chain scission of the mcl-PHA polymer chains *via* hydrolytic ester bond cleavage. The primary degradation products were a mixture of low molecular weight oligomeric hydroxyalkanoic acids which resulted from the hydrolysis of the ester linkages. A proportion of the degradation products could have undergone dehydration of the hydroxyl end groups, giving rise to alkenoic acid as secondary products. Fig. 4.25 showed the plausible chain cleavage mechanism in mcl-PHA polymers during the thermal degradation process.

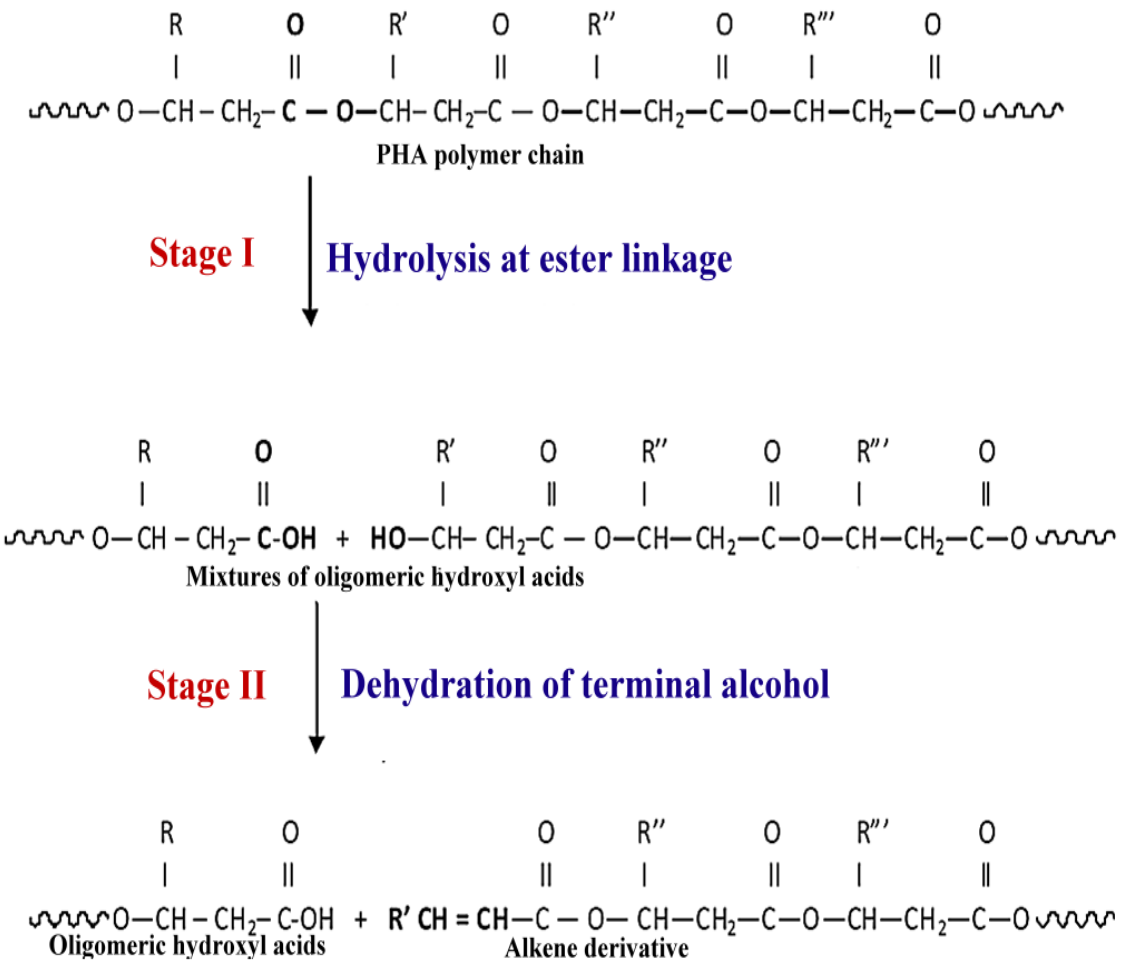

Fig. 4.25 A plausible chain cleavage mechanism in mcl-PHA during thermal degradation process. Stage I: Hydrolysis at the ester bond; Stage II: Dehydration of hydroxyl end group in the acidic environment

The above-mentioned mechanism does not agree with the β-chain cleavage mechanism in the thermal degradation of scl-PHA. For example, for PHB thermal decomposition, the mechanism pathway involved the 6-membered ring ester transition followed by synchronous breakage of the β-C-O and α-C-H bonds, producing oligomers with carboxyl and crotonyl terminals (Morikawa & Marchessault, 1981; Grassie et al., 1984; Kopinke et al., 1996; Erceg et al., 2005; Ariffin et al., 2008) as shown in Fig. 4.26. Formation of a stable intramolecular 6-membered ring ester intermediate is possible during the thermal degradation of scl-PHA as the R substituent consists of a methyl or

ethyl group. However, mcl-PHA contains bulky alkyl substituents with 3, 5, 7, 9 or 11 carbon atoms. These bulky R substituents could hinder the formation of a stable cyclic transition during the β-chain scission mechanism. Thus compared to the β-chain cleavage mechanism espoused for scl-PHA, hydrolysis of ester linkages might occur more readily in mcl-PHA during thermal degradation.

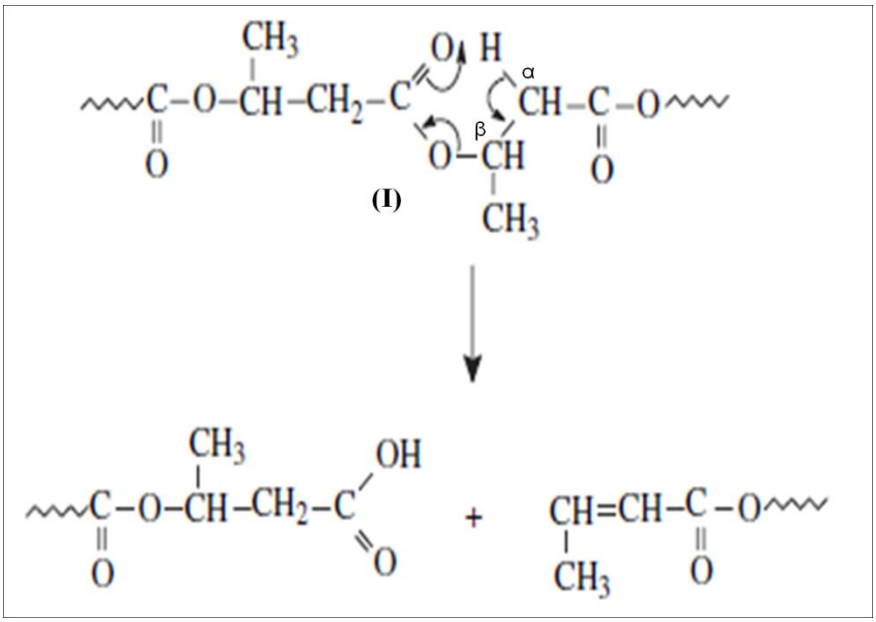

Fig. 4.26 A typical β-chain cleavage mechanism during PHB thermal decomposition. A 6-membered ring ester transition state (I) is involved followed by synchronous breakage of the β-C-O and α-C-H bonds

CHAPTER FIVE

PHA AS PLASTICIZER FOR POLY(VINYL CHLORIDE)

5.1 Mcl-PHA as natural-based plasticizer for PVC

Mcl-PHA, the polyester of bacterial origin has potential to act as a natural-based plasticizer for vinyl resins such as PVC. Both mcl-PHA in the original undegraded and degraded forms are considered to be compatible with PVC as they may have reasonable affinity to the PVC resin due to the dipole-dipole and hydrogen bonding interactions. They could be dispersed in the PVC polymer matrix on a molecular level and do not easily migrate out from the PVC compound as a result of entanglement. This is different from the conventional petrochemical-based plasticizers which are small molecules that intercalates into PVC and thus may have limited permanence in the PVC compound. Besides that, owing to its biocompatible and biodegradable properties, even if mcl-PHA diffused out from PVC, they would not be hazardous to human health and the environment.

5.1.1 Monomer compositions of the SPKO- and OA- derived polymeric and oligomeric mcl-PHA used in solution blending

Fig. 5.1 and Fig. 5.2 showed the molecular structure of the monomer units for the saponified palm kernel oil (SPKO) and oleic acid (OA)-derived mcl-PHA respectively, as analysed from the GC and ^{1}H-NMR spectra as discussed in Sections 4.4.1 and 4.4.3.

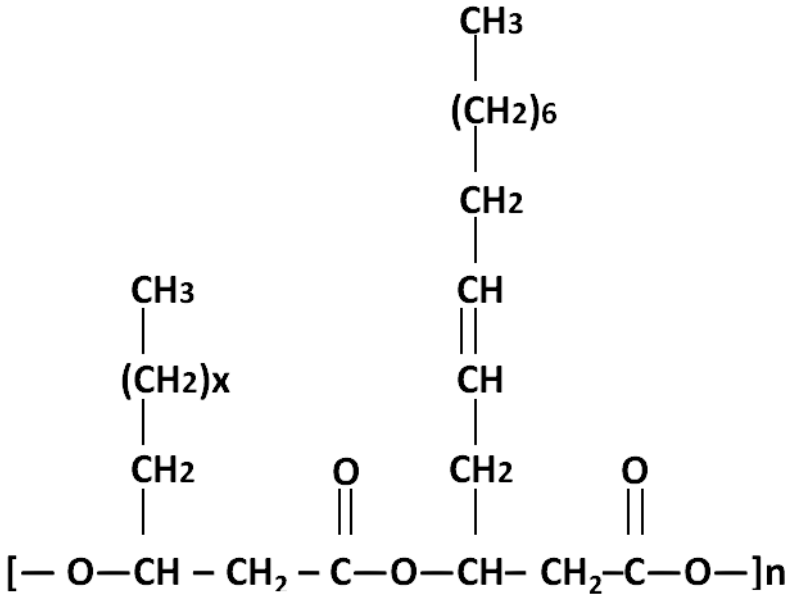

Fig. 5.1 Molecular structure of monomer units of PHA_{SPKO} (SPKO-derived PHA); x: 1, 3, 5, 7 and 9

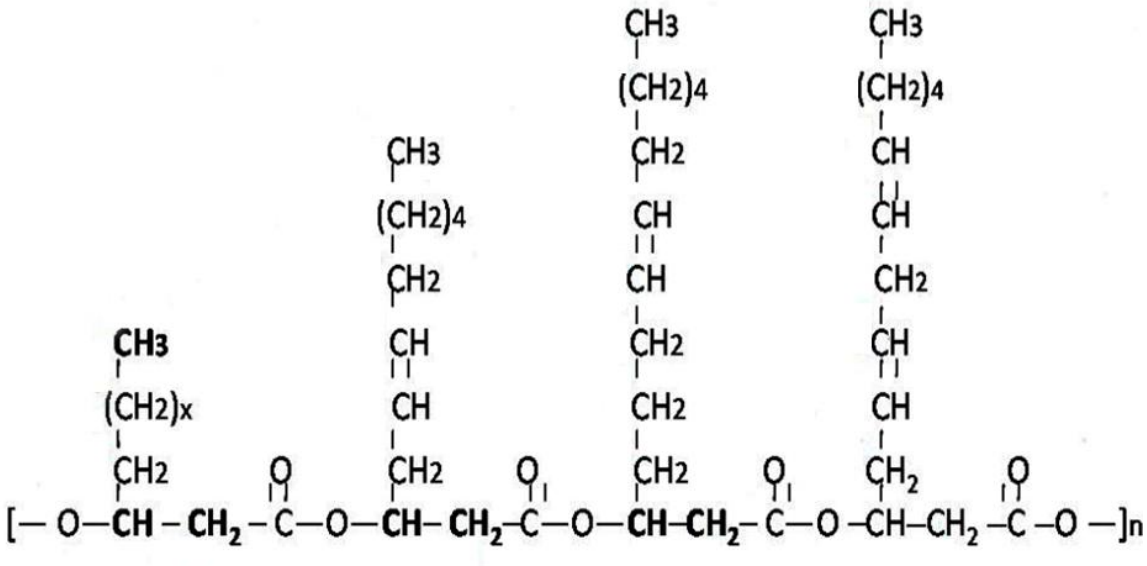

Fig 5.2 Molecular structure of monomer units of PHA_{OA} (OA-derived mcl-PHA); x: 1, 3, 5, 7 and 9

Table 5.1 showed the relative monomer compositions of the non-degraded and 170 ℃-treated mcl-PHA derived from SPKO and OA, which were used in the PVC

blending. The oligomeric PHA (170 ℃-treated PHA) contained higher amount of shorter side chain monomers (C_6 and C_8), compared to the polymeric PHA (non-degraded PHA). For example, the amount of shorter side chain monomers for 170 ℃-treated PHA_{SPKO} was 52.1 wt %, which was higher than those shorter side chain monomers present in polymeric PHA_{SPKO} (50.8 wt %). The amount of shorter side chain monomers for polymeric PHA_{OA} accounted for 43.7 wt %, and the amount was increased to 47.4 wt % after the heat treatment of PHA_{OA} at 170 ℃, with an additional $C_{6:1}$ monomer detected in the heat-treated sample.

Overall PHA_{OA} contained higher unsaturated monomers compared to PHA_{SPKO}. Both polymeric and oligomeric PHA_{OA} contained 17.4 wt % ($C_{12:1}$, $C_{12:2}$, $C_{14:1}$ and $C_{14:2}$) and 7.5 wt % ($C_{6:1}$, $C_{12:1}$ and $C_{14:1}$) unsaturated monomer contents, respectively. In the PHA_{SPKO}, the total unsaturated monomers content was much lower, with only 1.6 wt % for polymeric PHA_{SPKO} and 1.2 wt % for oligomeric PHA_{SPKO}. The GC chromatograms of the PHA samples were shown in Appendix G.

Table 5.1 Monomer compositions of the non-degraded and heat-treated SPKO- and OA-derived PHA determined by GC analysis

PHA sample / Compound [1]ID	Monomer composition (wt %)			
	[2]PHA_{SPKO}	**170 ℃ treated PHA_{SPKO}**	**[3]PHA_{OA}**	**170 ℃ treated PHA_{OA}**
C_6	4.51	4.86	4.26	5.03
$C_{6:1}$	-	-	-	0.58
C_8	46.29	47.21	39.42	41.81
C_{10}	32.59	32.36	29.70	33.62
C_{12}	13.42	12.59	9.21	11.53
$C_{12:1}$	-	-	2.16	0.75
$C_{12:2}$	-	-	2.92	-
C_{14}	1.60	1.74	-	0.55
$C_{14:1}$	1.59	1.24	10.01	6.13
$C_{14:2}$	-		2.32	-

[1]ID: Identity; [2]PHA_{SPKO}: Mcl-PHA derived from saponified palm kernel oil; [3]PHA_{OA}: mcl-PHA derived from oleic acid; **C_6**: 3-hydroxyhexanoic acid;

$C_{6:1}$: 3-hydroxyhexenoic acid; **C_8**: 3-hydroxyoctanoic acid;

C_{10}: 3-hydroxydecanoic acid; **C_{12}**: 3-hydroxydodecanoic acid;

$C_{12:1}$: 3-hydroxydodecenoic acid; **$C_{12:2}$**: 3-hydroxydodecadienoic acid;

C_{14}: 3-hydroxytetradecanoic acid; **$C_{14:1}$**:3-hydroxytetradecenoic acid; and

$C_{14:2}$: 3-hydroxytetradecadienoic acid

5.2 Miscibility of PVC and mcl-PHA

Specific interactions such as dipole-dipole interaction, hydrogen bonding, polar interaction or proton donor-proton acceptor interactions are important for achieving miscibility in polymer blends (Olabisi et al., 1979; Choe et al., 1995). Therefore the multiplicity of miscible systems containing poly(vinyl chloride) and polyester is possibly the result of specific interactions.

5.2.1 Solution blending and solvent casting

Mixing process has a pronounced effect on plasticizer distribution and homogeneity of the plasticized materials. More intimate dispersion could be achieved by mixing the two polymer solutions in a common solvent, in this case, chloroform.

Mcl-PHA has higher solubility in chloroform than PVC. Hence, PVC has higher tendency to precipitate out compared to PHA during the solution casting process. Therefore removal of the solvent during preparation of the polymer blend, the mixtures were stirred continuously to ensure uniform distribution of PHA into PVC

5.2.2 FTIR analysis of PVC-PHA system

Fourier transform infrared (FTIR) spectroscopy is often used in the analysis of polymer mixtures. In this study, FTIR spectroscopy was used to investigate whether specific interaction between the PHA and PVC had taken place, which could be observed from the shift of certain peaks in the spectrum.

The characteristic bands of PVC can be classified into three regions: (i) the C-Cl stretching region in the range from 600 to 700 cm^{-1}; (ii) the C-C stretching in the range from 900-1200 cm^{-1} and (iii) 1250 to 2970 cm^{-1}, attributed to numerous C-H modes in PVC (Rajendran et al., 2008). Table 5.2 showed the characteristic vibrational modes and wave numbers exhibited by PVC.

Table 5.2 Vibrational modes and wave numbers exhibited by PVC (adapted from Beltran & Marcilla (1997) and Pavia et al. (2009))

Vibrational mode	**Wave numbers (cm^{-1})**
Stretching C-H of CHCl	2970
Stretching C-H of CH_2	2912
C=C stretching of vinyl chloride	1645
Deformation (wagging) CH_2	1435, 1427
Deformation C-H of CHCl	1331, 1255
Stretching C-C	1099
Rocking CH_2	966
Stretching C-Cl	692, 637, 616

On the other hand, the mcl-PHA polyesters had characteristic strong absorbance band at around 1726 cm^{-1} for PHA_{SPKO} and 1735 cm^{-1} for PHA_{OA}, which were attributed to the C=O stretching. Therefore it is conveniently to differentiate the PHA from PVC by the carbonyl band.

Fig. 5.3 to Fig. 5.6 showed the FTIR absorption spectra of PVC/PHA_{SPKO}, PVC/deg$PHA_{SPKO,}$ PVC/PHA_{OA} and PVC/degPHA_{OA} polymer blends. The FTIR spectra of all the blends showed the characteristic peaks of both PVC and PHA components, i.e. the C=O stretching band at around 1737 to 1741 cm^{-1} and C-Cl stretching around 607 to 611 cm^{-1}. This showed that both polar functional groups of mcl-PHA and PVC were present in the PHA-PVC blends.

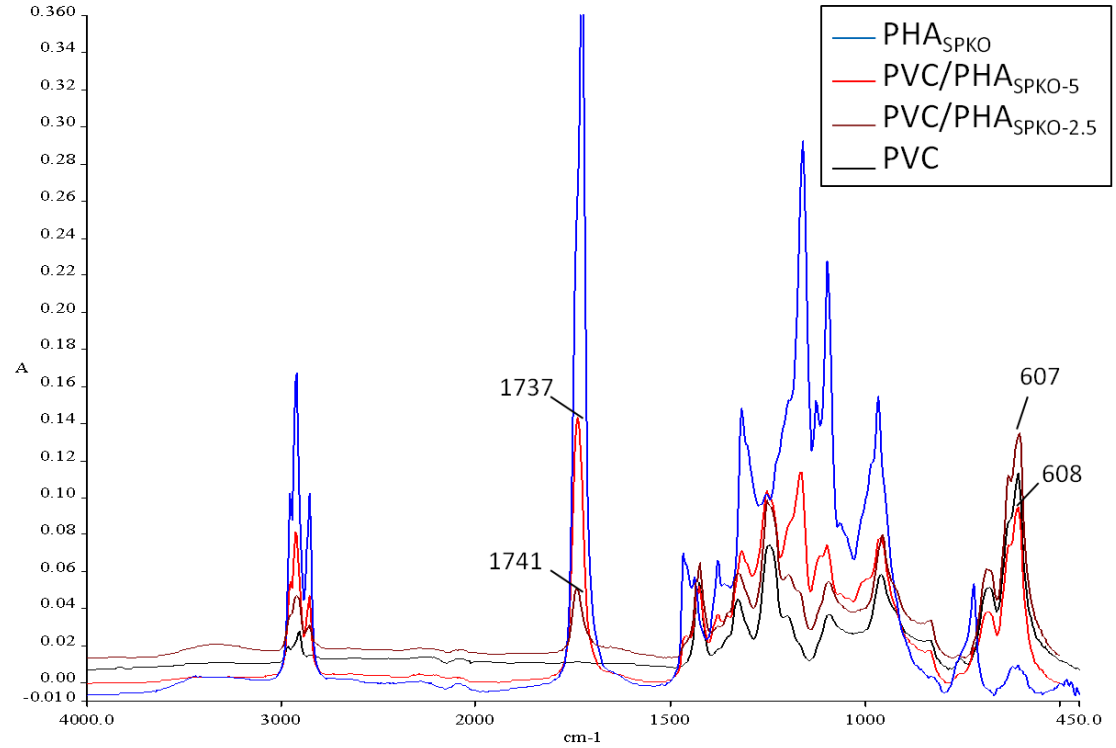

Fig. 5.3 FTIR absorption spectra of PVC, polymeric PHA_{SPKO} and the polymer blends: $PVC/PHA_{SPKO-2.5}$ and PVC/PHA_{SPKO-5}

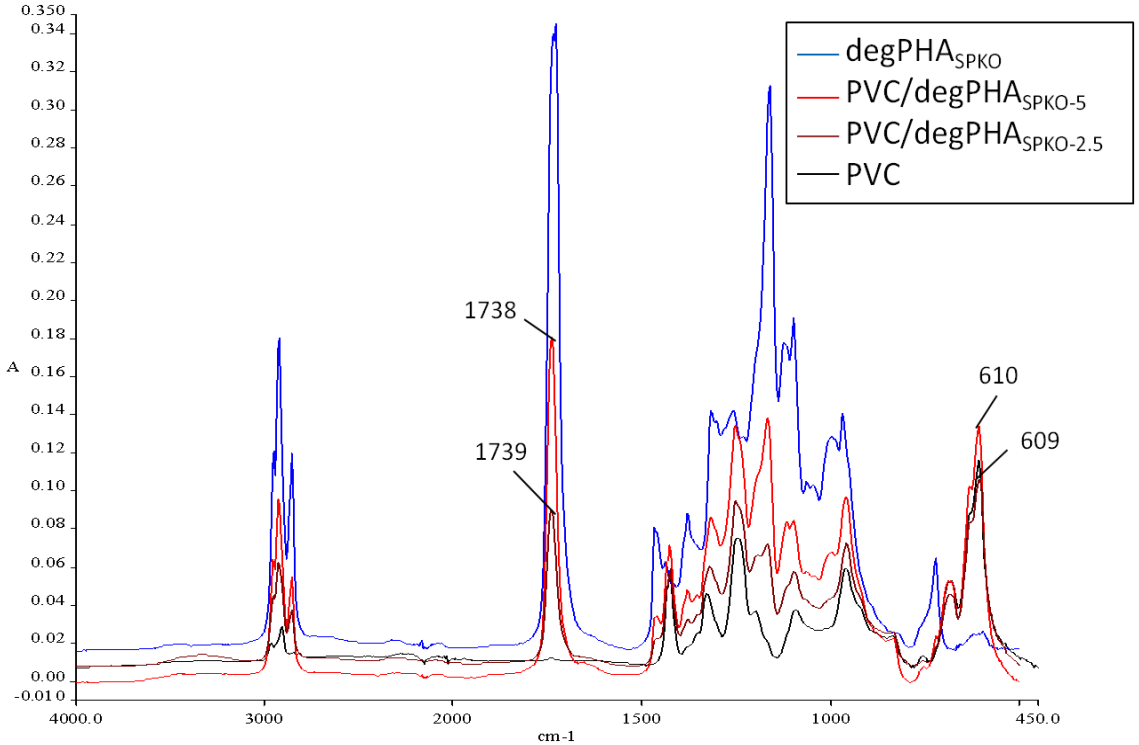

Fig. 5.4 FTIR absorption spectra of PVC, oligomeric PHA_{SPKO} ($degPHA_{SPKO}$) and the polymer blends: $PVC/degPHA_{SPKO-2.5}$ and $PVC/degPHA_{SPKO-5}$

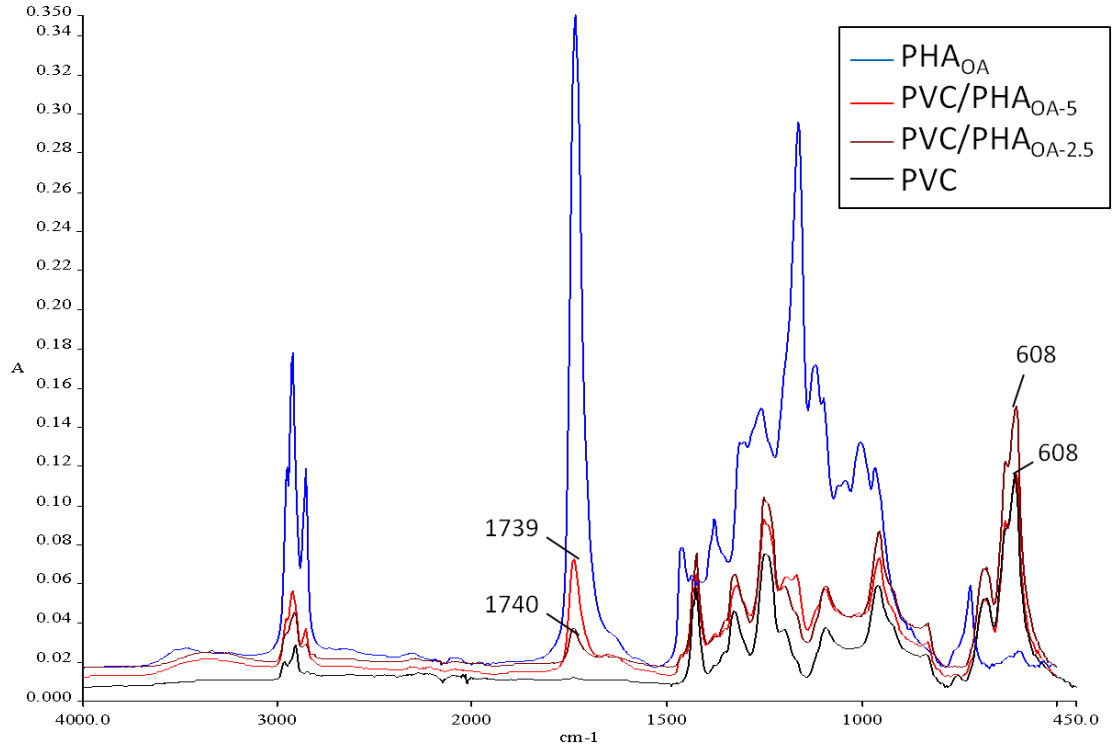

Fig. 5.5 FTIR absorption spectra of PVC, polymeric PHA_{OA} and the polymer blends: $PVC/PHA_{OA-2.5}$ and PVC/PHA_{OA-5}

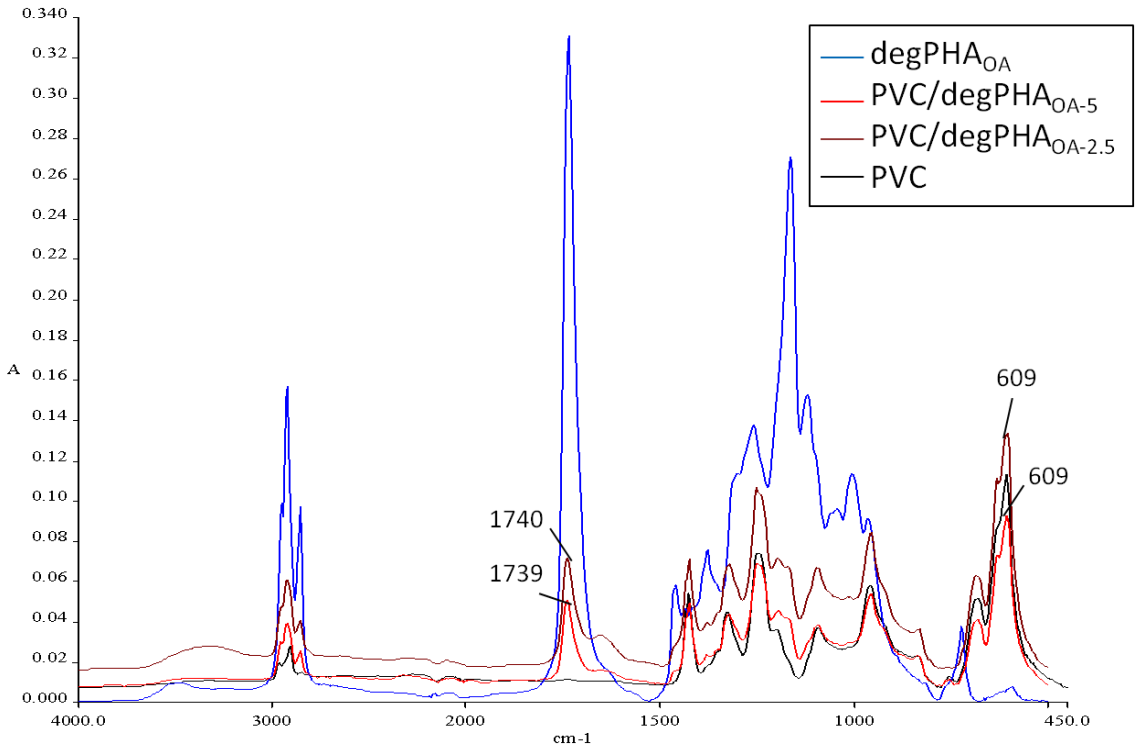

Fig. 5.6 FTIR absorption spectra of PVC, oligomeric PHA_{OA} ($degPHA_{OA}$) and the polymer blends: $PVC/degPHA_{OA-2.5}$ and $PVC/degPHA_{OA-5}$

Table 5.3 showed the relative intensity ratio of the absorbance value at C=O stretching present in mcl-PHA to the absorbance value of CH bending in PVC.

Table 5.3 Relative intensity ratio between absorbance value for C=O stretching in PHA and CH bending in PVC

PVC/PHA binary blends	**[5]Intensity ratio, A_{1739}/A_{1426} (C=O group of PHA to non-reactive CH_2 group of PVC)**	
	2.5 phr	**5 phr**
[1]PVC/PHA_{SPKO}	0.465	0.759
[2]PVC/degPHA_{SPKO}	0.394	0.631
[3]PVC/PHA_{OA}	0.392	0.728
[4]PVC/deg PHA_{OA}	0.282	0.563

[1]PVC/PHA_{SPKO}: PVC blend consisted of 2.5 or 5 phr polymeric PHA derived from SPKO; [2]PVC/degPHA_{SPKO}: PVC blend consisted of 2.5 or 5 phr oligomeric PHA derived from SPKO. [3]PVC/PHA_{OA}: PVC blend consisted of 2.5 or 5 phr polymeric PHA derived from oleic acid; [4]PVC/degPHA_{OA}: PVC blend consisted of 2.5 or 5 phr oligomeric PHA derived from oleic acid; [5]Intensity ratio, A_{1739}/A_{1426}: Height ratio of absorbance band at C=O stretching (A_{1739}= Base 1: 2776 cm^{-1}; Base 2: 1489 cm^{-1}) to CH bending (A_{1426}= Base 1: 1489 cm^{-1}; Base 2: 1392 cm^{-1})

PVC plasticized with polymeric PHA had higher relative ratio of A_{1739}/A_{1426} than with those plasticized with PHA oligoesters. Higher molecular weight and longer polyester chain has more ester C=O carbonyl group. Thus the polymeric PHA may have increased level of interaction with the PVC.

PVC plasticized with 5 phr PHA had higher relative ratio of A_{1739}/A_{1426} than with 2.5 phr PHA. As higher amount of PHA present in the polymer mixture, higher amount of polar groups in the polymer are available for possible interaction with PVC.

PVC plasticized with SPKO-derived PHA had higher relative ratio of A_{1739}/A_{1426} than with OA-derived PHA. SPKO-derived PHA had higher molecular weight and possessed a longer polymer chain compared to OA-derived PHA (referred to Table 3.2 and Appendix H). Thus SPKO-derived PHA was likely to have more interaction with PVC.

Fig. 5.7 to Fig. 5.10 showed the FTIR absorption spectra in the ester carbonyl (C=O) stretching region of PHA and PVC/PHA blends.

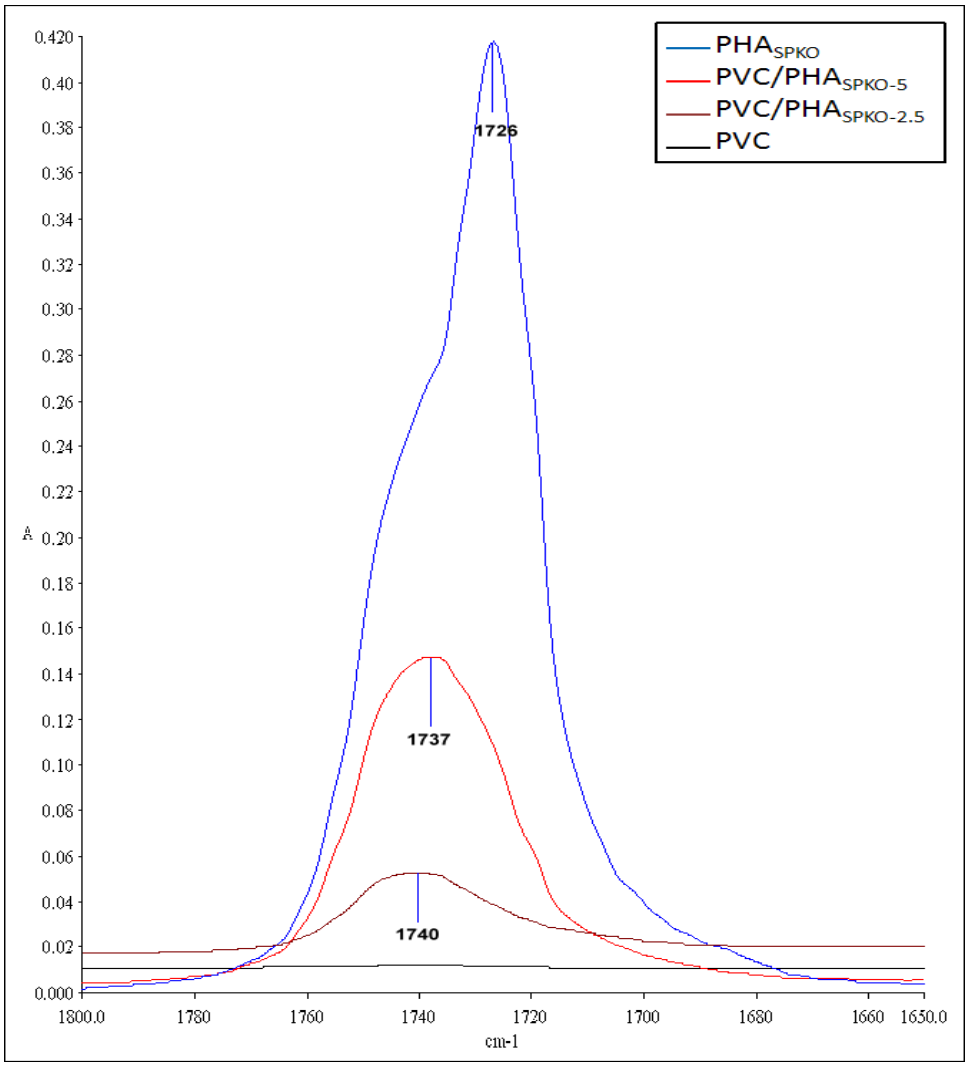

Fig. 5.7 FTIR absorption of PVC, PHA_{SPKO} and PVC/PHA_{SPKO} polymer blends in the region 1650 to 1800 cm^{-1}

The C=O stretching frequency for PHA_{SPKO} was observed at 1726 cm^{-1}, as shown in Fig. 5.7. After mixing the PVC with 2.5 and 5 phr of PHA_{SPKO}, the peak maximum position was shifted to higher frequency, i.e. 1737 cm^{-1} for PVC/PHA_{SPKO-5} and 1740 cm^{-1} for PVC/$PHA_{SPKO-2.5}$.

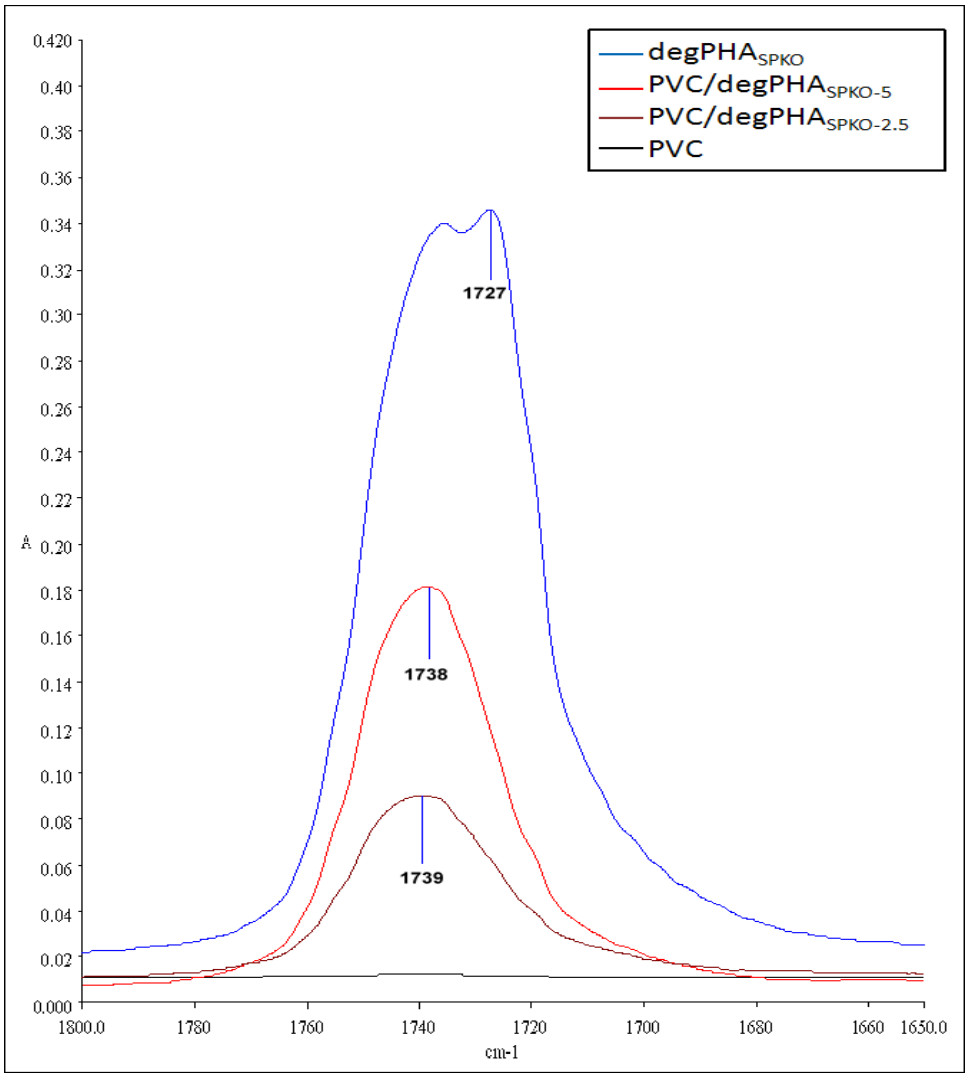

Fig. 5.8 FTIR absorption spectra of PVC, degPHA$_{SPKO}$ and PVC/degPHA$_{SPKO}$ polymer blends in the region 1650 to 1800 cm^{-1}

From Fig. 5.8, the ester carbonyl stretching frequency for oligomeric PHA_{SPKO} (degPHA$_{SPKO}$) was observed at 1727 cm^{-1}. After mixing the PVC with 2.5 and 5 phr of degPHA$_{SPKO}$, the peak maximum position was shifted to 1738 cm^{-1} for PVC/degPHA$_{SPKO-5}$ and 1739 cm^{-1} for PVC/degPHA$_{SPKO-2.5}$.

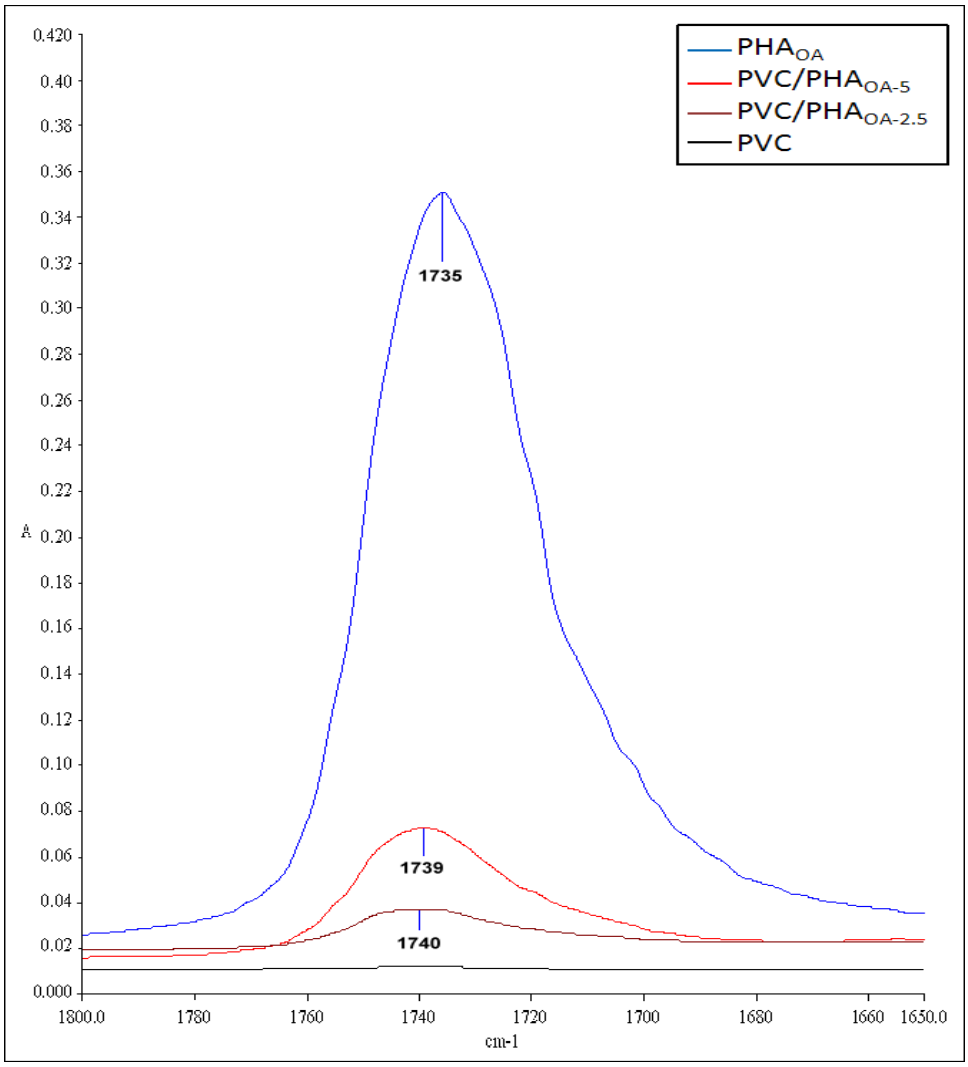

Fig. 5.9 FTIR absorption spectra of PVC, PHA_{OA} and PVC/PHA_{OA} polymer blends in the region 1650 to 1800 cm^{-1}

For PHA_{OA}, the ester carbonyl stretching frequency was observed at 1735 cm^{-1}, as shown in Fig. 5.9. The peak maximum position was shifted to higher frequency after the PVC was mixed with PHA_{OA} at different compositions, e.g. 1739 cm^{-1} for PVC/PHA_{SPKO-5} and 1740 cm^{-1} for PVC/$PHA_{SPKO-2.5}$.

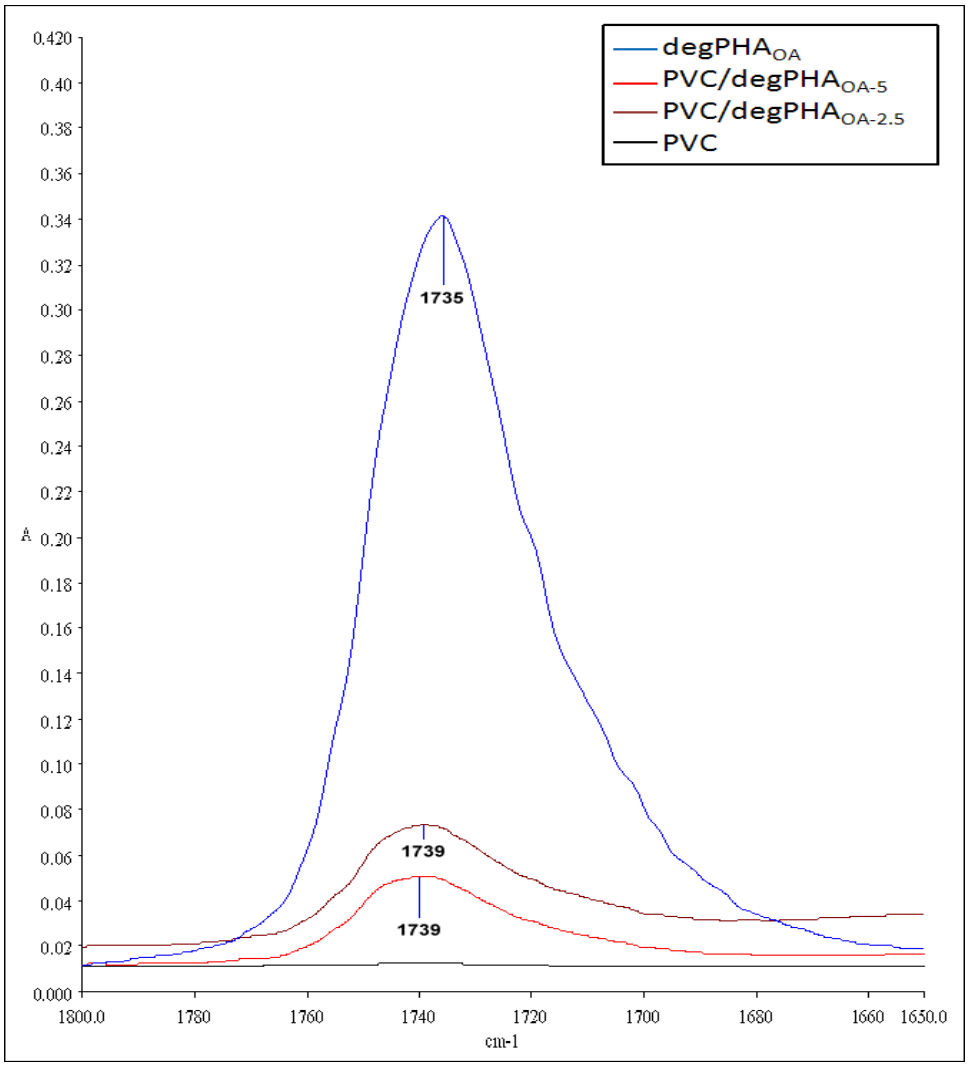

Fig. 5.10 FTIR absorption spectra of PVC, degPHA$_{OA}$ and PVC/degPHA$_{OA}$ polymer blends in the region 1650 to 1800 cm^{-1}

Similarly, the ester carbonyl stretching frequency for oligomeric PHA$_{OA}$ (degPHA$_{OA}$) was observed at 1735 cm^{-1}, as shown in Fig. 5.10. After mixing the PVC with degPHA$_{OA}$, the peak maximum position was shifted to 1739 cm^{-1} for both PVC/degPHA$_{SPKO-5}$ and PVC/degPHA$_{SPKO-2.5}$ binary blends.

From the observations for the shift of ester carbonyl stretching band in all polymer blends, it is believed that the C=O group in PHA could be responsible for the miscibility with the PVC, due to polar interactions in the system.

Fig. 5.11 to Fig. 5.14 showed the FTIR absorption spectra in the C-O-C and CH-Cl stretching region of PVC/PHA polymer blends. The CH-Cl deformation of PVC was assigned at 1328 cm^{-1}, whereas the C-O-C stretching vibration band for respective PHA was assigned at 1161 to 1164 cm^{-1}.

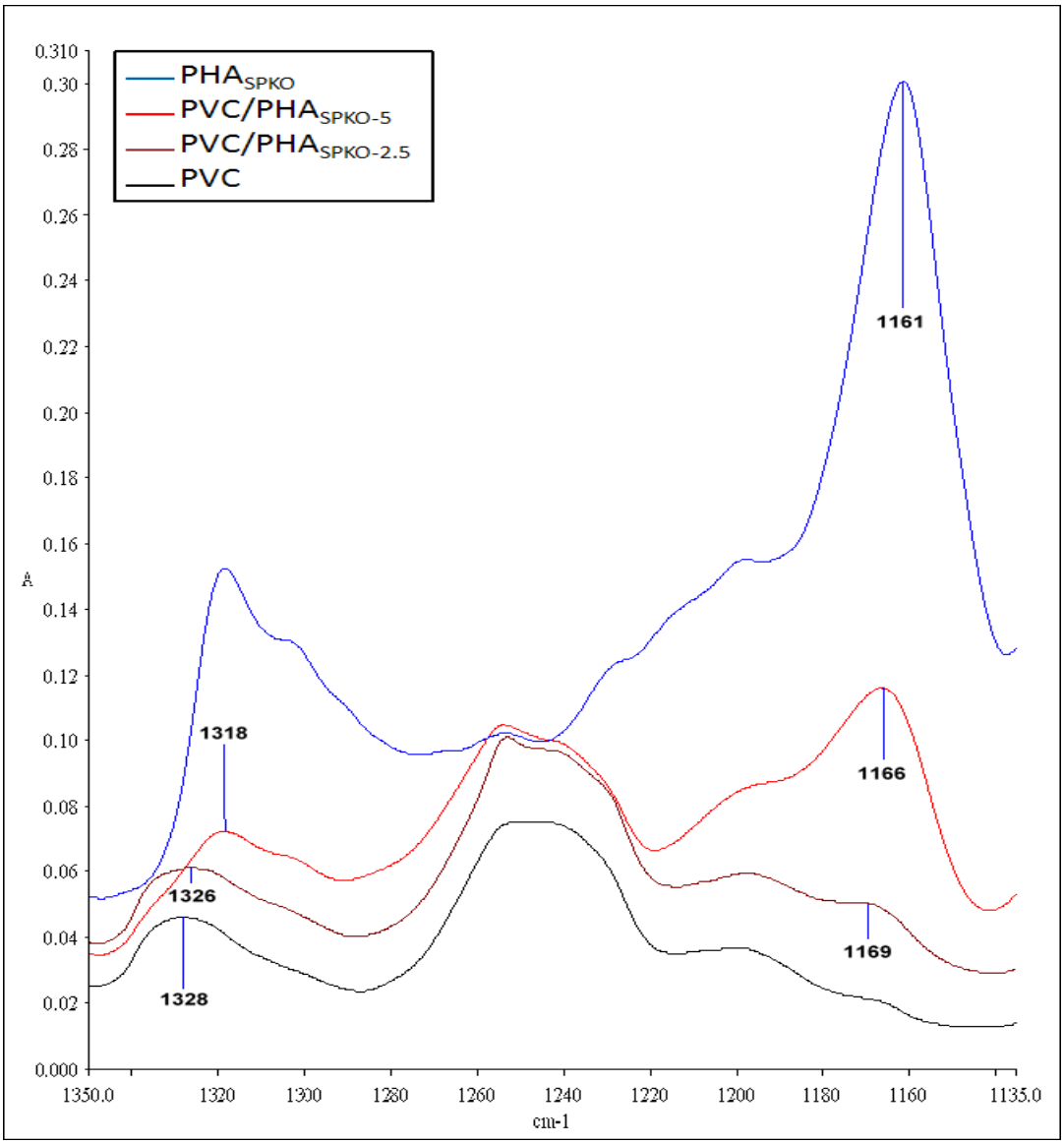

Fig. 5.11 FTIR absorption spectra of PVC, PHA_{SPKO} and PVC/PHA_{SPKO} polymer blends in the region 1135 to 1350 cm^{-1}

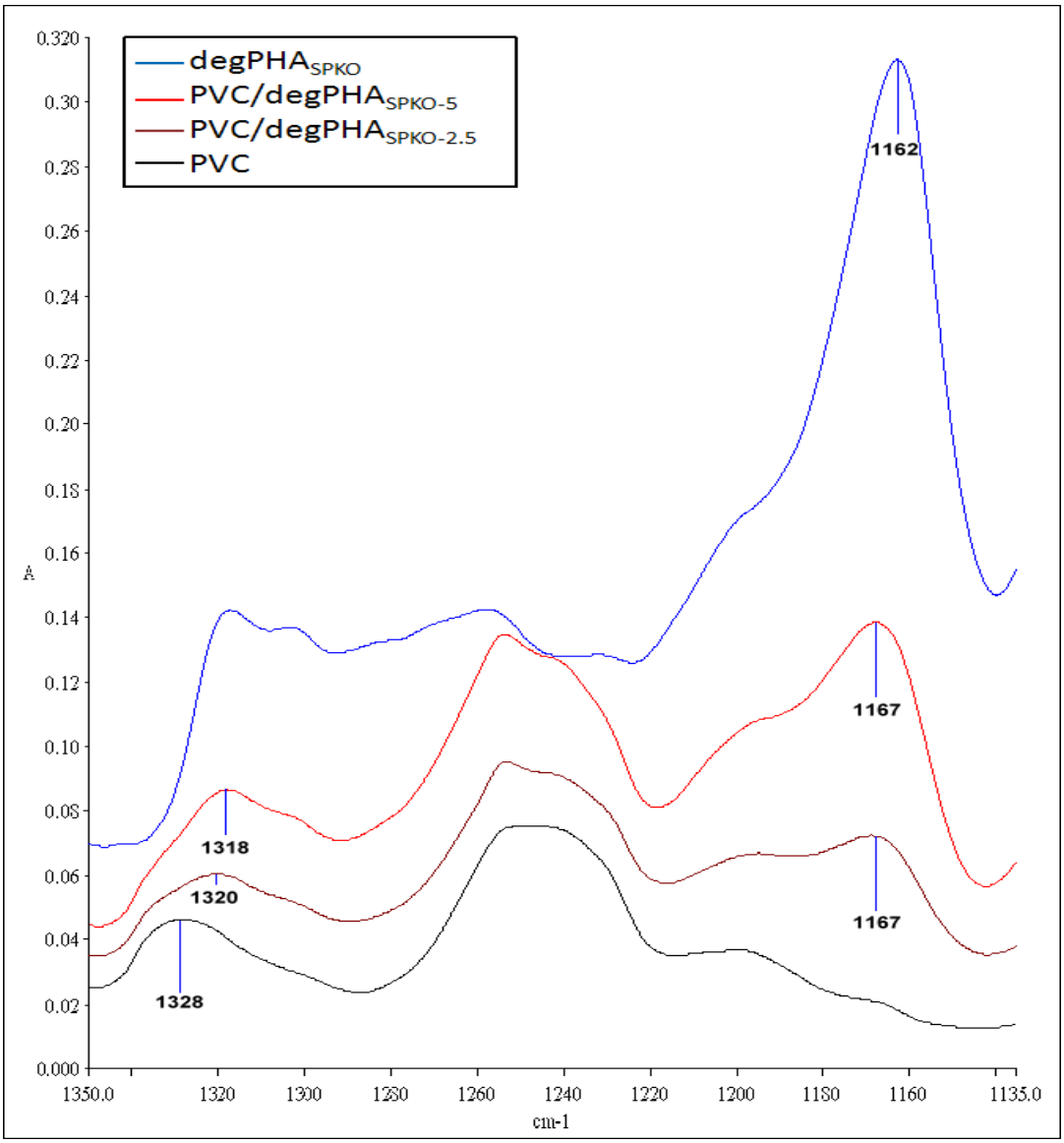

Fig. 5.12 FTIR absorption spectra of PVC, degPHA$_{SPKO}$ and PVC/degPHA$_{SPKO}$ polymer blends in the region 1135 to 1350 cm^{-1}

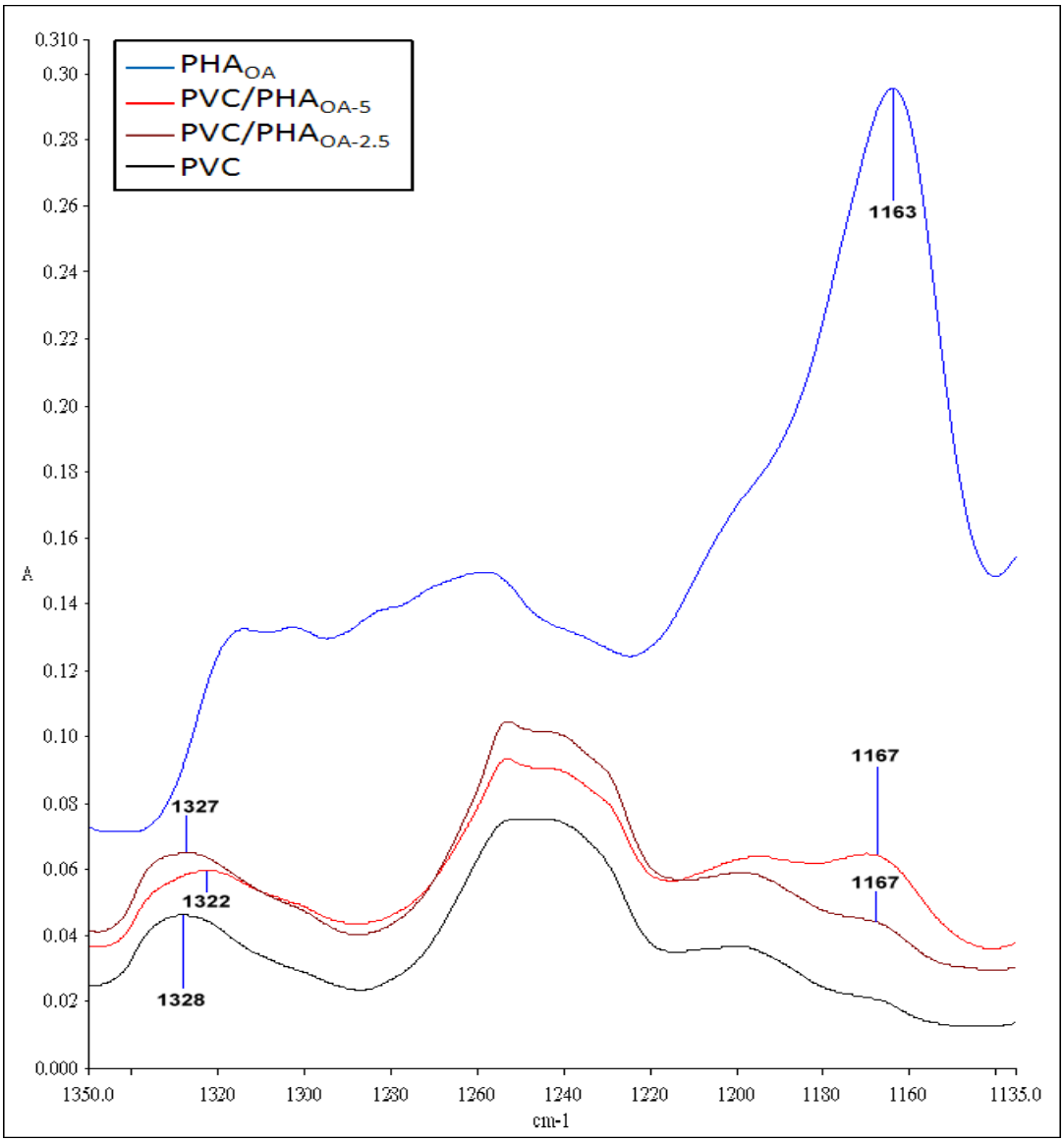

Fig. 5.13 FTIR absorption spectra of PVC, PHA_{OA} and PVC/PHA_{OA} polymer blends in the region 1135 to 1350 cm^{-1}

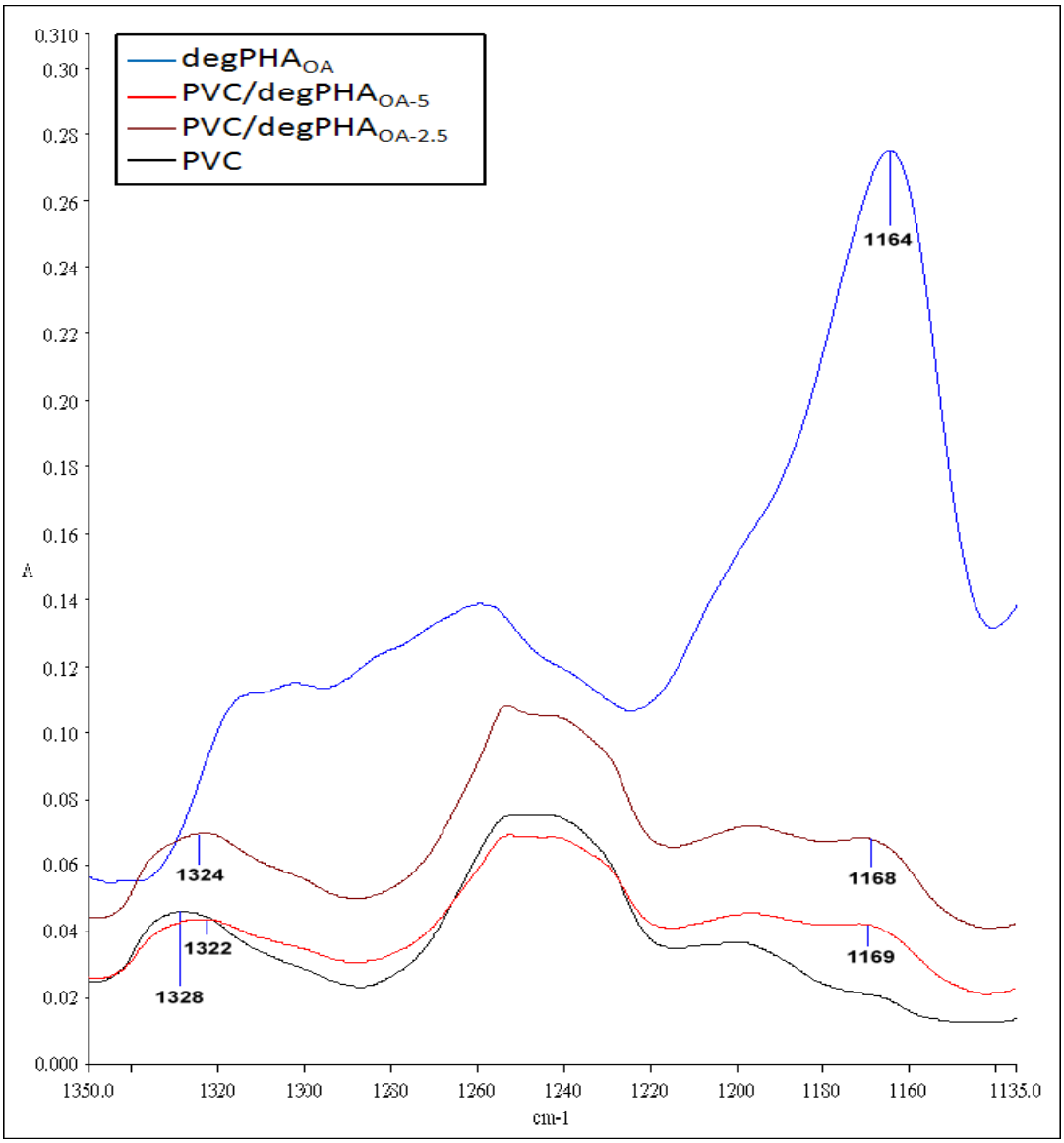

Fig. 5.14 FTIR absorption spectra of PVC, degPHA$_{OA}$ and PVC/degPHA$_{OA}$ polymer blends in the region 1135 to 1350 cm^{-1}

As shown in Fig. 5.11 to Fig. 5.14, the C-O-C stretching vibration of PHA and CH-Cl deformation of PVC for all the polymer blends were shifted. These showed the existence of specific interactions such as dipole-dipole and polar interactions between the two polymers.

5.2.3 ^{1}H-NMR analysis of PVC-PHA system

Nuclear magnetic resonance (NMR) spectroscopy is one of the techniques which could provide information on a molecular dimension scale (Havens & Koenig, 1983). The general molecular structure of the repeating unit for PVC and mcl-PHA is shown in Fig. 5.15 (a) and (b), respectively.

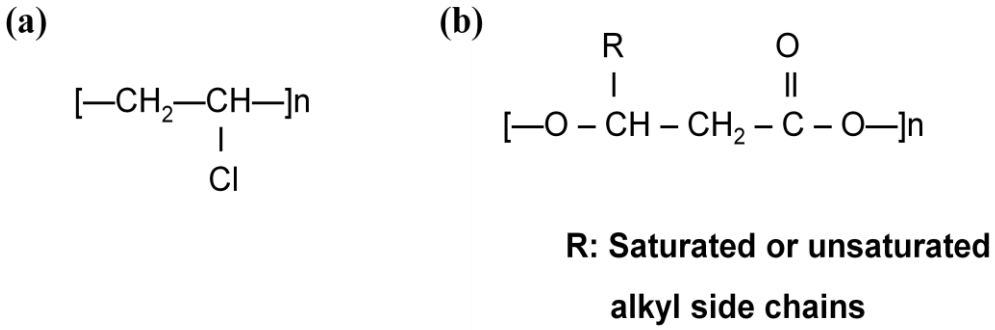

Fig 5.15 Structural formula of (a) PVC and (b) mcl-PHA monomer units

Fig. 5.16 and Fig. 5.17 showed the proton NMR spectra for PVC and the PHA (in this case, PHA_{OA}) used in the polymer blending.

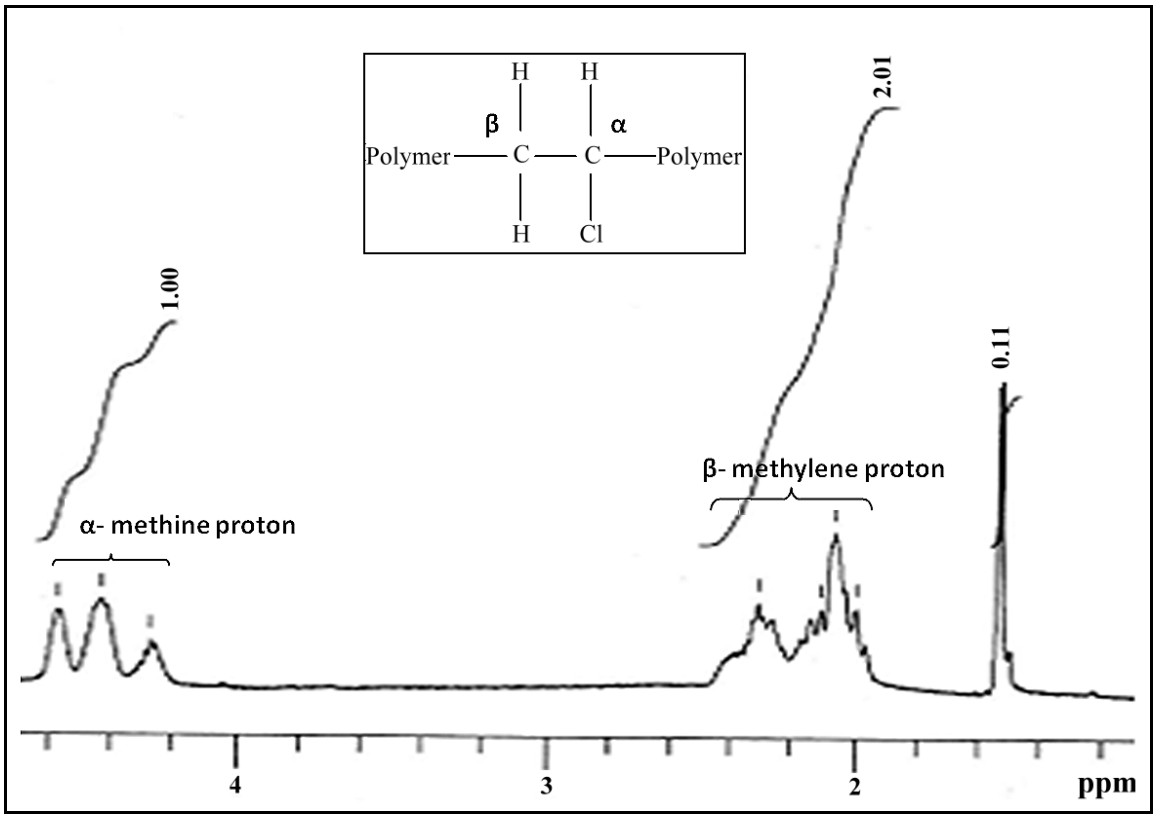

Fig. 5.16 ^{1}H-NMR spectrum of PVC. Chemical shift from 1.9 to 2.3 ppm was assigned to H_β of $–CH_2–$; chemical shift from 4.3 to 4.6 ppm was assigned to H_α of –CHCl–

In Fig. 5.16, the peaks around 4.3 to 4.6 ppm were assigned to the α-methine proton (–CHCl–) which attached to the electropositive carbon atom, and peaks around 1.9 to 2.3 ppm was assigned to the β-methylene proton ($–CH_2–$) in PVC. The relative intensity ratio of $^{\alpha}$H (α-methine proton) to $^{\beta}$H (β-methylene proton) was 1:2, in agreement to the structure of the repeating unit. The peak at 1.5 ppm was due to the moisture in the D-chloroform. This could be due to the relatively low solubility of PVC in the chloroform and therefore small amount of water in the solvent could be detected in the spectrum.

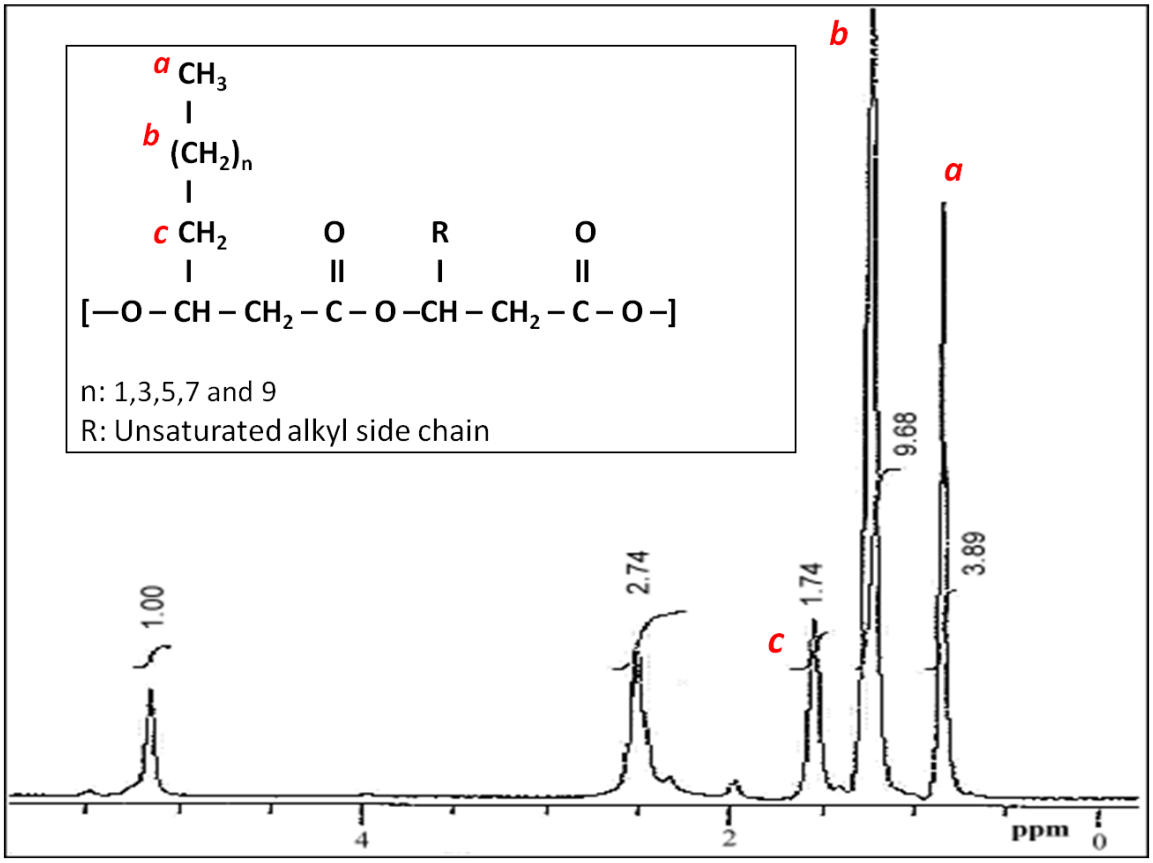

Fig. 5.17 ^{1}H-NMR spectrum of PHA_{OA}. The protons in the PHA_{OA} structure were denoted by the corresponding letters in the spectrum

Fig. 5.17 showed the ^{1}H-NMR spectrum of oleic acid derived mcl-PHA. The peak *a* at 0.8 ppm and peak *b* at 1.2 ppm were assigned to the methyl (-CH_3) and methylene (-$(CH_2)_n$-) group in the PHA side chain, respectively. Peak *c* at around 1.5 ppm was assigned to the methylene (-CH_2-) group attached to the carbon adjacent to the oxygen atom. These three peaks: *a, b* and *c* are the characteristic peaks of PHA, which could be used to validate the presence of polyester in the polymer blends.

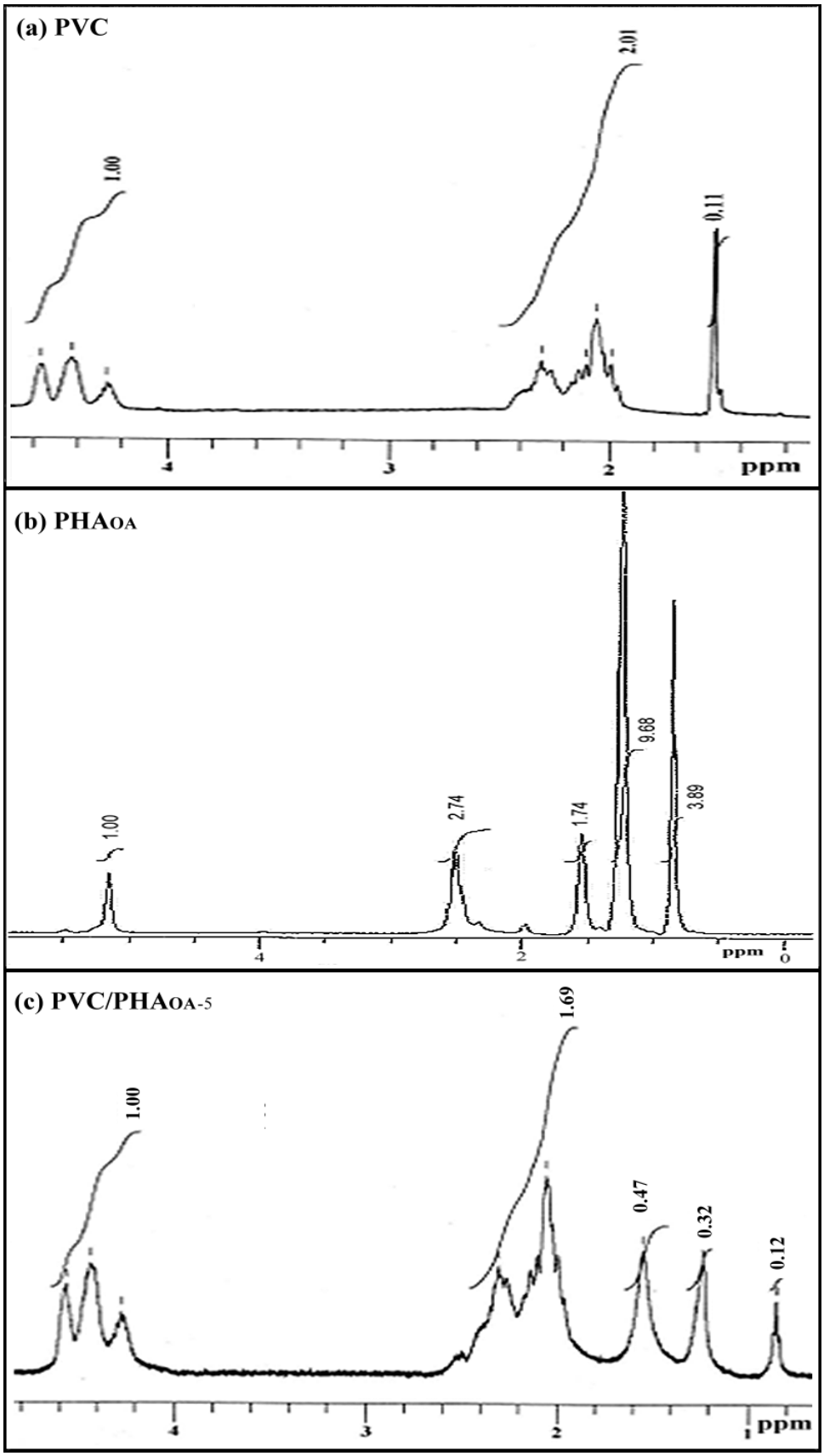

Fig. 5.18 ^{1}H-NMR spectra of (a) PVC, (b) PHA_{OA} and (c) PVC/PHA_{OA-5} polymer blends

Fig. 5.18 compared the ^{1}H-NMR spectra of (a) PVC and (b) PHA_{OA} with the polymer blend, (c) PVC/PHA_{OA-5}. As could be seen from Fig. 5.18 (c), the spectrum of PVC/PHA_{OA-5} polymer blend showed almost identical peaks as PVC, with three additional peaks being detected: 0.8 ppm, 1.2 ppm and 1.5 ppm which assignable to $–CH_3$, $-(CH_2)_n-$ and $–CH_2-$ groups in PHA, respectively. This showed that both PVC and PHA were present in the polymer. On the other hand, the relative intensity ratio of $^{\alpha}$H/ $^{\beta}$H in PVC/PHA_{OA-5} was reduced to 1.69, compared to PVC.

The ^{1}H-NMR spectra for the other polymer blends showed similar spectrum as PVC/PHA_{OA-5} and the relative intensity ratio of $^{\alpha}$H to $^{\beta}$H in the polymer blends were summarized in Table 5.4.

Table 5.4 Relative intensity ratio between $^{\alpha}$H (α-methine proton) to $^{\beta}$H (β-methylene proton) in polymer blends

PVC/PHA binary blends	**Relative intensity ratio of $^{\alpha}$H to $^{\beta}$H**	
	2.5 phr	**5 phr**
PVC/ PHA_{SPKO}	1/1.70	1/1.77
PVC/deg PHA_{SPKO}	1/1.57	1/1.66
PVC/ PHA_{OA}	1/1.77	1/1.69
PVC/degPHA_{OA}	1/1.64	1/1.69

From Table 5.4, the ratio of $^{\alpha}$H/$^{\beta}$H in polymer blends varied with the compositions and types of PHA present in the polymer blends. All the blends showed a reduced ratio of $^{\alpha}$H/$^{\beta}$H, compared to the PVC, indicating that the α-methine proton or/and β-methylene proton in the PVC could be interacted with the PHA, giving rise to the specific intermolecular interactions within the polymer mixture. These inter-polymer interactions could be probably attributed to the interactions of α-hydrogen as well as the

local dipole-dipole interaction between chlorines of PVC with the PHA, in which the two polymers may intermingle with each other on a molecular level.

5.3 Scanning electron microscopy (SEM) of PVC and plasticized PVC films

In order to understand how the surface morphology of the PVC film changes with the introduction of plasticizers, the SEM micrographs of the pure PVC and PHA-plasticized PVC films were taken. The simplest polymer blends are typically a two-phase system consisting of a rubbery impact modifier dispersed in a thermoplastic matrix such as PVC.

5.3.1 Morphology of PVC and PHA films by SEM

As shown in Fig. 5.19, cavities were present in the individual PVC film. The pores were distributed throughout the surface with the pore size in the range of 1 to 20 μm. These observations were similar to the findings reported by Stephan et al. (2000). Fig. 5.20 showed the surface morphology of PHA_{SPKO} film. PHA_{SPKO} physically and morphologically existed as softer and amorphous material and thus appeared as a smooth film, without any cavity, under the electron microscope.

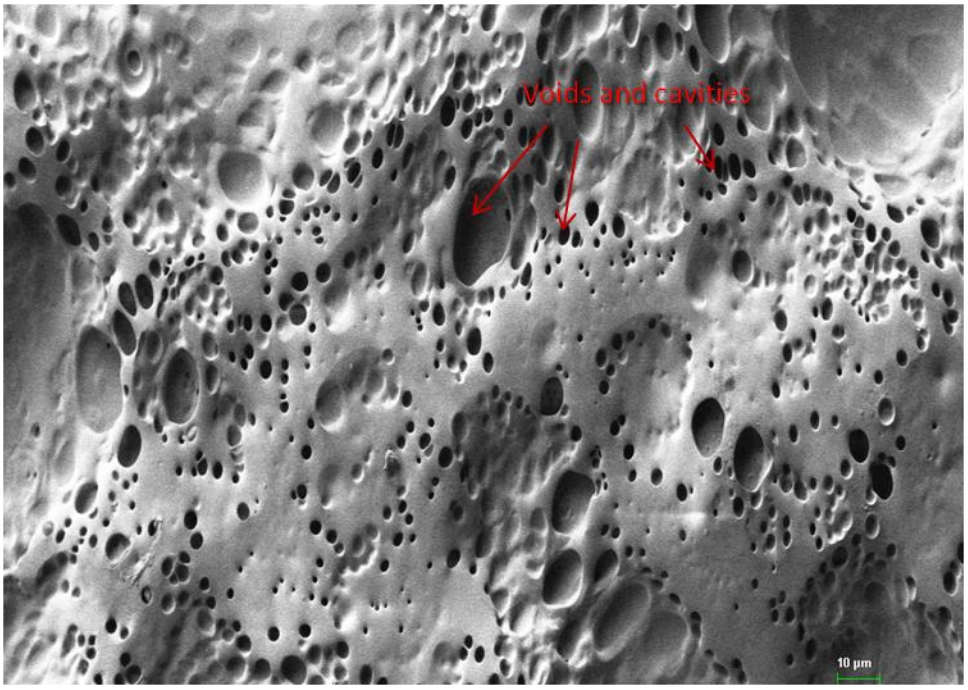

Fig. 5.19 SEM micrograph showing surface morphology of PVC. Voids and cavities were present in the PVC film (500 x magnification)

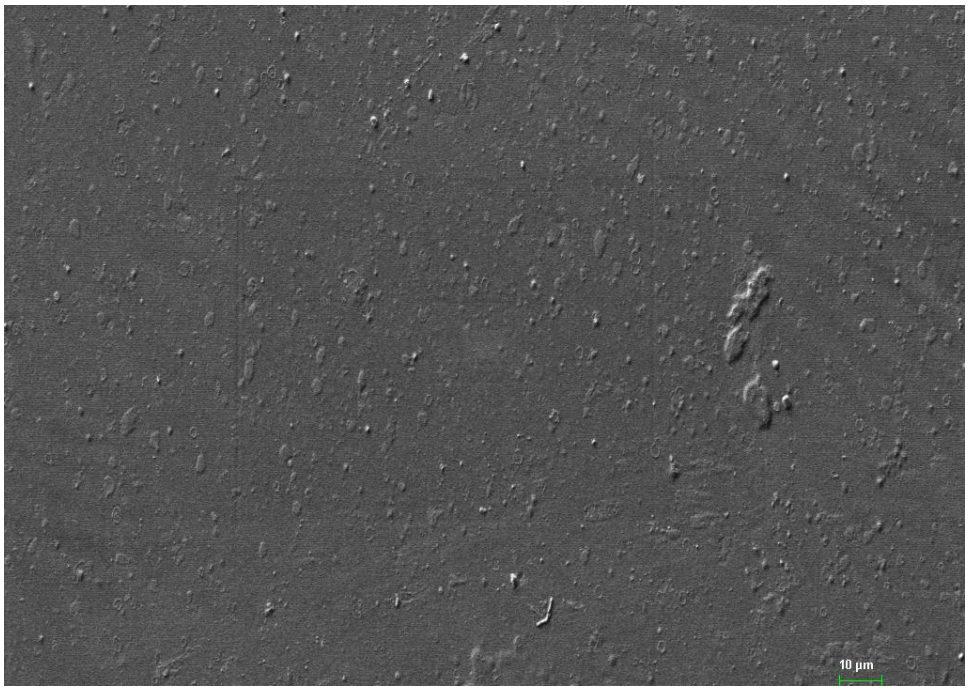

Fig. 5.20 SEM micrograph showing surface morphology of PHA_{SPKO} film (500 x magnification)

5.3.2 Qualitative comparisons of PVC/PHA binary blend morphologies by SEM

SEM is used to examine the surface variations of polymer blends and provide qualitative comparisons for blend morphology (Hobbs & Watkins, 2000). A basic function for the plasticizer is to act as a lubricant (Clark, 1941), embedding themselves between the polymer chains, reducing the internal resistance to sliding and thus allowing the polymer chains to move past each other rapidly.

Fig. 5.21 to Fig. 5.28 showed the SEM micrographs of PVC/PHA blend films prepared by solution casting.

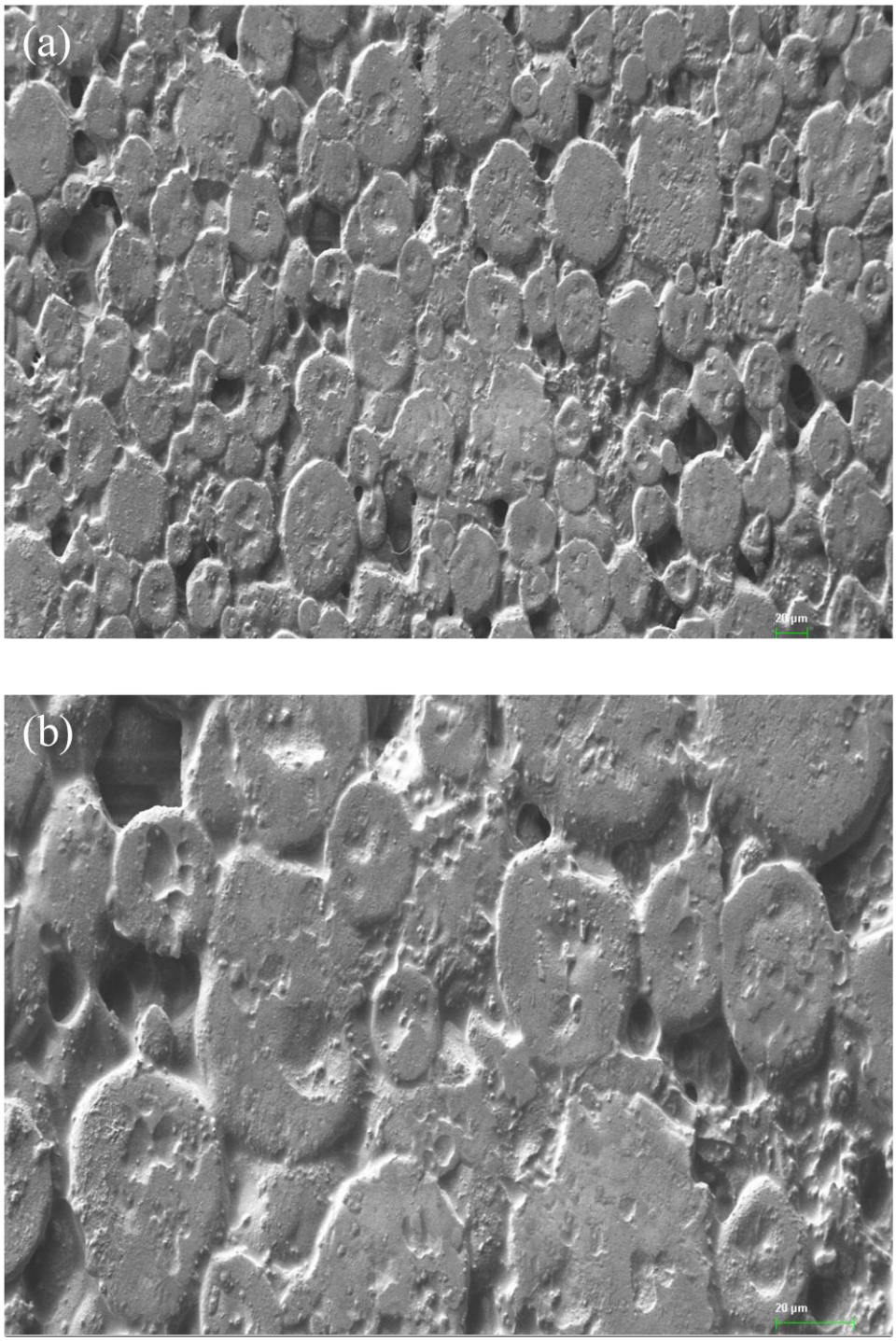

Fig. 5.21 SEM micrograph showing surface morphology of PVC/$PHA_{SPKO-2.5}$ film: (a)200 x; (b)500 x magnification

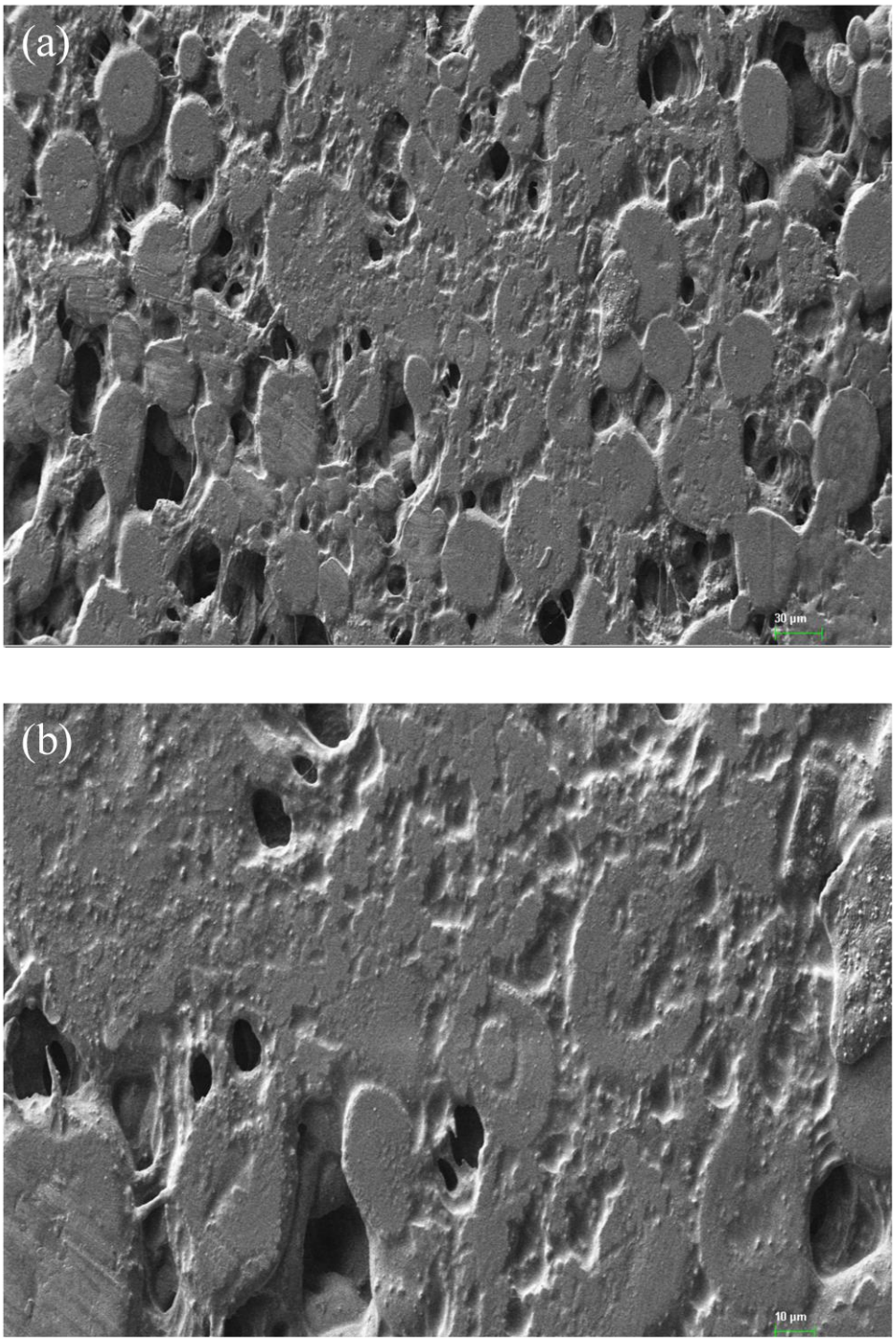

Fig. 5.22 SEM micrograph showing surface morphology of PVC/PHA_{SPKO-5} film: (a)200 x; (b)500 x magnification

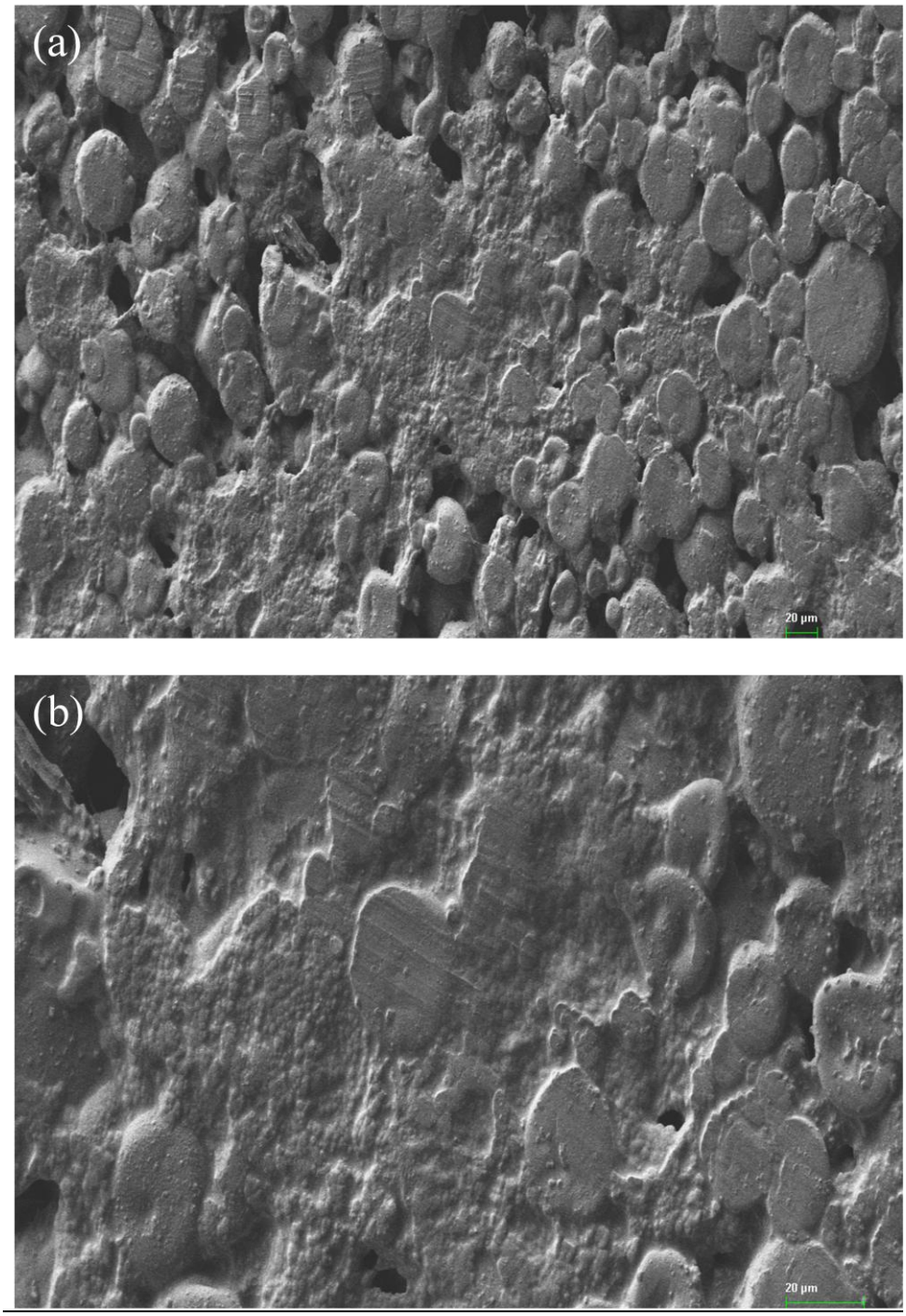

Fig. 5.23 SEM micrograph showing surface morphology of PVC/degPHA$_{SPKO-2.5}$ film: (a)200 x; (b)500 x magnification

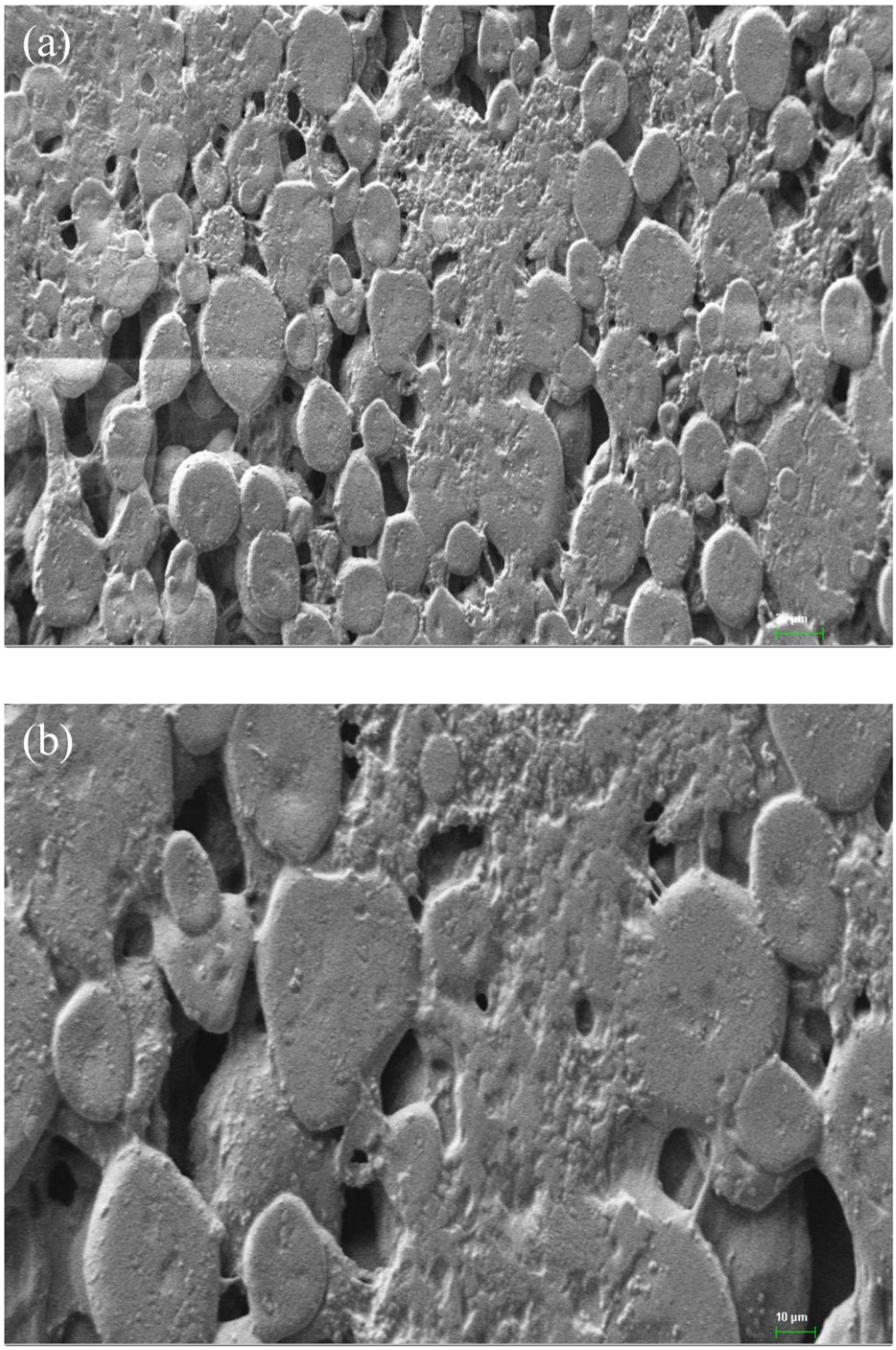

Fig. 5.24 SEM micrograph showing surface morphology of PVC/degPHA$_{SPKO-5}$ film: (a)200 x; (b)500 x magnification

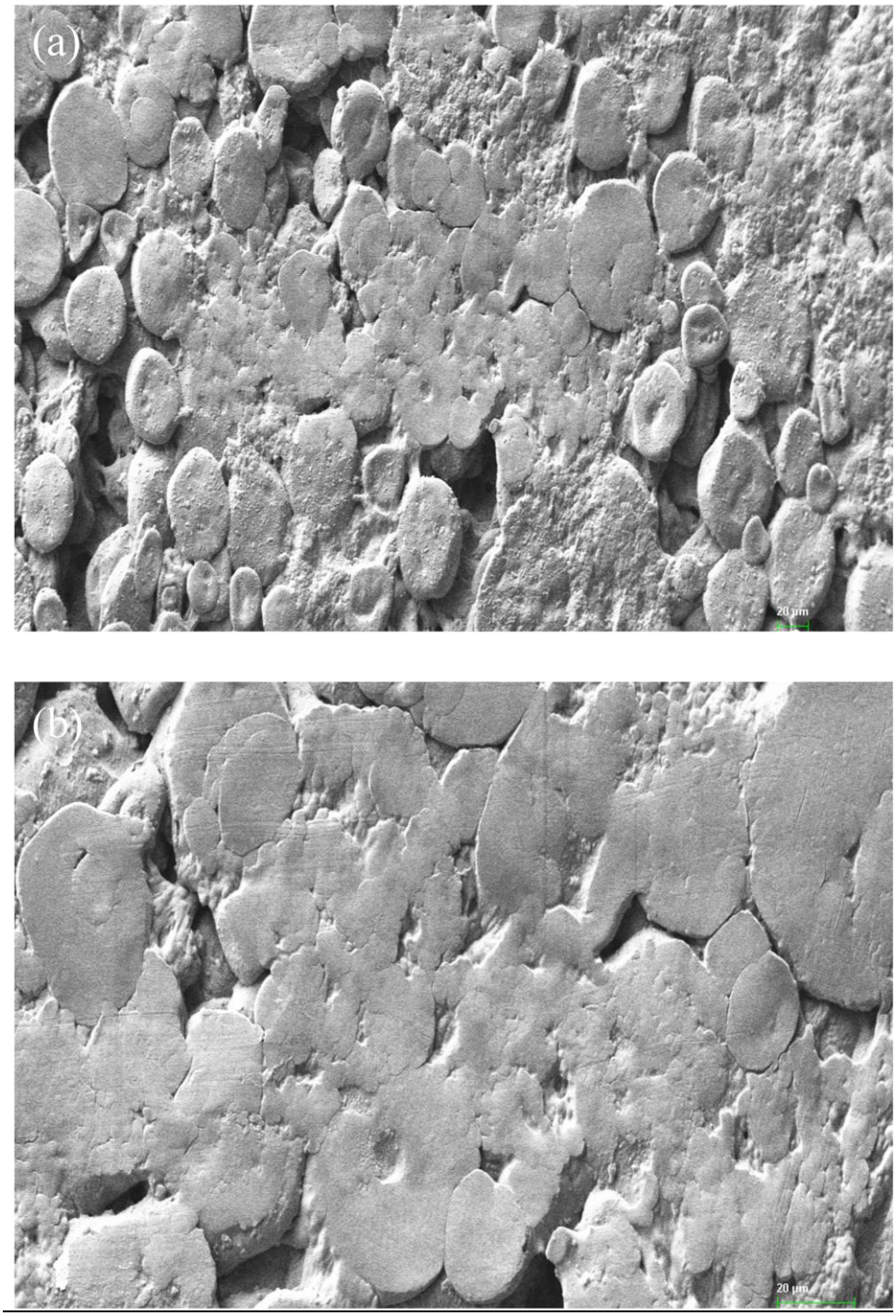

Fig. 5.25 SEM micrograph showing surface morphology of PVC/$PHA_{OA\text{-}2.5}$ film: (a)200 x; (b)500 x magnification

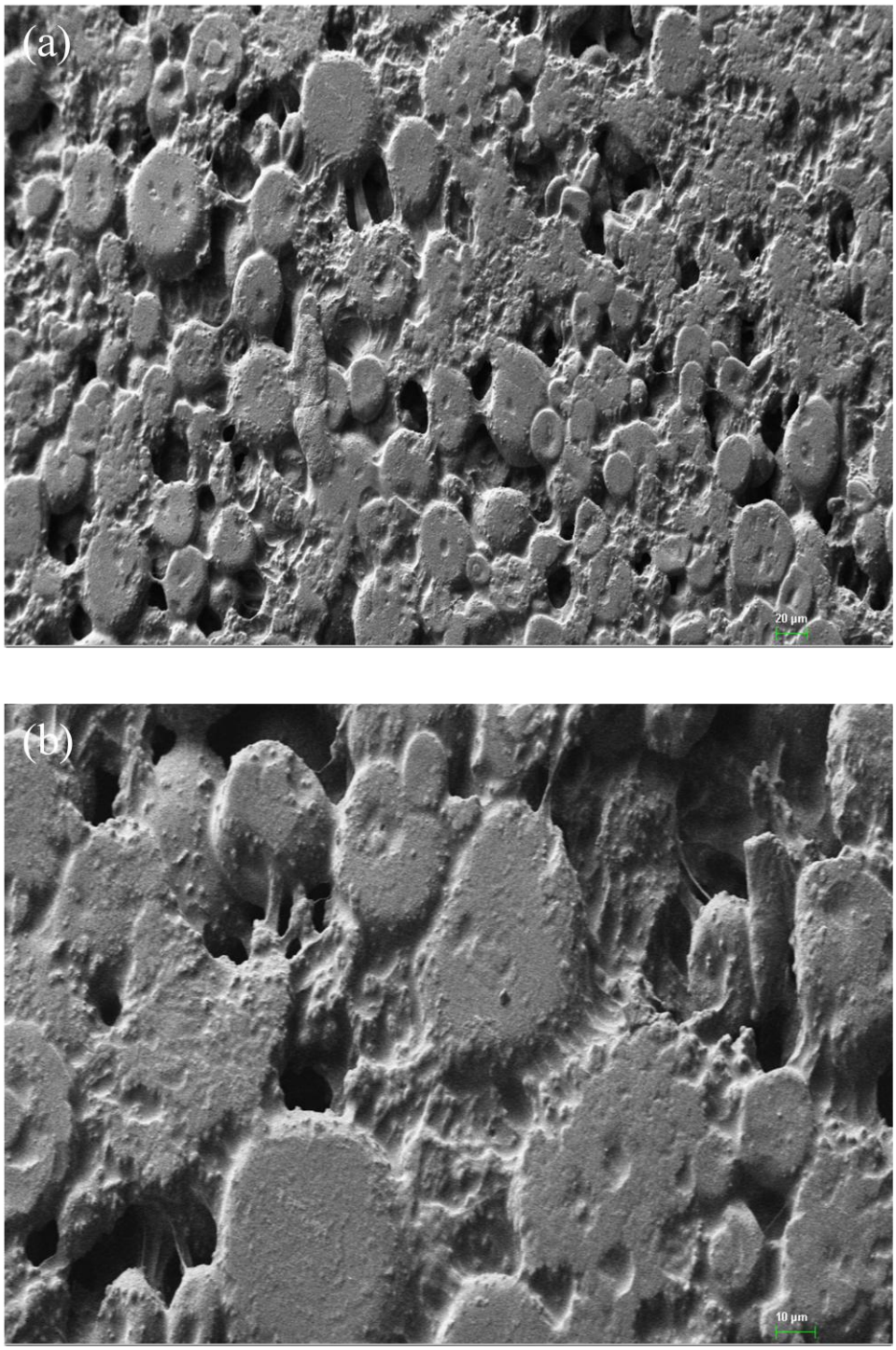

Fig. 5.26 SEM micrograph showing surface morphology of PVC/PHA_{OA-5} film: (a)200 x; (b)500 x magnification

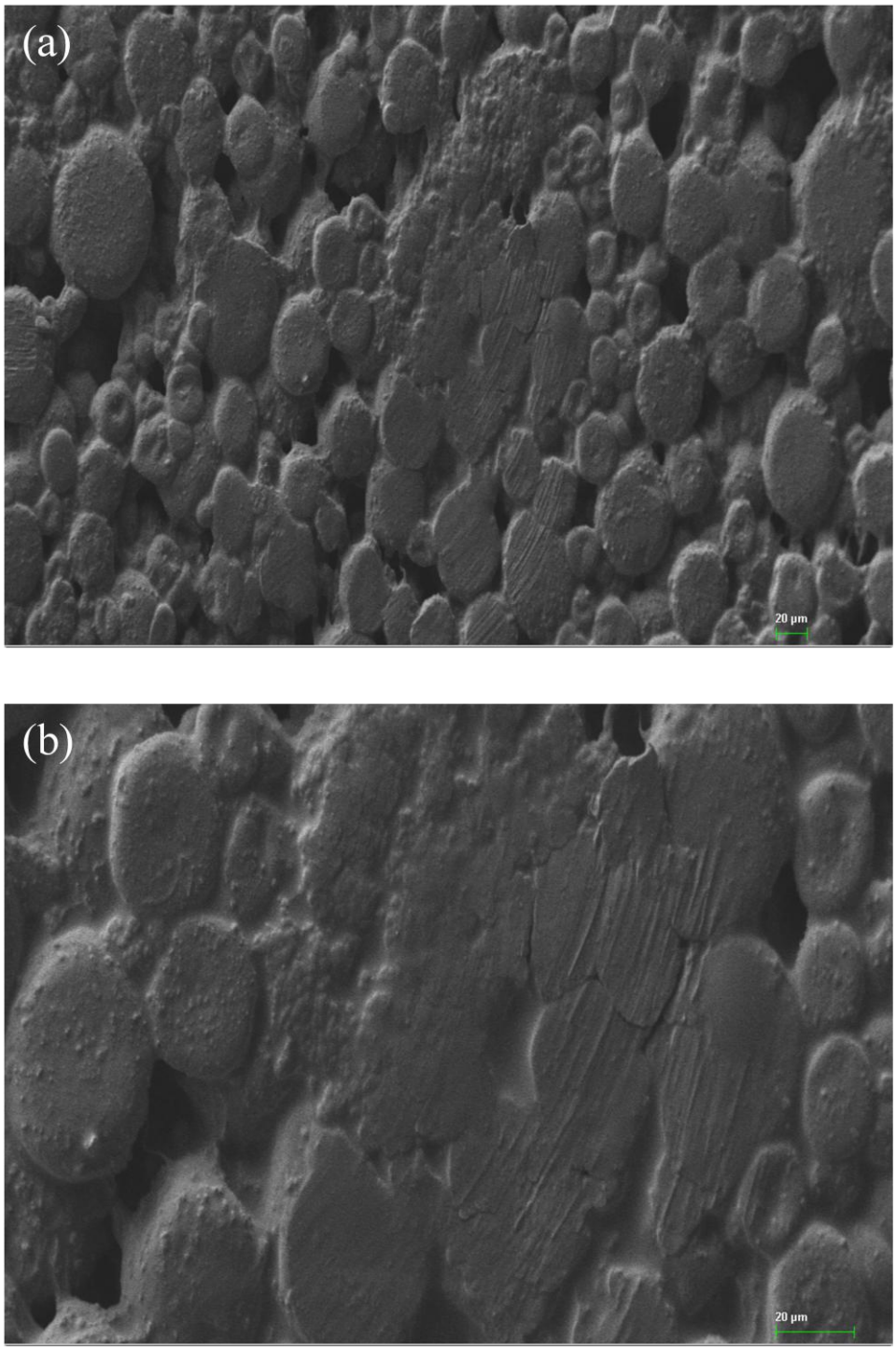

Fig. 5.27 SEM micrograph showing surface morphology of PVC/degPHA$_{OA\text{-}2.5}$ film: (a)200 x; (b)500 x magnification

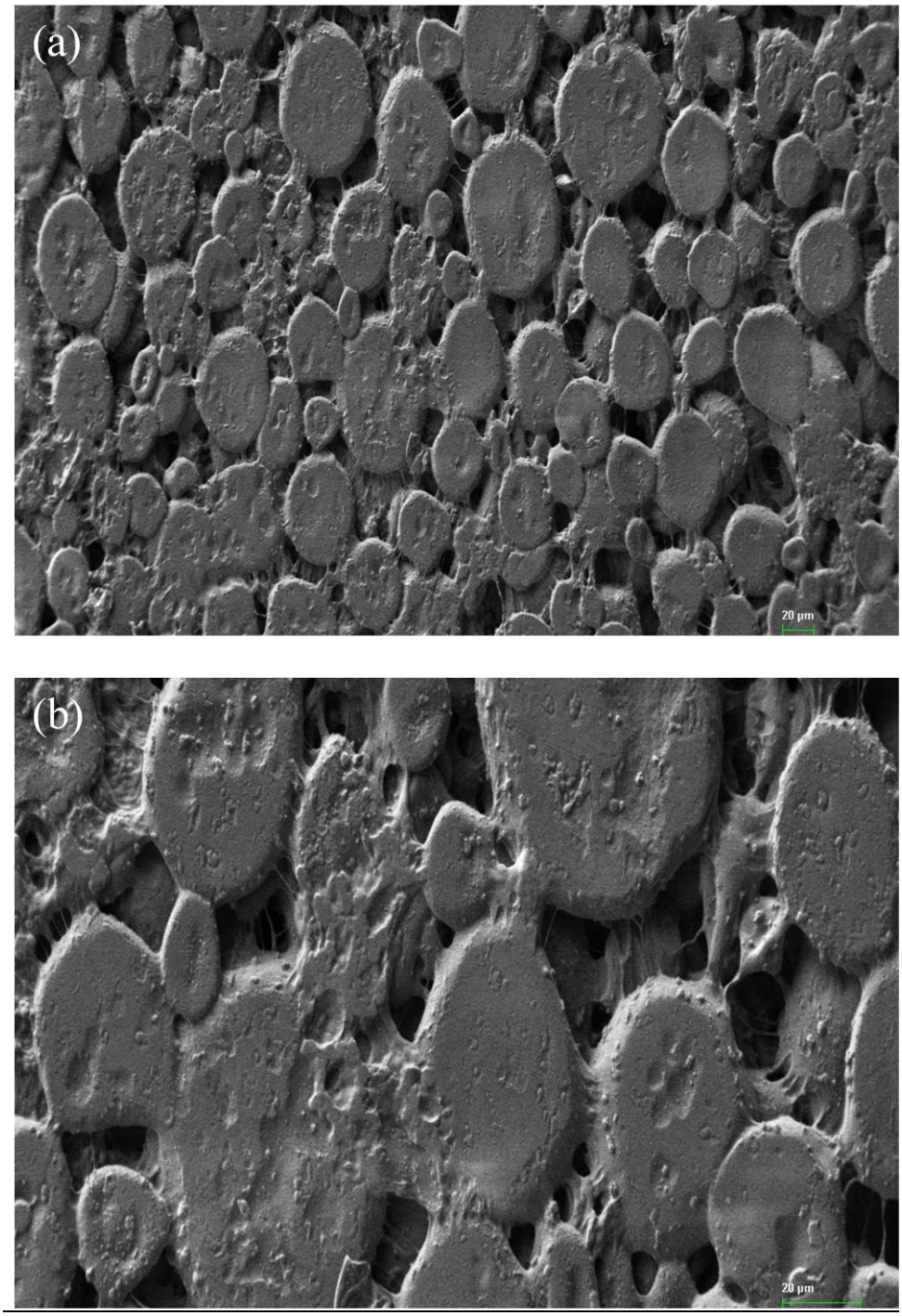

Fig. 5.28 SEM micrograph showing surface morphology of PVC/degPHA$_{OA-5}$ film: (a)200 x; (b)500 x magnification

As shown in the SEM micrographs of the polymer blends, after mixing the PVC with PHA, the cavities were not as clearly observed as in pure PVC. The PHA penetrated to some of the porous structures of PVC and interfused with the PVC polymer segments.

The dispersion of the PHA into the PVC matrix presumably increased the distance between PVC chains, by placing themselves in between the PVC polymers and separating the PVC chains further apart, therefore promoted higher degree of freedom of polymer conformation. The effectiveness in the dispersion of plasticizers in PVC matrix could be attributed to the molecular weight of the PHA and polar interactions between PVC and PHA phases. Low molecular weight oligoesters would have greater diffusion into the PVC matrix compared to polymeric PHA, leading to greater flexibility and polymer chain movements.

5.4 Thermal studies of PVC and PVC/PHA binary blends

The thermal stability of polymer blend is a vital parameter to characterize the plasticizing effect of the PHA on PVC. In this study, thermogravimetric analysis (TGA) was used to study the thermal stability of PVC and a series of PVC/PHA polymer blends consisting of PVC and different types of mcl-PHA as plasticizers. The derivative thermogravimetry (DTG) which is defined as the first derivative of the weight change of sample as a function of temperature was used to analyze overlapping decompositions where different components of the polymer blends could be separated and subsequently determined the thermal stability of each component.

Fig. 5.29 to Fig. 5.37 showed the respective TG and DTG curves of PVC and PVC/PHA polymer blends.

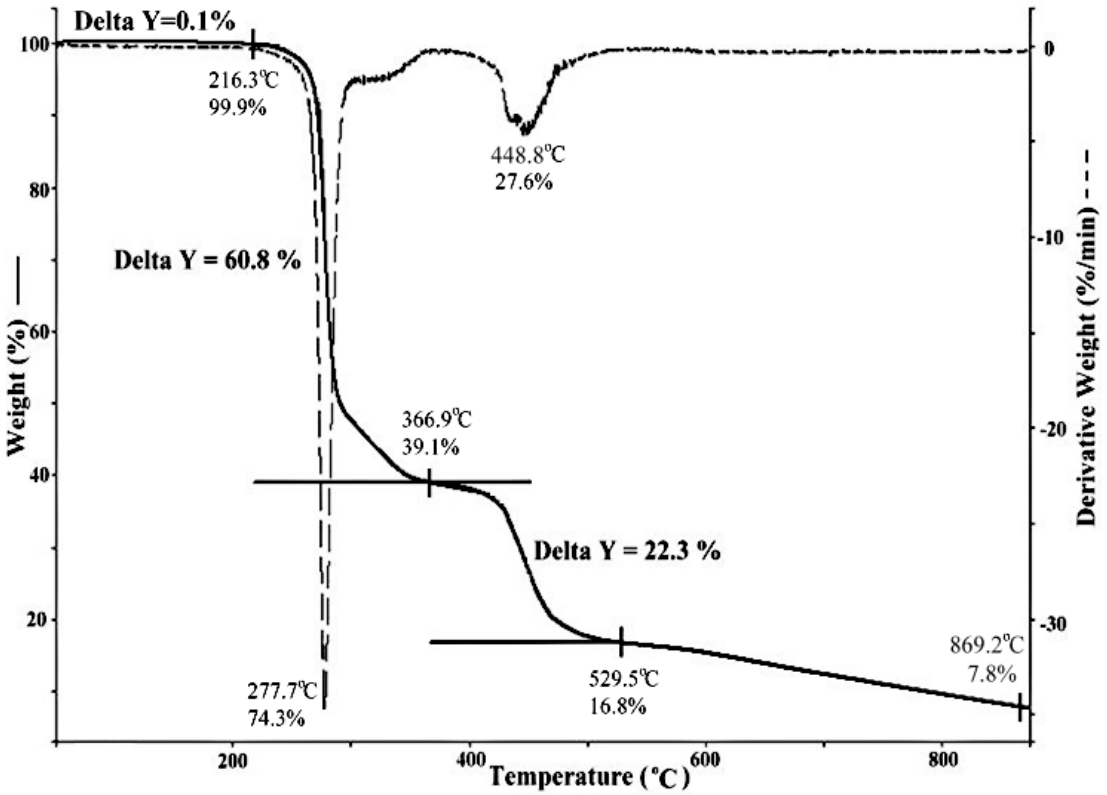

Fig. 5.29 TGA thermogram of PVC

Fig. 5.29 showed the TGA thermogram of PVC, which exhibited two distinct stages of thermal decomposition. The first decomposition started from 216 ℃ to 367 ℃ with a peak decomposition temperature at 278 ℃. This corresponded to the elimination of mainly hydrogen chloride. The second decomposition started from 367 ℃ to 530 ℃ with a maximum rate at 449 ℃, which presumably corresponded to the degradation of the resulting unsaturated hydrocarbons. There was a remaining 7.8% of residual carbon black since the heating was carried out under nitrogen atmosphere.

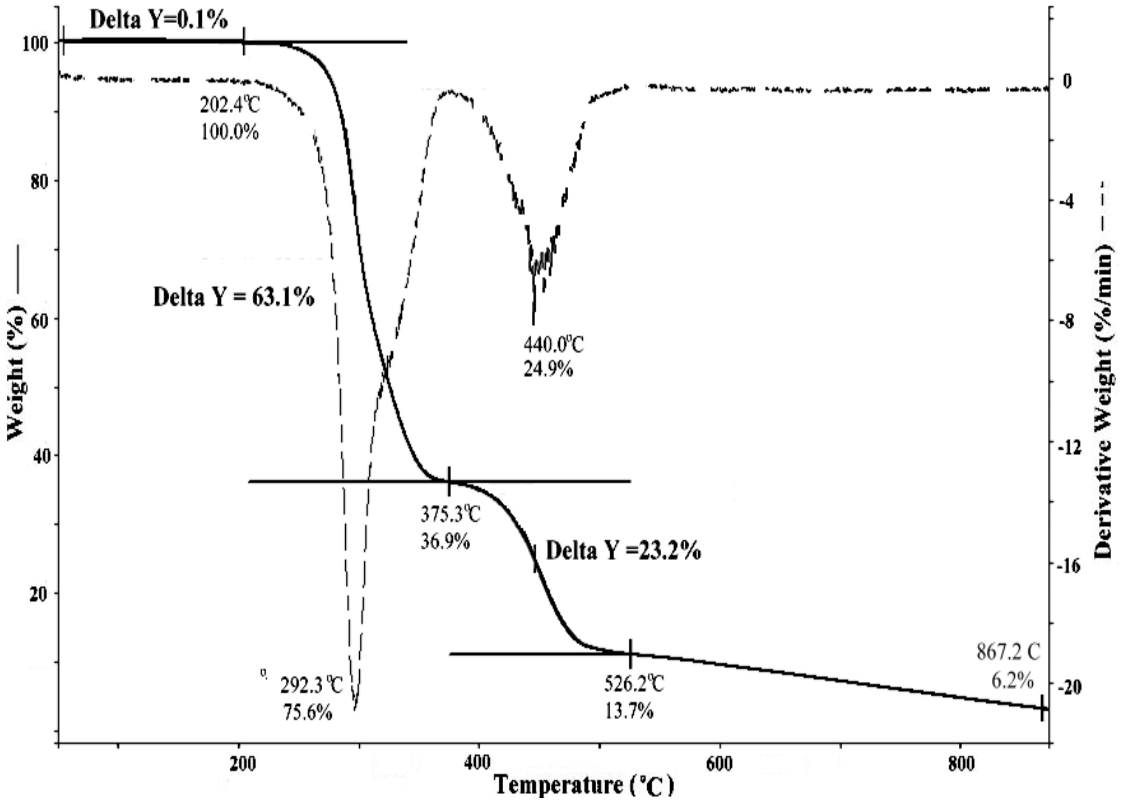

Fig. 5.30 TGA thermogram of PVC/$PHA_{SPKO-2.5}$

About 0.1% of weight loss was observed in PVC/$PHA_{SPKO-2.5}$ before 202 ℃, which was attributed to volatile components in the sample, as shown in Fig. 5.30. The first stage of decomposition started at 202 ℃ and ended at 375 ℃, with a maximum decomposition rate at 292 ℃. This weight loss could be attributed to the decomposition of PHA and evolution of chlorinated fragments comprising mainly HCl. The second stage of decomposition began from 375 ℃ to 526 ℃ with a maximum decomposition rate at 440 ℃. It was characterized by the decomposition of the unsaturated hydrocarbon structures which made up of 23.2% by weight. There was a remaining 6.2% of carbon black residue.

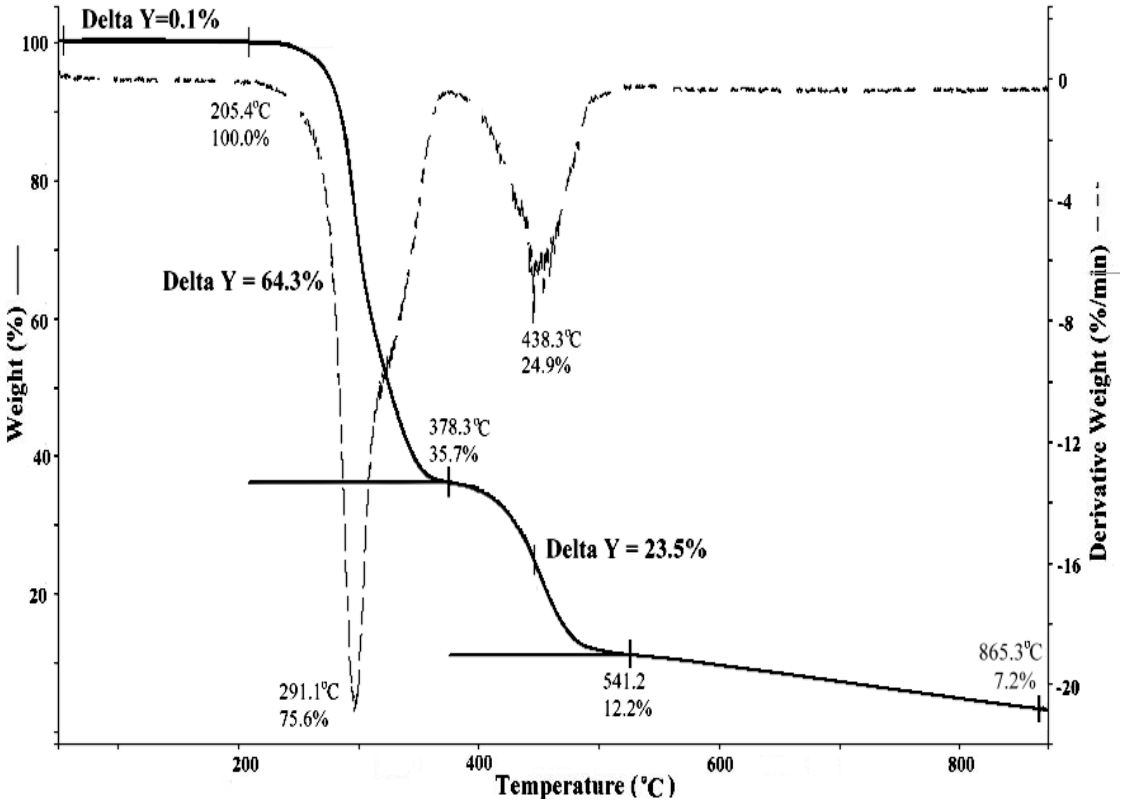

Fig. 5.31 TGA thermogram of PVC/PHA_{SPKO-5}

For PVC/PHA_{SPKO-5} as shown in Fig. 5.31, there was an initial weight loss of 0.1% prior to 205 ℃. The first stage of decomposition began at 205 ℃ and ended at 378 ℃ with a peak decomposition temperature at 291 ℃. The total weight loss at this stage was 64.3%. The second stage of decomposition commenced at 378 ℃ and ended at 541 ℃ with a peak decomposition temperature at 438 ℃. This corresponded to a weight loss of 23.5%. The remaining weight loss of 7.2% was attributed to the carbon black.

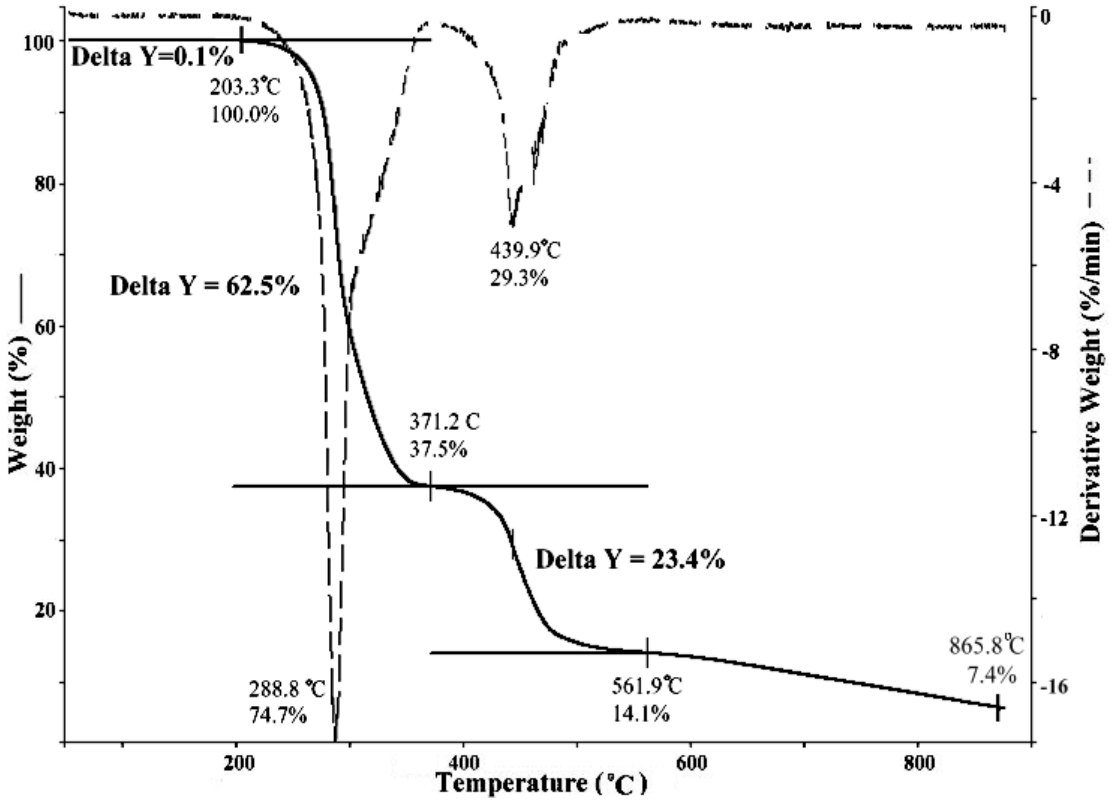

Fig. 5.32 TGA thermogram of PVC/degPHA$_{SPKO-2.5}$

From Fig. 5.32, around 0.1% of weight loss was observed in the PVC/degPHA$_{SPKO-2.5}$ before 203 ℃. The 62.5% of the blend decomposed at 203 ℃ to 371 ℃ during the first stage of decomposition, with a peak decomposition temperature at 289 ℃. The second stage of decomposition began from 371 ℃ to 562 ℃, with a peak decomposition temperature at 440 ℃ and this accounted for 23.4% of weight loss. The remaining 7.4% of total weight was attributed to the carbon residues.

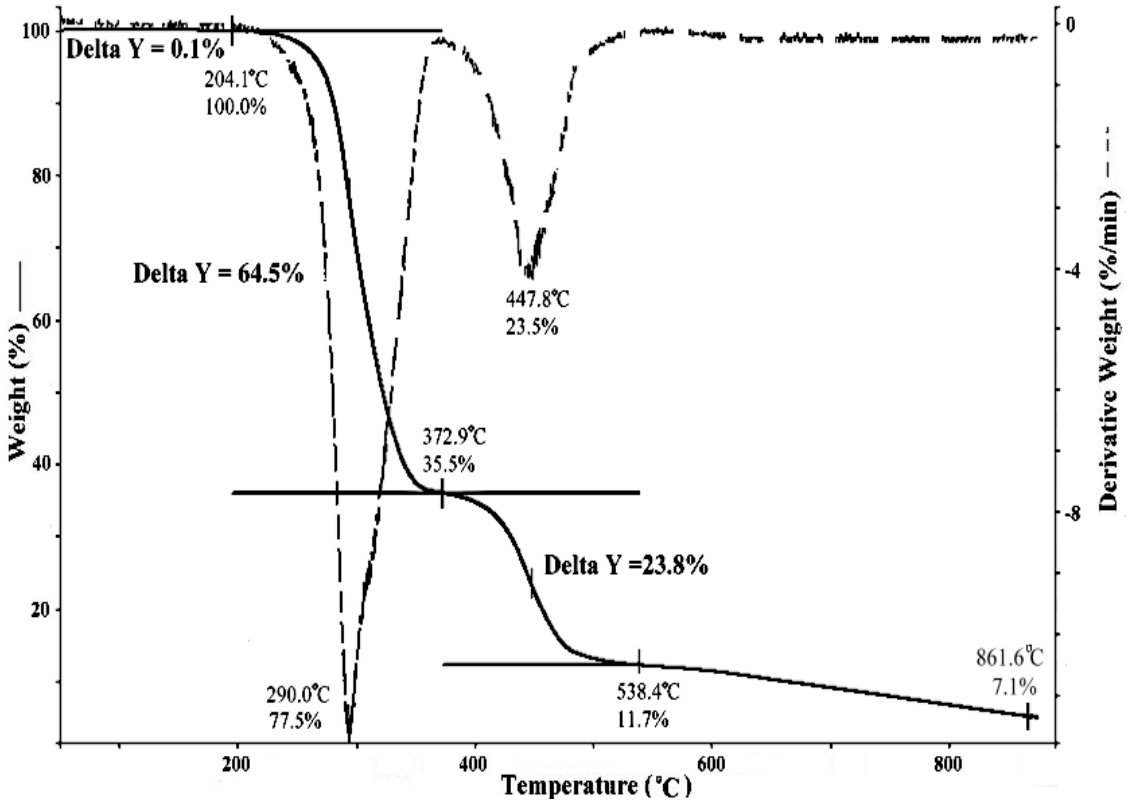

Fig. 5.33 TGA thermogram of PVC/degPHA$_{SPKO-5}$

As shown in Fig. 5.33, only 0.1% weight loss of PVC/degPHA$_{SPKO-5}$ occurred prior to 204 ℃. The first 64.5% weight loss occurred from 204 ℃ to 373 ℃ with a maximum decomposition rate at 290 ℃. The second 23.8% weight loss began from 373 ℃ to 538 ℃ with a maximum decomposition rate at 448 ℃. There was a remaining 7.1% of carbon black.

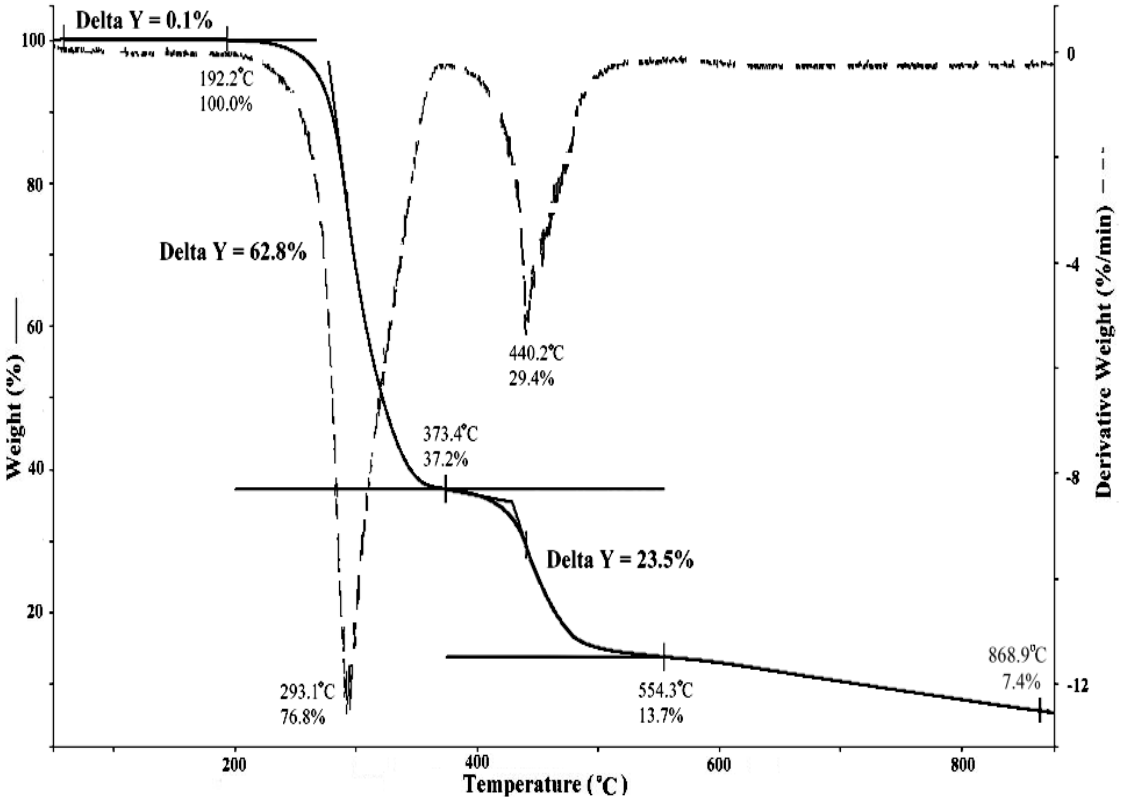

Fig. 5.34 TGA thermogram of PVC/$PHA_{OA\text{-}2.5}$

Fig. 5.34 showed the TGA result of PVC/$PHA_{OA\text{-}2.5}$. The first 62.8% of weight loss was observed from 192 ℃ to 373 ℃, with a peak decomposition temperature at 293 ℃. The second 23.5% of weight loss began from 373 ℃ and ended at 554 ℃, with a peak decomposition temperature at 440 ℃. There was a remaining 7.4% of carbon black.

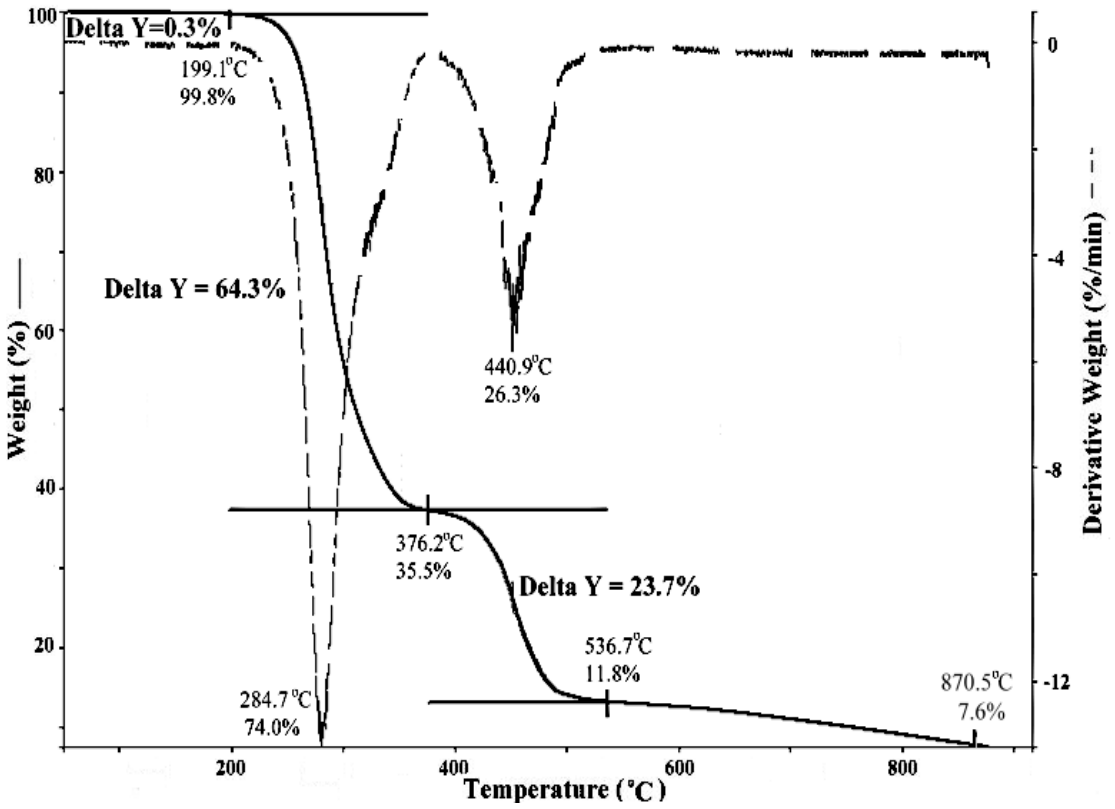

Fig. 5.35 TGA thermogram of PVC/PHA_{OA-5}

Slight weight loss of 0.3% was observed in the PVC/PHA_{OA-5} around 199 ℃, as shown in Fig. 5.35. The blend started to decompose at 199 ℃ and ended at 376 ℃ during the first stage of decomposition with a peak decomposition temperature at 285 ℃. This made up around 64.3% of the blend. The second stage of decomposition commenced from 376 ℃ to 537 ℃ with a peak decomposition temperature at 441 ℃ and this made up of 23.7% of total weight. The remaining 7.6% of total weight was attributed to the carbon black.

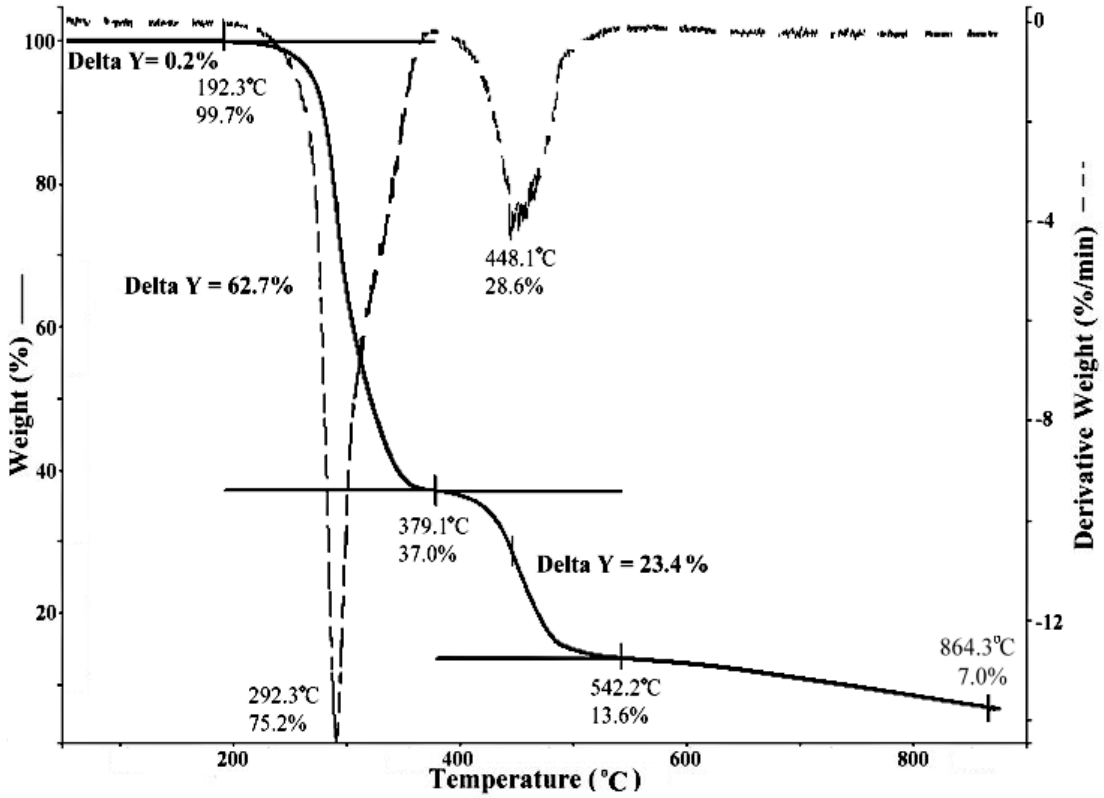

Fig. 5.36 TGA thermogram of PVC/degPHA$_{OA-2.5}$

The thermogram for PVC/degPHA$_{OA-2.5}$ was shown in Fig. 5.36. The first stage of decomposition began at 192 ℃ and ended at 379 ℃ with a peak decomposition temperature at 292 ℃. The total weight loss at this stage was 62.7%. The second stage of decomposition began at 379 ℃ and ended at 542 ℃ with a peak decomposition temperature at 448 ℃. This corresponded to a weight loss of 23.4%. The remaining 7.0% was attributed to the carbon black.

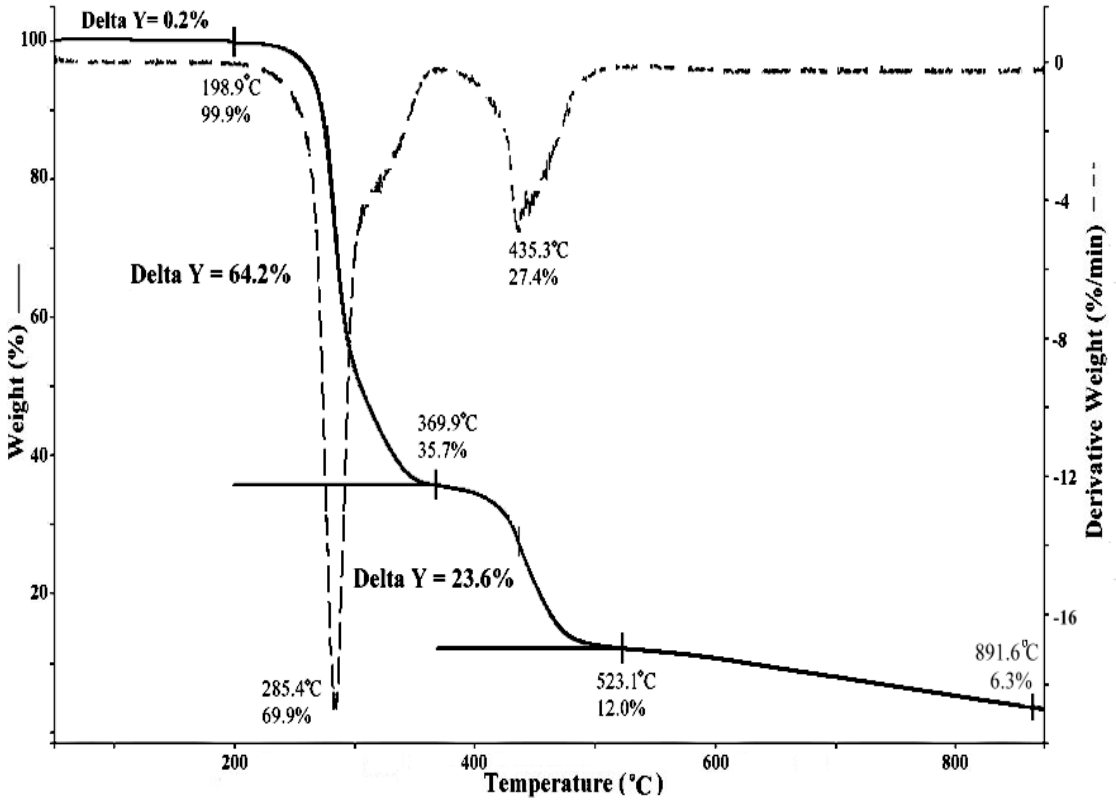

Fig. 5.37 TGA thermogram of PVC/degPHA$_{OA-5}$

Fig. 5.37 showed the thermal decomposition of PVC/degPHA$_{OA-5}$. The first 64.2% weight loss commenced from 199 ℃ to 370 ℃ with a maximum decomposition rate at 285 ℃. The second 23.6% weight loss began from 370 ℃ to 523 ℃ with a maximum decomposition rate at 435 ℃. There was 6.3% carbon black at the end of the TGA heating program.

5.4.1 Study of PVC-PHA interactions by TGA

All the TGA data from Fig. 5.29 to Fig. 5.37 were summarized in Table 5.5 and Table 5.6. The percentage of weight loss at first stage and second stage of degradation and the residual weight at 870 ℃ were summarized in Table 5.5.

Table 5.5 Weight loss of PVC, PHA and their blends at different stage of degradation at 10 ˚C min^{-1} heating rate under nitrogen atmosphere

Sample	Weight loss (%)		Total weight loss (%)	Residual weight at 870 ℃ (%)
	Stage 1	Stage 2		
PVC	60.8	22.3	83.1	7.8
PHA_{SPKO}	97.9	-	97.9	-
PHA_{OA}	99.0	-	99.0	-
PVC/PHA_{SPKO-5}	64.3	23.5	87.8	7.2
$PVC/degPHA_{SPKO-5}$	64.5	23.8	88.3	7.1
PVC/PHA_{OA-5}	64.3	23.7	88.0	7.6
$PVC/degPHA_{OA-5}$	64.2	23.6	87.8	6.3
$PVC/PHA_{SPKO-2.5}$	63.1	23.2	86.3	6.2
$PVC/degPHA_{SPKO-2.5}$	62.5	23.4	85.9	7.4
$PVC/PHA_{OA-2.5}$	62.8	23.5	86.3	7.4
$PVC/degPHA_{OA-2.5}$	62.7	23.4	86.1	7.0

As shown in Fig. 5.29 and Table 5.5, apparent two-stage degradation pattern was seen in the PVC decomposition, where the first stage of degradation was ascribed to mainly the dehydrochlorination process, leaving behind the unsaturated hydrocarbon structures and the second degradation was attributed to the decomposition of the resulting hydrocarbons.

Similarly, the thermal decomposition of all the polymer blends was found to occur through two stages as observed in PVC. From Fig. 5.30 to Fig. 5.37, two distinctive DTG peaks could be observed, with the first peak being ascribed to the decomposition of PVC and its plasticizer, as shown by the higher weight loss due to the added PHA in the PVC/PHA compared to the individual PVC (Table 5.5). There was no

significant change in weight loss at the second stage of decomposition as this stage of decomposition was mainly ascribed to the decomposition of fraction of resin with no plasticizer, since any PHA would have completely degraded at temperature above 400°C.

The temperature range of decomposition, temperature of onset of decomposition (T_{onset}) and temperature of fastest decomposition (T_p) during first stage and second stage of decomposition were summarized in Table 5.6.

Table 5.6 Thermogravimetric data of PVC blends and blend components at 10 ˚C min^{-1} heating rate

Sample	First Stage (˚C)			Second Stage(˚C)		
	Temp. range	$^1T_{onset}$	^2T_p	Temp. range	T_{onset}	T_p
PVC	219-367	271	278	367-530	426	449
PHA_{SPKO}	196-555	276	293	-	-	-
PHA_{OA}	187-520	269	282	-	-	-
$PVC/PHA_{SPKO-2.5}$	202-375	273	292	375-526	427	440
PVC/PHA_{SPKO-5}	205-378	272	291	378-541	432	438
$PVC/degPHA_{SPKO-2.5}$	203-371	274	289	371-562	429	440
$PVC/degPHA_{SPKO-5}$	204-373	275	290	373-538	424	448
$PVC/PHA_{OA-2.5}$	192-373	275	293	373-554	429	440
PVC/PHA_{OA-5}	199-376	262	285	376-537	430	441
$PVC/degPHA_{OA-2.5}$	192-379	275	292	379-542	430	448
$PVC/degPHA_{OA-5}$	199-370	270	285	370-523	424	435

$^1T_{onset}$: Temperature at onset of decomposition; ^2T_p: Temperature at fastest decomposition

The temperature scale of TGA instrument is calibrated by Curie-Points of certain metals and alloys, and the accuracy is in the order of ± 4 ℃. As shown in Table 5.6, there

was no significant difference in the T_{onset} between the pure PVC and those plasticized with PHA during the first stage of degradation, presumably the amounts of plasticizer at 2.5 and 5.0 phr were insufficient to produce any significant change to the onset of decomposition for PVC. However, the decomposition temperature range for the first stage of degradation showed a noticeable difference, whereby the plasticized samples degraded over a broader range, starting at a lower temperature. This effect could be due to the molecular interactions between the PVC and PHA plasticizer whereby the presence of PHA plasticizer fractions might influence the degradation of the PVC. Thus the plasticized samples would decompose earlier compared to the unplasticized PVC.

On the other hand, during the first stage of degradation, PVC/PHA blend revealed a higher temperature of fastest decomposition (T_p) than the pure PVC. This showed that the evolution of HCl during thermal degradation could be delayed as the fusion of PVC-PHA layers may act as a barrier and delay the diffusion of the volatile decomposition products.

There was no significant difference in the temperature range of decomposition, T_{onset} and T_p between PVC and PVC/PHA polymer blends at the second stage of decomposition. As almost no PHA plasticizer present in the blend at this stage of decomposition, the rate of degradation of the remaining hydrocarbon structures was about the same in the PVC and PVC/PHA polymer blends. Therefore it could be concluded that PVC decomposition was influenced by the presence of plasticizer mainly at the first stage of decomposition only.

5.4.2 Thermo-kinetic analysis of PVC/PHA binary blends

The kinetic parameters of the degradation studies of PVC/PHA blends and the blend components during first stage and second stage of decomposition were

summarized in Table 5.7 and Table 5.8. The descriptions of calculations of E_d, A and ΔS for the PVC and PVC/PHA blends were shown in Appendix I.

As could be seen from the tables, two degradation processes with different activation energies were observed in both PVC and the polymer blends.

Table 5.7 Thermo-kinetic parameters of PVC blends and blend components at first stage of decomposition

Samples	**Degradation activation energy, E_d (kJ mol^{-1})**	**Pre-exponential factor, A (s^{-1})**	**Entropy of activation, ΔS (J K^{-1} mol^{-1})**	**Correlation of coefficient, R^2**
PVC	138.2	1.18×10^{11}	-38.1	0.9726
PHA_{SPKO}	128.9	1.15×10^{10}	-57.6	0.9931
PHA_{OA}	85.3	6.07×10^{5}	-139.4	0.9019
$PVC/PHA_{SPKO-2.5}$	131.2	1.31×10^{10}	-56.5	0.9940
PVC/PHA_{SPKO-5}	125.1	2.81×10^{9}	-69.3	0.9784
$PVC/degPHA_{SPKO-2.5}$	122.5	1.83×10^{9}	-72.9	0.9946
$PVC/degPHA_{SPKO-5}$	117.7	5.62×10^{8}	-82.7	0.9938
$PVC/PHA_{OA-2.5}$	132.2	1.37×10^{10}	-56.2	0.9877
PVC/PHA_{OA-5}	128.1	8.21×10^{9}	-60.3	0.9932
$PVC/degPHA_{OA-2.5}$	125.2	2.97×10^{9}	-68.9	0.9871
$PVC/degPHA_{OA-5}$	119.0	1.06×10^{9}	-77.3	0.9722

For the first stage of decomposition, all the polymer blends showed a lower E_d and ΔS compared to the unblended PVC, with E_d and ΔS of PVC/PHA_5 blends lower

than PVC/$PHA_{2.5}$ blends; E_d and ΔS of PVC/PHA_{SPKO} blends lower than PVC/PHA_{OA} blends; E_d and ΔS of PVC/oligoesters blends lower than PVC/polyesters blends. These phenomena showed that thermal decomposition of plasticized PVC could depend on the type and concentration of the plasticizer used.

Table 5.8 Kinetic parameters of PVC blends and blend components at second stage of decomposition

Samples	**Degradation activation energy, E_d (kJ mol^{-1})**	**Pre-exponential factor, A (s^{-1})**	**Entropy of activation, ΔS (J K^{-1} mol^{-1})**	**Correlation of coefficient, R^2**
PVC k-60	360.0	$7.89x10^{23}$	205.1	0.9600
PHA_{OA}	-	-	-	-
PHA_{SPKO}	-	-	-	-
PVC/$PHA_{SPKO-2.5}$	337.7	$8.08x10^{22}$	186.4	0.9612
PVC/PHA_{SPKO-5}	211.4	$2.74x10^{13}$	5.1	0.9722
PVC/deg$PHA_{SPKO-2.5}$	286.9	$1.35x10^{19}$	114.1	0.9416
PVC/degPHA_{SPKO-5}	368.6	$7.87x10^{24}$	222.4	0.9712
PVC/$PHA_{OA-2.5}$	255.7	$5.36x10^{16}$	68.1	0.9801
PVC/PHA_{OA-5}	302.2	$1.66x10^{20}$	134.9	0.9668
PVC/deg$PHA_{OA-2.5}$	221.1	$8.53x10^{13}$	14.4	0.9817
PVC/degPHA_{OA-5}	208.2	$1.67x10^{13}$	1.0	0.9914

Similar with T_{onset} and T_p, there was no a clear trend of variation between the E_d, A and ΔS of PVC and PVC/PHA blends for the second stage of decomposition as this

stage of decomposition mainly consisted of the decomposition of unsaturated hydrocarbon structures.

E_d of second stage degradation was higher than the E_d of first stage of degradation for the PVC and all PVC/PHA binary blends. The possible reason for the higher E_d value of second stage degradation is explained by the stable C=C distribution in the unsaturated hydrocarbons remained in the PVC and PVC/PHA. The bond energies of the alkylene and aromatic chains are much higher than a single C-Cl and C-H bond where these weaker bonds were dissociated during the dehydrochlorination process. Therefore higher energy was required for the chain breaking during second stage of decomposition.

5.4.3 Thermal stability of PVC/$PHA_{2.5}$ and PVC/PHA_5 binary blends

Fig. 5.38 to Fig. 5.41 showed the DTG curves of PVC/$PHA_{2.5}$ and PVC/PHA_5 binary blends, composed of polymeric oleic acid-derived mcl-PHA (PHA_{OA}), oligomeric oleic acid-derived mcl-PHA ($degPHA_{OA}$), polymeric saponified palm kernel oil-derived mcl-PHA (PHA_{SPKO}) and oligomeric saponified palm kernel oil-derived mcl-PHA ($degPHA_{SPKO}$) as plasticizers for PVC, respectively.

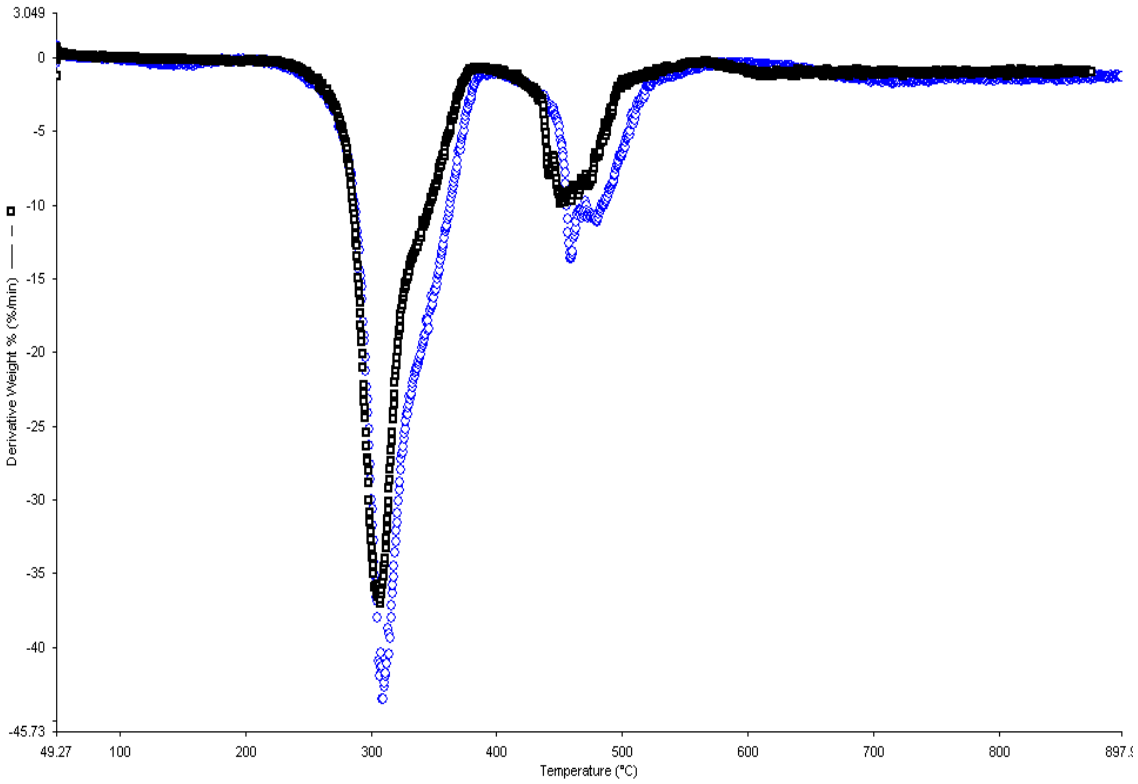

Fig. 5.38 DTG thermograms of PVC/ PHA_{SPKO} and PVC/PHA_{SPKO-5} binary blends. Black dots: PVC/PHA_{SPKO-5}; Blue dots: PVC/$PHA_{SPKO-2.5}$

By comparing the thermal stability of PVC/$PHA_{SPKO-2.5}$ and PVC/PHA_{SPKO-5} binary blend, PVC/PHA_{SPKO-5} showed an earlier decomposition in both first and second stage of decomposition. PVC/$PHA_{SPKO-2.5}$ was more thermo-stable by having DTG peaks of both stage of decomposition shifted to higher temperatures as shown in Fig. 5.38. These observations were supported by the magnitude of degradation activation energies of both binary blends where in the first and second stage of degradation: E_d of PVC/$PHA_{SPKO-2.5}$ > E_d of PVC/PHA_{SPKO-5}.

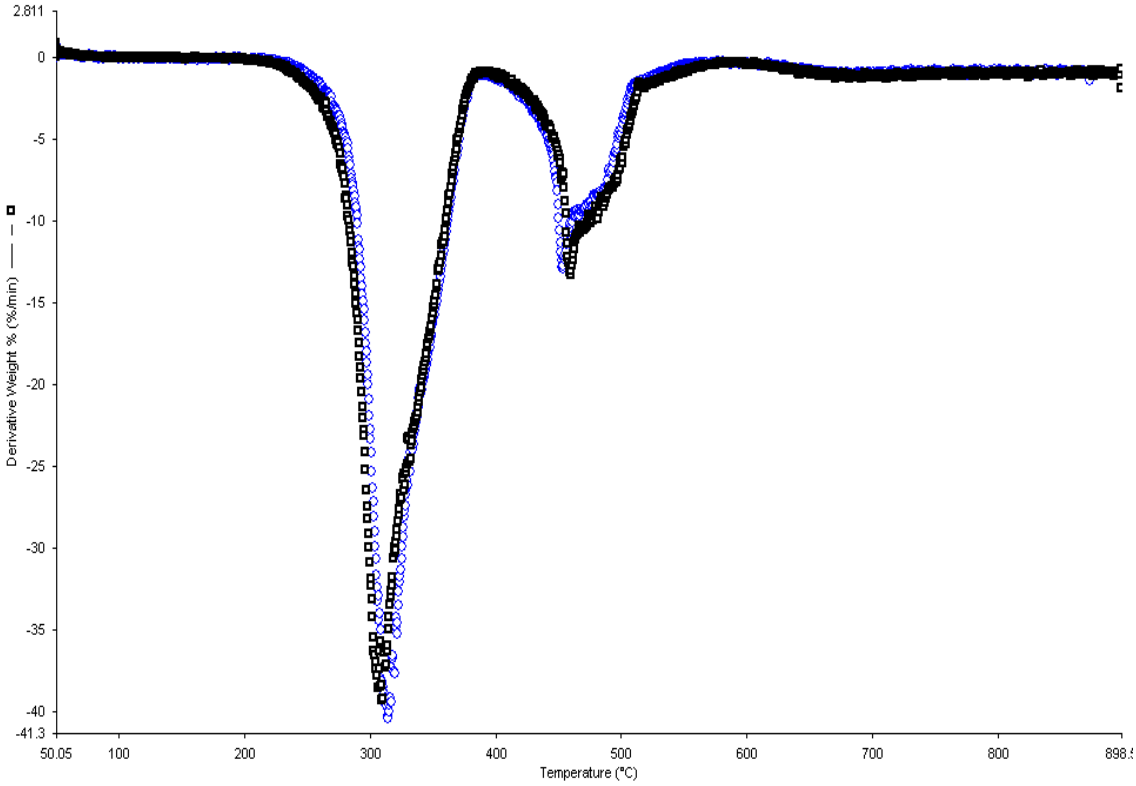

Fig. 5.39 DTG thermograms of PVC/degSPKO$_{2.5}$ and PVC/degSPKO$_5$ binary blends. Black dots: PVC/degPHA$_{SPKO-5}$; Blue dots: PVC/degPHA$_{SPKO-2.5}$

For PVC/degPHA$_{SPKO-2.5}$ and PVC/degPHA$_{SPKO-5}$ binary blends, the PVC/degPHA$_{SPKO-5}$ showed a lower thermal stability at first stage of decomposition. However, PVC/PHA$_{SPKO-2.5}$ appeared to be less thermo-stable in the second stage of decomposition as shown in Fig. 5.39. These observations were consistent with the magnitude of degradation activation energies for both binary blends where in the first stage of degradation: E_d of PVC/degPHA$_{SPKO-2.5}$ > E_d of PVC/degPHA$_{SPKO-5}$; in second stage of decomposition: E_d of PVC/degPHA$_{SPKO-2.5}$ < E_d of PVC/degPHA$_{SPKO-5}$.

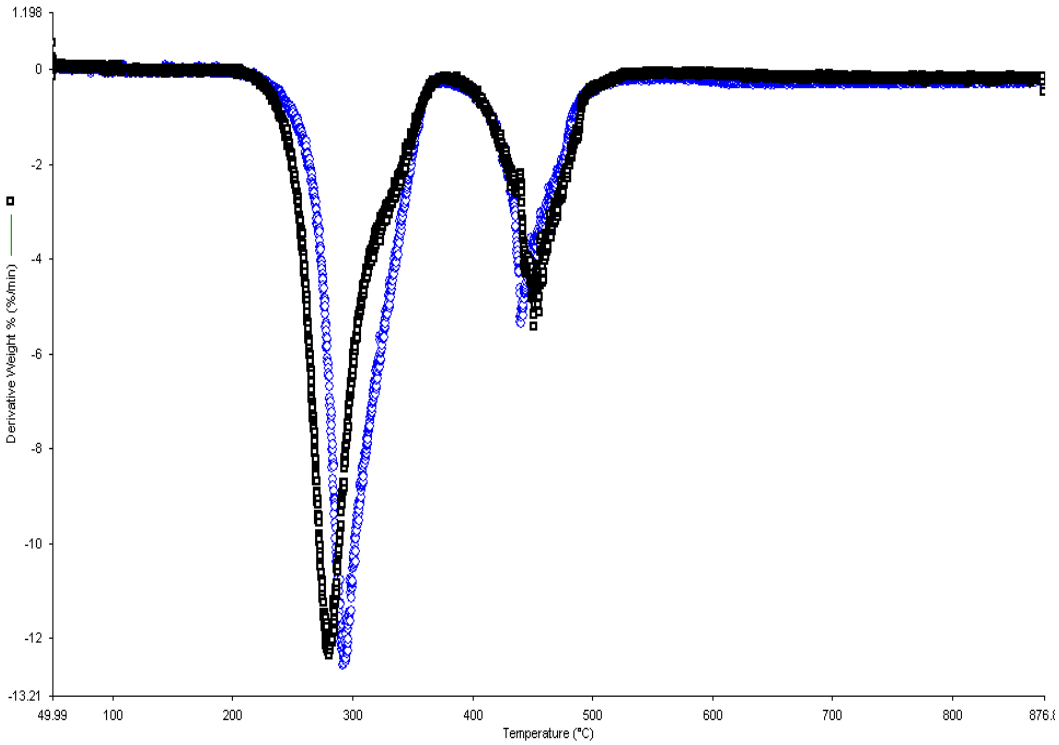

Fig. 5.40 DTG thermograms of PVC/$PHA_{OA-2.5}$ and PVC/PHA_{OA-5} binary blends. Black dots: PVC/PHA_{OA-5}; Blue dots: PVC/$PHA_{OA-2.5}$

Similarly, PVC/PHA_{OA-5} binary blend decomposed first in the first stage of decomposition, followed by PVC/$PHA_{OA-2.5}$ as shown in Fig. 5.40. However, PVC/$PHA_{OA-2.5}$ binary blend showed a lower thermal stability than PVC/PHA_{OA-5} binary blend by decomposed slightly earlier before PVC/PHA_{OA-5} at the second stage of decomposition. These observations were in agreement with the magnitude of degradation activation energies for both binary blends where in the first stage of degradation: E_d of PVC/$PHA_{OA-2.5}$ > E_d of PVC/PHA_{OA-5}; in the second stage of decomposition: E_d of PVC/$PHA_{OA-2.5}$ < E_d of PVC/PHA_{OA-5}.

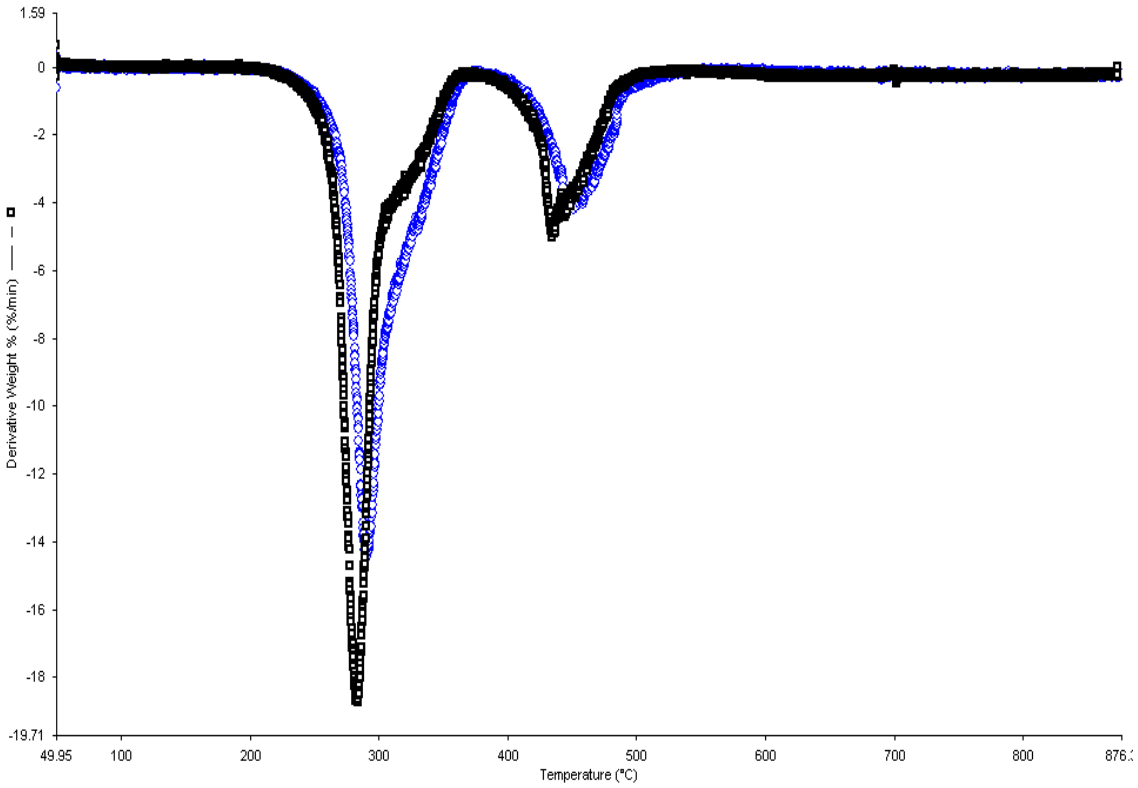

Fig. 5.41 DTG thermograms of PVC/degPHA$_{OA-2.5}$ and PVC/degPHA$_{OA-5}$ binary blends. Black dots: PVC/degPHA$_{OA-5}$; Blue dots: PVC/degPHA$_{OA-2.5}$

Comparing the thermal stability of PVC/degPHA$_{OA-2.5}$ and PVC/degPHA$_{OA-5}$ binary blend, PVC/degPHA$_{OA-5}$ showed an earlier decomposition at both first and second stage of decomposition as shown in Fig. 5.41. These observations were consistent with the magnitude of degradation activation energies of both binary blends where in the first and second stage of degradation: E_d of PVC/degPHA$_{OA-2.5}$ > E_d of PVC/degPHA$_{OA-5.}$

Judging from these observations, the PVC/PHA blends were less thermal stable than the unplasticized PVC. One possible explanation for these phenomena is plasticizer can induce the degrading effects to the polymer as a consequence of the fusion of plasticizer-PVC chains (Minsker et al., 1988). The effect was more pronounced when the amount of plasticizer was increased. This could be seen by the decrease in thermal stability and activation energy of the polymer blends in the first stage of degradation when the amount of PHA plasticizer was increased.

According to Tawfik et al. (2006), the decrease of thermal stability for the PVC mixture when PVC is mixed with any polyesters could be attributed to the partial hydrolysis of the polyesters with HCl gas evolved during first stage of decomposition. This would lead to the formation of acid chlorides which possess a catalytic effect on the further dehydrochlorination process, therefore accelerating the rate of decomposition and subsequently lower the initial temperature of decomposition.

5.5 Determination of T_g of PVC/PHA polymer blends by DSC analysis

The T_g values of PVC, PHA and PVC/PHA binary blends obtained from the DSC measurements were listed in Table 5.9 and 5.10. DSC thermograms of PVC, PHA and PVC/PHA samples which indicated T_g were shown in Appendix J.

Table 5.9 Glass transition temperatures of the polymer constituents in ℃ and ℉

Polymer	**Glass transition temperature, T_g**	
	℃	**℉**
PVC	78.6	351.6
PHA_{SPKO}	-44.4	228.6
170 ℃-treated PHA_{SPKO}	-47.5	225.5
PHA_{OA}	-44.1	228.9
170 ℃-treated PHA_{OA}	-47.3	225.7

From Table 5.9, T_g of PVC was 78.6 ℃. The corresponding values of polymeric and 170 ℃ heat-treated PHA_{SPKO} were -44.4 and -47.5 ℃; polymeric and 170 ℃ heat-treated PHA_{OA} were -44.1 and -47.3 ℃, respectively.

Table 5.10 Glass transition temperatures of PVC/PHA polymer blends in ℃ and ℉

PVC/PHA binary blends	**[1]T_g of blend**	
	℃	**℉**
PVC/$PHA_{SPKO-2.5}$	73.7	346.7
PVC/deg$PHA_{SPKO-2.5}$	73.0	346.0
PVC/PHA_{SPKO-5}	71.9	344.9
PVC/degPHA_{SPKO-5}	71.1	344.1
PVC/$PHA_{OA-2.5}$	74.5	347.5
PVC/deg$PHA_{OA-2.5}$	74.2	347.2
PVC/PHA_{OA-5}	72.6	345.6
PVC/degPHA_{OA-5}	72.4	345.4

All PVC/PHA binary blends showed a T_g lower than that of PVC (Table 5.10). Besides, the T_g was intermediate to those of the component polymers, indicating a good miscibility and compatibility within the system. The molecular basis of miscibility could be attributed to the polar and hydrogen bonding interactions between PHA and PVC.

Several factors are known to affect the T_g of the polymer blend. The most important factor is chain flexibility of the polymer. T_g will be lowered if flexibility is built into the polymer, for example, by a lubricant effect. A second factor in determining T_g value is the molecular polarity of the polymer. Increasing the polarity of a polymer increases its T_g. Some equations fail to correctly predict T_g of plasticizer-polymer mixture because it neglects specific PVC-plasticizer interactions (Nielsen & Landel, 1994).

In this study, reduction of the T_g for the polymer blends was observed when the proportion of PHA increased. The marked decrease in T_g values for the higher PHA

composition in the binary blends were in agreement with the observation of decreased E_d and ΔS values when the PHA content increased in the blend.

The reduction of T_g was lesser when polymeric PHA was used as the plasticizer instead of the oligomeric PHA. In other words, PVC plasticized with oligomeric PHA had lower T_g than PVC plasticized with polymeric PHA. Plasticization of PVC by oligomeric PHA greatly enhanced the segmental mobility of the polymers system compared to polymeric PHA, which in turn modified the glass transition temperatures and material properties of the polymer blend in a greater extent. This is because shorter plasticizer fragments could greatly increase the free volume in the polymer system compared to longer, less mobile chains. Therefore the presence of oligomeric PHA as plasticizer would contribute to better mobility and therefore lower T_g for the polymer mixture.

Polymeric PHA had longer polymer chain than the oligomeric PHA and so had more carbonyl group for hydrogen bonding and thus higher interacting surfaces and segments with the PVC, leading to a decrease of segmental flexibility of the polymer chains. Oligomeric PHA had lower molecular weight and more end groups. Although it had overall higher amount of terminal COOH and OH groups which could contribute to the dipole-induced dipole interactions with neighboring PVC polymer molecules, but it had less carbonyl group for hydrogen bonding and thus had weaker interaction and lesser entanglement with PVC. It should be noted that the short-range intermolecular forces contributed by the dipole-dipole interactions are not that strong as compared to the hydrogen bonding.

The reduction of T_g of PVC by PHA_{OA} was lesser compared to PHA_{SPKO}, indicating a lower extent of mobility of the molecular chain segments in the PVC plasticized with PHA_{OA}. Branching of plasticizer tend to hinder the movement of plasticizer within the polymer matrix (Marcilla et al., 2004). PHA_{OA} consisted of higher

amount of bulky alkyl side chains (C_{14} and $C_{14:1}$) which may decrease the molecular flexibility in the polymer blend whereby the highly branched PHA polymer chains were slightly hindered from sliding past each other in the polymer system.

Besides that, PHA_{OA} contained more long unsaturated side chains in which high electron density in the double bond of unsaturated pendant group would act as electron donating group to the electropositive carbon atom in C-Cl of PVC, leading to a strong specific interaction with the PVC segments which could subsequently decrease the segmental mobility and increase the T_g of the polymer blend.

5.5.1 Correlation of polymer-plasticizer interaction with T_g derived from Gordon-Taylor equation

Generally, the compositional dependence T_g of a compatible polymer blend lies between the T_g of the constituents and it can be expressed by Gordon-Taylor equation. According to An et al. (1997), Gordon-Taylor equation should be applicable to determine the T_g of blends with not very strong specific interactions within the mixture.

It should be pointed out here that the constant *k* in the Gordon-Taylor equation is the model fitting parameter which includes all the possible interactions within the polymer mixture. These interactions were actually difficult to be determined precisely by conventional empirical and mechanistic approach. Thus the *k*-variable is usually determined *via* data fitting.

DSC measurements yielded experimental T_g and the values were compared with the T_g determined from the Gordon-Taylor equation. The calculations of T_g of PVC/PHA blends using Gordon-Taylor equation *via* data substitution and simultaneous equation solution approaches were described in Appendix K and the data were tabulated in Table 5.11.

Table 5.11 T_g of PVC/PHA binary blends determined from DSC analysis and Gordon-Taylor Equation *via* data substitution and simultaneous equation solution approaches

PVC/PHA blend	**2.5 PHR**					**5 PHR**				
	[1]$T_{g\ exp}$ / ℃	**[2]$T_{g\ calc}$ / ℃**		**[3]lΔT_gl / ℃**	**k-factor**	**$T_{g\ exp}$ / ℃**	**$T_{g\ calc}$ / ℃**		**lΔT_g l / ℃**	**k-factor**
PVC/ PHA_{OA}	74.5	Software	75.4	0.9	0.91	72.6	Software	72.2	0.4	0.91
		Substitution	75.1	0.6	0.85		Substitution	71.7	0.9	0.85
PVC/degPHA_{OA}	74.2	Software	75.3	1.1	0.90	72.4	Software	71.9	0.5	0.90
		Substitution	75.0	0.8	0.83		Substitution	71.4	1.0	0.83
PVC/PHA_{SPKO}	73.7	Software	74.9	1.2	0.80	71.9	Software	71.3	0.6	0.80
		Substitution	74.6	0.9	0.74		Substitution	70.9	1.0	0.74
PVC/degPHA_{SPKO}	73.0	Software	74.4	1.4	0.72	71.1	Software	70.3	0.8	0.72
		Substitution	74.1	1.1	0.67		Substitution	69.8	1.3	0.67

[1]$T_{g\ exp:}$ experimental T_g from DSC measurement; [2]$T_{g\ calc}$: calculated T_g from Gordon-Taylor equation; [3]lΔT_gl: l$T_{g\ exp}$ - $T_{g\ calc}$l

It was found that the experimental T_g data for all the binary blends gave an excellent fit with those obtained from the Gordon-Taylor equation. From Table 5.11, the absolute values of ΔT_g ($|\Delta T_g|$) lied in the range of 0.4 ℃ and 1.4 ℃. These results were in satisfactory agreement with the Gordon-Taylor fitting approach, with the differences between the respective T_g values lied within experimental error (< 2 ℃) (Penzel et al., 1997).

The value of *k*-variable obtained from solving the simultaneous equations for PVC/SPKO blend was 0.80 and the *k*-variable obtained from the experimental data substitution approach was 0.74, which showed a small difference. For PVC/degSPKO blend, the value of *k*-variable obtained from the simultaneous equations solution was 0.72 and it differed with the *k*-variable (0.67) obtained from the substitution approach by a small margin.

For PVC/OA blend, the value of *k*-variable obtained from the simultaneous linear equations solution was 0.91. This value was close to the *k*-variable (0.85) obtained from the data substitution approach. For PVC/degOA blend, the *k*-variable obtained from the simultaneous linear equations solution was 0.90, which differed from the *k*-variable (0.83) obtained from the T_g substitution approach by 0.07.

The differences of the two estimates of *k*-variable were quite small with variations ranged from 0.05 to 0.07. This showed that there was insignificant difference between the T_g values obtained using the two different determination methods (simultaneous equations solution and substitution method) as the *k*-specific parameters were not likely to deviate greatly.

From Table 5.11, PVC/polyester and PVC/PHA_{SPKO} blends exhibited smaller variations between the experimental T_g data and the T_g calculated *via* Gordon-Taylor expression compared to PVC/oligoester and PVC/PHA_{OA} blends. On the other hand, compared to PVC/$PHA_{2.5}$ blends, PVC/PHA_5 blends showed a closer experimental T_g

value with the predicted T_g value as shown by the small $|\Delta T_g|$ value. This is due to the fact that by increasing the mass composition of PHA, the predictive power of the equation increased as the *k*-factor becomes more reliable variable component within the predictor.

5.5.2 Correlation of polymer-plasticizer affinity with T_g derived from Fox equation

Fox equation was adapted to correlate the PVC-plasticizer system by comparing the experimental T_g data obtained from DSC measurement with the T_g calculated from Fox equation. Based on the classical theory stated by Sears and Darby (1982), the compatibility of the polymer and plasticizer is related to the PVC-plasticizer interaction forces.

The good miscibility within PVC-PHA blends is believed to be the result of specific intermolecular attractions between the electron donating and electron accepting functional groups of the two polymers. This apparent affinity between the polymer and plasticizer resulted in the values of T_g for the blends from experimental measurement to be higher than expected.

A simplified model as shown in Fig. 5.42 was established to describe the factors influencing the T_g of polymer-plasticizer blend, where this model was previously established by Slark (1997) and tested with the solute-polymer T_g values for a combination of a solute in various polymers.

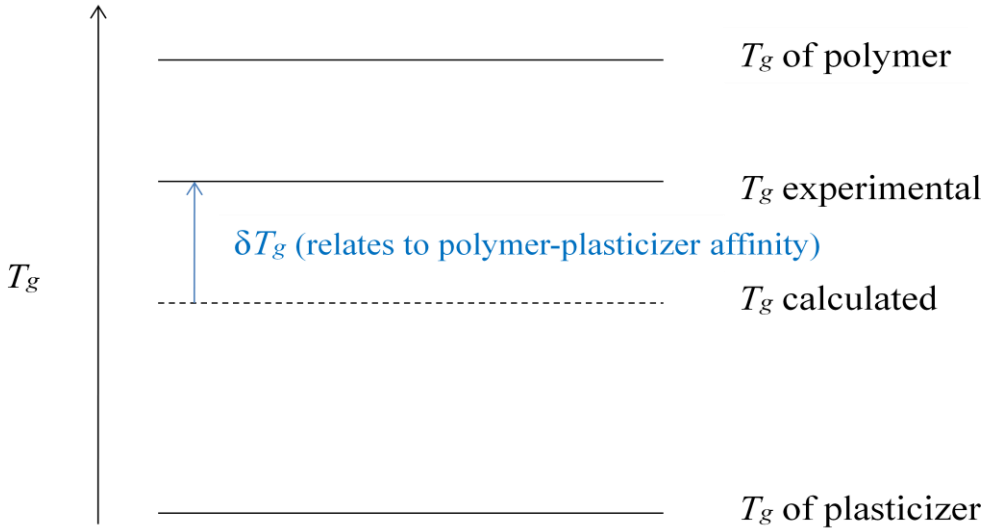

Fig. 5.42 Simplified model of factors affecting the T_g of polymer-plasticizer blends (Adapted from Slark, 1997)

Generally, the T_g in the absence of intermolecular interactions could be calculated using Fox Equation (3.9), as this equation does not take into account the relevant intermolecular forces. Hence two parameters: δT_g and ΔT_g were defined relating to the difference between the experimental T_g and calculated T_g as shown in the following relationships:

$$\delta T_g = T_{g_{exp}} - T_{g_{calc}} \quad (5.2)$$

$$\Delta T_g = (T_{g_{exp}} - T_{g_{calc}})/(T_{g_{pol}} - T_{g_{calc}})\, x\, 100 \quad (5.3)$$

where $T_{g\ \text{exp:}}$ experimental T_g from DSC measurement; $T_{g\ \text{calc}}$: calculated T_g from Fox equation; $T_{g\ \text{pol}}$: T_g of polymer.

Equation (5.3) was derived in the attempt to normalize for the differences in the $T_{g\ \text{pol}}$, in this case, the T_g of PVC since the magnitude of δT_g depends on the T_g of polymer (Slark 1997). The calculations of $T_{g\ \text{calc}}$, δT_g and ΔT_g for all the PVC/PHA binary blends were described in Appendix L and the values were summarized in Table 5.12.

Table 5.12 $T_{g\,exp}$, $T_{g\,calc}$, δT_g and ΔT_g of PVC/PHA binary blends determined from DSC analysis and Fox equation

PVC/PHA binary blend	2.5 phr				5 phr			
	$^1T_{g\,exp}$ / ℃	$^2T_{g\,calc}$ / ℃	δT_g / ℃	ΔT_g /%	$T_{g\,exp}$ / ℃	$T_{g\,calc}$ / ℃	δT_g / ℃	ΔT_g /%
PVC/PHA_{OA}	74.5	74.1	0.4	8.9	72.6	69.8	2.8	31.8
PVC/degPHA_{OA}	74.2	74.0	0.2	4.3	72.4	69.6	2.8	31.1
PVC/PHA_{SPKO}	73.7	74.1	-0.4	-8.9	71.9	69.7	2.2	24.7
PVC/degPHA_{SPKO}	73.0	73.9	-0.9	-19.1	71.1	69.4	1.7	18.5

$^1T_{g\,exp:}$ experimental T_g from DSC measurement; $^2T_{g\,calc}$: calculated T_g from Fox equation

The deviations of experimental T_g from that predicted by Fox equation would often be observed in systems with specific interactions (Zhang et al., 1997). From Table 5.12, most of the binary blends exhibited significantly higher T_g than the expected values. The T_g was elevated as a result of the presence of interactions between electron donating and electron accepting functional groups of the blend components as mentioned earlier.

A good plasticizer should have low affinity between plasticizer and polymer in order to have effective plasticization, which results in a higher chain mobility and lower T_g for the polymer blend. When the apparent affinity between plasticizer and polymer increased due to significant molecular interactions, the reduction of T_g of the polymer mixture would be lesser as the plasticizing effect to the polymer decreased.

ΔT_g was higher in the case of PVC/polyesters binary blend compared to PVC/oligoesters binary blends. The higher $T_{g\,exp}$ value in PVC/polyesters blends could be attributed to the presence of intermolecular forces i.e. hydrogen bonding existing in between polymeric PHA and PVC polymer chains in the PVC/PHA system. Polymeric

PHA had longer polymer chain than oligomeric PHA, and thus had more spatially aligned polar C=O groups to be contributed for the hydrogen bonding.

ΔT_g was higher in PVC/PHA_{OA} binary blend compared to PVC/PHA_{SPKO} blend. This was due to the higher intermolecular interactions present in the polymer mixture, which could be contributed to the probable π-electrons interaction in the electron acceptor, PVC with the electron donor, the double bond of the PHA_{OA}'s unsaturated side chains. The π-electrons in the double bond may interact with the electropositive carbon atom in the C-Cl bond of PVC, which may result in a relatively higher apparent affinity between the PHA_{OA} plasticizer and PVC polymer chains.

ΔT_g was very low for the PVC/$PHA_{SPKO\text{-}2.5}$ and PVC/deg$PHA_{SPKO\text{-}2.5}$ binary blends, which exhibited a negative value for the difference as both oligomeric and polymeric SPKO-PHA may have considerably weaker interactions with PVC.

ΔT_g was lower for PVC/$PHA_{2.5}$ binary blend compared to PVC/PHA_5 binary blend. This indicates that there was a relatively lower molecular interaction in terms of attractive forces between the two polymers as a result of lesser PHA plasticizer present in the polymer blend, and therefore lesser specific interactions within the system.

The maximum deviations of the experimental T_g-composition data from the T_g obtained from Fox equation strongly implied the existence (although limited to some extent) of intermolecular interactions between the constituents of the blend. This was due to the results of intermolecular forces between the PHA and PVC, which have more influence on the co-operative motions of polymer backbone associated with the T_g.

It is postulated that the extent of interactions between PHA and PVC may depends on the PVC tacticity, i.e. the arrangement of Cl atom along the PVC chain. The tacticity has a significant effect on the free volume within the polymer blends (Wypych, 2008). PVC with isotactic or syndiotactic segments may give different level of

interactions with PHA, either by having a closer chain interactions e.g. increased hydrogen bonding and lower mobility in the system, or vice versa.

5.5.3 Summary of DSC analysis

The glass transition temperature of pure PVC obtained in this work agreed well with reported values in the literature. The addition of mcl-PHA plasticizers to the PVC decreased the glass transition temperature of the polymer blend. A single transition was observed for all the polymer blends and the temperature shift pattern was that expected for a miscible blend. These results suggested that the polymeric and oligomeric SPKO- and OA-derived mcl-PHA were compatible and miscible with PVC when these biopolyesters as well as their oligoesters were used as plasticizers for PVC. However, the glass transition temperatures of the PVC/PHA_{SPKO} blends were found to be lower than the PVC/PHA_{OA} blends. On the other hand, PVC plasticized with oligomeric PHA showed lower T_g than those PVC plasticized with polymeric PHA.

In this study, two empirical formula suggested by Gordon-Taylor and Fox were used in the theoretical prediction of the T_g for the compatible polymer blends. The experimental T_g values from DSC were compared with theoretical T_g values predicted by the Gordon-Taylor and Fox equations. It was found that the experimental T_g results from DSC analysis fitted well with the Gordon-Taylor equation. However, the experimental T_g was generally higher than the values calculated from the Fox equation, as the intermolecular forces present in the polymer system were not taken into consideration in the equation. This study showed the existence of interpolymer interactions, to some limited extent, between PVC and mcl-PHA.

5.6 Dynamic mechanical analysis of PVC/PHA blends

Dynamic mechanical analysis (DMA) or viscoelastic measurement is an alternative method to study the polymers miscibility as well as the mechanical properties of the polymeric materials (Walsh et al., 1982).

5.6.1 Viscoelastic measurements of PVC, PHA & PVC/PHA binary blend

When there are specific polymer-polymer interactions in the mixture of two polymers, they form a miscible system. The mechanical properties of these compatible blends will show a single T_g value and a single modulus transition zone, which varies regularly with composition (Nielsen & Landel, 1994).

In this study, T_g was determined from the maximum peak of loss modulus (*E"*) curve as *E"* was shown to be more consistent compared with other determinations of T_g e.g. onset of storage modulus or maximum of tan δ curve. The loss modulus values change with the temperatures and transitions in the polymer blends. These transitions indicate subtler changes in the blend and the temperature peak of loss modulus is mainly affected by fusion of PVC crystallites (Menard, 2008).

For all PVC and PVC/PHA systems studied, the values of the T_g were obtained from the plots of loss modulus versus temperature and were evaluated from 40 to 140 ℃ for PVC; PHA from -60 to 30 ℃ and PVC/PHA blends from 40 to 120 ℃. The loss modulus curve of PHA_{SPKO} showed a peak at -36.8 ℃ which corresponded to the glass transition temperature (T_g) of PHA. PVC showed *E"* maximum at 91.9 ℃, as shown in the loss modulus versus temperature curve. Table 5.13 summarized the T_gs of the binary blends obtained from loss modulus peak versus temperature.

Table 5.13 T_g of PVC/PHA binary blends measured from loss modulus peak maxima in DMA

T_g / ℃ (Loss modulus peak maxima)	2.5 phr	5 phr
PVC/PHA_{SPKO}	83.4	82.7
PVC/degPHA_{SPKO}	80.9	79.7
PVC/PHA_{OA}	84.6	83.6
PVC/degPHA_{OA}	81.7	80.2

The T_g values obtained from the loss modulus maximum displayed similar trends to those T_g values obtained from DSC analysis. Both measurements of DMA and DSC gave consistent T_g results and showed a single T_g for all the PVC/PHA blends compared to the individual polymers, indicating that the mcl-PHA were highly miscible with PVC. Overall the T_g of all the binary blends were lower than the PVC, with T_g of PVC/PHA_5 lower than PVC/$PHA_{2.5}$; T_g of PVC/PHA_{SPKO} lower than PVC/PHA_{OA} and T_g of PVC/oligoesters lower than PVC/polyesters.

It should be noted that exact T_g values from DMA measurement usually were not similar with the values reported from DSC as the glass transition is a range of behavior where scientists have agreed to accept a single temperature as the indicator per certain standards. Nevertheless different industries use different points from the same data set that can vary as much as 15 ℃. DSC and DMA measure different processes and thus, the numerical value can vary quite a bit (Turi, 1997).

The loss modulus curves of PVC, PVC/$PHA_{2.5}$ and PVC/PHA_5 binary blends which consisted of polymeric PHA (PHA_{SPKO} and PHA_{OA}) and oligomeric PHA (degPHA_{SPKO} and degPHA_{OA}) as plasticizers were compared in Fig. 5.43, Fig. 5.44, Fig. 5.45 and Fig. 5.46.

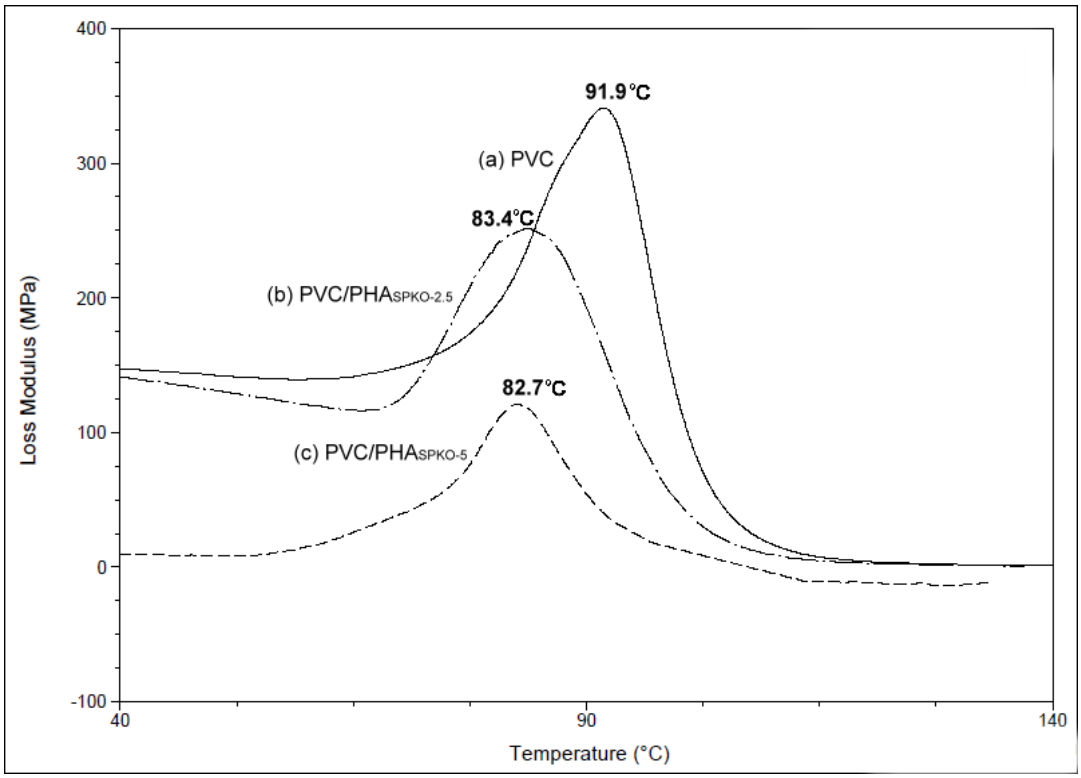

Fig. 5.43 T_g values obtained from the peak of loss modulus vs. temperature curves of (a) PVC, (b) $PVC/PHA_{SPKO-2.5;}$ and (c) PVC/PHA_{SPKO-5}

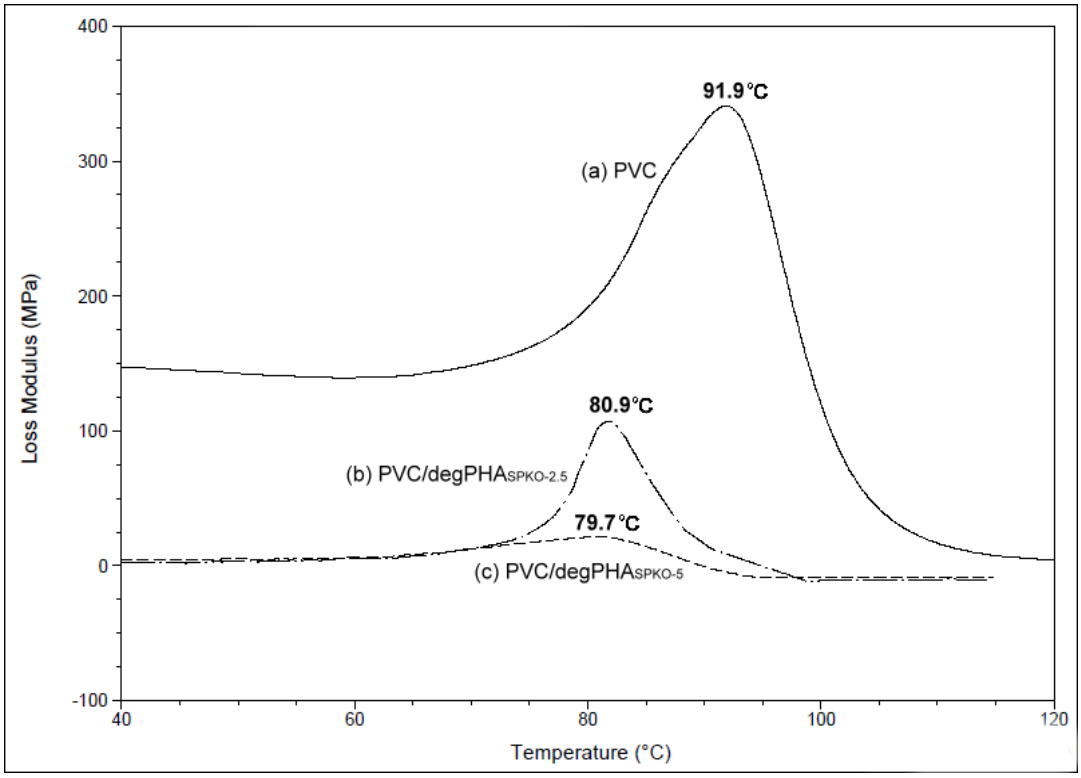

Fig. 5.44 T_g values obtained from the peak of loss modulus vs. temperature curves of (a) PVC, (b) $PVC/degPHA_{SPKO-2.5}$; and (c) $PVC/degPHA_{SPKO-5}$

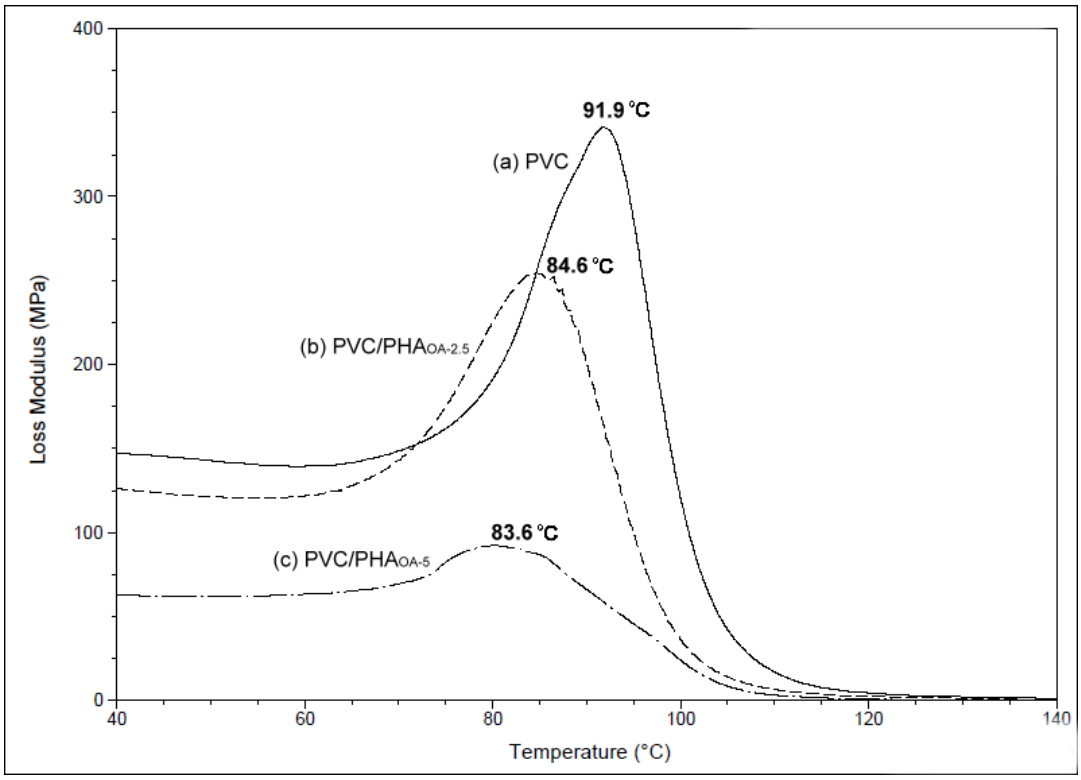

Fig. 5.45 T_g values obtained from the peak of loss modulus vs. temperature curves of (a) PVC, (b) PVC/PHA$_{OA-2.5}$; and (c) PVC/PHA$_{OA-5}$

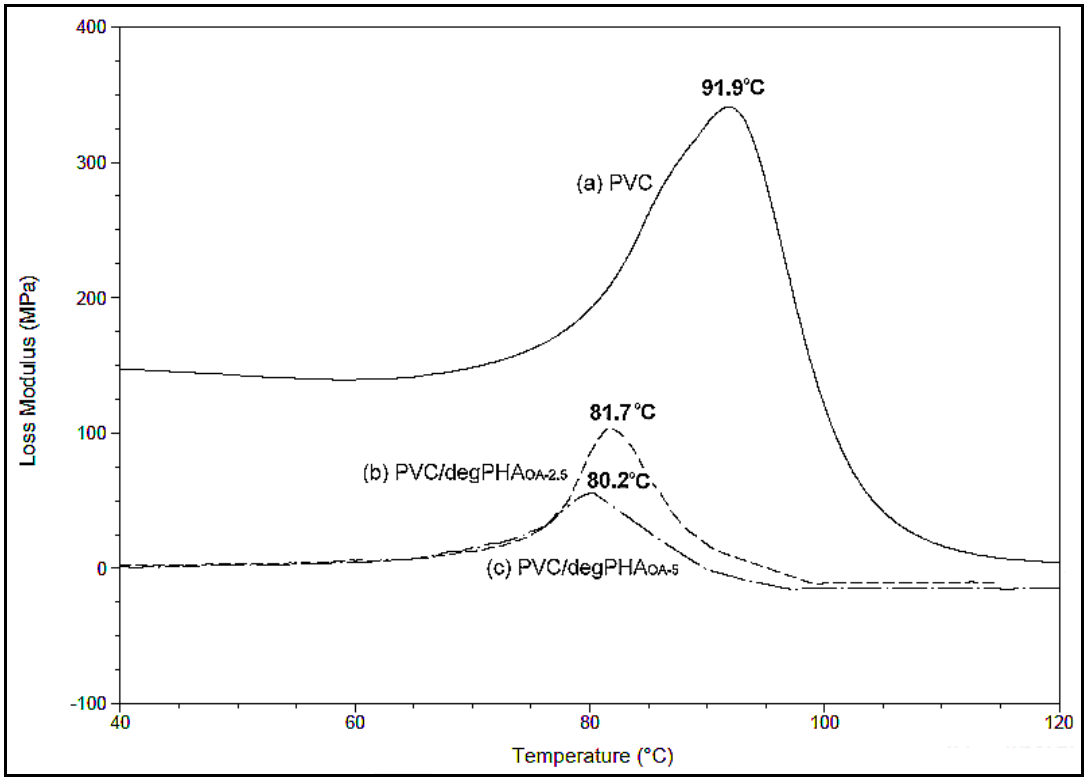

Fig. 5.46 T_g values obtained from the peak of loss modulus vs. temperature curves of (a) PVC, (b) PVC/degPHA$_{OA-2.5}$; and (c) PVC/degPHA$_{OA-5}$

Fig. 5.43 to Fig. 5.46 clearly showed that the glass transition temperature was shifted to lower temperature when PVC was mixed with PHA. The order of magnitude of lowering the T_g value gets higher when the PHA content gets higher in the blend. This means that the plasticization of PVC by higher amounts of mcl-PHA reduced the T_g of the polymer blends more effectively. A higher PHA content imparted better plasticization to the PVC due to more PHA plasticizer embedding themselves between the PVC chains, thus spacing them further apart to increase the free volume and polymer chain mobility. This in turn lowered the T_g of the polymer blend more significantly.

Besides that, the loss modulus value of pure PVC as seen in Fig. 5.35 to Fig. 5.38 had been reduced with the increase in the PHA content. The loss modulus (E") is related to the energy dissipated as heat upon deformation. It describes the ability of a material to dissipate energy and provides an indication of the damping capacity of the material. Low loss modulus indicates low damping properties and hence elastic behavior. Therefore by increasing the PHA content in the polymer blend, the blended material is transforming to a more elastic behaviour. This agrees with Ahmad et al. (2007) where low value of loss modulus shows an elastic polymeric behaviour.

5.6.2 Stiffness of PVC/PHA blends

The extent of decrease in stiffness and changes in the softness of the plasticized PVC depend on both the level of plasticization and the nature of the plasticizer (Hernandez et al., 2000). As discussed earlier, introduction of the plasticizer into the polymer system greatly increased the mobility among the polymer chain, and this subsequently increased the softening properties of the polymer. Fig 5.47 to Fig. 5.50 revealed the temperature variation of film's stiffness for the PVC/PHA_{SPKO}, PVC/degPHA_{SPKO}, PVC/PHA_{OA} and PVC/degPHA_{OA} polymer blends.

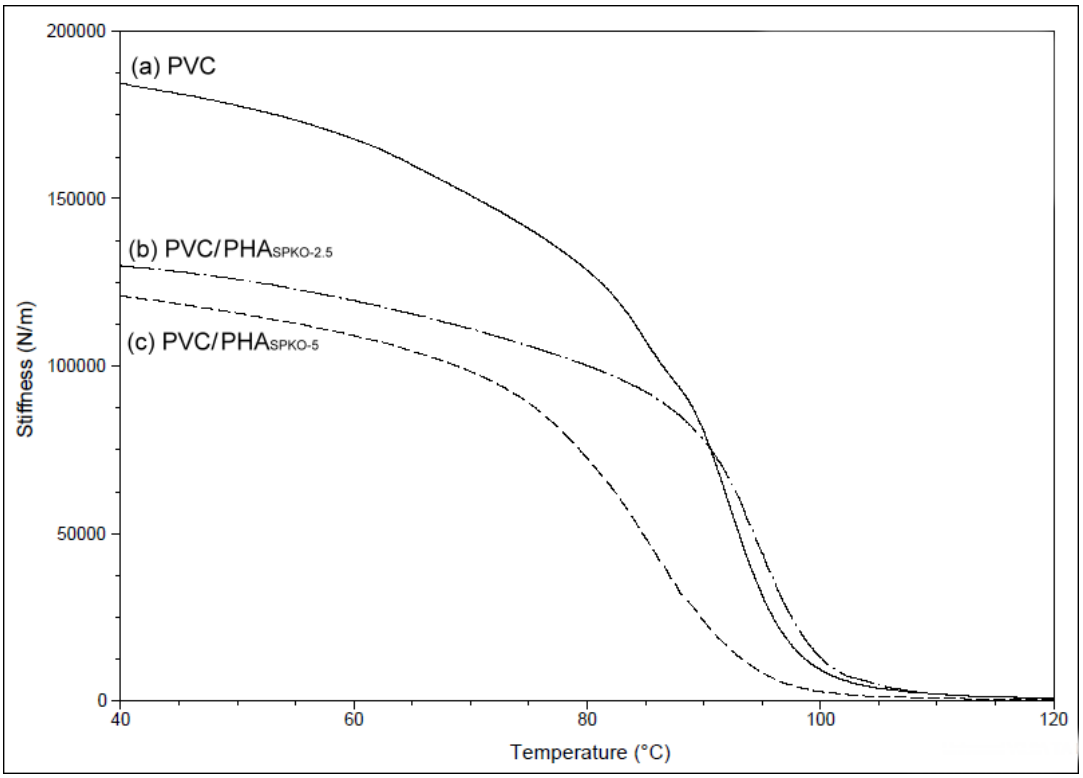

Fig. 5.47 Temperature variation of film's stiffness for (a) PVC, (b) PVC/PHA$_{SPKO-2.5}$; and (c) PVC/PHA$_{SPKO-5}$

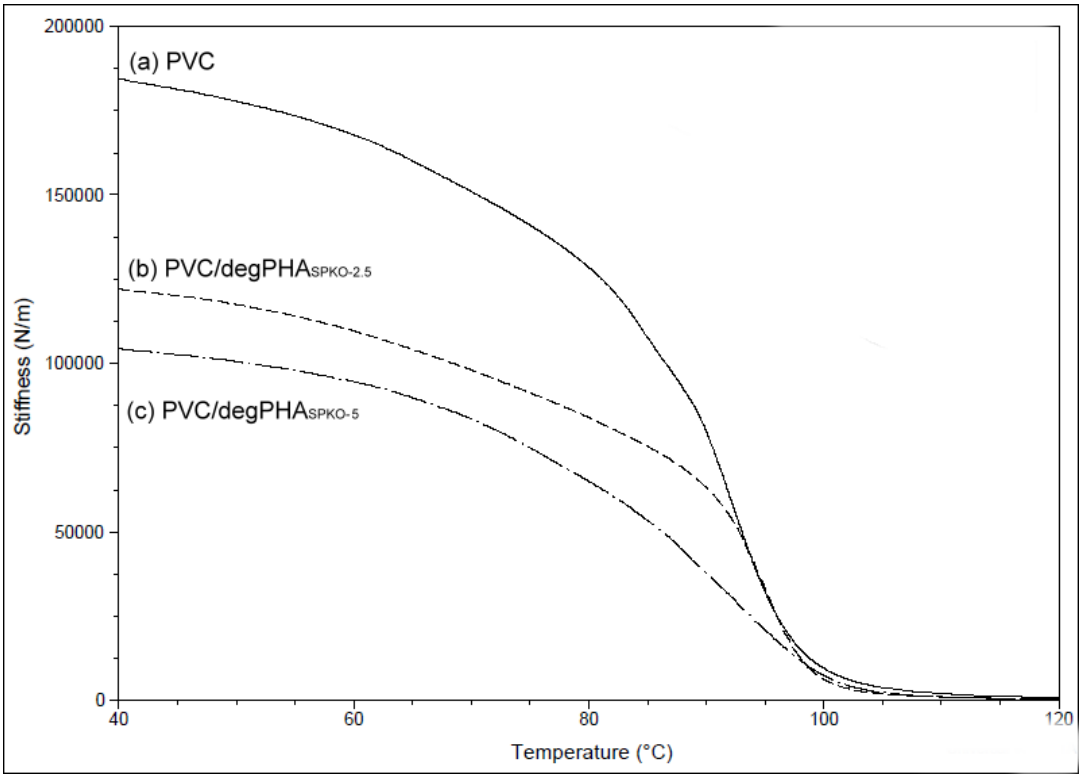

Fig. 5.48 Temperature variation of film's stiffness for (a) PVC, (b) PVC/degPHA$_{SPKO-2.5}$; and (c) PVC/degPHA$_{SPKO-5}$

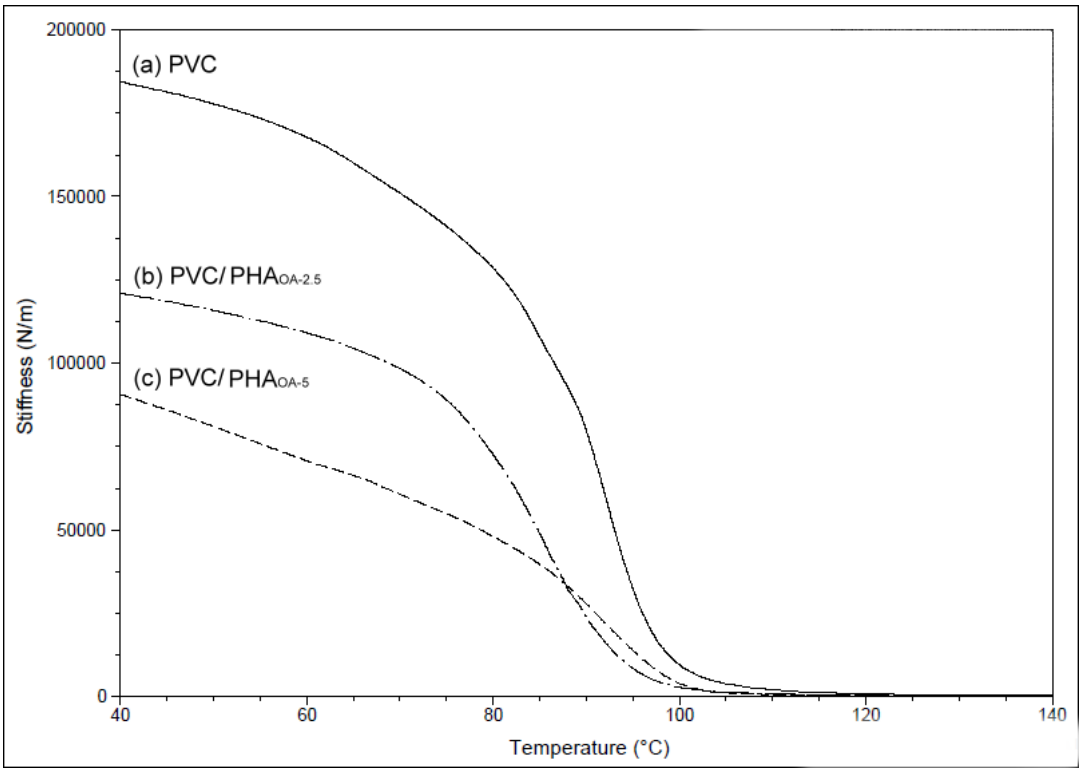

Fig 5.49 Temperature variation of film's stiffness for (a) PVC, (b) PVC/$PHA_{OA-2.5}$; and (c) PVC/PHA_{OA-5}

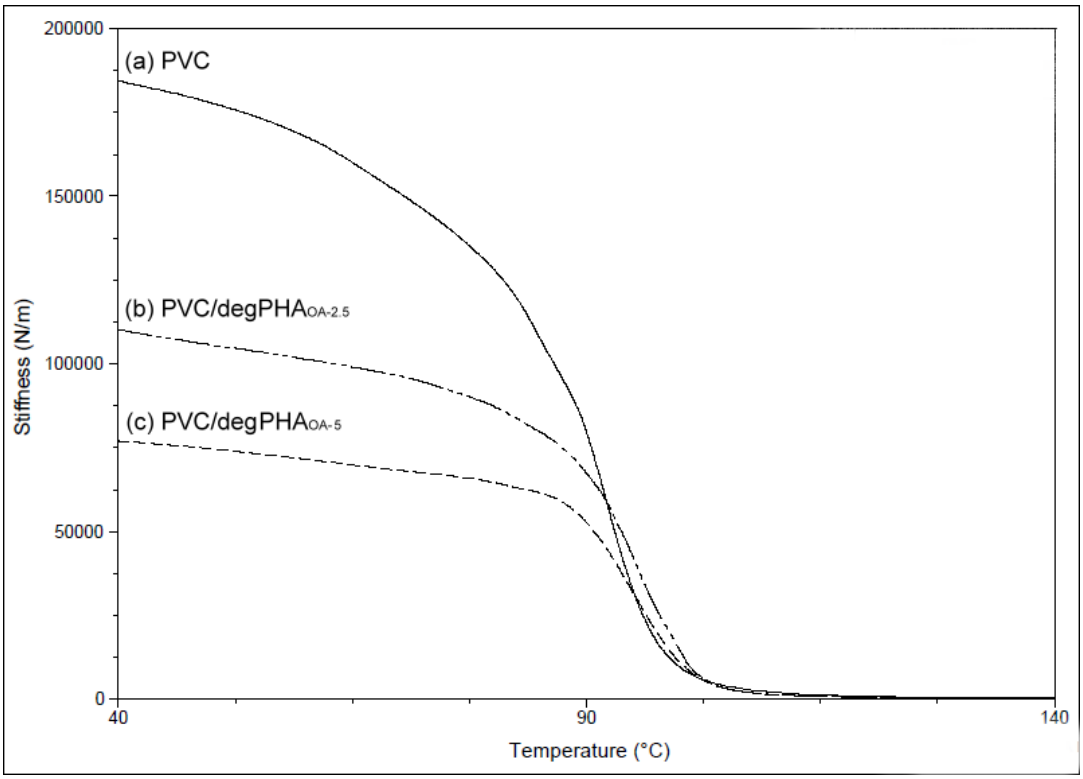

Fig. 5.50 Temperature variation of film's stiffness for (a) PVC, (b) PVC/deg$PHA_{OA-2.5}$; and (c) PVC/degPHA_{OA-5}

As shown from Fig. 5.47 to Fig. 5.50, the stiffness of the polymer blends decreased when the proportion of PHA increased. According to Wypych (2004), when larger quantities of PHA plasticizers were added into the PVC, more amorphous areas of the polymer became swollen. This would lead to increased ease of movement of the macromolecules, thus making the PVC-PHA blends to be more flexible.

On the other hand, by comparing the film's stiffness of the PVC/PHA with PVC/degPHA blends at 40 ℃, it could be seen that addition of oligomeric PHA could provide greater flexibility to the rigid PVC compared to the polymeric PHA, by introducing greater internal lubrication effect. The effectiveness in the lubrication effect could be attributed to the widespread specific interactions between the shorter chain fragments of oligomeric PHA with PVC, promoted by the increased hydroxyl and carboxyl end groups.

5.6.3 Comparison of elastic modulus of PVC and PVC/PHA binary blends

As elaborated in Section 3.2.2.4.5.1, the elastic modulus (*E*) is a measure of the stiffness of a component and its tendency to be deformed elastically when a force is applied to it.

For rigid PVC, typical elastic modulus lies between 2.4 to 4.1 GPa. In this study, the calculated elastic modulus for the unplasticized PVC was around 3.92 GPa. Subsequent elastic modulus values for the binary blends were summarized in Table 5.14.

Table 5.14 Elastic modulus values for PVC/PHA binary blends

Elastic Modulus (GPa)	2.5 phr	5 phr
PVC/PHA_{SPKO}	3.26	1.72
PVC/degPHA_{SPKO}	1.94	1.49
PVC/PHA_{OA}	3.67	2.61
PVC/degPHA_{OA}	2.85	2.1

As shown from Table 5.14, it can be seen that PVC plasticized with mcl-PHA showed a considerable lower elastic modulus than individual PVC, with the elastic modulus of both SPKO- and OA-derived PHA decreasing in the following order: PVC > PVC/$PHA_{2.5}$ > PVC/deg$PHA_{2.5}$ > PVC/PHA_5 > PVC/deg$PHA_{5.}$ These results were in agreement with the decrease in the stiffness of the binary blends.

Overall, the effectiveness of reducing the elastic modulus of the polymer was found to be better in PVC/PHA_5 binary blends as compared to PVC/$PHA_{2.5}$ binary blends; better in PVC/PHA_{SPKO} binary blends as compared to PVC/PHA_{OA} binary blends; and better in PVC/oligoesters binary blends as compared to PVC/polyesters binary blends.

5.6.4 Comparison of storage modulus between binary blends

As elaborated in Section 3.2.2.4.5.2, storage modulus (*E'*) provides an indication of rigidity of the material and its ability to resist deformation under an applied dynamic stress. The decrease in *E'* indicates a decrease in rigidity as well as the film stiffness.

The overall variation of storage modulus with temperature for PVC, PVC/$PHA_{2.5}$ and PVC/PHA_5 binary blends which consisted of polymeric PHA (PHA_{SPKO} and PHA_{OA}) and oligomeric PHA (degPHA_{SPKO} and degPHA_{OA}) as plasticizers are compared in Fig. 5.51, Fig. 5.52, Fig. 5.53 and Fig. 5.54.

From Fig. 5.51 and Fig. 5.52, respectively, the order of storage modulus for both PVC/PHA_{SPKO} and PVC/degPHA_{SPKO} blends decreased in the following sequence: PVC > PVC/$PHA_{SPKO-2.5}$ > PVC/$PHA_{SPKO-5,}$ and PVC > PVC/deg$PHA_{SPKO-2.5}$ > PVC/degPHA_{SPKO-5} whereas the storage modulus for both PVC/PHA_{OA} and PVC/degPHA_{OA} blends decreased in the following order: PVC > PVC/$PHA_{OA-2.5}$ > PVC/PHA_{OA-5} and PVC > PVC/deg$PHA_{OA-2.5}$ > PVC/deg$PHA_{OA-5,}$ as shown in Fig. 5.53 and Fig. 5.54, respectively.

Both observations indicated that the rigidity of the polymer blends is affected by the composition and amount fraction of the PHA plasticizer in the polymer mixture.

The modulus values of the all binary blends decreases with increasing temperature. This behavior may be due to the softening effect of the PVC/PHA matrix at high temperatures which has higher polymer chain mobility (Lawrence et al., 2004) and the modulus eventually drops to zero when the polymer melts.

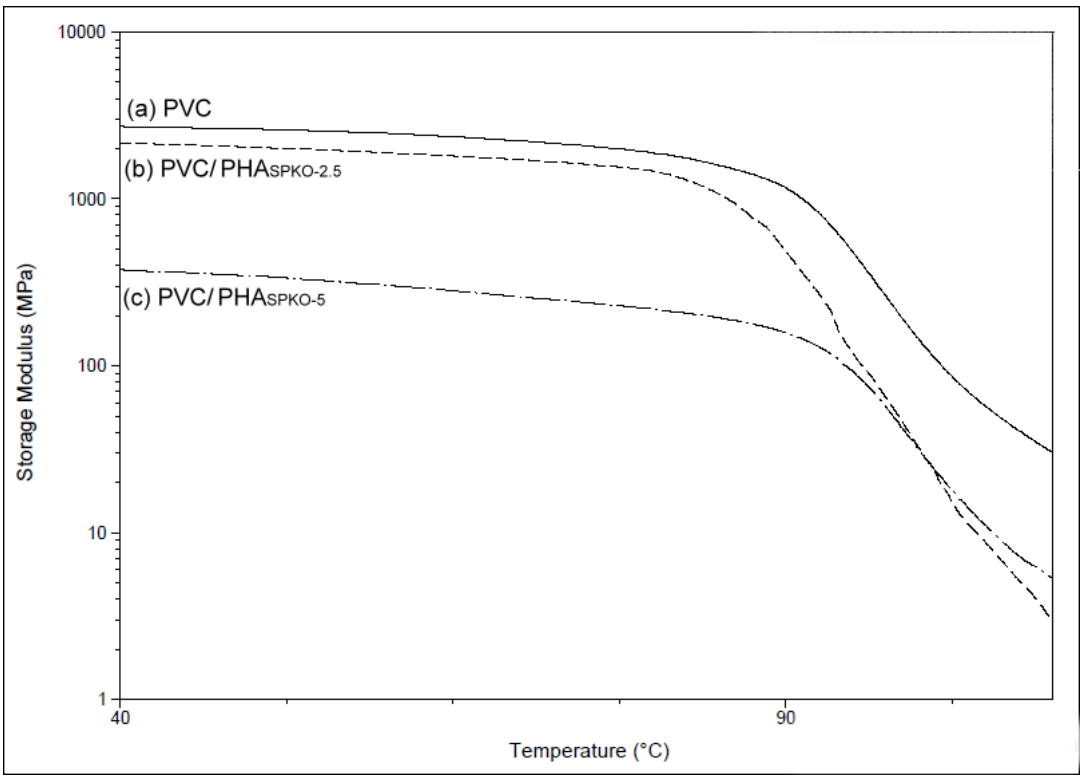

Fig. 5.51 Temperature variation of storage modulus for (a) PVC; (b) PVC/$PHA_{SPKO-2.5}$, and (c) PVC/PHA_{SPKO-5}

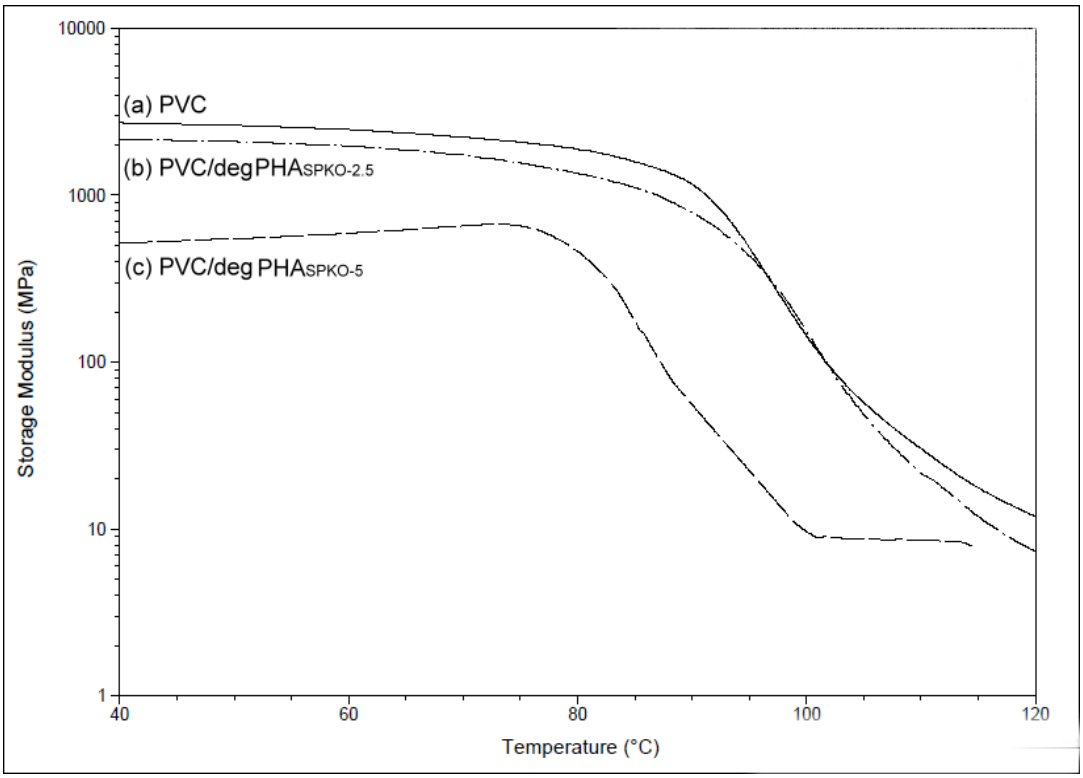

Fig. 5.52 Temperature variation of storage modulus for (a) PVC; (b) PVC/degPHA$_{SPKO-2.5}$, and (c) PVC/degPHA$_{SPKO-5}$

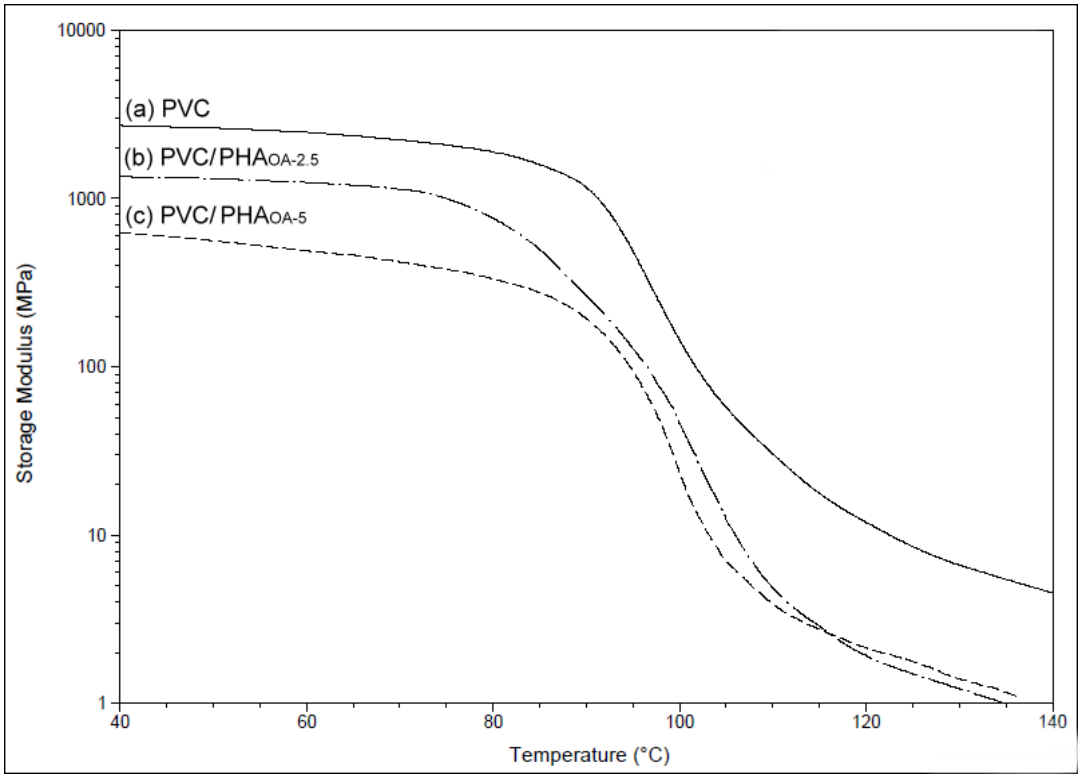

Fig. 5.53 Temperature variation of storage modulus for (a) PVC; (b) PVC/PHA$_{OA-2.5}$, and (c) PVC/PHA$_{OA-5}$

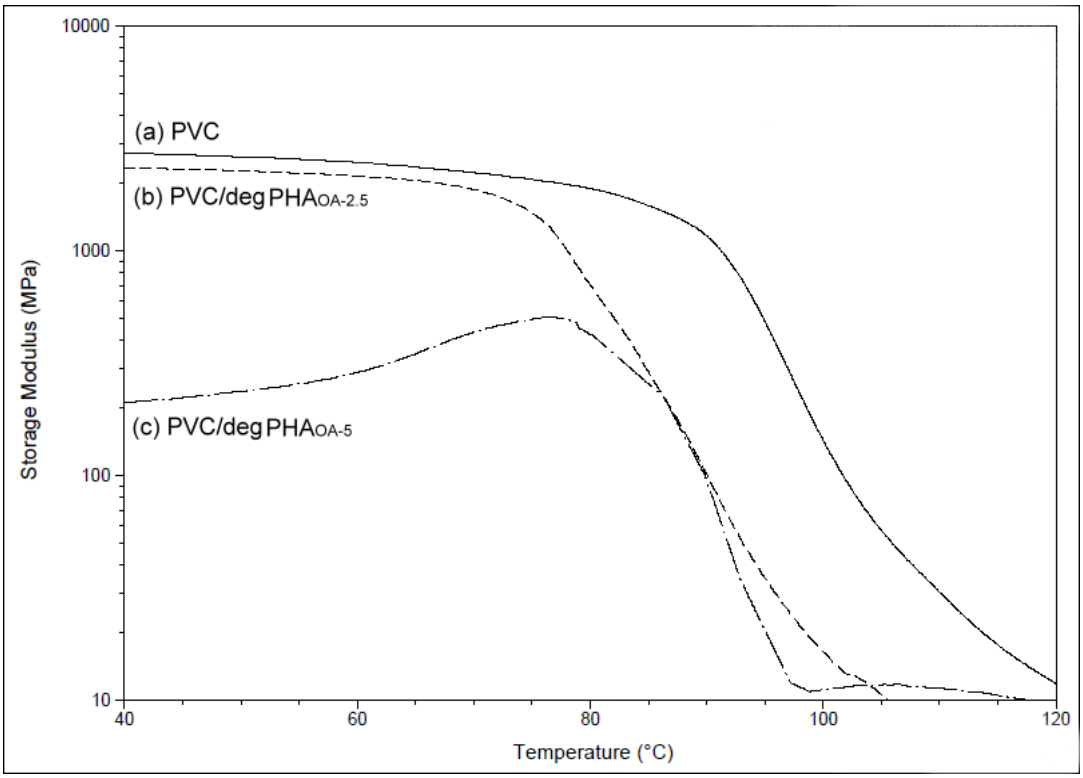

Fig. 5.54 Temperature variation of storage modulus for (a) PVC; (b) PVC/degPHA$_{OA-2.5}$, and (c) PVC/degPHA$_{OA-5}$

5.7 Summary

Results from FTIR and ^{1}H-NMR spectroscopic analyses showed that PVC-PHA miscibility was possibly due to the presence of specific interactions existed between the two polymers. These inter-polymer attractions were probably attributed to the interactions of α-hydrogen as well as the local dipoles between chlorines of PVC with the C=O and C-O-C groups of PHA. Under the SEM examination, most of the observed areas of the blends were composed of a dispersed phase, in which the individual PVC particles had been swollen as a consequence of plasticizer absorption.

Thermal analytical techniques such as TGA, DSC and DMA had been applied to the characterization of polymer blends as such techniques are particularly relevant to the characterization of polymer material. Since PVC and PHA are viscoelastic, their properties are temperature dependent and thus the thermal history of these polymeric

materials is an important variable. TGA study showed that PVC/mcl-PHA blend exhibited similar two-stage degradation as PVC. Both degradation of mcl-PHA and dehydrochlorination took place simultaneously in the first stage of degradation. All the binary blends had lower thermal stability, E_d and ΔS than unplasticized PVC. These findings were consistent with the T_g results obtained from DSC and DMA studies where the binary blends had a lower and single glass transition temperature than the PVC. These show that the polymer blends were miscible and compatible. Higher reduction of E_d, ΔS and T_g was observed when the proportion of PHA was increased in the blend; and when oligoesters were used as the plasticizer instead of polyesters, resulting in a more flexible and softer plasticized PVC film. The SPKO derived PHA was also found to exert a stronger plasticising effect than OA derived PHA.

In summary, small additions of PHA (2.5 and 5 phr.) to the PVC could effectively reduce the T_g of the polymer and impart flexibility to the PVC compound. Mcl-PHA and the oligoesters were shown to be a compatible plasticizer for PVC as they have reasonable apparent affinity towards the PVC resin due to the presence of some levels of intermolecular attraction between the polymers. The mcl-PHA also enhanced the segmental mobility of PVC by increasing the free volume of the system and therefore decreasing the glass transition temperature of the polymer blend and imparted greater flexibility to the PVC compound.

CHAPTER 6

CONCLUSION

6.1 Conclusion

The bacterial polyester, medium-chain-length poly(3-hydroxyalkanoates) (mcl-PHA), biosynthesized from two different palm oil-based carbon substrates, oleic acid and palm kernel oil were heat treated at various decomposition temperatures. The thermal, physical and structural properties of the un-degraded polyesters and their decomposition products, low molecular weight hydroxyacids oligoesters were characterized to study the thermal decomposition mechanism of the polymers. The polyesters and oligoesters were then assessed for the ability to act as plasticizer for poly(vinyl chloride) (PVC).

6.1.1 Thermal degradation of mcl-PHA

Oleic acid and SPKO-derived mcl-PHA were thermally degraded at 160 ℃ to 180 ℃; and at 160 ℃ to 190 ℃ respectively prior to the onset of rapid decomposition of the polymers, to generate low molecular weight hydroxyacids oligoesters. The degradation activation energy (E_a), pre-exponential factor (A) and change of activation entropy (ΔS) for oleic acid-derived PHA were 85.3 kJ mol^{-1}, 6.07 x 10^5 s^{-1} and -139.4 J K^{-1}, respectively; whereas for SPKO-derived PHA, the values were found to be 128.9 kJ mol^{-1}, 1.15 x 10^{10} s^{-1} and -57.6 J K^{-1}, respectively. Thermodegradation of mcl-PHA resulted in a progressive reduction in the polymer molecular weight, generating useful oligomeric hydroxyl acids with functional end-groups which could be used as biodegradable additives, plasticizers, or as blending materials in a polymerization process.

The thermal, physical and structural properties of the mcl-PHA changed dramatically when subjected to moderately high temperatures of degradation. Glass

transition temperatures (T_g) and initial degradation temperatures for both types of mcl-PHA decreased when the polymers were heat treated at increasing temperature. The morphology of the polymers was altered following thermal treatments. Acid values obtained from end group analysis showed that thermally-degraded PHA contained higher concentration of carboxylic terminals and lower M_n compared to control PHA (non heat-treated). The acid numbers of heat-treated PHA increased with increasing treatment temperatures, with 180˚C-treated oleic acid-derived mcl-PHA and 190˚C-treated SPKO-derived PHA contained the highest acid number, the highest concentration of terminal carboxylic acids and the lowest number average molecular weight. These results were corroborated with the decreased M_n from the GPC analysis. An increase in the acidity of the decomposition products was probably due to the formation of low molecular weight water-soluble hydroxyl acids in which the numbers of hydrogen and alkyl substituents were greatly decreased in the polymer chains. The standard Gibbs free energy (ΔG°) for the heat-treated PHA were positive, showing that dissociation of the weak hydroxyalkanoic acids into thermodynamically stable hydroxyl-carboxylate and hydrogen ions was not spontaneous, requiring energy input into the system to occur. Analyses of GC, FTIR and ^{1}H-NMR spectra suggested the thermal degradation mechanism of mcl-PHA involved random hydrolytic chain scission which initiated at the weak links of the ester linkages, producing a mixture of low molecular weight hydroxyacids accompanied by proportional increase in the hydroxyl and carboxyl end groups. Subsequent heating in the acidic environment at high temperature would lead to dehydration of some hydroxyl terminal groups, producing alkenoic acids as additional end product.

6.1.2 Assessment of PHA and its oligoesters as plasticizers for PVC

FTIR analysis confirmed the presence of both polar functional groups of PHA and PVC in the binary blends. The amount of polar C=O groups varied with the composition and type of PHA present in the binary blends. It is postulated that the PVC-PHA miscibility was possibly due to the specific interactions between the ester C=O group of PHA with the CH-Cl group of PVC.

Results from ^{1}H-NMR spectroscopic analysis also showed that the inter-polymer attractions between the two polymers were probably attributed to the α-hydrogen as well as the local dipole-dipole interaction between chlorines of PVC with the PHA.

SEM micrographs of PVC/PHA films showed that plasticization of PVC involved the PHA polymers penetrated in some of the porous structures of PVC, and interfused with PVC polymer segments. These PHA polymers possibly embedded themselves between PVC chains and increased the free volume in the system, by separating the PVC chains further apart and therefore promoted higher polymer chain movements

PVC/PHA blends exhibited similar two-stage degradation pattern as PVC, where the degradation of PHA and dehydrochlorination simultaneously took place in the first stage of degradation. At the first stage of degradation, the thermal stability, degradation activation energy (E_d), pre-exponential factor (A) and change of activation entropy (ΔS) decreased in the following order: PVC>PVC/PHA$_{2.5}$>PVC/PHA$_{5.}$ The PHA plasticizer can induce the degrading effects to the PVC possibly as a consequence of the solvation of plasticizer-polymer chains and the effect was more pronounced when the amount of plasticizer increased. Besides that, polymer blends consisting of PHA oligoesters (compared to the longer polyesters) and the SPKO-derived mcl-PHA (compared to the oleic acid derived PHA) as plasticizer had the lower thermal stability, E_d, A and ΔS. These findings were consistent with the T_g results obtained from DSC and DMA. There

was no a clear trend of variation between the E_d, A and ΔS of PVC/PHA blends for the second stage of decomposition as this stage of decomposition mainly consisted of the decomposition of unsaturated hydrocarbon structures.

The miscibility of the PVC with PHA and its oligoesters was shown by the PVC/PHA blend having a single glass transition based on DSC and DMA analyses. The T_g of the blends decreased with increasing the amount of mcl-PHA as more PHA plasticizer embedding themselves between the PVC chains, spacing them further apart to increase the free volume and therefore imparting the plasticizing effect more significantly. Polymer blends composed of PVC and the oligoesters as plasticizer showed lower T_g than the blends composed of polymeric polyesters. As low molecular weight plasticizers possessed more end groups, this would accordingly increase the free volume and mobility among the PVC polymer chains, thus softer plasticized films with better plasticizing effect would be formed. Oleic acid-derived mcl-PHA either in polymeric or oligomeric form imparted lower plasticizing effect to the PVC compared to SPKO-derived mcl-PHA by reducing the T_g of the polymer blends less effectively. A plausible reason for that is that mcl-PHA derived from oleic acid consisted of polymer chains with numerous longer side chains compared to mcl-PHA derived from SPKO, and this would cause a decrease in chain hydrodynamic volume in the PVC system, resulting in a less flexible and harder plasticized PVC film. The experimental T_g values from DSC analysis were compared with theoretical T_g values predicted from the Fox and Gordon-Taylor equations. It was found that the experimental T_g fitted well with the Gordon-Taylor equation. However, the experimental T_g was generally higher than the values calculated from the Fox equation, as the intermolecular forces present in the polymer system were not taken into consideration in the equation, and therefore the differences between the theoretical and experimental values can be used to predict the level of intermolecular attractions between PVC and the plasticizers.

Both measurements of DSC and DMA gave consistent results where the dynamic viscoelastic measurements showed a single T_g for the PVC/PHA blends and a lower loss modulus peak compared to the PVC, indicating the PHA were highly miscible with PVC. Decreased T_g, stiffness, storage modulus and elastic modulus were observed in the polymer blends with higher amounts of PHA, and PHA in the form of oligoesters. When larger quantities of PHA plasticizers were added to the PVC, more amorphous areas of the PVC particles would be swollen and this would lead to increased ease of movement of the PVC macromolecules. On the other hand, low molecular weight PHA plasticizer would increase the degree of chain movement and segmental flexibility to the PVC chains in a greater extent and would therefore increase the softening properties of the blends.

In summary, oligomeric and SPKO-derived mcl-PHA were shown to be more compatible plasticizers for PVC compared to polymeric and oleic acid-derived mcl-PHA. These plasticizers enhanced the segmental mobility of PVC more effectively by increasing the free volume and macromolecular mobility of the system.

6.2 Future research plan

For future study, a bigger size of the PVC-PHA plasticized films is needed for measurements relating to mechanical properties i.e. tensile strength and elongation at break. It would be of interest also to study the migration of the plasticizer from the PVC-PHA compound, for example migration of the plasticizer on heating, resistance of plasticizer to extraction by chemicals e.g. water, soap solution, polar or organic solvents in order to investigate whether the plasticizers studied have sufficient affinities for the PVC to resist migration from the internal regions to the surface.

The work presented here studied the lightly plasticized PVC at low level of mcl-PHA. It is also interesting to investigate the effects of higher level of plasticizer in

formulations such as 10, 20, 30 and 40 parts of mcl-PVC per hundred parts of PVC resin in terms of thermal and physical properties of the blends as well as to determine the optimum point of plasticizer concentration. In terms of compound production, it is also interesting to investigate the effect of mixing time in solution blending under defined conditions, on the physical properties of the PVC/mcl-PHA binary blends.